ABUNDANCE AND SIZE OF THE SEA SCALLOP POPULATION IN THE MID-ATLANTIC BIGHT

by

Justin H. Walker

A thesis submitted to the Faculty of the University of Delaware in partial fulfillment of the requirements for the degree of Master of Science in Geology

Spring 2013

© 2013 Justin H. Walker
All Rights Reserved

ABUNDANCE AND SIZE OF THE SEA SCALLOP POPULATION

IN THE MID-ATLANTIC BIGHT

by

Justin H. Walker

Approved: _____
Arthur C. Trembanis, Ph.D.
Professor in charge of thesis on behalf of the Advisory Committee

Approved: _____
James E. Pizzuto, Ph.D.
Chair of the Department of Geological Sciences

Approved: _____
Nancy M. Targett, Ph.D.
Dean of the College of Earth, Ocean, and Environment

Approved: _____
James G. Richards, Ph.D.
Vice Provost for Graduate and Professional Education

ACKNOWLEDGMENTS

I am extremely grateful for the support and mentorship provided by my advisor, Dr. Art Trembanis. I am thankful to my committee member, Dr. Douglas Miller, for helping this geologist explore the world of marine biology. Thanks to my other committee member, Dr. John Madsen, for years of guidance. To the late Dr. William Phoel for showing me that age should never slow you down. I would like thank my past and present lab mates: Stephanie Nebel, Carter DuVal, Trevor Metz, Nicole Raineault, Ashley Norton, Jonathan Gutsche, Bryan Keller, and Adam Skarke for continual help and support on my project and for being an amazing group of people that I am proud to be associated with. I am indebted to the captains and crew of the F/V CHRISTIAN AND ALEXA: Arthur Ochse, Kenny Ochse, Mike Newman, Dave Crosson, and Robert Adam. I am thankful to Mike Carrington for his help during the scallop cruise. Thanks to Dr. Dvora Hart for helping me to understand the sea scallop. This project would not have been possible without the scripting savvy of Vinar Amrutia. I am thankful to all of the scallop counters: Brandon Reed, Thomas Santangelo, and Dave Wessel. Thanks to Val Schmidt for teaching me about the AUV and expanding my technical horizons. To Meg Christie and Elyse Williamson for consistently keeping my sanity in check. To my officemate James Heiss for always listening whenever I got stuck understanding a concept during late nights at the office. My thanks to Dr. Ron Martin for inspiring me to always take an interest in earth history.

I owe a special thanks to my parents, Rickey and Maria Walker, and to my sister, Jessica Pinson, for their continued love, support, and understanding in everything that I have done.

TABLE OF CONTENTS

LIST OF TABLES ix
LIST OF FIGURES xi
LIST OF EQUATIONS xvii
LIST OF VARIABLES xviii
ABSTRACT xix

Chapter

1 INTRODUCTION 1

1.1 Scope of Research 1
1.2 Mid-Atlantic Bight Sea Scallop Fishery 3

1.2.1 History of the Fishery 3
1.2.1 Magnuson-Stevens Act 7
1.2.2 Overfishing in the 1990s 8

1.3 The Sea Scallop 9

1.3.1 Origin of the Scallop 9
1.3.2 Morphology and Habitat 9

1.4 Mid-Atlantic Bight Geologic Background 13

1.4.1 The Coastline 13
1.4.2 Shelf Seafloor 16
1.4.3 Regional Geologic Framework 20

2 DEVELOPMENT AND IMPLEMENTATION OF AN AUV BASED SEA SCALLOP IMAGE SURVEY 24

2.1 Introduction 24
2.2 Study Area 26
2.3 Methods 26

2.3.1 Autonomous Underwater Vehicle 26

2.3.1.1 The AUV Camera 31

2.3.1.2 Navigation System 34
2.3.1.3 Side-Scan Sonar and Bathymetric Sonar 35

2.3.2 F/V Christian and Alexa 39
2.3.3 Survey Mission Design 40
2.3.4 Image Processing 43

2.3.4.1 A Single Image 43
2.3.4.2 Sea Scallop Enumeration and Sizing 46

2.3.5 Bed Type 50
2.3.6 Processing Side-scan Sonar 52
2.3.7 Processing Bathymetric Data 52
2.3.8 Dredge Efficiencies 53
2.3.9 Scallop Biomass 54
2.3.10 Variograms 55

2.4 Results 57

2.4.1 Survey Stratum 1 57
2.4.2 Survey Stratum 2 58
2.4.3 Survey Stratum 3 61
2.4.4 Survey Stratum 4 61
2.4.5 Survey Stratum 5 65
2.4.6 Survey Stratum 6 65
2.4.7 Survey Stratum 7 66
2.4.8 Survey Stratum 8 69
2.4.9 Mid-Atlantic Bight Summary 77
2.4.10 Simulation of Abundance Results 86
2.4.11 Dredge Efficiency Analysis 89

2.5 Discussion and Conclusion 92

2.5.1 AUV as a Survey Platform 92
2.5.2 Sea Scallop Stock Assessment 92

3 QUANTIFYING SEA SCALLOP FISHING EFFORT AND A LOOK AT OTHER MID-ATLANTIC BIGHT EPIFAUNAL ORGANISMS 94

3.1 Introduction 94

3.1.1 Closed Area 94
3.1.2 Study Area 96

3.2 Methods 99

3.2.1 Image Analysis 99
3.2.2 Statistical Analysis 103
3.2.3 Dredge Scar Area 104

3.3 Results 107

3.3.1 Species Diversity Analysis 107
3.3.2 Sea Scallop Fishing Effort 111

3.4 Discussion and Conclusion 121

3.4.1 Species Diversity Analysis 121
3.4.2 Fishing Effort 122

4 CONCLUSIONS 124

4.1 Stock Assessment 124
4.2 Future Work 125

REFERENCES 127

Appendix

A AUV MISSION BUBBLE PLOTS 132

A.1 Introduction 132
A.2 AUV Mission Bubble Plots 133

B SHELL HEIGHT BOX PLOTS 146

B.1 Introduction 146
B.2 Shell Height Box Plots 147

C OMNIDIRECTIONAL VARIOGRAMS 155

C.1 Introduction 155
C.2 Sea Scallop Survey Variograms 156

D SHELL HEIGHT HISTOGRAMS 181

D.1 Introduction 181
D.2 Shell Height Histograms 182

E SIDE-SCAN MOSAICS WITH DIGITIZED DREDGE SCARS 208

E.1 Introduction 208
E.2 Side-Scan Sonar Mosaics 209

F MATLAB CODE 236

F.1 Biomass 236
F.2 Semivariogram 237
F.3 Dredge Scar Area 239
F.4 Image Sample Model 242

G QUALITY CONTROL 244

H DREDGE SCAR AREA AND ROSE PLOTS 246

H.1 Introduction 246
H.2 Dredge Scar Rose Plots 247

LIST OF TABLES

Table 1.1: Cumulative sea scallop landings for the United States and Canada 1978-1998. Years of heavy fishing are boldfaced. Adapted from Naidu and Robert (2006). 6

Table 2.1: AUV Mission Summary Table 28

Table 2.2: Point Grey Scorpion 20SO AUV research camera specification. 32

Table 2.2: Table of scallop survey mission data for survey strata 1-3. 71

Table 2.3: Table of scallop survey mission data for survey strata 4-6. 72

Table 2.4: Table of scallop survey mission data for survey strata 7 and 8. 73

Table 2.5: Scallop shell height data and distribution statistics for each digital image survey within survey strata 1-6. 74

Table 2.6: Scallop shell height data and distribution statistics for each digital image survey within survey strata 7 and 8. 75

Table 2.7: Biomass and harvestable biomass calculated for each mission based on scallop shell height and water depth. 76

Table 2.8: 2011 sea scallop survey season summary. 79

Table 3.1 Environmental and bathymetric data for the dredged (U1, U2, and U3) and non-dredged missions (P1, P2, and P3). 97

Table 3.2: Benthic organisms identified and enumerated from the 12,000 image subset. 102

Table 3.3 Simpson's Diversity and Shannon-Wiener Indices for the dredged (U1-3) and non-dredged missions (P1-3). Simpon's Diversity values approaching 1 represent a lower diversity. Shannon-Weiner values approaching 0 represent a lower diversity. 109

Table 3.4: T-test analysis of each identified species between the dredged (U1-3) and non-dredged (P1-3) missions. Degrees of freedom is 4 (6 missions – 2). p is probability that the difference observed in species densities between the dredged and non-dredged areas is by random chance. The threshold for $p<0.1$ is $t \geq 2.13$ and for $p<0.05$, $t \geq 2.78$.. 110

Table 3.5: Results of the dredge scar area analysis and vessesl monitoring system nearest neighbor values. 114

LIST OF FIGURES

Figure 1.1: U.S.A landings of the Atlantic Sea Scallop for the years 2002 – 2011. The year 2011 saw a record 7-year high of over $500 million in sea scallop landings. From *Fisheries of the United States* (2012). 5

Figure 1.2: Specimens of *Placopecten magellanicus* dredged from the seafloor by the F/V Christian and Alexa. Note the symmetric circular shape and orange color. 12

Figure 1.3: The general coastal geology of the Mid-Atlantic Bight and other providences as interpreted from vibratory cores and acoustic data from Field and Duane (1976). 15

Figure 1.4: The depositional geomorphology of the Mid-Atlantic Bight. From Swift (1976). 18

Figure 1.5: Side-scan sonar (900 KHz) image of a sorted bedform on the seafloor of the Mid-Atlantic Bight. Bright areas illustrate high backscatter. The white boundary highlights the sharp contact between rippled and flat bed. 19

Figure 1.6: The geologic framework of the Mid-Atlantic Bight and surrounding areas. The majority of the Mid-Atlantic Bight resides atop the Baltimore Canyon Trough. From Hutchinson and Grow (1985). 22

Figure 1.7: Interpretation of the Baltimore Canyon trough from seismic stratigraphy, Continental Off-shore Stratigraphic Test (COST) wells B-2 and B-3, and gravity models. From Sawyer *et al.* (1982). 23

Figure 2.1: The eight survey substrata chosen for the 2011 scallop image surveys. The eight strata fall within the colored NMFS sea scallop survey strata. 27

Figure 2.2: The AUV was configured for seafloor imaging and mapping. In addition to the 250,000 seafloor images that were collected, the AUV also gathered data about water temperature, salinity, dissolved oxygen, bathymetry (500kHz phase differencing bathymetric sonar), and seafloor features (900 kHz side-scan sonar). The AUV can operate at depths of 500m, and can operate for 3 hours before the batteries need to be recharged. 30

Figure 2.3: The hull mounted AUV camera on the nose cone, and the hull mounted LED strobe system on the command module. 33

Figure 2.4: AUV mission data demonstrating the terrain following behavior of the vehicle over seafloor while adhering to a predefined altitude. Standard deviation of 16 cm. 37

Figure 2.5: Plan view of AUV survey mission track designs. 42

Figure 2.6: An image of the seafloor with 15 scallops in it. Image dimensions are defined in terms of length and width. This image represents an area of seafloor 2.6 m^2 (1.86 m x 1.4 m). 45

Figure 2.7: Visual representation of the scallop sizing algorithm. Green circles were sized, and therefore counted. The red circle represents a scallop that could not be sufficiently sized. Image dimensions: 1.86 m x 1.4 m. 47

Figure 2.8: The user interface of the sea scallop counting and sizing program. Scallop were sized by using a built in length tool (the red lines in the image). Other attributes such as the bed type and image quality were also input by the user. 48

Figure 2.9: Image references for the bed type classification scheme. 51

Figure 2.10: Experimental variogram with a spherical fit model. Variograms assist in understanding the spatial structuring of the scallop populations within each mission. This mission has an autocorrelation length of 400 m. 56

Figure 2.11: A comparison of images of the seafloor taken at night versus during the day. Attached histograms of the RBG channel in each image show that the daytime photo has undersaturated reds and overexposed greens, which can make it difficult to identify a scallop shell. The nighttime photos have a much better color balance. 59

Figure 2.12: Bubble plot of mission 110709_Scallop_D3_M1_Corey. Each bubble represents 1 seafloor image. The size of the bubble corresponds to the number of scallops counted in that image. This mission does not display any noticeable scallop grouping. 60

Figure 2.13: Mission 110710M1_ArtiesRun showing a higher density grouping of scallops on the western side of the mission. 62

Figure 2.14: Shell Height histogram for mission 110711_DV115 showing a negatively skewed distribution. 64

Figure 2.15: Bubble plot of mission 110728_D3_R6_M1 showing a steadily increasing scallop density to the south. 67

Figure 2.16: Box plots for the missions within survey stratum 6 showing a large range of digitally measured shell heights within each mission. 68

Figure 2.17: Side-scan sonar mosaic of a ripple field. The blue dots represent locations of identified scallops within an image classified rippled bed. . 70

Figure 2.18: Mission scallop densities compared to near bed (altitude of 2 m) water temperature. Highest densities occur near 9 degrees Celsius. 80

Figure 2.19: A plot of near bed temperature and depth for each survey showing a correlation between temperature and depth. 81

Figure 2.20: Sea scallop shell height distributions for the Mid-Atlantic Bight 82

Figure 2.21: A 3-dimensional variogram comparing shell height distribution to depth. Shell heights are negatively distributed below depths of 45 m. .. 83

Figure 2.22: Plot of digitally measured mean shell height versus scallop density. A relationship was not found to exist. 84

Figure 2.23: Bed type distribution of sized scallops identified in seafloor photographs. 98.6% of all identified scallops occurred on a sandy classified bed. 85

Figure 2.24: Results of Monte Carlo simulation. The response of the abundance estimate to the portion of the available images that are analyzed. 87

Figure 2.25: Plot of relative accuracy of abundance estimate for a range of analyzed images. 88

Figure 2.26: Comparison of AUV image measured shell heights and dredge measured shell heights for the same survey line. 90

Figure 2.27: Comparison of AUV image shell height distributions and dredged shell height distributions for the same survey line. 91

Figure 3.1: Study area of non-dredged (missions P1, P2, P3) versus heavily dredged (U1, U2, U3) sea scallop survey missions. Note that each mission is a subset of a sea scallop survey mission. 98

Figure 3.2: Section of a side-scan sonar mosaic of the seafloor from mission U2 (110709_Scallop_D3_M1_Corey) showing multiple intersecting commercial scallop dredge scars. 106

Figure 3.3: Log plot of the benthic organism species densities for each protected (P1, P2, P3) and unprotected (U1, U2, U3) missions. The relationship of scallop densities and sand sea star densities are inversed from protected to unprotected missions. Note the density units are 10^{-3} of the y-axis value. 108

Figure 3.4: Plot of dredged seafloor area versus scallop density. The plot shows that fishing vessels will allocate considerable dredging effort (>15% area dredged) when the scallop density is greater than 0.06 scallops/m^2 115

Figure 3.5: A plot showing the inverse relationship that exists between mean sea scallop shell height and dredging for scallop missions that showed minimal dredging effort (>5% area dredged). 116

Figure 3.6: Plot of shell height distribution skewness compared to seafloor dredge area. Increased dredging shifts the shell height distribution more positive due to size selectivity of the commercial scallop dredge. 117

Figure 3.7: Map showing VMS fishing effort data (log transform). Fishing effort trends parallel with depth contour. South of Hudson Shelf Valley, fishing effort is concentrated seaward of the 47 m depth contour. North of Hudson Canyon, fishing effort is concentrated between the 32 and 47 m contour. 118

Figure 3.8: Plot of VMS fishing effort versus sea scallop density. 119

Figure 3.9: A semi-log plot of the two fishing effort proxies used in this study: VMS data and side-scan sonar derived percent area dredged. There exists an exponential relationship between the two methods. 120

Figure E.1: 110708_Scallop_DvoraRun 209
Figure E.2: 110708_ScallopD2_M4 210
Figure E.3: 110708_ScallopD2 211
Figure E.4: 110708_SM2 212
Figure E.5: 110709_Scallop_D3_M1_Corey 213
Figure E.6: 110709_ScallopDay3_DV119 214
Figure E.7: 110710_DV117 215
Figure E.8: 110710_DV118 216
Figure E.9: 110710_M1_ArtiesRun 217
Figure E.10: 110711_DV115 218
Figure E.11: 110726_ScallopD1_DV2_M2 219
Figure E.12: 110726_ScallopD1_DV44_M3 220
Figure E.13: 110727_D2_R2_M2 221
Figure E.14: 110727_D2_R3_M3 222
Figure E.15: 110726_D2_R4_M4 223
Figure E.16: 110727_D2_R5_M5 224
Figure E.17: 110727_ScallopD2_R1_M1 225
Figure E.18: 110728_D3_DV062_M3 226
Figure E.19: 110728_D3_DV063_M4 227
Figure E.20: 110728_D3_R6_M1 228
Figure E.21: 110728_D3_R7_M2 229
Figure E.22: 110728_D3_R8_M5 230
Figure E.23: 110729_D4_DV0105_M2 231

Figure E.24: 110729_D4_DV0106_M1 232

Figure E.25: 110729_D4_DV0112_M3 233

Figure E.26: 110729_D4_DV0113_M4 234

Figure E.27: 20110726_ScallopD1_M1 235

Figure G.1: Plot showing the consistency of repeated image counts by multiple analysts. 244

Figure G.2: Results of N=53 repeated digital measurements of the same scallop in a photo by a single analyst. 245

LIST OF EQUATIONS

Equation 2.1: Acoustic impedance contrast 38

Equation 2.2: Seafloor image width 43

Equation 2.3: Dredge/image transect length 49

Equation 2.4: Scallop density 49

Equation 2.5: Dredge efficiency 54

Equation 2.6: Sea scallop biomass 54

Equation 2.7: Semivariogram 55

Equation 3.1: Simpson diversity index 103

Equation 3.2: Shannon-Wiener 103

Equation 3.3: Student's t-test 103

Equation 3.4: Dredge scar area 104

LIST OF VARIABLES

α	autocorrelation length
a	abundance of scallops in an image
α_D	abundance of scallops captured in a single dredge tow
α_h	horizontal field of view (in water)
α_T	abundance of scallops identified from images for a single mission
A	area contained within an image
A_D	percent area dredged
d	depth
D	Simpson diversity index
D_S	scallop density
e	dredge efficient
$E_{\mathrm{T_{end}}}$	easting end coordinate of AUV or dredge transect
$E_{\mathrm{T_{start}}}$	easting start coordinate of AUV or dredge transect
h	lag distance
H	Shannon-Wiener index
H_s	shell height of scallop
H	dimensional height of an image
l_D	total dredge path length
l_T	total survey line length
n_i	number of individuals per species
N	number of data pairs
$N_{\mathrm{T_{end}}}$	northing end coordinate of AUV or dredge transect
$N_{\mathrm{T_{start}}}$	northing start coordinate of AUV or dredge transect
N	total number of individuals counted
p_i	n_i/N
S	total number of species counted
T	AUV transect
v	sound velocity of material
W_m	meat weight
W	dimensional width of an image
$\overline{W_T}$	mean image width of an AUV transect
$\overline{x_1}$	mean of the population of the species in the protected area
$\overline{x_2}$	mean of the population of the $\overline{x_1}$ species in the unprotected area
x_i	scallop image from a mission
z	altitude above the seafloor
Z	acoustic impedance contrast
ρ	density of the material
$\hat{\gamma}$	semivariance
θ_p	pitch attitude of the AUV

ABSTRACT

The stock of the Mid-Atlantic Bight sea scallop fishery is assessed every year through the use of various dredging and imaging techniques. The sustainability of the fishery depends on the proper setting of the yearly catch limits based on the assessment of the preceding year. Within the past 10 years, digital image surveys have been explored as a potential method to supplement the yearly dredged based surveys. AUVs have been shown to be a successful platform for rapidly and accurately performing seafloor image surveys of benthic habitats. In 2011, a Teledyne-Gavia autonomous underwater vehicle (AUV) with a hull-mounted camera was used to non-invasively optically and acoustically image 313 km of the seafloor within the Mid-Atlantic Bight at a constant altitude of 2 m. Survey transects were completed at 24 open access ground locations and 3 additional locations within the Elephant Trunk Access Area. Trained image analysts, using a scallop counting and sizing algorithm developed for this stock assessment, were able to enumerate and size sea scallops within the collected 250,000 seafloor images, finding that the region had an overall scallop density of 0.027 scallops/m^2. Georeferenced data was tagged by the AUV inertial navigation system (INS) to every seafloor image, allowing for unprecedented meter scale spatial analysis of the sea scallop distribution. The relationship between image subsampling and the accuracy of the resulting scallop density was explored via simulations run on the image analysis results. Eight AUV transects were resurveyed by a New Bedford commercial scallop dredge for shell height calibration data and to calculate the harvest efficiency of the dredge (0.60).

Image analysis and backscatter data collected by the AUV's 900 kHz side-scan sonar were used to classify seafloor substrate types. The surveyed scallop strata were classified as 98.6% sandy seafloor with the remaining 1.4% representing intermittent shell hash, mounds, and ripples. The side-scan backscatter data revealed other varied seafloor texture, including escarpments from scallop dredge trawling and wave created sorted bedforms. Seafloor dredge scar area measured from the side-scan backscatter data and National Oceanic and Atmospheric Administration (NOAA) vessel monitoring system (VMS) tracking data were used as a proxy for fishing effort. Increased dredging was found to positively skew shell height distributions.

Chapter 1

INTRODUCTION

1.1 Scope of Research

During the past decade, sea scallop (*Placopecten magellanicus* (Gmelin, 1791)) annual landings have averaged 26,000 metric tons of scallop meat per year in the United States. The Mid-Atlantic region has been a historically high production region, with landings peaking in 2004 at 24,494 mt (NMFS, 2010). The sea scallop abundance and size distribution in the Mid-Atlantic region has been monitored by the National Marine Fisheries Service (NMFS) through annual sampling via dredging of the seafloor.

Dredging is a method for collecting sea scallops and other macrofauna from the seafloor and hauling them to the deck of a vessel. While dredging has been shown to not only alter the surficial geology of the seafloor, it has also been known to selectively increase mortality of certain species like the spider crab (Currie and Parry, 1999). In the 2010 NMFS sea scallop stock assessment report, NMFS defined the need to develop and apply analytic approaches for single and multi-year stock projections (NMFS, 2010).

Since 2002, it has been shown that image sampling techniques can be used to estimate sea scallop populations (Stokesbury, 2002). The first system devised to visually measure scallop abundances and sizes on the seafloor was a stationary pyramid platform consisting of video cameras that was lowered from a vessel to the

seafloor. A more recent system developed called HabCam uses a towed camera sled tethered to a ship to gather images of scallops on the seafloor (Rosenkranz *et al.*, 2008).

This study utilized an autonomous underwater vehicle (AUV) as the platform to collect seafloor images, geoacoustic data, and water quality data in the Mid-Atlantic region. AUVs have been previously shown to be useful in marine habitat mapping (Raineault *et al.*, 2011; Seiller *et al.*, 2012). Whereas dredging has been shown to only have an efficiency of 0.3 to 0.6 for sea scallops, this study aims to use a photographic analysis method that has an efficiency that approaches 1 (NMFS, 2010). It will also be shown that the AUV platform can noninvasively sample a greater area in a shorter amount of time than the current dredging method. This refined method will give a more accurate estimate of the scallop population density and whole stock abundance in the Mid-Atlantic region so that the fisheries can give more precise landing restrictions that maximize economical benefit, while ensuring the stock does not become overfished.

The primary research objectives of this study are:

1. To quantify the varying sea scallop densities across the different survey stratum of the Mid-Atlantic Bight.
2. To estimate the biomass of the sea scallop population within the study area.
3. To quantify the spatial distribution and patchiness of the sea scallop population within the Mid-Atlantic Bight.

4. To correlate distribution of sea scallops to bedform morphology, sediment type, and environmental conditions.
5. To quantify dredge efficiencies for the 15 ft (4.572 m) New Bedford commercial dredge.
6. Calculate the necessary image subset sample size necessary to accurately estimate varying scallop densities.

1.2 Mid-Atlantic Bight Sea Scallop Fishery

To understand the need for improved sea scallop stock assessment techniques, it is important to examine the history of the fishery as a whole, and the regulations that had to be enacted in order to protect the fishery from collapse.

1.2.1 History of the Fishery

The sea scallop northwest Atlantic fishery extends from Cape Hatteras, North Carolina to the Gulf of the St. Lawerence. In the United States, the sea scallop fishery has been commercially active for over 100 years, and as of 2011 it is the third most valuable domestic U.S. fishery at a value of $587 million (Figure 1.1). The fishery was first commercially harvested in the 1880s when scallop grounds were discovered off the coast of Maine (Schick and Feindel, 2005). Maine remained the center of the United States scallop harvesting until the 1920s when economically viable grounds were discovered off Long Island, New York. In the 1930s, production shifted for the final time to ports in Massachusetts with the discovery of the Georges Bank scallop grounds (Naidu and Robert, 2006).

Since the 1930s, the majority of U.S. sea scallop production has been split between Georges Bank and the Mid-Atlantic Bight grounds. The Georges Bank

scallop beds are the largest single scallop resource in the world (Caddy, 1989). The unusually dense scallop beds can be explained by the presence of a summer counterclockwise gyre that forms. The gyre has the effect of trapping planktonic scallop larvae within the region until the time that they undergo metamorphosis and settle on the seafloor (Larsen and Lee, 1978). The Georges Bank fishery saw heavy harvesting in the 1970s from both the United States and Canada (Table 1.1). As a result, measures needed to be taken in order to prevent overfishing and to protect the sustainability of the fishery. The protective measures put in place were in response to the passing of the Magnuson-Stevens Fisheries and Conservation Act.

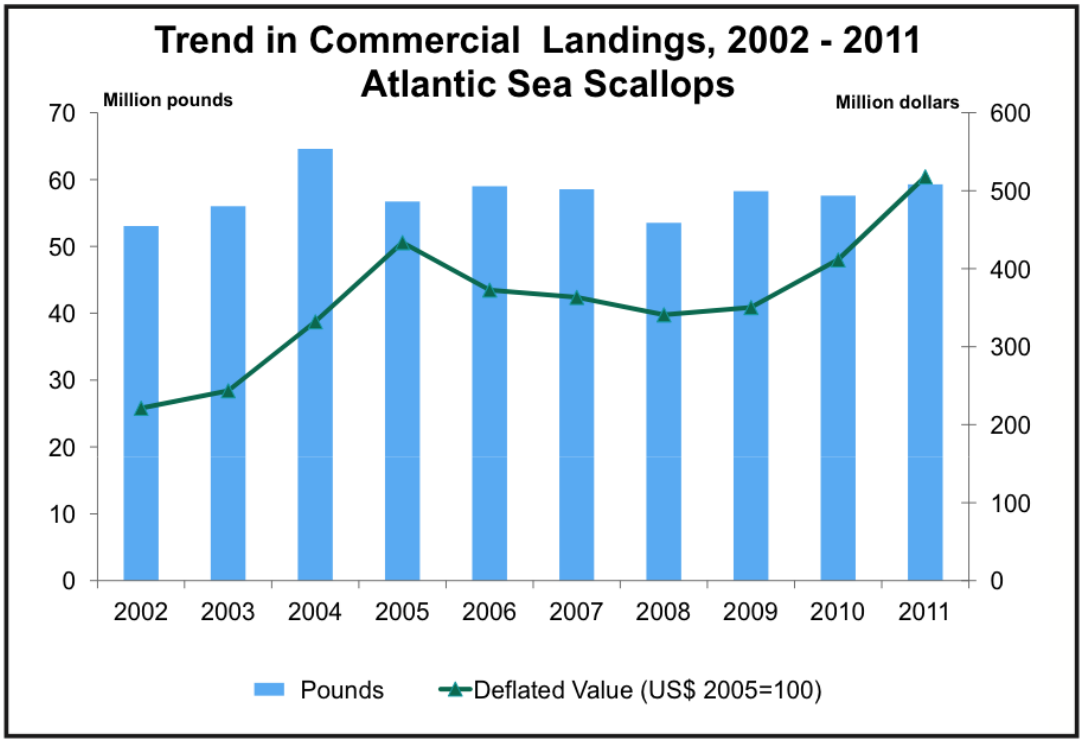

Figure 1.1: U.S.A landings of the Atlantic Sea Scallop for the years 2002 – 2011. The year 2011 saw a record 7-year high of over $500 million in sea scallop landings. From *Fisheries of the United States* (2012).

Year	USA (metric tons)	Canada (metric tons)	Total (metric tons)
1978	**120,209**	**109,402**	**238,534**
1979	**118,325**	**89,491**	**222,623**
1980	**104,298**	**70,475**	**201,757**
1981	97,459	89,897	172,524
1982	75,065	65,097	147,391
1983	72,326	51,286	136,560
1984	64,234	36,470	120,359
1985	56,125	47,210	128,011
1986	71,886	57,063	181,670
1987	**109,784**	**73,903**	**219,327**
1988	**109,543**	**77,854**	**233,827**
1989	**124,284**	**92,188**	**269,625**
1990	**145,341**	**83,278**	**288,159**
1991	**142,818**	**79,538**	**260,736**
1992	117,918	92,163	178,458
1993	60,540	90,749	124,359
1994	63,819	91,626	129,439
1995	65,620	68,670	131,157
1996	65,537	59,987	117,039
1997	51,502	66,023	97,160
1998	45,658	63,030	45,658

Table 1.1: Cumulative sea scallop landings for the United States and Canada 1978-1998. Years of heavy fishing are boldfaced. Adapted from Naidu and Robert (2006).

1.2.1 Magnuson-Stevens Act

The overfishing of the sea scallop in the United States was not an isolated incident. Other U.S. fisheries were struggling to maintain sustainability as a result of unchecked industrialization. Other species affected in addition to the sea scallop included the summer flounder, groundfish, cod, sablefish, monkfish, vermillion snapper, North Atlantic swordfish, and other economic fish stocks (Roughgarden and Smith, 1996). In response to collapsing fisheries and a slew of other environmental issues, the Environmental Protection Agency (EPA) and National Oceanic and Atmospheric Administration (NOAA) were founded. One of the mandates of these newfound organizations was the enforcement of environmental protection legislation, including the eventual Magnuson-Stevens Act.

The Magnuson-Stevens Act was signed on April 13, 1976. One of the major points of the act was the extension of the U.S. exclusive economic zone (EEZ) from 3 nautical miles to 200 nautical miles off of the coasts. Without this mandate, other nations could continue to harvest from U.S. fisheries without regulation, which would jeopardize any future efforts at conservation. The United Nations (UN) would later adopt the 200 nautical miles definition of EEZ for all nations in the 1982 UN Law of the Sea. Other regulations in the Manguson-Stevens Act included regulations on yearly catch limits and the creation of a fishery management council system. The regulations put in place were adequate for a period, but eventually the act had to undergo numerous reauthorizations (namely in 1996) as domestic fishing infrastructure rapidly progressed to the point that overfishing was once again occurring (Naidu and Robert, 2006).

1.2.2 Overfishing in the 1990s

In 1982, following the Magnuson-Stevens Act, the Sea Scallop Fishery Management Plan (FMN) was implemented for the specific regulation of the U.S. northwest Atlantic sea scallop fishery. The plan contained regulation strategies that included days-at-sea allocations, gear restrictions that aimed to prevent the capture of recruit-sized scallops, and vessel crew restrictions. The regulations proved to be ineffective overtime as the catch limits were set too high (Naidu and Robert, 2006).

The late 1980s and early 1990s saw a boom in sea scallop landings comparable to the overfishing of the 1970s (Table 1.1). The landings were deemed to be unsustainable, and as a result, amendments were made to the FMN to better protect the fishery. New regulations included stricter catch limits and the closing of the Georges Bank area. Considerations for bycatch (the unintended landing of other marine organisms in the scallop dredge) of other regulated marine species (notably the yellowtail flounder) were also included. In 2003, the official adoption of Amendment 10 to the FMN resulted in an area-based management strategy. Areas within the fishery would be rotationally closed for periods of months to years to allow the sea scallop population to rebound.

The threatening of the sea scallop fishery during the early 1990s is a good example of how regulations can be ineffective if the parameters of fishery sustainability are not fully understood. The catch limits of the 1980s were set too high, and as a result the fishery was overfished (Naidu and Robert, 2006). Conversely, catch limits that are set too conservatively would lead to unnecessary economic losses that could have negative effects on the industry. Every year, NMFS performs stock assessments to monitor the fishery areas and to set catch limits for the following year. The catch limits strive to maximize economic output, while

maintaining the sustainability of the fishery and the minimization of bycatch. Thus, it is important that stock assessment methods continually improve and incorporate new technologies that lead to more accurate assessments. The use of a near-bed AUV based image survey in this study allows for the evaluation of the currently used dredging and image survey methods.

1.3 The Sea Scallop

1.3.1 Origin of the Scallop

The scallop family (Pectinidae) is classified within the order Osteroida, the class Bivalvia, and the phylum Mollusca. The Pectinidae split from the Aviculopectinoidea family during the Middle Triassic when the first scallops evolved (Hautmann, 2010). One of the key family defining characteristics of the Pectinidae family is the presence of a ctenolium. The ctenolium of a scallop is a row of denticles that are found on the ventral edge of the byssal notch. The ctenolium is used to spread byssal threads, which increases the attachment strength of the byssus.

1.3.2 Morphology and Habitat

Scallops are sessile epifaunal organisms found in all of the world's oceans. Scallops are easily identified, as they possess the classical bivalve structure of two hinged valves with a distinctive sculpturing consisting of radial ridges on the shell. The scallop family Pectinidae is named from the latin root *Pecten*, which means "comb". The comb structure of longitudinal ridges running along the outside of the shell is a famous feature of scallop shells. The ridges on the sea scallop's shell are relatively subdued compared to most other scallop species. The upper left cuspate

valve of the sea scallop is light to dark orange in color. The right valve of the sea scallop sits in contact with the seafloor and is flatter and lighter in color than the left valve (Naidu and Robert, 2006). The concentric rings that radiate from the hinge of the shell are annual growth rings (Stevenson and Dickie, 1954). The shape of the sea scallop shell is circular with the exception of two symmetric triangular shaped auricles near the hinge. The size of the scallop shell, or shell height, is measured by taking the taking the dorsal-ventral tangential length that bisects the hinge (Naidu and Robert, 2006). Sea scallops can typically have shell heights over 200 millimeters (mm), and have been known to live for almost 30 years (Naidu and Robert, 2006).

The valves are held together by a singular adductor muscle, which is attached to the interior of each shell. The adductor muscle is the reason scallops are harvested around the world for the food industry. The adductor muscle is used for defense, swimming, and eating. Contracting the adductor muscle will cause the valves to be pulled together. This can be a defensive reflex if the scallop detects a predator nearby, either at a distance from the use of chemoreceptors or at proximity from the scallop's light detecting eyes (Barbeau and Scheibling, 1994). The sea scallop can also sharply contract and relax the adductor muscle in a clapping motion, combined with jetting water from the mantle to swim. The scallop cannot sharply contract its shell more than a few times before it must rest (Brand, 2006). Relaxing the adductor muscle allows the shell to open so that the scallop can feed.

The scallop filters phytoplankton out of the water column in order to feed (Cranford and Grant, 1990). Suspension feeding in the scallop is done by the assistance of cilia. Cilia of the folded gill waves water past a second set of cilia, which act as a trap for food particles. The food becomes stuck in mucus and is

transported to an anteroposterior groove, where it continues towards the mouth. Larger particles are able to fall out before reaching the mouth via labial palps, while smaller particles are eaten. Digestion is aided by enzymes within the stomach.

Scallops prefer sandy to gravely seafloor to bottoms of finer grain size (Kostylev *et al.*, 2001). Silt can be detrimental to the scallop as it can clog the gills, impeding filtration (Crandford and Gordon, 1992). Gravel, shell hash, and other coarse features are popular settling grounds for spat as hard surfaces offer protection and a firm surface for byssal attachment. Gravel can be advantageous to adult scallops, as it can offer protection from predators such as crabs (Barbeau and Scheibling, 1994).

Besides bed type and potential lethal amounts of silt in the water column, the other habitat controls for sea scallops are water temperature, salinity, predators, food availability, and depth (Naidu and Robert, 2006). Scallops generally inhabit fully saline water (greater than 30 ppt) (Naidu and Robert, 2006). Depth is considered a major factor in sea scallop distribution, but it is likely a direct result of water temperature. The sea scallop is generally found at depths between 18-110 m, but has been observed at depths of 384 m (Merrill, 1959). Each scallop species is known to inhabit a particular spectrum of temperatures, and will die if it is exposed to temperatures out of that range for an extended period of time (mostly due to lethargy that makes them susceptible to predators).

Figure 1.2: Specimens of *Placopecten magellanicus* dredged from the seafloor by the F/V Christian and Alexa. Note the symmetric circular shape and orange color.

1.4 Mid-Atlantic Bight Geologic Background

1.4.1 The Coastline

The Mid-Atlantic Bight is an embayed coastline that is the product of post-Pleistocene sea level rise. There are two major estuaries, Delaware Bay and Chesapeake Bay, which are responsible for transporting a combined 4,680 metric tonnes of sediment per year onto the Atlantic shelf (Gibbs, 1981). Some of the river sediment discharge will continue to travel along the relict path of the river and be deposited on the shelf's edge, while the rest of the sediment will be transported along the coast due to tidal and wave forces.

River estuaries are not the only evidence that the Mid-Atlantic Bight is a drowned coastline. In-situ peat horizons that extend to the shoreface indicate that the shoreline is transgressing. The peat is the result of rapid burial of decaying marsh flora, such as smooth cord grass, S*partina alterniflora*, and other marsh grasses, by marsh silts and clays behind a barrier beach (Kraft, 1971). As the shoreface transgresses, the dune complex of the beach and the back barrier marsh moves landward. Eventually the dunes move horizontally over the peat layer, where wave forces at the shoreline will expose it.

The southern portion of the transgressing Mid-Atlantic Coast is moving over generally Pleistocene age deposits, while areas to the northeast of Long Island are atop Triassic age bedrock (Figure 1.3). Sediment is deposited along the coast in barrier structures including barrier islands, barrier spits, barrier beaches, and in tidal marshes. Over 500km of Mid-Atlantic Coast is either a barrier island or spit (USACE, 2002). Tidal inlets sparsely cut the extensive barrier systems. Barrier structures protect the coast from the destructive wave energy of storms. Larger storms, such as nor'easters,

can cause major reworking of barrier sand. Overwash deposits can occur over beach dunes or on the landward side of barrier islands. Inlets can be greatly widened, or entirely new inlets can be formed at weak points in the barrier. Paleochannels can often be observed in ground-penetrating radar (GPR) on land and sub-bottom profiles near or under barrier islands, showing that tidal inlet migration is a relatively common occurrence (Nebel *et al.*, 2012).

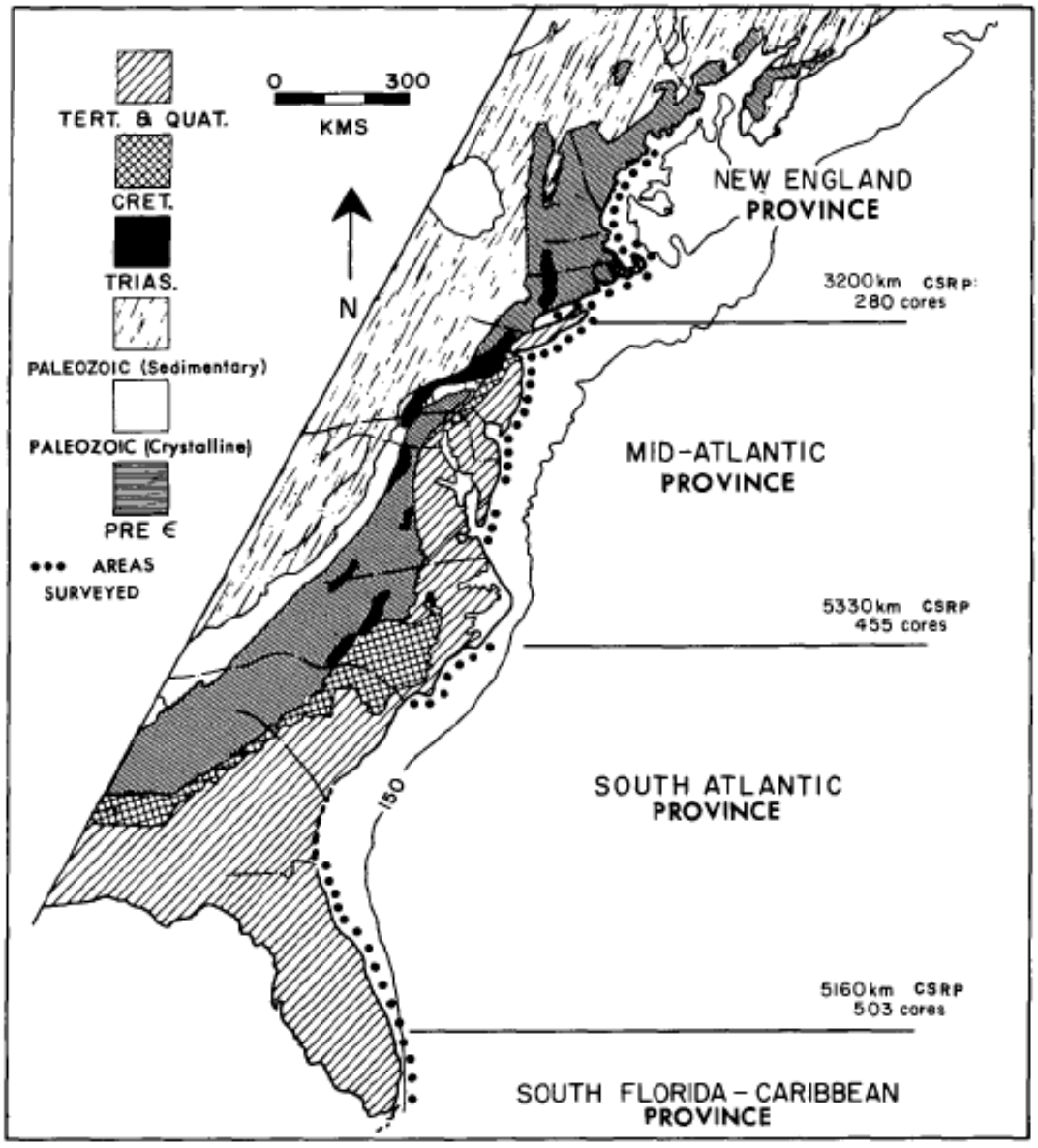

Figure 1.3: The general coastal geology of the Mid-Atlantic Bight and other providences as interpreted from vibratory cores and acoustic data from Field and Duane (1976).

1.4.2 Shelf Seafloor

The Mid-Atlantic shelf at its southern edge extends 60 km from Roanoke Island, Virginia seaward. The shelf generally widens northward, and is almost 200 km wide directly south of Cape Cod, Massachusetts. The major rivers have valleys that cut across the shelf and terminate at the shelf edge, representing Pleistocene river drainage paths (Schlee, 1973). The shelf near the coast is composed of ridge and swale topography that trends generally shore parallel or more easterly (Figure 1.4). The ridges are likely the result of storm currents or the reworking of tidal deposits during transgression, and are probably only mobilized during storm events (Swift, 1973; McBride and Moslow 1991). Nearshore topography starting at Long Island and heading eastward is composed of offshore glacial moraine deposits.

The seafloor of the Mid-Atlantic continental shelf is blanketed by a layer of fine to medium quartzose sand (Schlee, 1973). The presence of the moraines from Long Island to Massachusetts results in a gravelly seafloor near the coast in those regions. The sediment across the shelf may be reworked depending on local depth, storm, and current activity. Sorted bedforms (Figure 1.5) are a common feature that occur on the shelf and are the result of reworking coarse material into rippled beds (Goff *et al*., 2005; McNinch, 2004). The rippled pattern of the coarse sediment causes an increase in turbulence in near bottom currents, which inhibits the deposition of fine sediment. Once the water current is over a flatter terrain (finer sediment), the turbulence dissipates and the finer sediment is allowed to deposit. If the coarse sediment is ultimately buried under fine sediments due to a prolonged period of low shear stress near the bed, during the next major storm event that has waves with a high enough periodicity to interact with the seafloor, the fine sediment will be entrained,

and the coarse material will be re-exposed and mobilized into ripples (Trembanis and Hume, 2011).

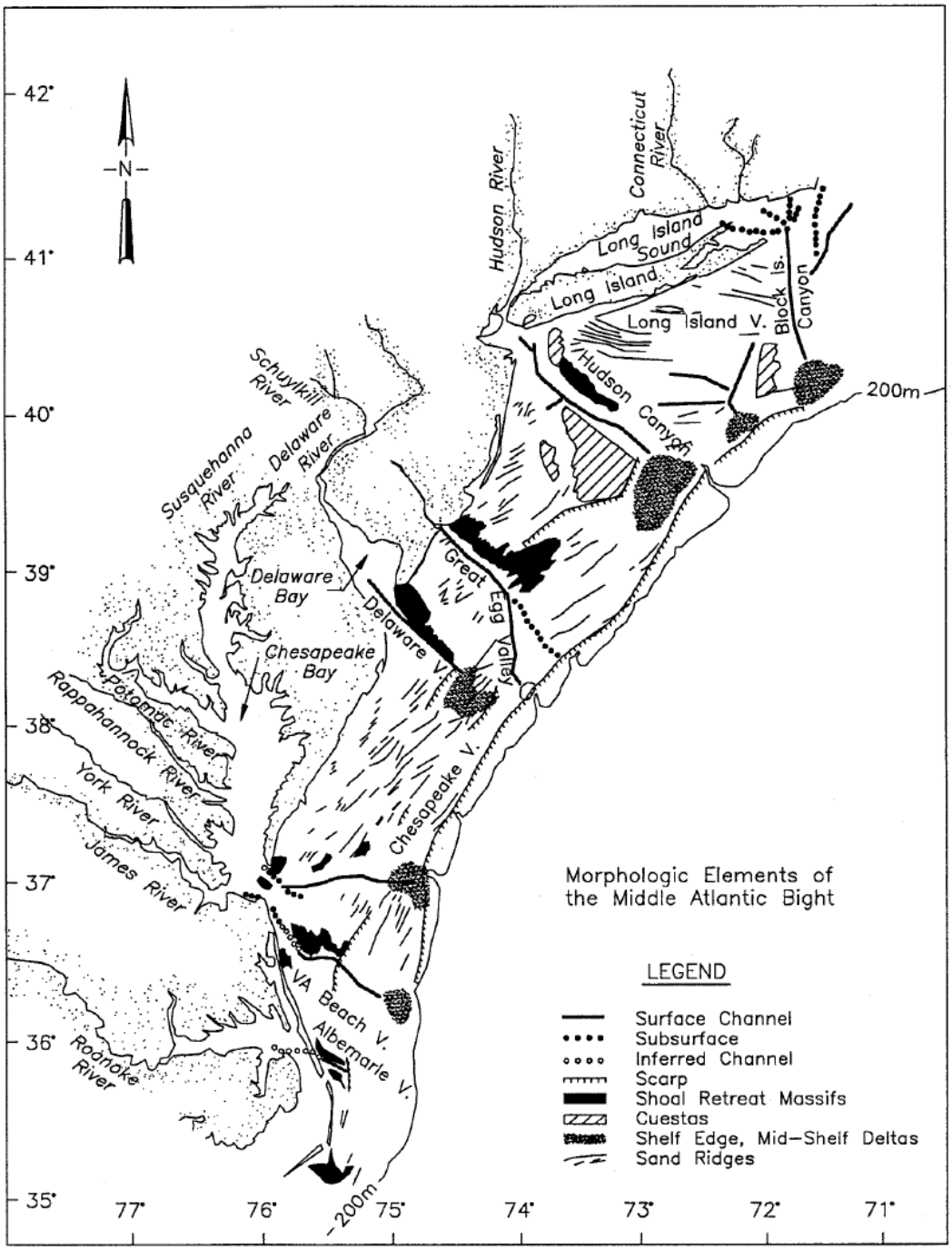

Figure 1.4: The depositional geomorphology of the Mid-Atlantic Bight. From Swift (1976).

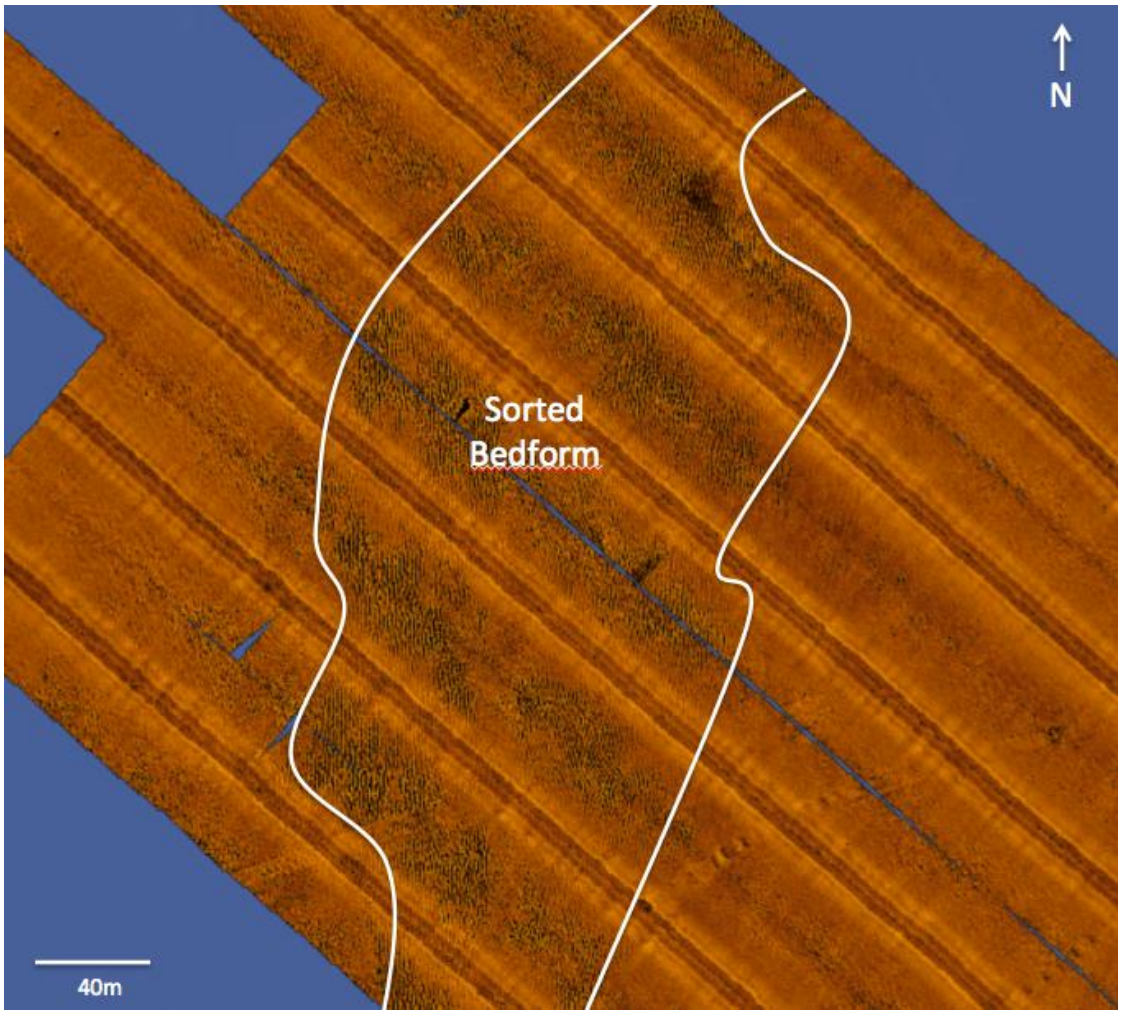

Figure 1.5: Side-scan sonar (900 kHz) image of a sorted bedform on the seafloor of the Mid-Atlantic Bight. Bright areas illustrate high backscatter. The white boundary highlights the sharp contact between rippled and flat bed.

1.4.3 Regional Geologic Framework

The history of the Mid-Atlantic Bight begins with the rifting of Pangea during the Middle Jurassic. The rifting of continental crust between Gondwana and Laurasia resulted in the formation of the Atlantic Ocean. As mafic magma continually upwelled at spreading centers, new seafloor was created that widened the Atlantic Basin and continued to further separate the rifting continental crust (Schettino and Turco, 2009).

The Mid-Atlantic Bight is a passive continental margin. The shelf of the Mid-Atlantic Bight resides atop a planform oval shaped 13 km thick sedimentary wedge known as the Baltimore Canyon trough (BCT) (Trehu *et al.*, 1989). The BCT is approximately bounded to the south by the Norfolk fault zone and to the northeast by the Long Island fault zone (Figure 1.6). Both fault zones are similar to transform faults that form perpendicular to seafloor spreading centers. The eastern (seaward) edge of the BCT is the East Coast Magnetic Anomaly (ECMA), which coincides in this region with the East Coast Boundary Fault. The western extent of the BCT is the basement hinge zone, where seaward dipping basement rock steepens as a result of Triassic subsidence between the coastal plain and the trough (Harry and Sawyer, 1992). The hinge zone occurs approximately 30 km seaward of Delaware Bay at a depth of 5000 m. The hinge zone moves farther offshore northward where it is ultimately 65 km off of Long Island.

The stratigraphy of the BCT rests on a basement of rifted crust on the west and ocean crust to the east (see Figure 1.7). The trough is composed of sediments that have been deposited since the Jurassic. The Jurassic layer of sediment thickens from the shore, reaches maximum thickness below the ECMA, and then begins to thin seaward. Within the Jurassic sedimentary layer is a carbonate facies that is up to 5 km

thick. The eastern extent of the carbonate strata (150 km off the modern coast) represents the Jurassic paleoshelf (Trehu *et al.,* 1989). The geology under the carbonate layer is not well understood as seismic waves are unable to penetrate deeply below the layer. A 2 - 3 km Cretaceous sedimentary layer caps the Jurassic layer. Lastly, a Tertiary sedimentary layer extends from the Cretaceous layer to the seafloor. The crust/mantle boundary (Moho) is believed to be at a depth of 35 km below the coastline and shallows seaward

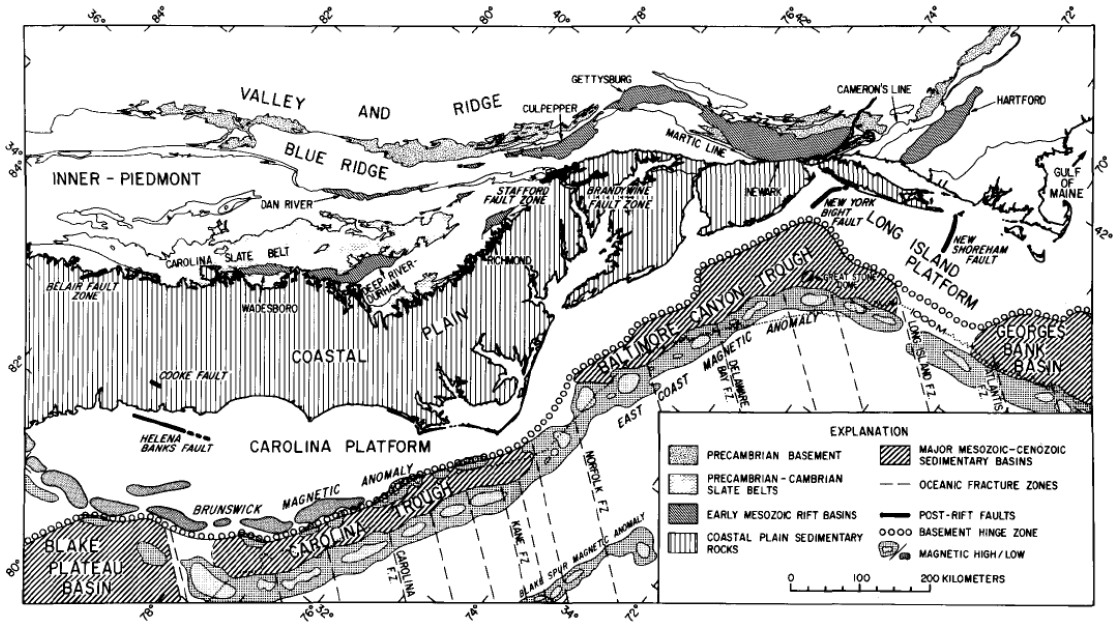

Figure 1.6: The geologic framework of the Mid-Atlantic Bight and surrounding areas. The majority of the Mid-Atlantic Bight resides atop the Baltimore Canyon Trough. From Hutchinson and Grow (1985).

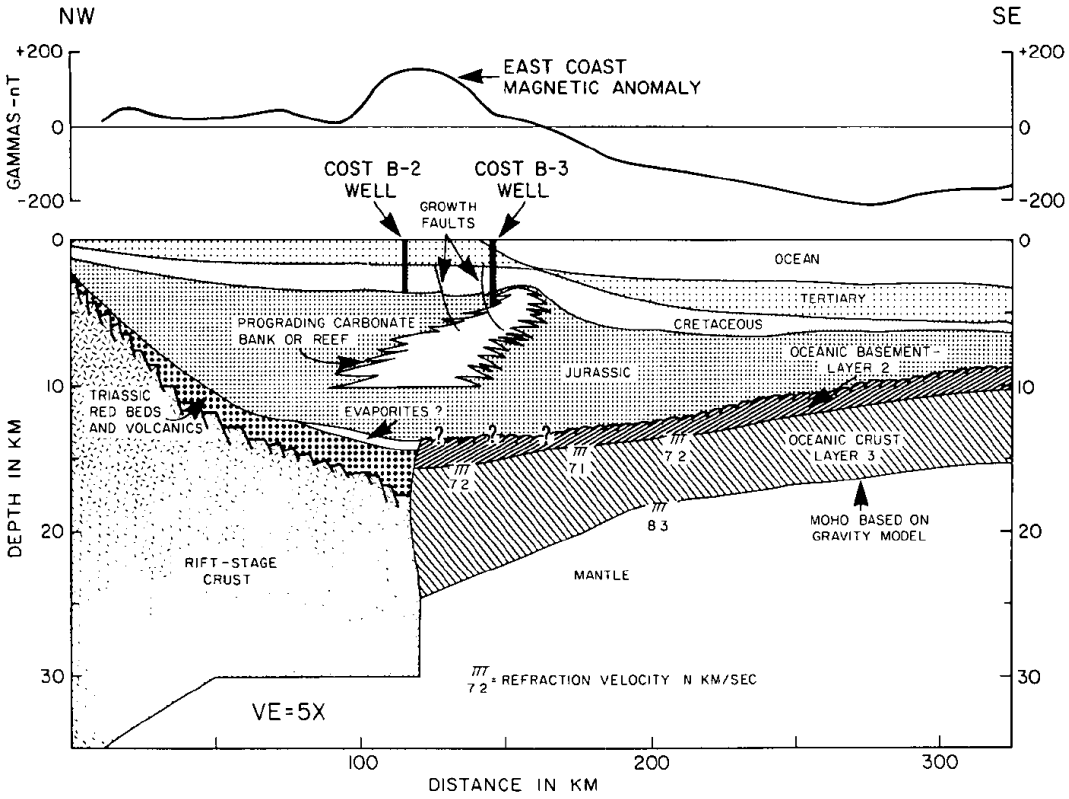

Figure 1.7: Interpretation of the Baltimore Canyon trough from seismic stratigraphy, Continental Off-shore Stratigraphic Test (COST) wells B-2 and B-3, and gravity models. From Sawyer *et al.* (1982).

Chapter 2

DEVELOPMENT AND IMPLEMENTATION OF AN AUV BASED SEA SCALLOP IMAGE SURVEY

2.1 Introduction

Each year, the sea scallop stock within the Mid-Atlantic Bight is evaluated utilizing a combination of dredge and image survey methods. The results of these stock assessments are used to monitor the scallop population and to set annual catch limits (NMFS, 2010). A better fundamental understanding of the spatial structure and distribution of the sea scallop is needed to improve the accuracy of stock surveys.

Sea scallops inhabit the Mid-Atlantic Bight fisheries in kilometer size groups known as beds (Hart, 2004). The scallop beds are heterogeneously distributed, making it difficult to accurately quantify the scallop population in each bed. They are distributed in meter to tens of meter scale groups known as patches. These patches have never been quantified; likely due to sampling limitations of current dredge surveys (Brand, 2006). Dredge surveys average a scallop population over the entire area that is dredged, integrating any small-scale spatial structure. The inadequacies of dredge surveys have led to the recent innovation of digital image surveys.

Digital image surveys have been shown to be a valid method for habitat mapping (Forrest *et al*., 2012; Seiler *et al.,* 2012). Since 2003, it has been shown that image sampling techniques can not only be used to estimate sea scallop populations, but can also be used to study sea scallop spatial distribution (Stokesbury *et al.*, 2004). The first system devised to visually measure scallop abundances and sizes on the

seafloor was a stationary pyramid platform consisting of video cameras that was lowered from a vessel to the seafloor (Stokesbury, 2002). Each deployment of the platform results in a 3.2 m^2 image of the seafloor, and because it is lowered through the water column it cannot be precisely aimed to a location on the seafloor. Due to the small area photographed for each sample and the imprecise deployment method, it is cumbersome and inefficient for precision area studies. A more recent system developed called HabCam uses a towed camera sled tethered to a ship to gather images of scallops on the seafloor (Rosenkranz *et al.*, 2008). While HabCam can photograph scallops in their natural habitat, the system is towed from the surface making it susceptible to oscillations by waves.

The use of geostatistics as a tool for studying ecological distributions has been shown previously for a wide-range of marine organisms (Bulit *et al.*, 2003). Previous studies have used geostatistics to quantify sea scallop grounds and beds in the Mid-Atlantic Bight (Adams *et al.*, 2010). Adams showed using variograms that scallop beds ranged in diameter from 3 to 25 km in the Mid-Atlantic Bight and adjacent Georges Bank area. My study uses a sampling design that allows the spatial structure of scallop patches to be quantified.

Current stock assessments of *P. magellanicus* within the Mid-Atlantic Bight use regular grids ranging in size from 1.5 to 5.0 km (NMFS, 2010). The distance of autocorrelation of an organism being studied has major implications for how surveys must be designed in order to accurately estimate the population. This study employed the use of an AUV to take continuous images of the seafloor at a constant 2 m height above the seafloor. The AUV is able to operate below the depth of surface wave interaction in sufficiently deep water, and is able to precisely follow predefined

mission paths, which is crucial for studying small scale spatial spreading. The findings of this study are that the sea scallop has an autocorrelation length of at least 300 m when spatial structuring is present.

2.2 Study Area

The Mid-Atlantic Bight is the shallow portion of the continental shelf that extends from Cape Hatteras, NC to Cape Cod, MA. The area was chosen by the needs of the Mid-Atlantic Council's Research Set-Aside (RSA) program to survey inshore heavily fished grounds. Mission sites were subsampled from pre-existing NMFS scallop stock assessment sites (half of the missions), and were all within 70 km of the coast of Delaware, New Jersey, or New York. The water depths sampled ranged from 20-55 m, which are often cited as the normal habitable zone for the sea scallop. The sites that were surveyed in the summer of 2011 are shown in Figure 2.1 and Table 2.1.

2.3 Methods

2.3.1 Autonomous Underwater Vehicle

The 2011 scallop survey was conducted with the use of the Coastal Sediments, Hydrodynamics, and Engineering Lab's (CSHEL) autonomous underwater vehicle (AUV) DORA. DORA is a Teledyne-Gavia class AUV that has an operational depth limit of 500 m, which exceeds the depths of the Mid-Atlantic Bight. An AUV is unique compared to other underwater research robots in that it is unmanned and untethered.

The AUV is designed around a compartmentalized modular platform, meaning that the instrument load of the AUV can be changed depending on the needs of the

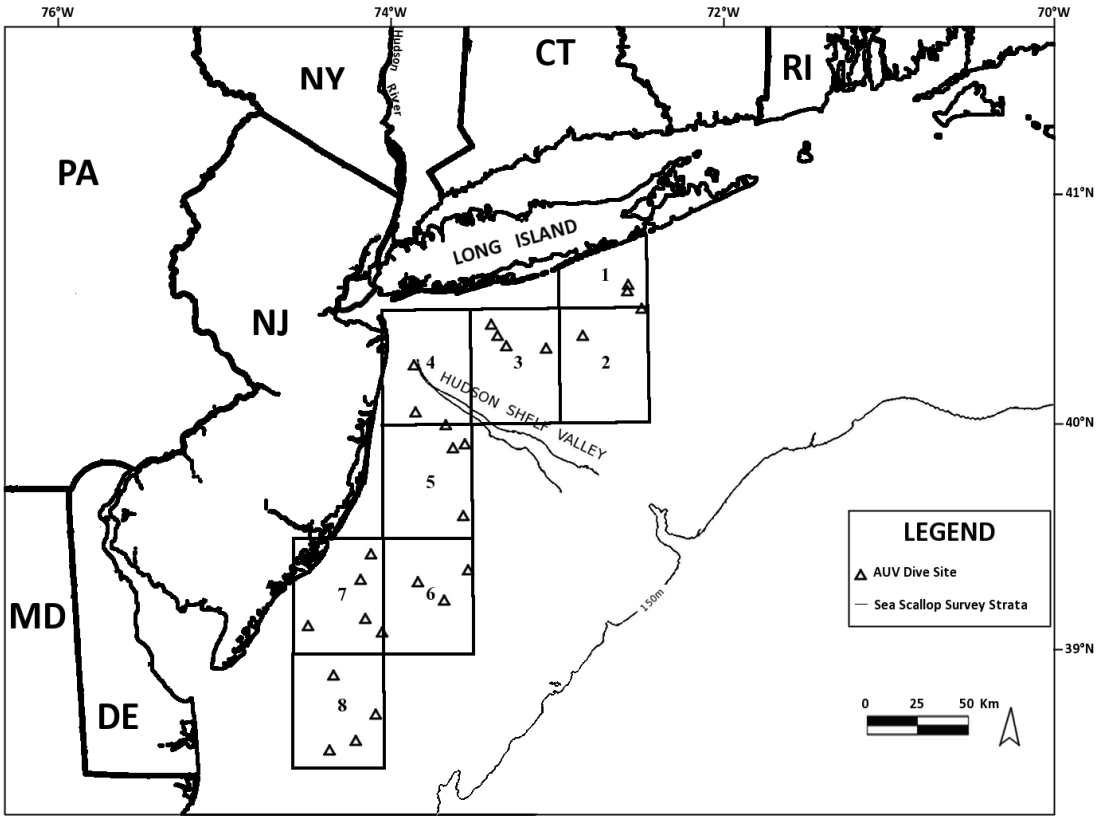

Figure 2.1: The eight survey substrata chosen for the 2011 scallop image surveys. The eight strata fall within the colored NMFS sea scallop survey strata.

Mission Names	Date	Mission Length (Km)	Images	Depth (m)	Lat Start	Lon Start
110708_Scallop_DvoraRun	7/8/11	10.34	8066	43	40.5503	-72.5872
110708_ScallopD2	7/8/11	15.904	12775	41	40.5529	-72.5899
110708_ScallopD2_M4	7/8/11	3.015	2388	41	40.5503	-72.5872
110709_Scallop_D3_M1_Corey	7/9/11	12.28	9993	44	40.3449	-72.8817
110708_SM2	7/8/11	3.199	2688	41	40.5502	-72.625
110709_ScallopDay3_DV119	7/9/11	10.773	8339	40	40.3111	-73.0825
110710_DV117	7/10/11	14.211	11330	30	40.3961	-73.3818
110710_DV118	7/10/11	12.271	10164	32	40.3551	-73.3483
110710_M1_ArtiesRun	7/10/11	12.154	9781	33	40.3213	-73.2749
110711_DV115	7/11/11	10.398	9142	33	40.2249	-73.7828
20110726_ScallopD1_M1	7/26/11	12.713	10475	45	38.5600	-74.3177
110726_ScallopD1_DV44_M3	7/26/11	15.913	12036	47	38.7372	-74.0551
110727_D2_R2_M2	7/27/11	11.791	9171	20	39.0907	-74.447
110727_D2_R3_M3	7/27/11	13.499	10392	36	39.1432	-74.0397
110727_D2_R4_M4	7/27/11	12.207	7346	37	39.1432	-74.0397
110727_D2_R5_M5	7/27/11	8.292	6286	24	39.4200	-74.0267
110727_ScallopD2_R1_M1	7/27/11	12.127	11098	39	38.9049	-74.3271
110728_D3_DV062_M3	7/28/11	12.196	12069	45	39.2178	-73.6423
110728_D3_DV063_M4	7/28/11	12.149	9528	49	39.3477	-73.5099
110728_D3_R6_M1	7/28/11	13.086	10951	38	39.3536	-73.7925
110728_D3_R7_M2	7/28/11	12.331	9438	40	39.1226	-73.984
110728_D3_R8_M5	7/28/11	11.691	9545	39	39.6209	-73.5386
110729_D4_DV0105_M2	7/29/11	12.181	9075	31	39.8959	-73.6105
110729_D4_DV0106_M1	7/29/11	11.752	9426	35	39.8963	-73.5318
110729_D4_DV0112_M3	7/29/11	12.133	9282	36	39.9783	-73.6383
110729_D4_DV0113_M4	7/29/11	12.511	9524	26	40.0173	-73.8078
110726_ScallopD1_DV2_M2	7/26/11	11.699	9256	52	38.6021	-74.1828
Summary		**312.81**	**249564**			

Table 2.1: AUV Mission Summary Table

particular mission. For the scallop surveys, the AUV was configured for imaging and mapping (Figure 2.2) with the following modules: nose cone, battery module, Geoswath phase measuring bathymetric sonar module, inertial navigation system / Doppler velocity log (INS/DVL) module, command module, and the propulsion module. Some of the modules and systems will be explained in greater detail in the following sections. Once deployed, the AUV executes a predefined mission that includes navigation and scientific instrument instructions. During a mission, the AUV can simultaneously take digital images of the seafloor, acoustically map the seafloor, and record environmental conditions of the seawater (salinity, temperature, dissolved oxygen, turbidity).

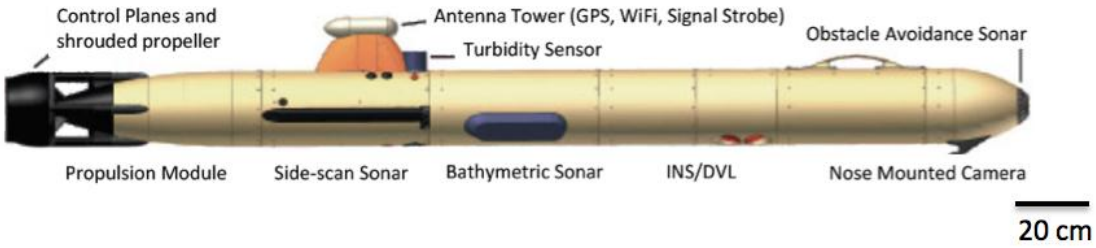

Figure 2.2: The AUV was configured for seafloor imaging and mapping. In addition to the 250,000 seafloor images that were collected, the AUV also gathered data about water temperature, salinity, dissolved oxygen, bathymetry (500kHz phase differencing bathymetric sonar), and seafloor features (900 kHz side-scan sonar). The AUV can operate at depths of 500m, and can operate for 3 hours before the batteries need to be recharged.

2.3.1.1 The AUV Camera

The AUV nose cone module contains a hull mounted Point Grey Scorpion 20SO research camera (Table 2.2). The Point Grey is an ideal camera for the AUV because it has low power consumption (<3.5 W), is small (5 cm x 5 cm x 4 cm) and is designed to work in low light conditions, such as those found at depths within the ocean. The camera is housed directly in the nose cone module, and the lens of the camera is protected by a secondary viewport lens in the nose cone. The AUV camera is 2.11 mega pixels with a maximum resolution capability of 1600 x 1200 and a horizontal field of view of 49.92° (in water). The camera is focused to take images at a distance of 2 m. When taking photographs underwater, it is important to remember that light entering the lens of the camera is changing mediums from water to air; therefore, there will be refraction of the light as it enters the camera. As such, it is imperative that the field of view of the camera be calculated underwater rather than in air.

The image sensor within the camera is a Sony charged coupled device (CCD). The CCD is a silicon chip that functions similar to analogue film. The chip has electron wells at the site of each pixel. Each well builds a charge as photons collide with it. The CCD is sensitive enough that 90% of photons colliding with it produce a useable charge. The digital analogue converter (A/D) then converts the voltages of each pixel. A gain setting can be applied to amplify the voltage of each photon. Lastly, an 8-bit value is assigned to each pixel. The A/D is capable of assigning a 12-bit value, but the camera images are saved as jpegs, and jpegs are an 8-bit format.

The shutter of the camera is digitally controlled by the camera.xml configuration file in the Linux PC104 computer housed in the nose cone. For these

Point Grey Scorpion 20SO Research Camera	
Mega Pixels	2.11 (2.01 effective)
Sensor Resolution	1600x1200 (800x600 actual image settting)
Image Sensor	8.923mm (diagonally) Sony CCD
Shutter Speed	0.03ms – 533ms
Dimensions	50mm x 50mm x 40mm
Operational Temperature	0 – 45 degrees Celsius
Power Consumption	< 3.5W
Mass	125 grams
Analogue to Digital Converter	12-bit A/D
Horizontal Viewing Angle	49.92 degrees (underwater)
Memory	Computer in the nose cone of AUV

Table 2.2: Point Grey Scorpion 20SO AUV research camera specification.

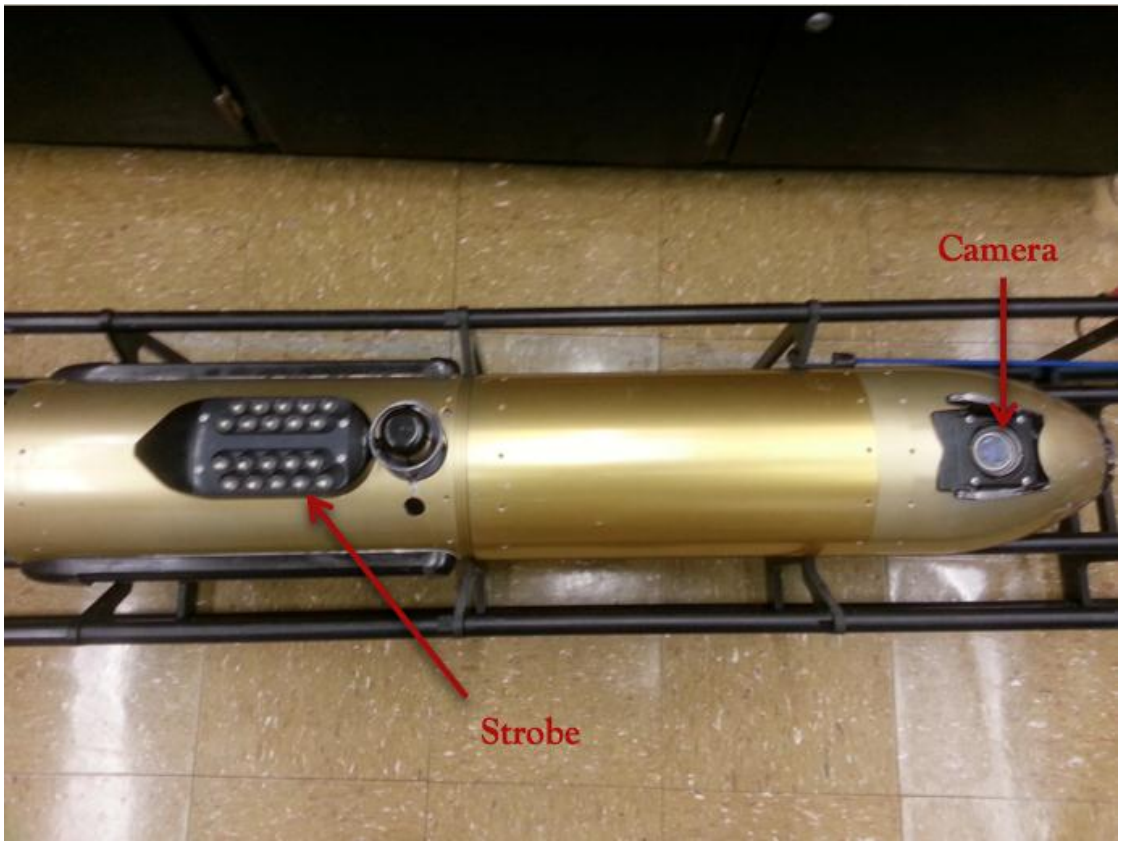

Figure 2.3: The hull mounted AUV camera on the nose cone, and the hull mounted LED strobe system on the command module.

image surveys, the shutter and exposure speeds of the camera were configured to "auto". Because the AUV camera uses a CCD, the shutter operates differently than a typical film camera. The shutter is the amount of time that the CCD is allowed to gather photons before pixel voltages are quantified and reset.

The strobe for the camera is an LED array mounted to the hull of the control module. The strobe is offset from the camera to prevent over-saturating the pixels of the camera. Also, the angle between the strobe and the camera limits the reflection of light off of suspended particles. There are numerous settings for the strobe, but for these surveys the strobe was configured to flash for every image taken.

2.3.1.2 Navigation System

The AUV relies on a suite of instrumentation in order to navigate and to resolve its current position. When the AUV is on the deck of a ship or the surface of the water, the differential GPS receiver in the command module resolves the AUVs position via a GPS fix. Once the AUV dives below the surface of the water, it will no longer be able to receive GPS updates, so it must use other instrumentation to resolve its positioning.

The INS/DVL module is critical in the navigation of the AUV. The INS is a Kearfott KN-5053 T24 MRLG (Monolithic Ring Laser Gyros) Seaborne Navigation System. The INS is a mechanical system of accelerometers and gyros that are able to detect motion in relation to reference frames that include magnetic north and the center of the earth. The INS receives inputs from the GPS, DVL (1200 kHz Teledyne), and the pressure sensor. The error of the INS is 0.1% of distance traveled.

The DVL is able to acoustically measure velocity in relation to the seafloor when it has "bottomlock" (within 35 m of the seafloor) or the water current velocity below the vehicle when it cannot resolve the seafloor. The pressure sensor is in the command module, and it is able to determine the water depth of the AUV. The INS is able to take inputs from these instruments in order to determine positioning, heading, pitch, roll, depth, and the altitude of the AUV. A command altitude above the seafloor can be set for the AUV to adhere to because of the precise dynamic positioning of the AUV. Figure 2.4 shows the ability of the AUV to fly at a preset altitude. The scallop missions were all performed at a command altitude of 2 m.

The nose cone of the AUV also contains a collision avoidance sonar, which will result in the AUV executing avoidance strategies in the event that an obstacle is detected in the path of the AUV. The positioning of the AUV can be monitored Mid-mission from the research vessel by deploying an acoustic towfish that can communicate with the acoustic modem on the AUV.

2.3.1.3 Side-Scan Sonar and Bathymetric Sonar

The dual frequency (900 kHz/1800 kHz, 15 Hz sampling frequency) side-scan sonar transducers are laterally mounted to the hull of the command module at an elevation angle of 30 degrees down from horizontal. The side-scan is used to acoustically map the texture of the seafloor. All of the scallop missions were completed at a frequency of 900 kHz because the 1800 kHz was non-functional at the time, and because lower frequencies are able to survey a wider swath (Johnson and Helferty, 1990).

The transducer transmits sound at 900 kHz for a duration of 6.67 μs. The acoustic energy radiates outwards until it reaches the seafloor. Most of the

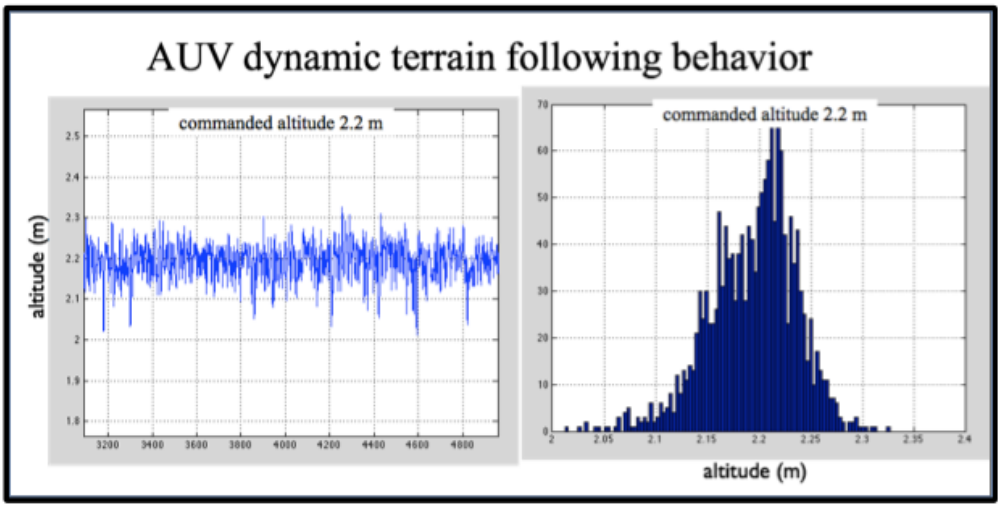

Figure 2.4: AUV mission data demonstrating the terrain following behavior of the vehicle over seafloor while adhering to a predefined altitude. Standard deviation of 16 cm.

acoustic energy will reflect off the seafloor and travel away from the vehicle; however, small and large scale topographic features will reflect a detectable backscatter signal. The amplitude of the signal depends on the acoustic impedance contrast of the seawater and seafloor. The acoustic impedance contrast (Z) is given by:

$$Z = \rho v \qquad \text{Eq. 2.1}$$

where ρ is the density of the medium and v is the travel velocity of sound through the medium (Johnson and Helferty, 1990).

Once the ping has been sent, the transmit circuitry of the transducer switches off and the receive circuitry activates. The returning backscatter energy is continually recorded. Return signal from targets closest to the transducer are received first, followed by returns from continually farther away from the vehicle track up until a backscatter limit where the signal attenuates too much to be detected (Johnson and Helferty, 1990). Each return signal is timed from the moment of transmission to return, so that a travel distance can be calculated. Each ping of the AUV's side-scan was able to record a range up to 20 m across track and <10 cm along track (at normal survey speeds of 1.5 m/s). As the wave radiates away from the transducer, the intensity of the wave diminishes with increased distance. Additionally, acoustic energy is lost from the scattering caused by bubbles and particles suspended in the water column, and absorption by magnesium sulfate (Johnson and Helferty, 1990). The side-scan sonar processor automatically applies a time-varying gain to correct for the attenuation of the sound wave.

The Geoswath module is a 500 kHz phase measuring bathymetric sonar (PMBS). Like the side-scan sonar, the PMBS collects backscatter data, but unlike the

side-scan, it also records bathymetric data. The bathymetric data can be recorded because the sonar array contains multiple receiver arrays. An echo from the same target will reach each receiver at a slightly different time. Based on the amount of time it took from transmitting the ping to receiving the echo it is possible to calculate the path length of the target. Comparing the difference in the path lengths allows for the approximation of the elevation angle of the target (Lurton, 2000). The elevation angle can then be used to calculate the bathymetry of the target.

The side-scan sonar and Geoswath PMBS collected acoustic data during all 27 scallop missions. The backscatter data is useful in a habitat study because it has been shown that classification schemes can be automatically applied that can determine changes in seafloor sediment texture (Mackinson *et al.,* 2004; Raineault *et al.*, 2011; Raineault *et al.*, 2013). Bathymetric data can be used to resolve areas of local relief that may have an impact on habitat.

2.3.2 F/V Christian and Alexa

The CHRISTIAN AND ALEXA is a 30 m commercial scallop fishing vessel equipped with port and New Bedford commercial scallop dredges. In each stratum, the F/V CHRISTIAN AND ALEXA made one 15-minute dredge tow along the AUV transect to ground-truth the presence of scallops and other fauna and provide calibration for the size distribution. The vessel was maintained on the dredge track by using DGPS. The tows were made with the starboard 15 ft (4.572 m) wide New Bedford style commercial dredge at the commercial dredge speed of 4.5 – 5.0 knots. The commercial scallop dredges were fitted with 4 inch (in) interlocking rings to coincide with the 4 in (101.6 mm) shell height limit of a harvestable sea scallop.

Where dredging was accomplished the catch was sorted, identified, and weighed. Length-frequency data were obtained for the scallops. This information was recorded onto data logs and then entered into a laptop computer database aboard ship for comparison to the camera image estimates.

2.3.3 Survey Mission Design

Given the pilot study nature of this project, variable sampling designs were chosen to assess optimal image sampling utilizing an AUV. The goal of the study was to photograph 45,000 m^2 of seafloor in the eight inshore NMFS sea scallop survey strata (Figure 2.1). An AUV image of the seafloor is typically about 2 m wide, meaning that the AUV had to complete approximately 23 km of transects in each strata to get the desired coverage. A minimum of two missions were run in each strata to increase the number of sampling sites. A mission is defined as the AUV sampling path completed in a single dive and surfacing deployment.

The staircase (Figure 2.4) sampling design consists of the AUV completing orthogonal transects of equal length that mimics the profile view of a staircase. Of the 27 missions, two utilized this sampling design. The advantage of this design over the other designs chosen is that it samples from the largest distributed area given the same battery usage, while maintaining two distinct spatial dimensions of sampling. This sampling design would be recommended for generally quantifying a large area in a single mission.

The snake (Figure 2.4) sampling design is similar to the staircase (equidistant orthogonal transects), except that it propagates along only one of the transect axes. We utilized this sampling design for 6 missions. This sampling design is

recommended for generally sampling a large area in which the scallops form an elongated bed.

The lawnmower (Figure 2.4) pattern consists of running parallel transects, typically at a small lateral spacing (4 – 40 m). This survey method was most preferred for this project (56% of the missions) as it precisely samples a small area, while utilizing the high accuracy navigation and maneuverability of the AUV. A lawnmower pattern can achieve up to 100% photographic coverage of a 30,000 m^2 rectangular survey area in a single mission. This sampling design can also perform accurate structured grids, which are preferred in many biological statistical analyses.

The fourth sampling design category consists of non-regular designs that are uniquely designed to the special needs of a mission. Reasons for using a non-regular design include experimentation, terrain limitation, or surveying a specific topographical feature, such as a submarine canyon.

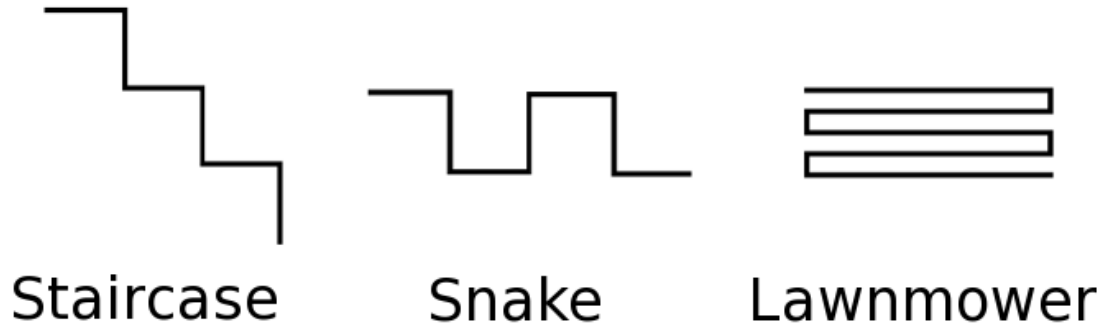

Figure 2.5: Plan view of AUV survey mission track designs.

2.3.4 Image Processing

2.3.4.1 A Single Image

The hull-mounted camera in the AUV took images during every mission at a fixed altitude of 2 m above the seafloor. The resolution of each image was 800 x 600. The camera lens has a horizontal viewing angle (α_h) of 49.92 degrees. Knowing the viewing angle and distance to the object being photographed, it is possible to calculate the true dimensions of the seafloor that was imaged. For example, it can be calculated that an image at 2 m altitude covered 1.86 m x 1.40 m of seafloor. This yields a pixel width and height within in each image of 2.3 mm. The general formula used for calculating the seafloor width (W) in the image is:

$$W = 2\tan\left(\frac{\alpha_h}{2}\right)\left[z - 1.3\tan(\theta_p)\right] \quad \text{Eq. 2.2}$$

where z is height (meters) of the AUV above the seafloor. θ_p is the pitch (degrees) of the AUV. A negative pitch refers to the AUV nose pointed towards the seafloor below horizontal. The coefficient of 1.3 is the lever arm distance (meters) from the camera to the location of the vehicle navigation reference point. The height (H) of the image is equal to 0.75W. The area (A) of the seafloor represented in a single image is therefore just A = W*H. Equation 2.2 assumes that the seafloor is flat, and it also does not account for the roll of the AUV. Image width error is less than 1% if AUV roll is less than 5° from horizontal. These equations allowed scallops to be precisely sized given the varying altitude and pitch of the AUV at the time each image was taken. Figure 2.6 shows a standard nighttime image of the seafloor taken by the AUV camera showing 15 scallops in a 2.6 m^2 area.

The AUV automatically tags each image captured with navigation and environmental data that pertains to the moment that the image was taken. Some of the metadata that is recorded in each image includes the latitude, longitude, capture time, depth, altitude, and pitch of the AUV when the image was captured.

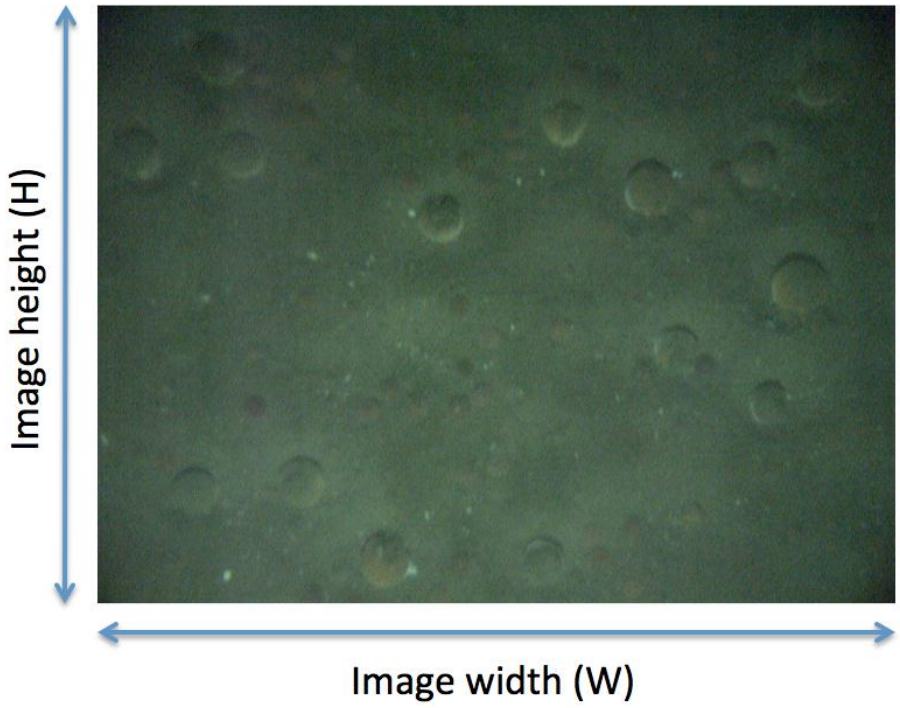

Figure 2.6: An image of the seafloor with 15 scallops in it. Image dimensions are defined in terms of length and width. This image represents an area of seafloor 2.6 m^2 (1.86 m x 1.4 m).

2.3.4.2 Sea Scallop Enumeration and Sizing

In order to estimate the scallop populations within the region, manual counts of the scallop population within the surveyed areas have been done from the images. The scallops were counted, sized, and logged as follows (see Figure 2.7 for a visual representation of the sizing rules):

1. All images for a mission that were taken at a height above the seafloor between 1.5 m and 2.5 m are counted.
2. Each scallop in an image is counted individually, unless a scallop has already been counted from an image that overlapped the same section of seafloor. Analyzers examined photos sequentially and were trained to recognize when images overlap, so that scallops would not be counted more than once.
3. Each scallop is sized based on the distance from the hinge to the end of the shell bisecting the scallop using a pixel measuring tool (where the real-world length represented by the pixels can be calculated based on the metadata of the image).
4. The scallop size is **not** recorded if more than half of the entire scallop is not contained within the frame.
5. A dead scallop is not sized or counted. A dead scallop was identified as a disarticulated shell or a shell in a nonlife position (resting on right valve).
6. The final count for a mission is the number of live scallops that could be sized.

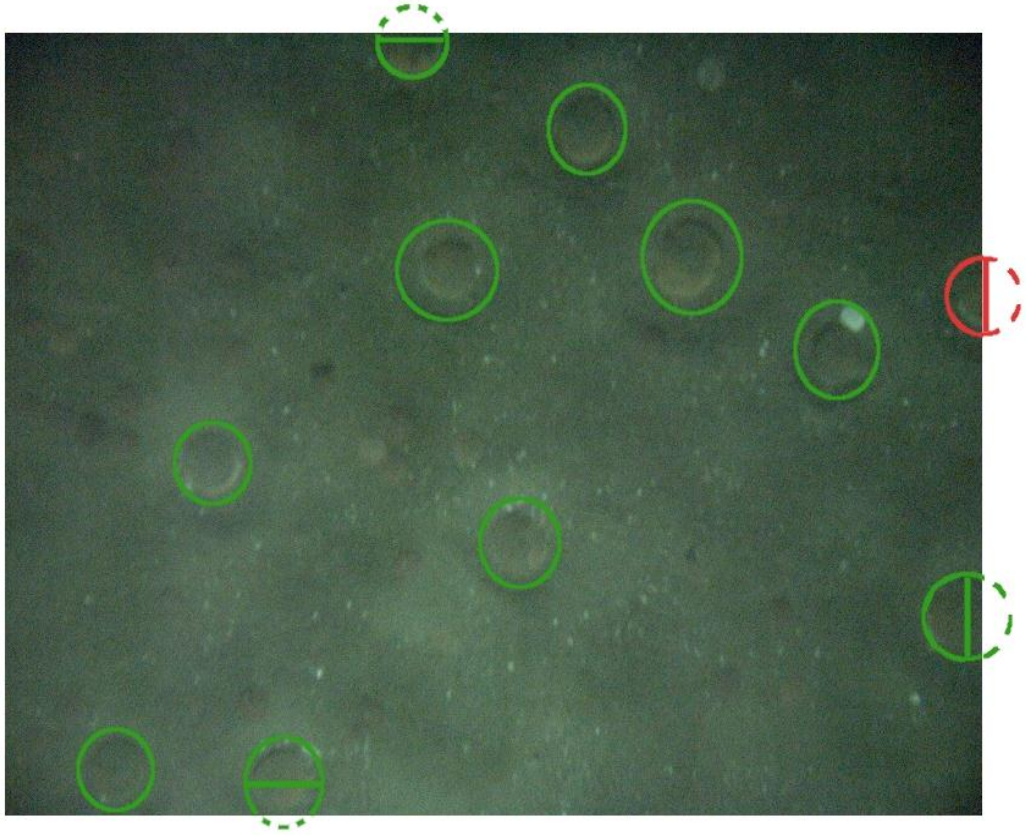

Figure 2.7: Visual representation of the scallop sizing algorithm. Green circles were sized, and therefore counted. The red circle represents a scallop that could not be sufficiently sized. Image dimensions: 1.86 m x 1.4 m.

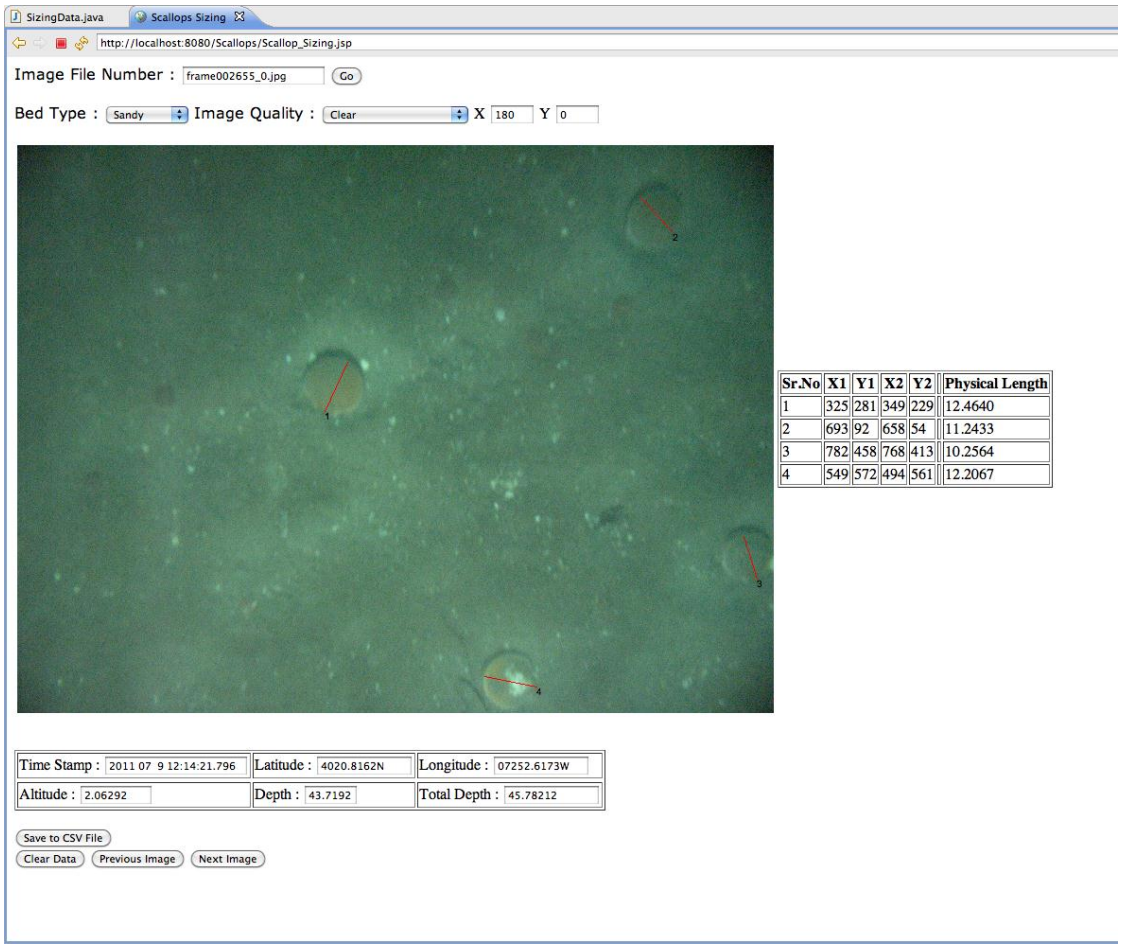

Figure 2.8: The user interface of the sea scallop counting and sizing program. Scallop were sized by using a built in length tool (the red lines in the image). Other attributes such as the bed type and image quality were also input by the user.

The data was logged in Microsoft Excel spreadsheets that were divided by mission. Interns and myself completed scallop counts in January 2012. Each volunteer received training on how to identify a scallop from an image, and how to size it. After being trained, each analyzer was given a standardized packet of 100 images to analyze. Each intern correctly identified at least 97% of the scallops in the test packet. After an analyzer completed counting all of the scallops for a mission, I would personally reanalyze a subset of their images to confirm their results.

In order to aid the process of scallop counting and to further standardize the process for volunteers, a web-based program was developed by the CSHEL IT consultant. The software offered a user-friendly environment that was completely mouse click driven. Data such as the number of scallops, the size of the scallops, the seabed type, and image quality was manually inputted by the user and automatically recorded into the database. Shown in Figure 2.8 is the user interface of the scallop sizing program.

Scallop density (D_s) for a mission was calculated by summing all of the sized scallops from mission photos (a_T, mission total scallops), and dividing by the imaged seafloor area (m^2). Simply summing the photo areas could result in overestimating the area of seafloor photographed. Instead, the length (l_T, Pythagorean theorem of start and end coordinates in Northings and Eastings) of each AUV run transect (T) within a mission was calculated and multiplied by the mean image width ($\overline{W_T}$, found by solving Equation 2.2 in terms of the mean image altitude for the transect).

$$l_T = \sqrt{\left(\left(N_{\mathrm{T_{end}}} - N_{\mathrm{T_{start}}}\right)^2 + \left(E_{\mathrm{T_{end}}} - E_{\mathrm{T_{start}}}\right)^2\right)} \qquad \text{Eq. 2.3}$$

$$D_s = \frac{a_T}{\sum_1^T \overline{W_T} l_T} \qquad \text{Eq. 2.4}$$

2.3.5 Bed Type

Seabed was classified for every scallop containing image. The choices for the bed type were sandy, shell hash, mounds, ripples, and boulders (Figure 2.9). The sandy bed type was defined as a sandy sediment texture that lacked morphological features. Shell hash was defined as weathered or fragmented pieces of shell that made up more than 10% of the visible surface sediment. Mounds were defined as round or oval morphological seafloor features. Ripples were defined as trough separated elongate crests (typically parallel in orientation).

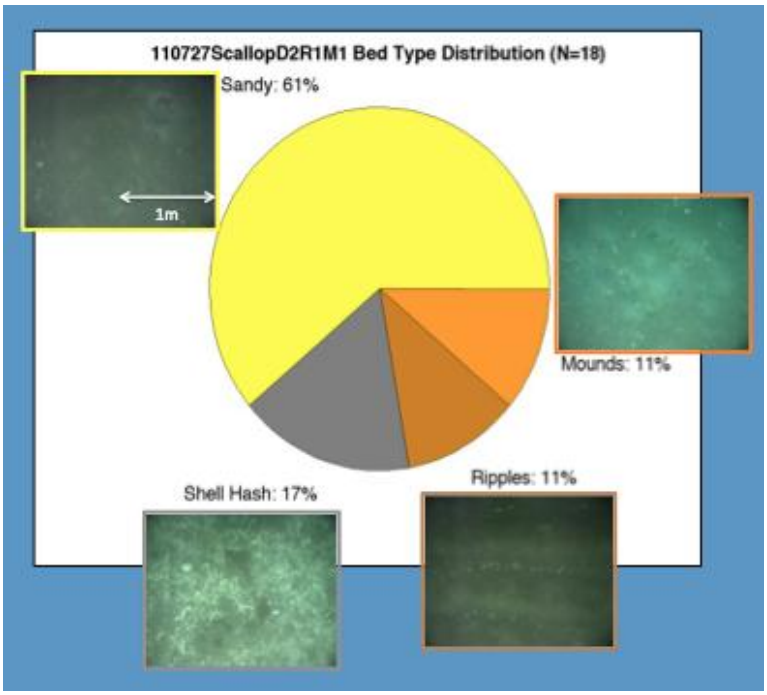

Figure 2.9: Image references for the bed type classification scheme.

2.3.6 Processing Side-scan Sonar

Processing of the side-scan sonar imagery was done using Chesapeake Technologies SonarWiz 5. An individual project was created for each scallop mission. The marine sonic (.mst) files were batch imported for a single scallop mission. The water column was then removed from each file using the bottom-tracking tool built into the software. Other processing of the side-scan data included cropping files that included noisy or erroneous data. Once the data had been processed, it was exported as a geotiff (.tiff) mosaic with a 0.25 m resolution. The geotiff mosaics were then exported as KMLs so that the processed data could be viewed in Google Earth. The mosaic files have been archived on a publically available website (www. http://cshel.geology.udel.edu/kml_files/Scallop/).

2.3.7 Processing Bathymetric Data

While all 27 missions collected bathymetric data via the Geoswath PMBS, only the mission 110710_M1_ArtiesRun was processed as a test case. The bathymetry was processed using Caris Hips & Sips. The raw Geoswath files (.rdf) were imported using the import wizard. A vessel file was created for the AUV, where the offsets of the transducers in reference to the INS were input along with uncertainties for the instrumentation. Next, a tide file and a sound velocity profile file were applied. Total propagated uncertainty (TPU) was then computed. A depth filter was then applied to filter out any data points that were grossly out of observed depth ranges (>40 m depth). The data was then manually "cleaned" by deleting data points that occurred above or below the seafloor return. The data from all of the sources (xyz, tide, SVP, TPU, etc.) were then merged so that a Combined Uncertainty and Bathymetric Estimator (CUBE) surface could be produced. The CUBE surface is a

best estimate bathymetric surface of the seafloor that is produced from a statistical hypothesis.

The remaining missions were not processed because it was found that the side-scan sonar mosaics were able to provide the necessary information about seafloor morphology (ripples, sediment texture, etc.). Also, it was evident from the side-scan sonar mosaics that there were not any areas of significant local relief within any of the missions that would require further investigation through the use of high resolution bathymetry.

2.3.8 Dredge Efficiencies

Dredging data were collected and utilized in two independent ways for this project. The first instance of dredging has been previously done and completed by Dr. Hart for NMFS during the spring of 2011 (NEFSC internal document). The sampling was done in the Mid-Atlantic region utilizing an 8 ft (2.438 m) wide standard survey dredge. Additionally, the dredge had a 1.5 in liner and a 3.5 in twine top diamond mesh (DuPaul and Rudders, 2008). The second instance of dredging took place during summer 2011aboard the F/V CHRISTIAN AND ALEXA. The F/V CHRISTIAN AND ALEXA ran a single dredge during sampling missions over the same tow done by Hart previously in the year. The tows were run from the start and end latitude and longitudinal coordinates provided by Dr. Hart (personal communication, July 7, 2011).

The F/V CHRISTIAN AND ALEXA dredge is 15 ft (4.572 m) wide and has rings that are 4 in (101.6 mm) in diameter. The ring sizes of the commercial dredges are larger than that of survey dredges so that smaller, juvenile scallops will be preferentially left on the seafloor. The difference in the sieve size of the dredges, and in their respective widths must be normalized so that the data from the two can be

accurately compared. The way that this was done was to calculate a scallop density for the area dredged. The survey area for the commercial scallop dredge was calculated by multiplying the length of the dredge line by the width of the dredge (4.572 m). The abundance of scallops captured by the dredge (a_D) was then divided by the survey area. The dredged scallop density was then divided by the image survey scallop density (D_s, Equation 2.4), yielding the dredge efficiencies (e).

$$e = \frac{\left[\frac{a_D}{4.572\sqrt{\left(\left(N_{\mathrm{T_{end}}} - N_{\mathrm{T_{start}}}\right)^2 + \left(E_{\mathrm{T_{end}}} - E_{\mathrm{T_{start}}}\right)^2\right)}}\right]}{D_s} \qquad \text{Eq. 2.5}$$

2.3.9 Scallop Biomass

The meat weight (weight of the adductor muscle, W_m) of a scallop has been shown to covariate with the depth (d) that the sea scallop inhabited and the shell height (H_s) of the specimen (Rothschild *et al.*, 2009). Geographic location (latitude and longitude) has also been shown to have an effect (Hennen and Hart, 2012). The reason that meat weights decrease with depth is believed to be due to reduced phytoplankton (food) at greater depths. The shell height-meat weight conversion formula chosen for this study was (NMFS, 2010):

$$W_m = e^{-8.94 + 2.94 \ln H_s - 0.43 \ln d} \qquad \text{Eq. 2.6}$$

The chosen formula lacks variables for latitude and longitude because it has already been calibrated to the sea scallop population of the Mid-Atlantic region. The meat weight of every scallop in a mission was calculated using a Matlab script (see Appendix F) and then summed to give a total mission biomass.

2.3.10 Variograms

Geostatistics was originally developed by Matheron (1963) as a method to categorize geologic formations of mining interest. Since then, it has been used in broader applications, specifically in the fields of hydrogeology and ecology distribution mapping. The method begins by the construction of a (semi)variogram for a data set. The variogram is then fit with a model (spherical, exponential, Gaussian) that best fits the data.

Variograms quantify the variance within the data at different spatial scales. The plot is produced from the data of a single mission. First, data points were comprehensively paired. For each pair (*N*), a lag (*h*) was calculated (the distance between the points) and the variance of abundance (*a*). The points were then grouped by similar lag sizes. A tolerance was then applied to the lag sizes to account for any minor variations in lag, so that similar lags were grouped together. The data points with similar lags are then summed and averaged over the total number of points to get $\hat{\gamma}(h)$.

$$\hat{\gamma}(h) = \frac{1}{2N}\sum_{i=1}^{N}[a(x_i) - a(x_i + h)]^2 \qquad \text{Eq. 2.7}$$

Plotting $\hat{\gamma}(h)$ yields a variogram. The *sill* is the value of $\hat{\gamma}(h)$ for which the data asymptotes (see Figure 2.10). The *range* is the value of *h* at which the data reaches the sill. The *range* also corresponds to the distance of autocorrelation (α). Values that occur within the range of autocorrelation are affected by the values of neighboring points. The *nugget* accounts for the randomness of values of $\hat{\gamma}(h)$ extremely close to each point (as *h* goes to 0).

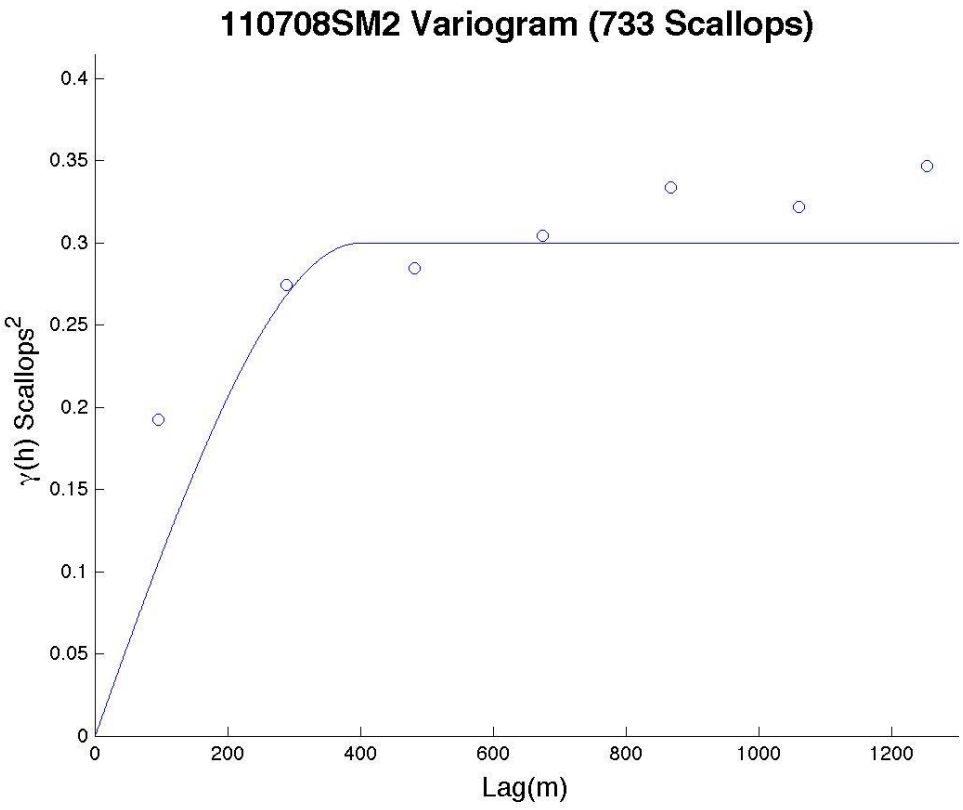

Figure 2.10: Experimental variogram with a spherical fit model. Variograms assist in understanding the spatial structuring of the scallop populations within each mission. This mission has an autocorrelation length of 400 m.

Once the variograms were plotted, each one was analyzed individually to determine the best model to be applied to the data. There are numerous types of models, but the three main types are spherical, exponential, and Guassian.

2.4 Results

2.4.1 Survey Stratum 1

Survey stratum 1 was defined as the region bounded by 40.5 - 41°N latitude and 72.5 - 73°W longitude (off the southeastern coast of Long Island). Three scallop survey missions were performed within the stratum on July 8, 2011 (Table 2.2). Missions 110708_ScallopD2_M4 and 110708_SM2 surveyed the same 3 km line 7 hours apart. The intent of this experiment was to compare the effect that daylight has on the ability to discern scallops in the images (Figure 2.11). Daytime photos are typically overexposed in the green channel, while the red channel is undersaturated. The result is that all of the features and objects in the image appear various shades of green, including the normally orange colored scallop shells. The counts for the two missions differed by 187 scallops (21%). Assuming that the AUV resurveyed the exact same section of seafloor, and that none of the scallops had moved over the 7 hours between the missions, this shows that the daytime photos can result in artificially decreased scallop abundances due to the increased difficulty to identify scallops in daytime photos.

The three missions surveyed a combined area of 42,495 m^2. The total scallop density for the strata was found to be 0.09 scallops/m^2. Mission 110708_SM2 (Figure 2.10) was found to have an autocorrelation length (α) equal to 400 m at a

semivariance of 0.3 scallops^2. Gaussian distributions that were moderately skewed towards smaller shell heights were found for the shell height distributions. Mean shell height for the strata was 136.9 mm. No recruits (H_s < 70 mm) were observed. The scallop population in this stratum is extremely mature, being >99% harvestable ($H_s > 101.6$ mm) with a corresponding biomass of 161,699 g (Table 2.7).

Image analysis found that the survey area for mission 110708_SM2 was predominately sandy featureless seabed (94%) with the remaining 6% being shell hash. The area surveyed in missions 110708_ScallopD2_M4 and 110708_SM2 were both >98% sandy. The side-scan sonar mosaics are in agreement with the image based seabed classification.

2.4.2 Survey Stratum 2

Stratum 2 was surveyed on July 8 – 9, 2011, and was defined as the region bounded by 40.0 - 40.5°N latitude and 72.5 - 73°W longitude. A total of 2 missions were run with the AUV that captured a combined 18,057 images. The images covered a combined area of 45,140m^2. Scallop counters were able to identify and size 5,071 scallops, yielding a stratum scallop density of 0.11 scallops/m^2. An autocorrelation model could not be applied to either mission. Figure 2.12 shows how the scallops in mission 110709_Scallop_D3_M1_Corey did not form any spatial groups at this scale.

Even though this stratum had the lowest mean shell height (115.3 mm), less than 1% of the digitally measured scallops were recruits. The shell distributions were both moderately skewed towards larger shell heights.

Missions 110708_Scallop_DvoraRun and 110709_Scallop_D3_M1_Corey were both found to be >99% featureless sandy bed according to image classification.

The side-scan sonar mosaics for both missions did not contain any well-formed ripple or mound beds, agreeing with the image analysis findings.

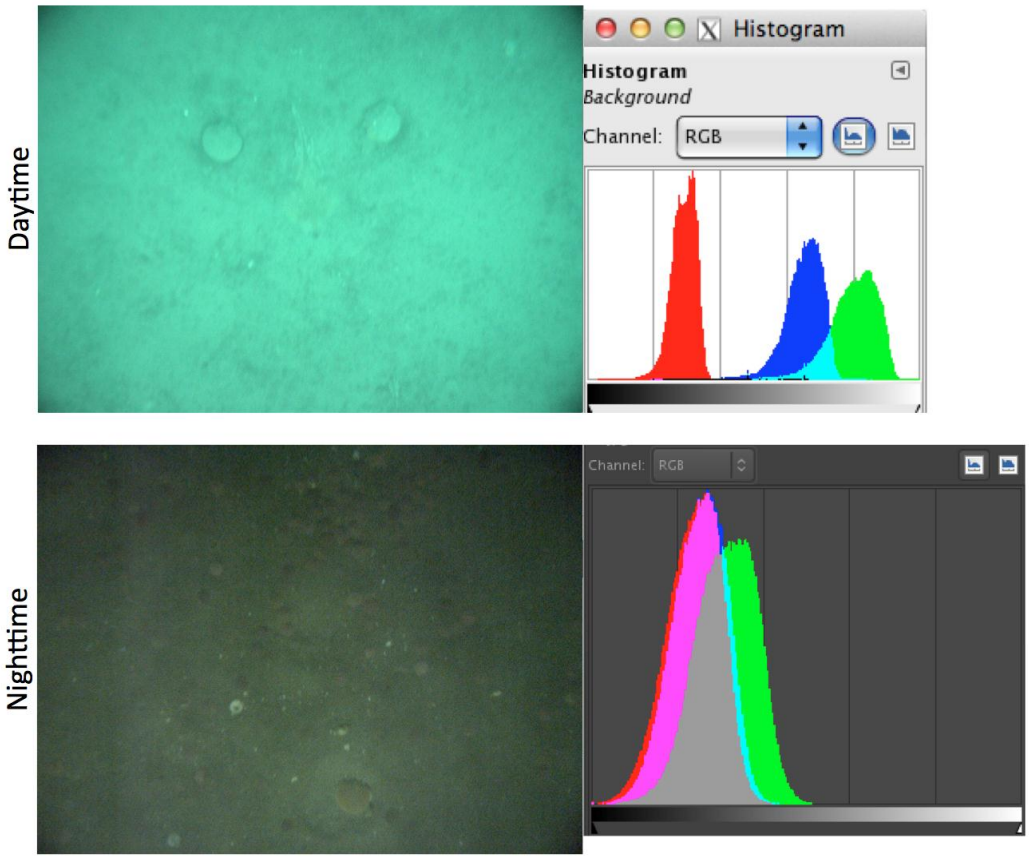

Figure 2.11: A comparison of images of the seafloor taken at night versus during the day. Attached histograms of the RBG channel in each image show that the daytime photo has undersaturated reds and overexposed greens, which can make it difficult to identify a scallop shell. The nighttime photos have a much better color balance.

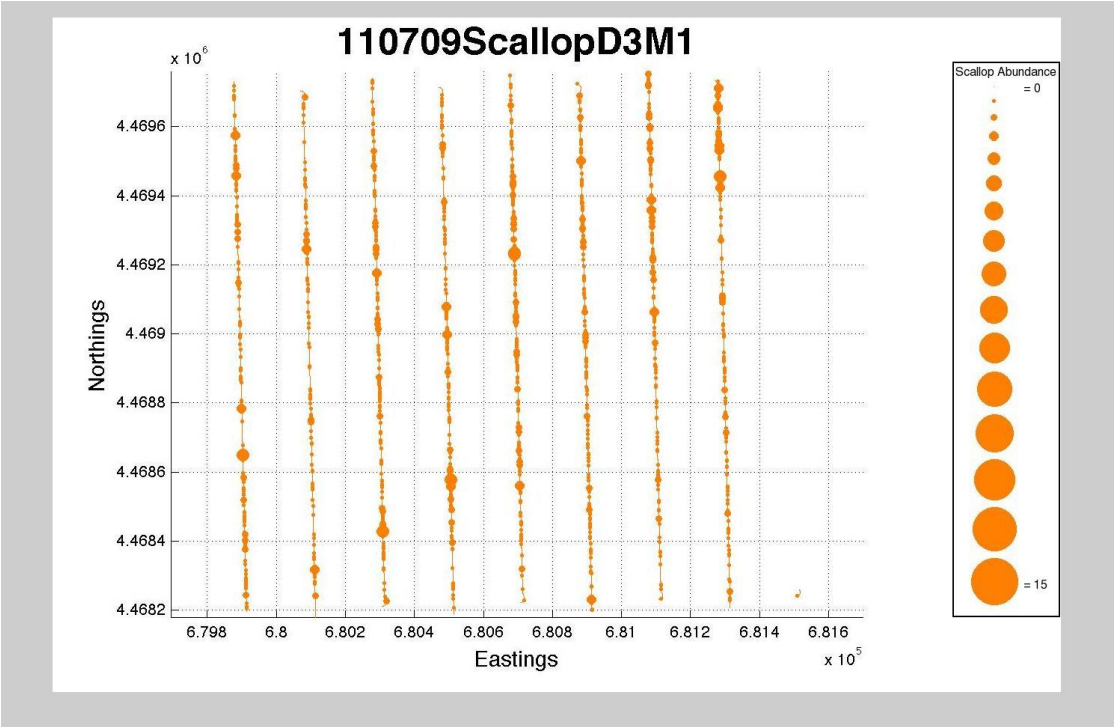

Figure 2.12: Bubble plot of mission 110709_Scallop_D3_M1_Corey. Each bubble represents 1 seafloor image. The size of the bubble corresponds to the number of scallops counted in that image. This mission does not display any noticeable scallop grouping.

2.4.3 Survey Stratum 3

Stratum 3 (40.0 - 40.5°N latitude and 73 – 73.5°W longitude) was directly south of Long Island, and was surveyed on July 9-10, 2011. Over the course of 4 separate missions, 39,600 images of the seafloor were produced, covering an area of 95,519 m^2. Missions 110710_DV117, 110710_DV118, and 110710_M1_ArtiesRun were all located in the northwestern section of stratum 2, while mission 110709_ScallopDay3_DV119 was on the boarder of survey strata 2 and 3. The stratum had an overall scallop density of 0.04 scallops/m^2. 110710_M1_ArtiesRun was the only mission to show an organizational spatial structuring (Figure 2.13), with an autocorrelation length of 500 m at a variance of 0.23 $scallops^2$. The proximity of mission 110709_ScallopDay3_DV119 to the boarder of stratum 2 likely explains why the scallop density and shell height statistics more closely match the missions from stratum 2 than the other missions in stratum 3. Over 80% of the scallops had a harvestable shell height among all 4 missions (126,565 g harvestable biomass). Recruits accounted for 0.5% of the observed scallops.

Bed type classification from images containing scallops yields a near 100% sandy bottom. (<1% ripples). The side-scan sonar mosaics for all 4 missions are lacking well-formed morphological features, implying that the image classification is accurate.

2.4.4 Survey Stratum 4

Stratum 4 was surveyed on the first survey cruise on July 11, 2011 and again during the second survey cruise on July 29, 2011. The survey stratum is bounded by 40.0 - 40.5°N latitude and 73.5 – 74°W longitude and is positioned at the bight of New

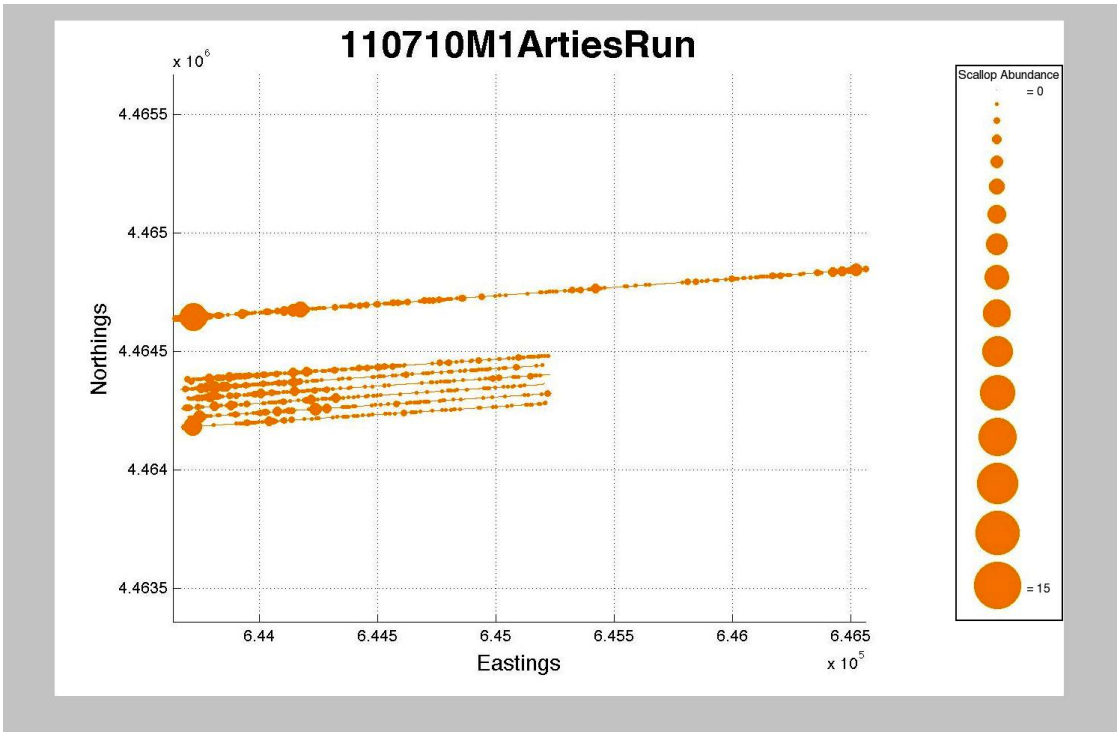

Figure 2.13: Mission 110710M1_ArtiesRun showing a higher density grouping of scallops on the western side of the mission.

York and New Jersey. Two AUV missions were run in this stratum, producing 18,664 images, which covered an area of 43,848 m^2. Only 98 scallops were identified between the two missions, meaning the resulting density was near 0 (0.003 scallops/m^3). This stratum is notable as it had the warmest near bed water temperatures recorded (11.3°C). Mission 110711_DV115 was very skewed towards small shell heights (Figure 2.14), likely from the inclusion of a younger size class. Approximately 4% of the observed scallops within the stratum were recruits, while >90% were harvestable sized scallops. The mean shell height for the stratum was 123.5 scallops/m^2. The harvestable biomass of the surveyed area was 4054 g. The low number of counted scallops prevented meaningful variogram analysis.

The bed type of mission 110729_D4_DV0113_M4 was found to be 13% shell hash and 87% sandy featureless bottom, while 110711_DV115 was 100% sandy. The side-scan sonar mosaic for mission 110729_D4_DV0113_M4 reveals that there were two ripple beds both containing 1 m wavelength megaripples (see Figure 1.5). The beds cut across the long axis of the survey extending for over 250 m. One of the scallop containing images occurred within the sorted bedform, but was not identified by the image observer. The reason is that the field of view of the image is too small to be able to delineate 1 m wavelength megaripples.

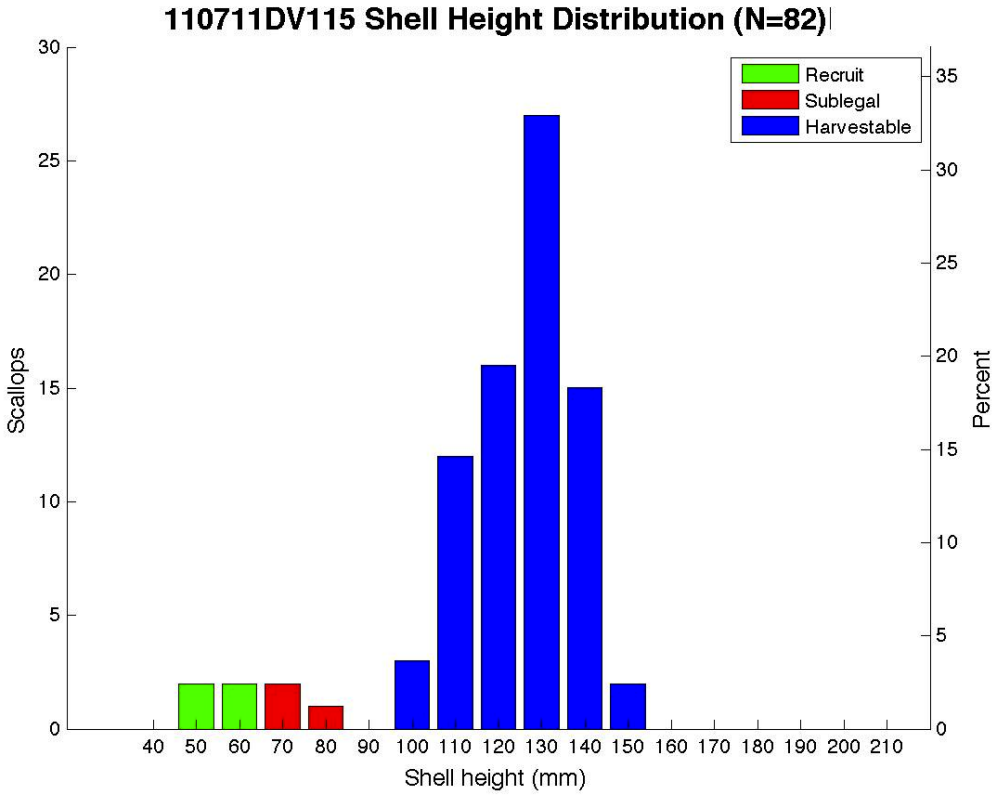

Figure 2.14: Shell Height histogram for mission 110711_DV115 showing a negatively skewed distribution.

2.4.5 Survey Stratum 5

Survey Stratum 5 was off the eastern coast of New Jersey (39.5 - 40.0°N latitude and 73.5 – 74°W). Four missions were completed on July 28-29, 2011. Over 37,000 images were captured by the AUV camera, representing 47,758 m^2 of seafloor. Scallop counters were able to identify 1,852 scallops within the images, resulting in a 0.02 scallops/m^2 density. Experimental variograms from the 4 missions were all nonstationary (do not asymptote at a variance), and therefore autocorrelation lengths could not be calculated. The scallop population was overwhelmingly mature with >89% of all scallops being harvestable. Less than 1% of the observed population was recruit size. All of the distributions were negatively skewed towards smaller shell heights.

All 4 missions were overwhelmingly sandy, but two missions had shell hash components of 9% (110728_D3_R8_M5) and 17% (11029_D4_DV01050_M2). The side-scan sonar mosaics reveal that 110729_D4_DV0106_M1 had a sand wave bed less than 100 m in length that scallops were identified in from images, but the wavelengths of the megaripples were 1 – 3 m, and therefore too large scale to identify from a 2 m altitude photo.

2.4.6 Survey Stratum 6

Survey stratum 6 started 50 km off the east coast of New Jersey (39.5 - 40.0°N latitude and 73.5 – 74°W) and was surveyed on July 28, 2011. A total of 3 surveys were completed that photographed 1,169 scallops. The scallop densities across all 3 missions were within 0.01 scallops/m^2, with a total density for the stratum of 0.02 scallops/m^2. Mission 110728_D3_R6_M1 was not evenly distributed. Scallop

densities within the southern survey lines were 3 to 4 times greater than the northern lines. This stratum had the highest mean shell height (139 mm). Only 6 recruits (0.5%) were observed within all of the stratum photographs, with the majority of the scallop population being greater than the harvestable limit. All 3 missions had negatively skewed shell height distributions, and 110728_D3_DV063_M4 had one of the widest spread of shell sizes with σ=31.4 mm (Figure 2.16).

The entire stratum was identified predominately sandy bottom (98%), with 110728_D3_DV062_M3 having a 2% shell hash component, and 110728_D3_R6_M1 being <1% rippled. Side-scan mosaics reveal the stratum to match the photo classified bed types.

2.4.7 Survey Stratum 7

Survey stratum 7 was directly off the southeastern coast of New Jersey (39.0 – 39.5°N latitude and 74 – 74.5°W) on July 27-28, 2011. This stratum was photographed the most with 42,628 images over 112,019 m^2. Five total missions were run, 3 of which were at shallow depths (20-30 m), and 4 of which at relatively warm near bed water temperatures of 10 – 11°C. Four of the missions had 4 or less total scallops resulting in scallop densities of or near 0 scallops/m^2. The mission 110728_D3_R7_M2 was performed at the greatest depth of all 5 missions, and had a scallop density of 0.001 scallops/m^2. Mean shell height for the stratum was 114.3 mm, which was the smallest of all 8 strata. Recruits represented 1% of the digitally sized scallops.

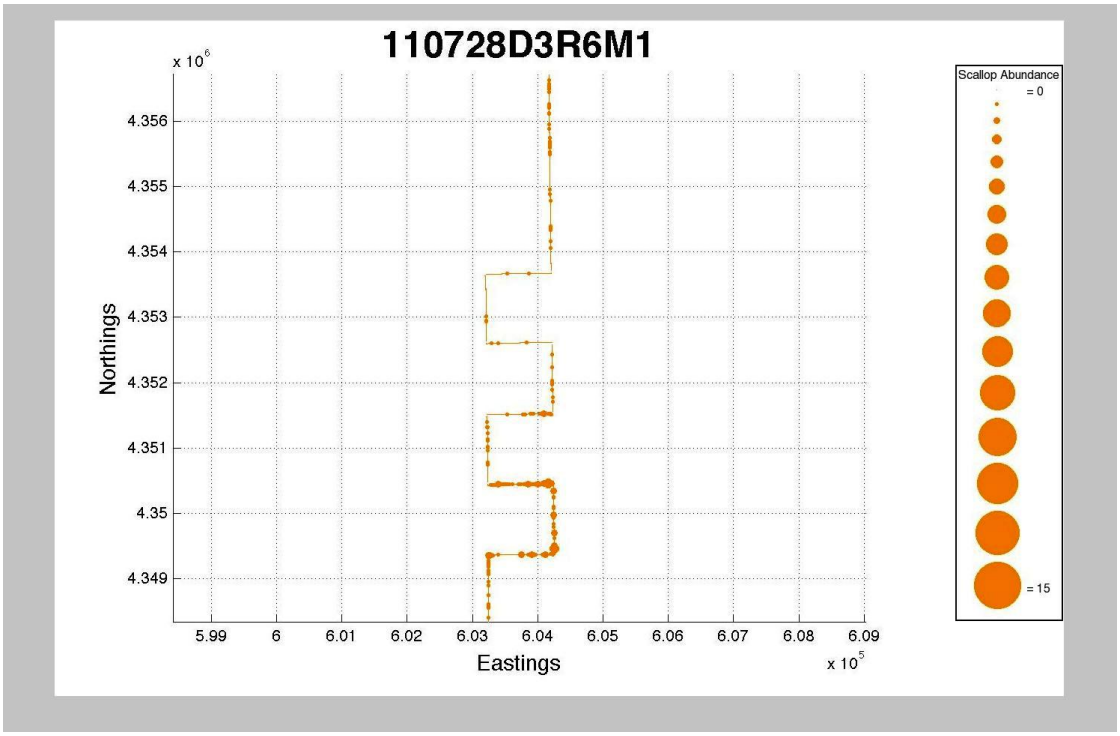

Figure 2.15: Bubble plot of mission 110728_D3_R6_M1 showing a steadily increasing scallop density to the south.

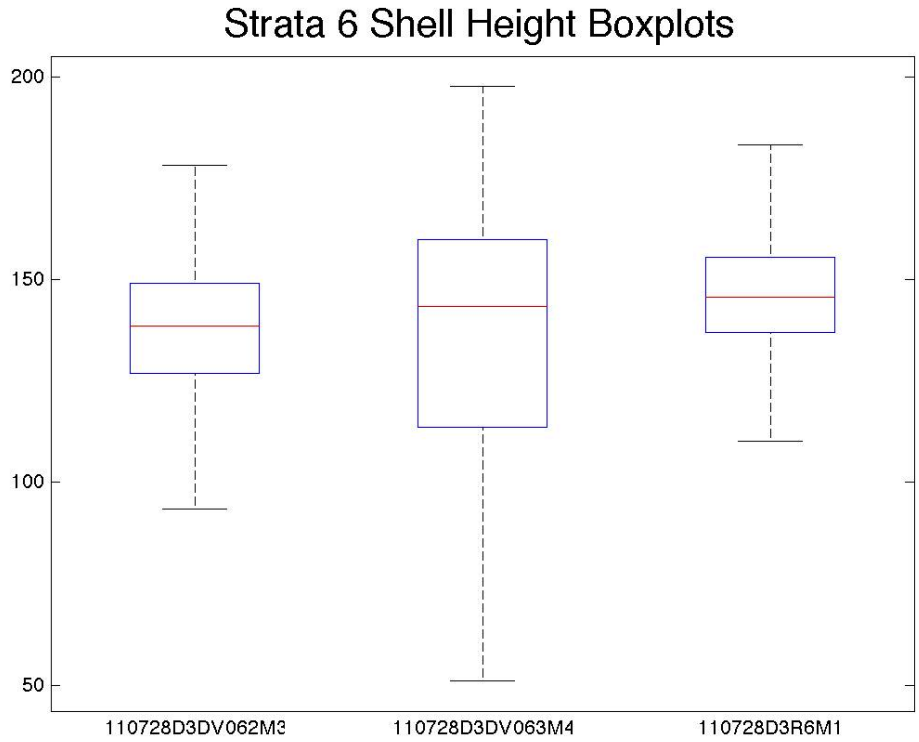

Figure 2.16: Box plots for the missions within survey stratum 6 showing a large range of digitally measured shell heights within each mission.

The scallop containing images were overwhelmingly classified as sandy bottom (86%), with ripples representing 10%, and shell hash the remaining 4%. Figure 2.17 shows the location of seafloor ripples from 110728_D3_R7_M2 where the corresponding scallop images were classified as rippled bed type.

2.4.8 Survey Stratum 8

The final survey stratum was located east of the Delaware coast (38.5 – 39.0°N latitude and 74 – 74.5°W). Four surveys completed on July 26 - 27, 2011. A total of 492 scallops were identified from 103,595 m^2 of seafloor photography, resulting in a stratum density of 0.005 scallops/m^2. The missions were surveyed at depths of 46 – 54 m, making this the deepest surveyed stratum. All 4 missions had scallop populations that were evenly distributed throughout the survey areas. Mean shell height of the digitally sized scallops was 136 mm, with a large range of sizes in all missions (σ>25 mm).

Bed types varied the most in this stratum with shell hash varying from 0 – 17% between missions, and mission 110727_ScallopD2_R1_M1 containing 11% mounds and 11% ripples.

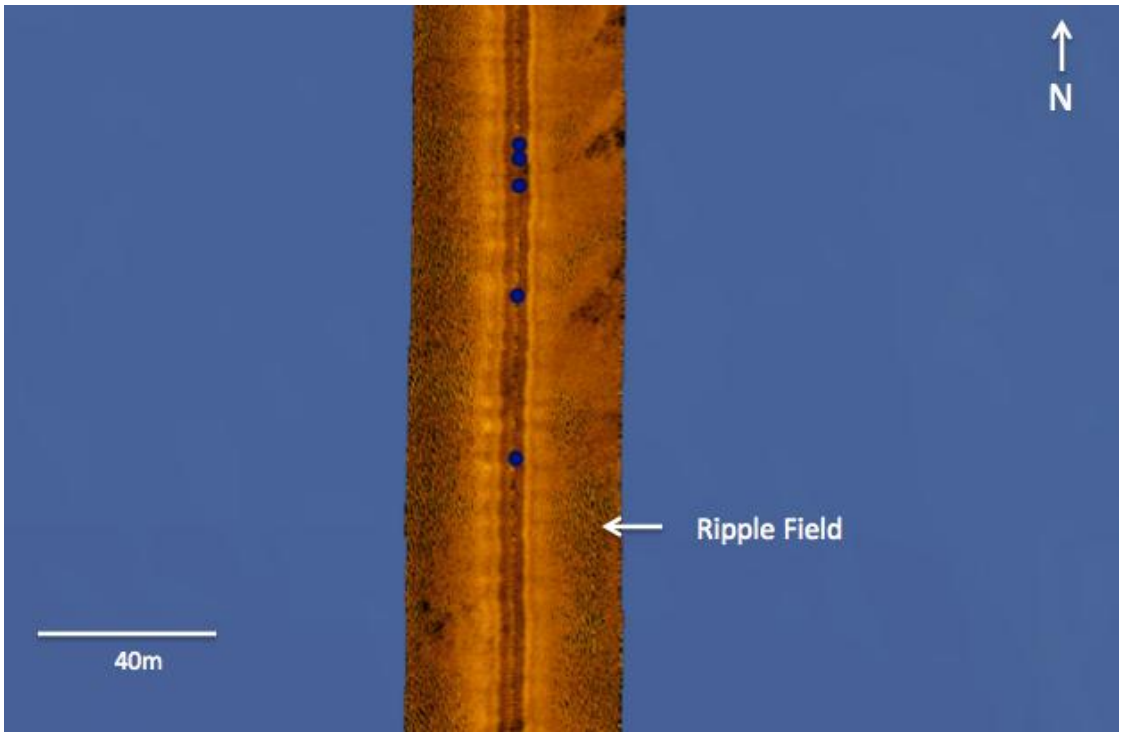

Figure 2.17: Side-scan sonar mosaic of a ripple field. The blue dots represent locations of identified scallops within an image classified rippled bed.

Survey Strata 1 (40.5 - 41N, 72.5 - 73W)

Mission	Images	Total Scallops	Survey Length (m)	Survey Area (m^2)	Scallop Density (scallops/m^2)	Mean Shell Height (mm)	Depth (m)	Near Bed Water Temp (^oC)
110708_ScallopD2	14,742	2,172	15,904	30,416	0.07	136.4	41.9	8.8
110708_ScallopD2_M4	2,387	894	3,015	5,985	0.15	138.6	43.5	8.8
110708_SM2	3,031	707	3,199	6,094	0.12	137.6	43.3	8.8
Summary	20,160	3,773	22,117	42,495	0.09	136.9	42.3	8.8

Survey Strata 2 (40 - 40.5N, 72.5 -73W)

Mission	Images	Total Scallops	Survey Length (m)	Survey Area (m^2)	Scallop Density (scallops/m^2)	Mean Shell Height (mm)	Depth (m)	Near Bed Water Temp (^oC)
110708_Scallop_DvoraRun	8,065	3,706	10,337	20,556	0.18	116.8	45.4	8.5
110709_Scallop_D3_M1_Corey	9,992	1,365	12,280	24,584	0.06	114.1	45.8	8.6
Summary	18,057	5,071	22,617	45,140	0.11	115.3	45.6	8.6

Survey Strata 3 (40 - 40.5N, 73 - 73.5N)

Mission	Images	Total Scallops	Survey Length (m)	Survey Area (m^2)	Scallop Density (scallops/m^2)	Mean Shell Height (mm)	Depth (m)	Near Bed Water Temp (^oC)
110709_ScallopDay3_DV119	8,338	1,850	10,773	21,633	0.09	114.1	42.1	8.9
110710_DV117	11,329	422	14,211	26,606	0.02	112.8	31.7	11.9
110710_DV118	10,163	227	12,271	23,105	0.01	126.9	33.7	10.8
110710_M1_ArtiesRun	9,780	1,403	12,154	24,175	0.06	117.4	35.3	9.8
Summary	39,610	3,902	49,410	95,519	0.04	117.8	35.3	10.4

Table 2.2: Table of scallop survey mission data for survey strata 1-3.

Survey Strata 4 (40 – 40.5N, 73.5 - 74W)

Mission	Images	Total Scallops	Survey Length (m)	Survey Area (m^2)	Scallop Density (scallops/m^2)	Mean Shell Height (mm)	Depth (m)	Near Bed Water Temp (^oC)
110711_DV115	9,141	82	10,398	20,044	0.004	120.0	35.5	11.0
110729_D4_DV0113_M4	9,523	16	12,511	23,804	0.001	126.9	27.7	11.5
Summary	18,664	98	22,909	43,848	0.003	123.5	31.2	11.3

Survey Strata 5 (39.5 - 40N, 73.5 - 74W)

Mission	Images	Total Scallops	Survey Length (m)	Survey Area (m^2)	Scallop Density (scallops/m^2)	Mean Shell Height (mm)	Depth (m)	Near Bed Water Temp (^oC)
110728_D3_R8_M5	9,544	508	11,691	21,626	0.02	131.1	41.5	8.4
110729_D4_DV0105_M2	9,479	212	12,181	21,614	0.01	146.8	32.8	9.1
110729_D4_DV0106_M1	9,425	801	11,752	23,169	0.03	131.9	36.9	9.2
110729_D4_DV0112_M3	9,281	331	12,133	22,710	0.01	135.0	37.9	9.4
Summary	37,729	1,852	47,758	89,119	0.02	136.2	37.2	9.0

Survey Strata 6 (39 - 39.5N, 73.5 - 74W)

Mission	Images	Total Scallops	Survey Length (m)	Survey Area (m^2)	Scallop Density (scallops/m^2)	Mean Shell Height (mm)	Depth (m)	Near Bed Water Temp (^oC)
110728_D3_DV062_M3	12,068	506	12196	20,662	0.02	135.9	46.6	8.0
110728_D3_DV063_M4	9,572	140	12149	22,676	0.01	136.0	50.7	8.2
110728_D3_R6_M1	10,950	523	13086	24,602	0.02	145.2	40.0	9.5
Summary	32,590	1,169	37430	67,940	0.02	139.1	45.6	8.6

Table 2.3: Table of scallop survey mission data for survey strata 4-6.

Survey Strata 7 (39 - 39.5N, 74 - 74.5W)

Mission	Images	Total Scallops	Survey Length (m)	Survey Area (m^2)	Scallop Density (scallops/m^2)	Mean Shell Height (mm)	Depth (m)	Near Bed Water Temp (^oC)
110727_D2_R2_M2	9,170	3	11,791	22,375	0.00	104.5	21.9	11.6
110727_D2_R3_M3	10,391	1	13,499	26,703	0.00	97.2	38.7	10.0
110727_D2_R4_M4	7,345	0	12,207	23,463	0.00		28.2	11.6
110727_D2_R5_M5	6,285	0	8,292	15,295	0.00		20.1	12.7
110728_D3_R7_M2	9,437	90	12,331	24,182	0.004	142.7	42.0	9.2
Summary	42,628	94	58,121	112,019	0.001	114.3	26.7	11.0

Survey Strata 8 (38.5 - 39N, 74 - 74.5W)

Mission	Images	Total Scallops	Survey Length (m)	Survey Area (m^2)	Scallop Density (scallops/m^2)	Mean Shell Height (mm)	Depth (m)	Near Bed Water Temp (^oC)
20110726_ScallopD1_M1	10,474	132	12,713	25,453	0.01	140.2	46.9	7.6
110726_ScallopD1_DV44_M3	12,035	113	15,913	31,101	0.01	136.2	48.8	7.4
110727_ScallopD2_R1_M1	11,097	18	12,127	23,612	0.00	141.4	40.7	9.0
110726_ScallopD1_DV2_M2	9,255	229	11,699	23,428	0.01	124.7	53.8	7.3
Summary	42,861	492	52,452	103,595	0.005	136.0	47.6	7.8

Table 2.4: Table of scallop survey mission data for survey strata 7 and 8.

Mission Name	Scallops	Mean (mm)	<70mm (%)	70<Hs<101.6 mm (%)	>101.6 mm (%)	Median (mm)	Standard Deviation (mm)	Skewness	Kurtosis	Survey Strata
110708SM2	707	137.6	0	0.8	99.2	139	16.2	-0.4	3.79	1
110708ScallopD2M4	894	138.6	0	0.3	99.7	140.1	15.7	-0.43	3.32	1
110708ScallopD2	2,172	136.4	0	0.9	99.1	137	15	-0.28	3.88	1
110708ScallopDvoraRun	3,706	116.8	0.1	11.5	88.4	114.8	19.1	0.25	2.64	2
110709ScallopD3M1	1,365	114.1	0.1	11.9	88.1	112.1	17.3	0.4	3.2	2
110709ScallopDay3DV119	1,850	115.7	0.1	9	91	112.8	17.6	0.55	3.22	3
110710DV117	422	112.8	1.7	17.1	81.3	112.9	20.5	-0.12	2.68	3
110710DV118	227	126.9	0	4	96	127.8	17.1	-0.16	3	3
110710M1ArtiesRun	1,403	117.4	0.6	9.7	89.7	117.6	17.6	-0.19	3.55	3
110711DV115	82	120	4.9	3.7	91.5	126.7	21.1	-1.78	6.2	4
110729D4DV0113M4	16	126.9	0	6.2	93.8	120.9	19.4	-0.1	1.92	4
110728D3R8M5	508	131.1	0.6	10.4	89	135.8	25.9	-0.49	2.77	5
110729D4DV0105M2	212	146.8	0.5	0.9	98.6	148.5	17.5	-0.72	5.24	5
110729D4DV0106M1	801	131.9	0	4.7	95.3	134.4	19.5	-0.37	2.86	5
110729D4DV0112M3	331	135	0	1.8	98.2	135.5	16.5	-0.52	3.88	5
110728D3DV062M3	506	135.9	0.4	3	96.6	138.7	19.6	-0.82	4.18	6
110728D3DV063M4	140	136	2.9	7.1	90	143.4	31.4	-0.5	2.64	6
110728D3R6M1	523	145.2	0	1.9	98.1	145.7	18.2	-0.66	4.85	6

Table 2.5: Scallop shell height data and distribution statistics for each digital image survey within survey strata 1-6.

Mission Name	Scallops	Mean (mm)	<70mm (%)	70<Hs<101.6 mm (%)	>101.6 mm (%)	Median (mm)	Standard Deviation (mm)	Skewness	Kurtosis	Survey Strata
110727D2R2M2	3	104.5	0	33.3	66.7	113.3	21.3	-0.63	1.5	7
110727D2R3M3	1	97.2	0	0	100	97.2	0	-	-	7
110727D2R4M4	0	-	-	-	-	-	-	-	-	7
110727D2R5M5	0	-	-	-	-	-	-	-	-	7
110728D3R7M2	90	142.7	1.1	2.2	96.7	142.2	21.1	-0.58	6.24	7
110726ScallopD1DV2M2	229	124.7	0	6.6	93.4	115.2	26.6	0.63	2.5	8
110726ScallopD1DV44M3	113	136.2	0.9	8	91.2	140.7	31.9	-0.12	2.2	8
110726ScallopD1M1	132	140.2	0	4.5	95.5	143	25.5	-0.31	2.39	8
110727ScallopD2R1M1	18	141.4	5.6	0	94.4	149	27.9	-1.14	4.4	8
Season Summary	16451	125.4	0.2	7.1	92.7	126.6	21.4	-0.02	2.71	8

Table 2.6: Scallop shell height data and distribution statistics for each digital image survey within survey strata 7 and 8.

Mission	Harvestable Biomass (g)	Total Biomass (g)	Percent Harvestable
110708SM2	37,349	37,722	99.0
110708ScallopD2M4	48,095	48,479	99.2
110708ScallopD2	113,604	114,306	99.4
110708ScallopDvoraRun	110,016	124,244	88.5
110709ScallopDay3DV119	54,834	61,863	88.6
110709ScallopD3M1	36,182	42,049	86.0
110710DV117	12,984	15,216	85.3
110710DV118	10,413	10,817	96.3
110710M1ArtiesRun	48,334	52,799	91.5
110711DV115	3,228	3,313	97.4
110726ScallopD1DV2M2	8,438	9,072	93.0
110726ScallopD1DV44M3	5,898	6,165	95.7
110726ScallopD1M1	7,414	7,543	98.3
110727D2R2M2	87	101	85.7
110727D2R3M3	0	20	0
110727D2R4M4	0	0	0
110727D2R5M5	0	0	0
110727ScallopD2R1M1	1,120	1,126	99.5
110728D3DV062M3	2,5087	25,580	98.1
110728D3DV063M4	7,194	7,405	97.1
110728D3R6M1	33,760	33,988	99.3
110728D3R7M2	5,541	5,569	99.5
110728D3R8M5	24,492	25,532	95.9
110729D4DV0105M2	15,472	15,513	99.7
110729D4DV0106M1	40,399	41,509	97.3
110729D4DV0112M3	17,597	17,782	99.0
110729D4DV0113M4	826	844	97.9
Total	**668362**	**708552.6**	**94.3**

Table 2.7: Biomass and harvestable biomass calculated for each mission based on scallop shell height and water depth.

2.4.9 Mid-Atlantic Bight Summary

A total of 27 AUV based survey were completed in July 2011 within the Mid-Atlantic Bight. The AUV surveyed 312 km of seafloor, producing over 250,000 images that covered 600,000 m^2. The overall density found for the region was 0.027 scallops/m^2. The scallop population was not evenly distributed; rather 78% of the population was concentrated to the northeastern survey strata (1-3). Scallop densities decrease rapidly to the south starting at stratum 4. Scallop densities were also found to be related to near bed water temperature (Figure 2.18). The highest densities occurred at a temperature of 9°C, while densities approached 0 below 7°C and above 13°C. The same relationship holds for depth, as near bed water temperature was found to directly correlate to depth for all mission sites (Figure 2.19).

Digitally sized sea scallop shell heights showed that all survey sites contained mature scallop populations. Figure 2.20 shows the shell height distributions at each mission location. Recruit sized scallops only accounted for 0.2% of observed scallops. Shell height distributions for the scallop population northeast of the Hudson Shelf Valley (strata 1 – 3) were found to have a higher proportion of sublegal (70 mm < $H_s < 101.6$ mm) scallops than southern missions. The reason for this could be due to the presence of a younger scallop class in the northeastern strata or due to higher dredging efforts by fishermen causing a bias towards scallop sizes that are too small to be captured by a commercial dredge. The effects of dredging on a scallop size class will be explored in Chapter 3. The shell height distribution skewness for the entire Mid-Atlantic Bight was -0.02, which is a near symmetrical distribution. This is illustrated in Figure 2.21. A correlation between shell height and scallop density was not found to exist (Figure 2.22).

Bed type was classified for every image containing a scallop as part of thee counting process. It was found that 98.61% of all identified scallops occurred on a bed type classified as sandy (featureless), 1.27% occurred on shell hash, 0.001% on ripples, and only 2 scallops were identified as occurring on mound topography. Mean shell height for sandy bottom type was found to be 125 mm, 140 mm for shell hash, 130 mm for ripples, and 150 mm for mound topography (see Figure 2.23).

Season Summary	
Season Total Missions:	**27**
Season Total Mission Lines:	**189**
Season Total Mission Images:	**249,564**
Season Total Line Length (m):	**312,814**
Season Total Sea Scallop Abundance:	**16,451**
Season Total Area Surveyed (m^2):	**599,675**
Season Total Density (Scallops/m^2):	**0.027**
Season Total Avg Shell Height (mm):	**125.2**
Season Total Scallop Biomass (g):	**708,553**

Table 2.8: 2011 sea scallop survey season summary.

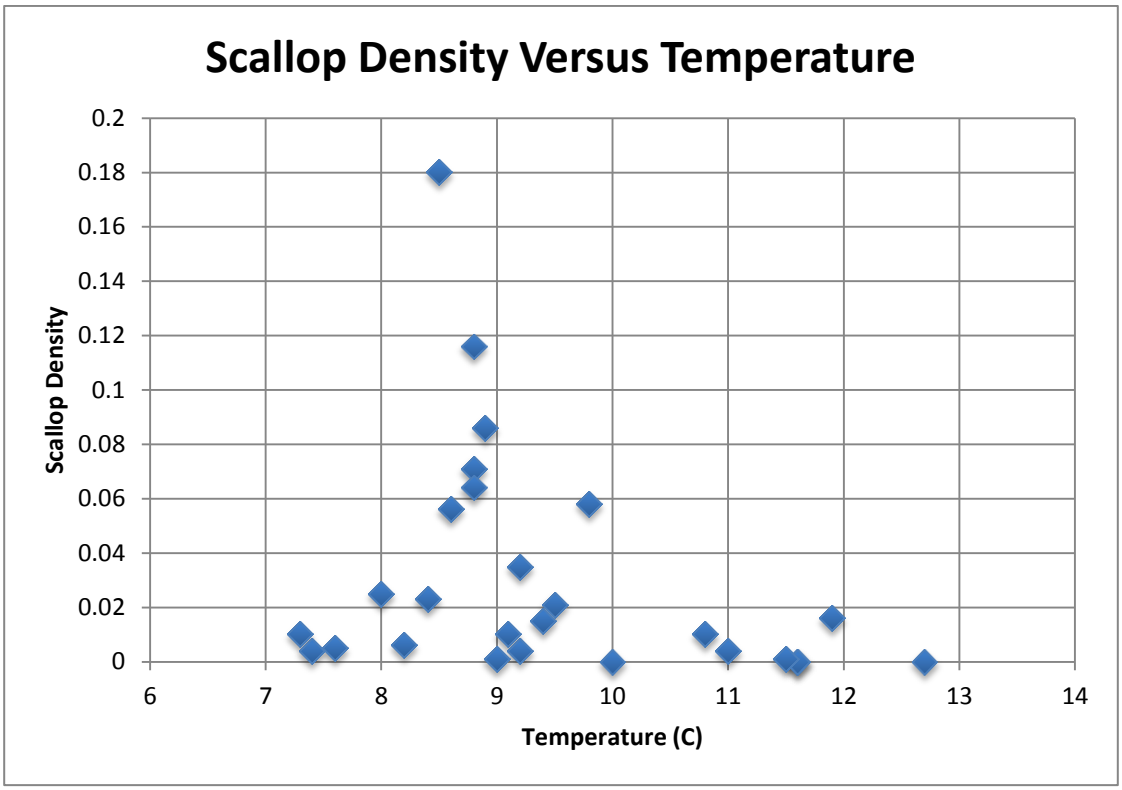

Figure 2.18: Mission scallop densities compared to near bed (altitude of 2 m) water temperature. Highest densities occur near 9 degrees Celsius.

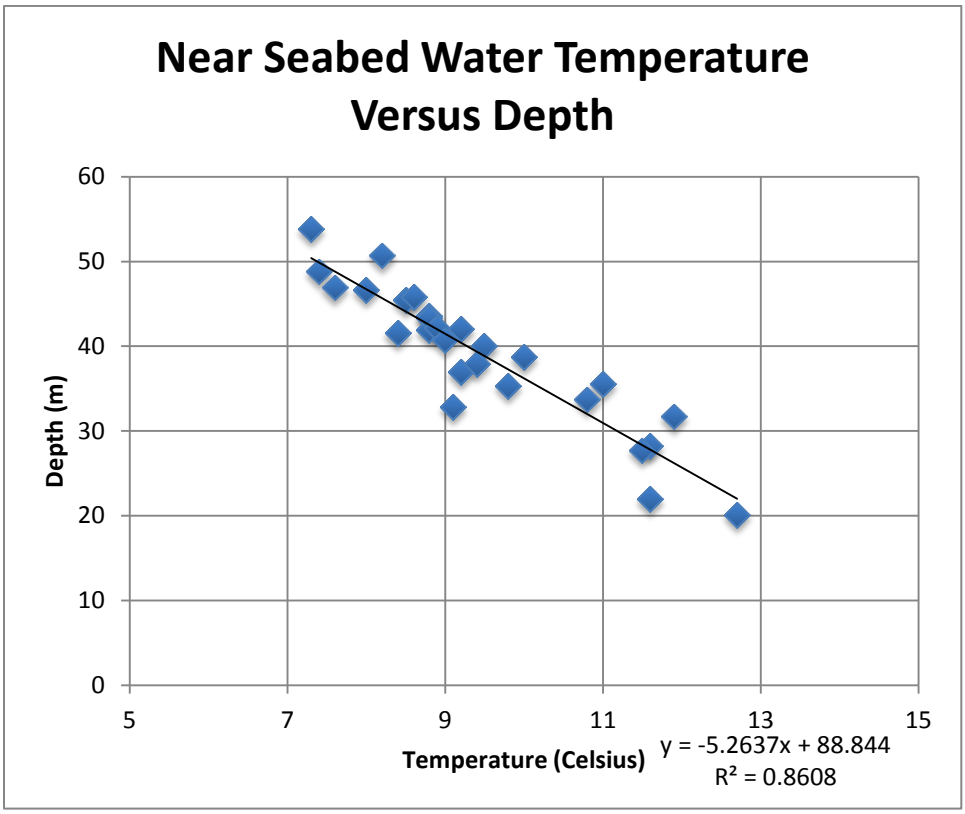

Figure 2.19: A plot of near bed temperature and depth for each survey showing a correlation between temperature and depth.

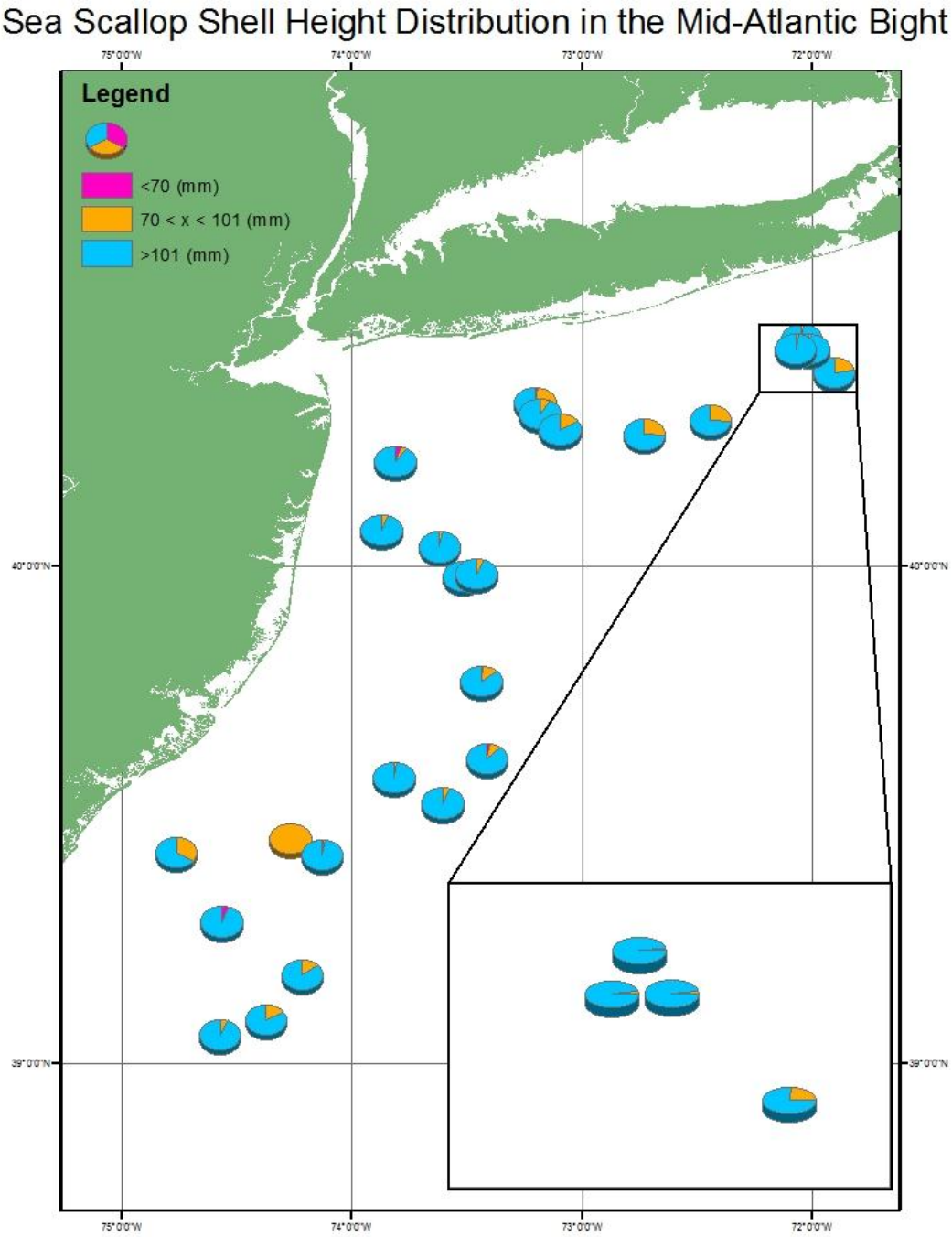

Figure 2.20: Sea scallop shell height distributions for the Mid-Atlantic Bight

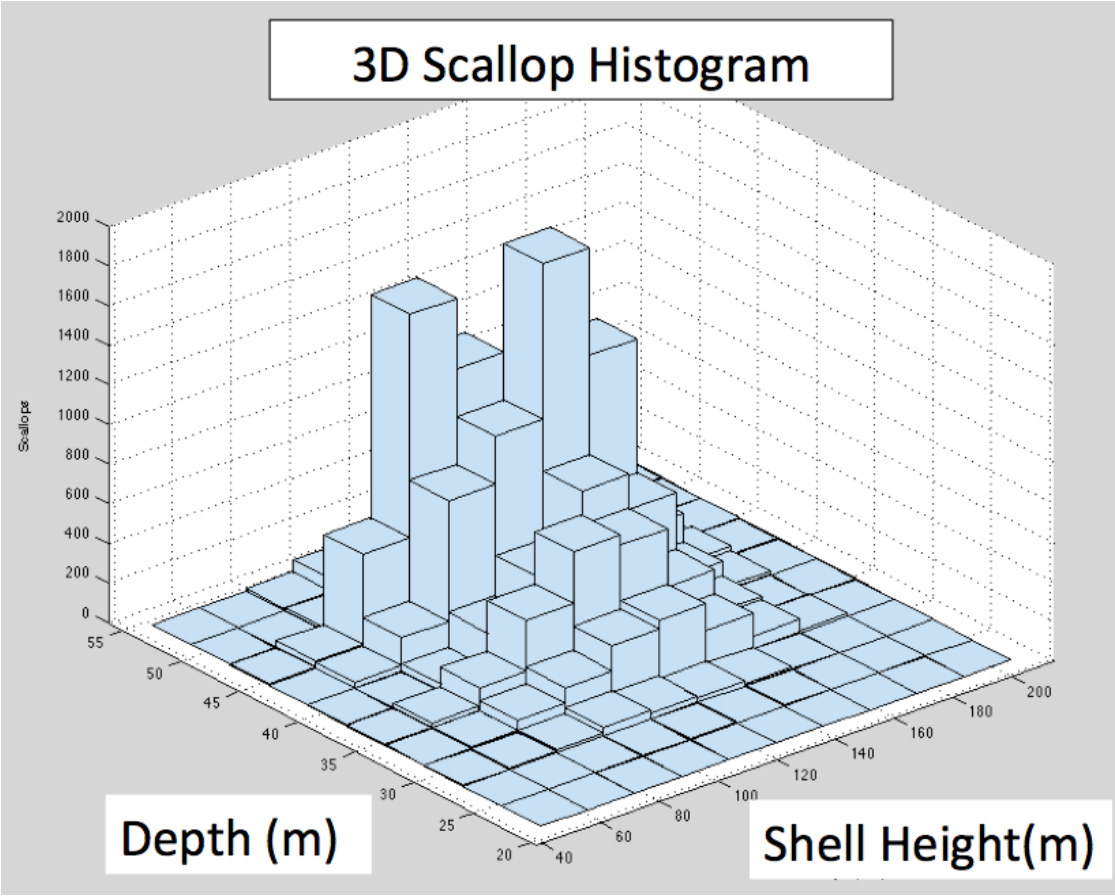

Figure 2.21: A 3-dimensional variogram comparing shell height distribution to depth. Shell heights are negatively distributed below depths of 45 m.

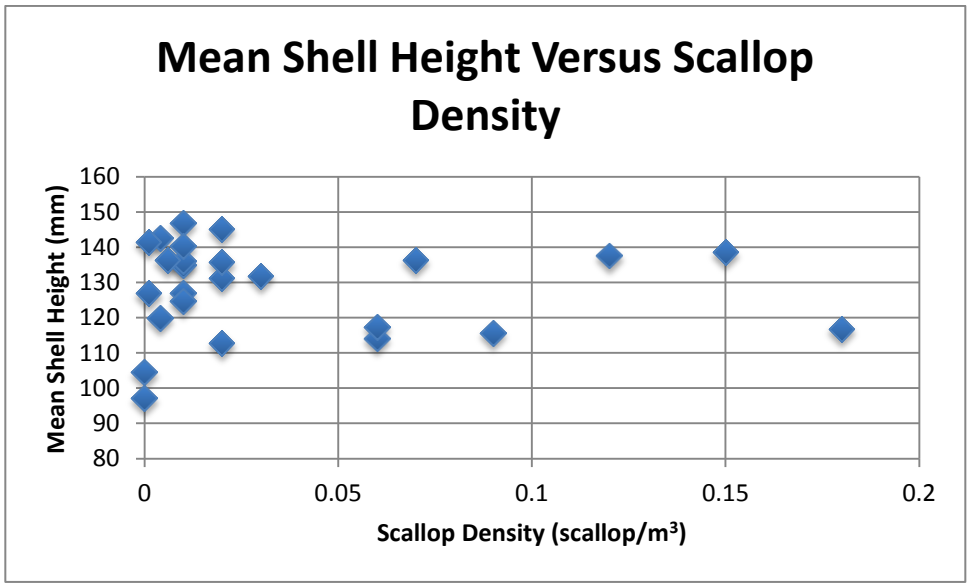

Figure 2.22: Plot of digitally measured mean shell height versus scallop density. A relationship was not found to exist.

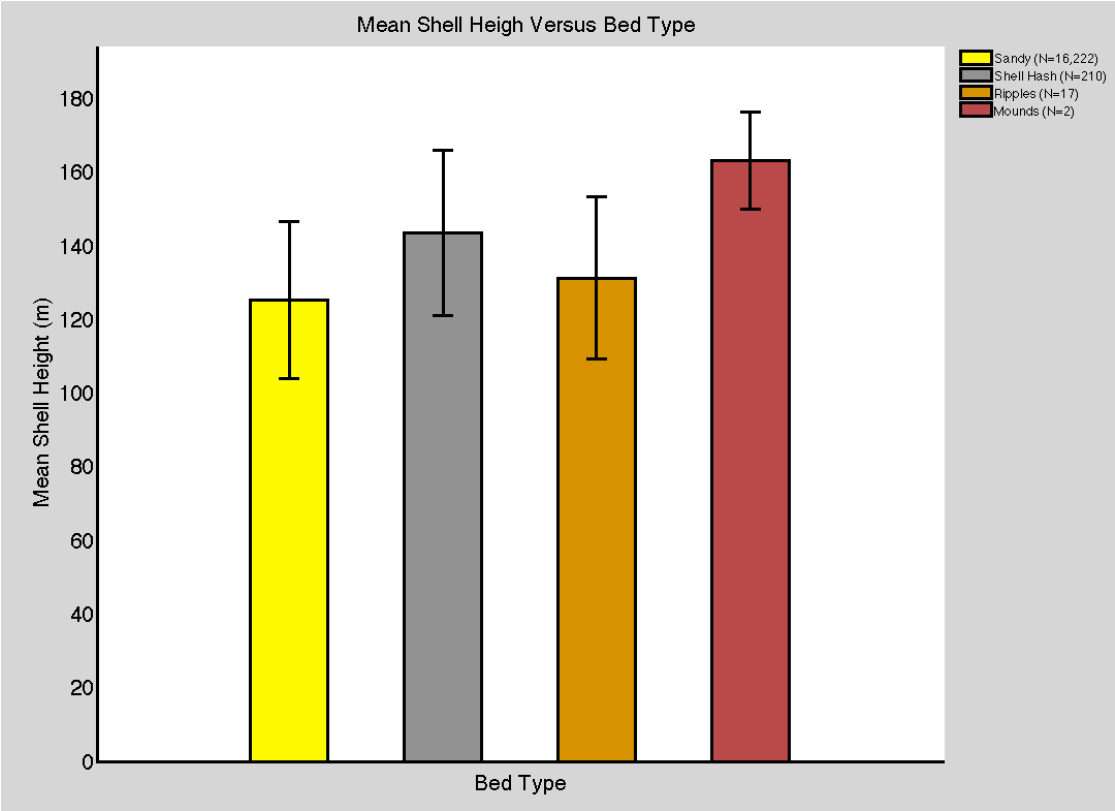

Figure 2.23: Bed type distribution of sized scallops identified in seafloor photographs. 98.6% of all identified scallops occurred on a sandy classified bed.

2.4.10 Simulation of Abundance Results

A unique aspect of this study was that 100% of images were examined and analyzed. The efficiency provided by the scallop sizing program and effort in training image analysts resulted in the 250,000 images being analyzed in 120 total man hours. To examine the effect of looking at various random subsets of the complete image database on the overall abundance estimate, a simulation was performed by repeatedly drawing (N=100 times) a random set of images from the entire database spanning the range from 1% up to 100% in 5 percentage increments (i.e. 1, 5, 10, 15, etc.) and calculating the normalized abundance relative to the value obtained from the analysis of all 100% images. The results are displayed in Figure 2.24, and illustrate the wide spread of estimates for analysis of small portions of the total database (portions below 15-20%) and the convergence that occurs as greater and greater portions of the full record are analyzed. This type of simulation is useful in helping to assess the potential uncertainty of analyzing only a subset of the images.

Furthermore, this simulation allows for the assessment of trade offs between the speed of analyzing a portion of the images versus analyzing every available image in terms of accuracy thresholds. By reconfiguring the simulation as shown in Figure 2.25, one can establish the minimum number of images that need to be analyzed for a given uncertainty tolerance. For example, a tolerance requirement of achieving results within 9 percent of the complete value can reasonably be expected from an analysis of 20% of the images, whereas achieving results within 5% requires analyzing 50% of the images.

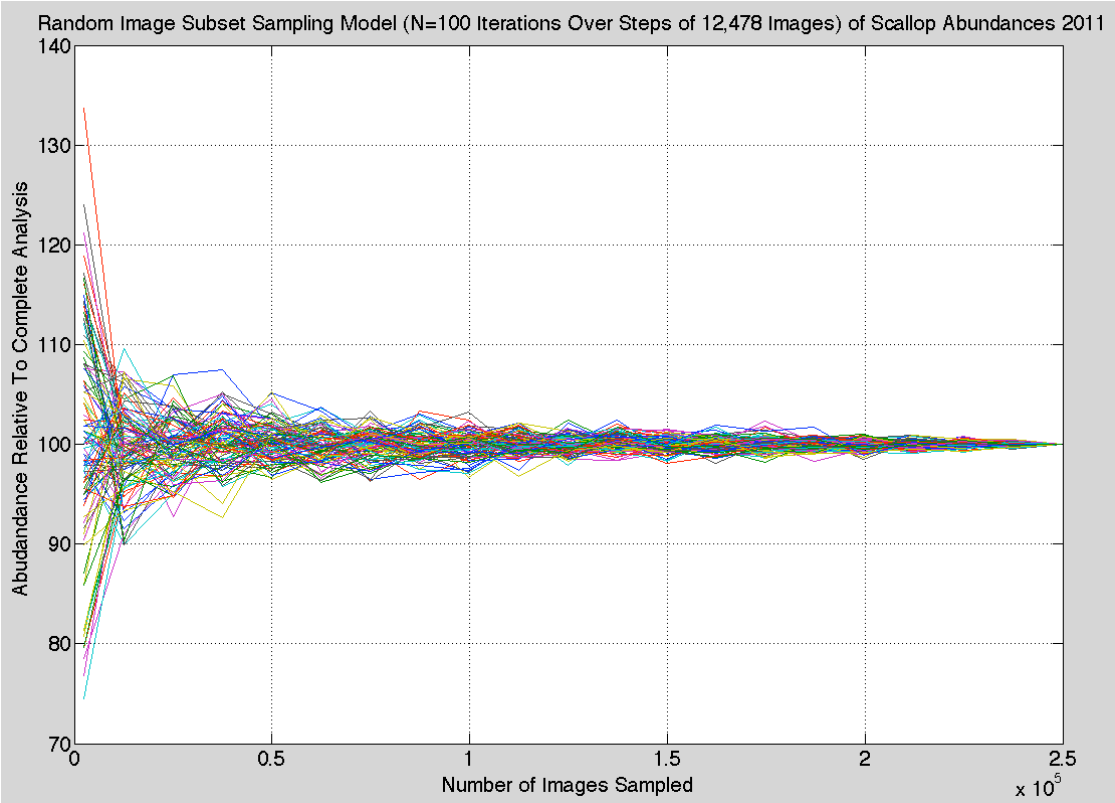

Figure 2.24: Results of Monte Carlo simulation. The response of the abundance estimate to the portion of the available images that are analyzed.

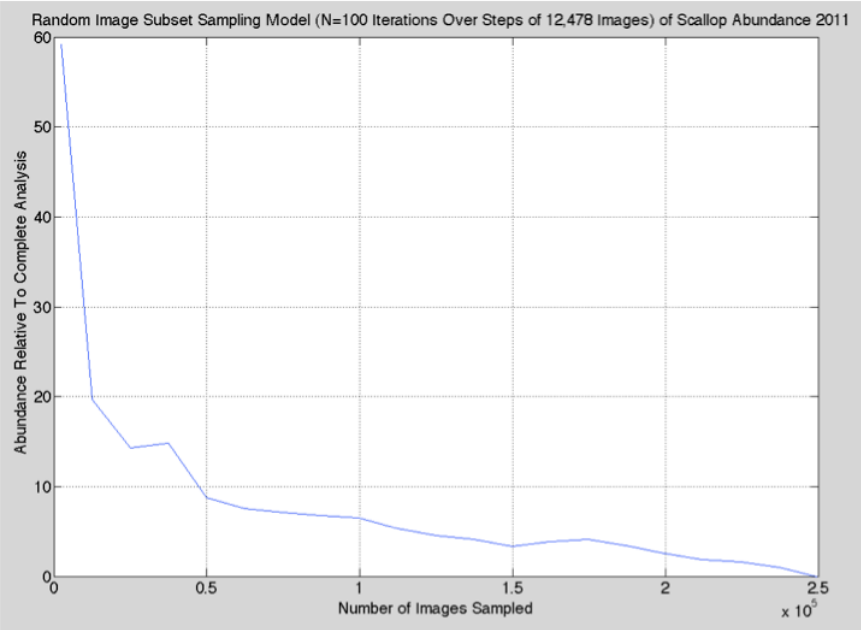

Number of Photos Examined	% Proximity to Complete Value
2496	59.2
12478	19.7
24956	14.3
37435	14.8
49913	8.8
62391	7.6
74869	7.1
87347	6.8
99826	6.6
112304	5.3
124782	4.6
137260	4.1
149738	3.3
162217	3.9
174695	4.1
187173	3.4
199651	2.6
212129	1.8
224608	1.6
237086	1.0
249564	0.0

Figure 2.25: Plot of relative accuracy of abundance estimate for a range of analyzed images.

2.4.11 Dredge Efficiency Analysis

At a select set of scallop survey sites, the AUV would begin a survey with a 1.5 – 3 km transect that was separate from the tightly spaced lawnmower survey pattern of the rest of mission, which was followed by a dredge tow using a New Bedford commercial scallop dredge. The purpose of the dredge tow was to compare image results of the first survey line with the coeval survey dredge line. From this, efficiencies for the New Bedford dredge could be calculated. Figure 2.26 compares the mean shell height from images to the mean shell height from manually sized scallops. Scallops that are dredged are sized using a 5 mm binned sizing chart. It is shown that shell height digital measurements are in agreement with manually sized measurements. Figure 2.27 shows the digital shell height distribution and dredged shell height distribution, showing that the AUV camera is able to capture a wider range of scallops due to more data points and because the commercial dredge is designed to only catch scallops >101.6 mm in size. Assuming the images have an efficiency of 1, it was found that the New Bedford scallop dredge had an efficiency of 0.60 on sandy bottom.

Mission Name	Image Measurement Size (+/- 5mm)	Dredge Measurement (+/- 5mm)	Difference
20110726_ScallopD1_M1	140	133	7
110726_ScallopD1_DV44_M3	136	144	8
110728_D3_DV062_M3	136	124	12
110728_D3_DV063_M4	136	126	10
110729_D4_DV0105_M2	147	135	12
110729_D4_DV0106_M1	132	122	10
110729_D4_DV0112_M4	135	127	8
110726_ScallopD1_DV2_M2	125	129	4
		Mean:	8.9
		Standard Deviation:	2.7

Figure 2.26: Comparison of AUV image measured shell heights and dredge measured shell heights for the same survey line.

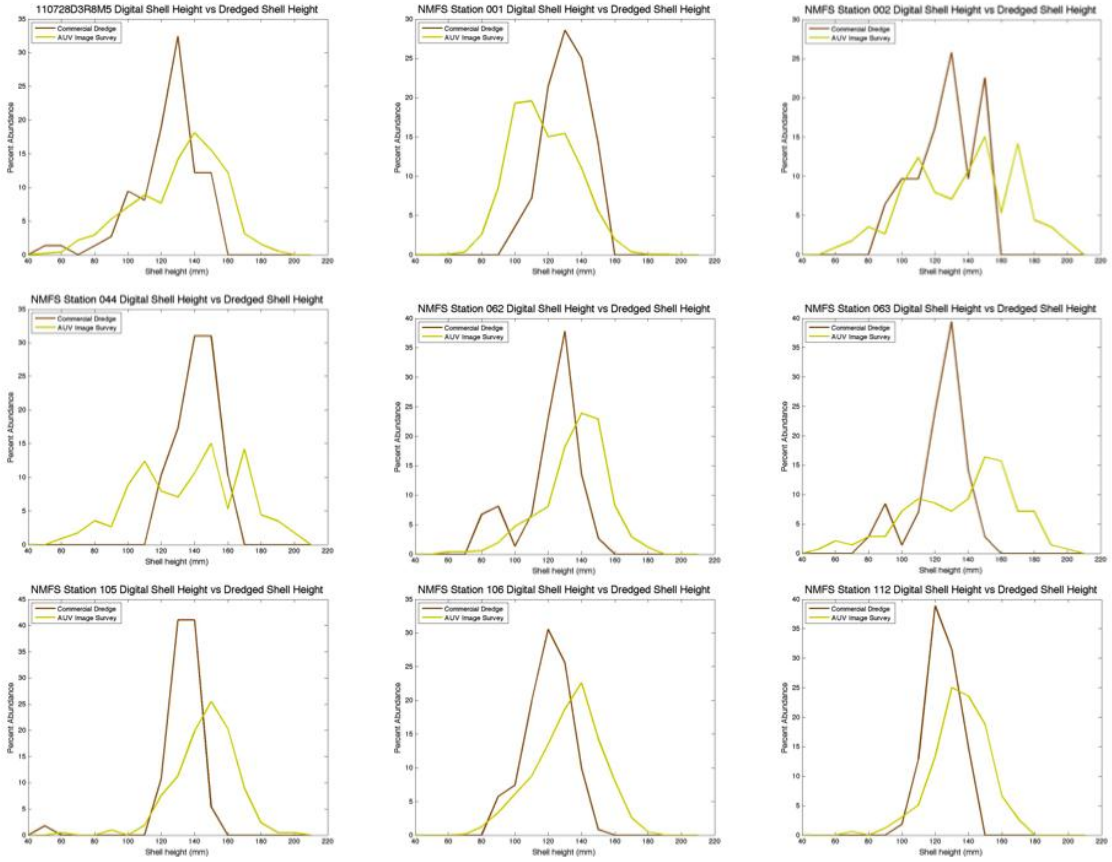

Figure 2.27: Comparison of AUV image shell height distributions and dredged shell height distributions for the same survey line.

2.5 Discussion and Conclusion

2.5.1 AUV as a Survey Platform

This is the first study to date to perform a sea scallop stock assessment with the use of an AUV. It has been shown that the AUV can work in tandem with the current stock assessment methodologies; namely, producing results in agreement with dredging enumeration and sizing and even calculating the harvest efficiency of dredges. The AUV also presents numerous advantages that can be exploited in quantifying the sea scallop population. Images of the seafloor allows for unprecedented analysis of the small and large scale spatial structuring of the sea scallop population. The suite of acoustic mapping sensors on the AUV allows for mapping and classification of large swaths of sea scallop strata, and georeferenced images provide ground-truthing to the acoustic data. The rapid deployment and highly accurate navigation system of the AUV allows for more efficient and repeatability data acquisition compared to other current image capture survey techniques.

2.5.2 Sea Scallop Stock Assessment

The sea scallop population within the shallow survey grounds of the Mid-Atlantic Bight is most densely concentrated off the shores of Long Island. There is a noticeable change in shell height distribution and scallop densities between the Long Island strata and the strata off the coast of New Jersey and Delaware. The increased population in this region has been hypothesized to be due to a combination of seeding from the Georges Bank area, and because there is no major influx of fresh water to interrupt the transport of larvae (Law, 2007).

The results of this study have shown that the recruit population in the Mid-Atlantic Bight was extremely low during 2011, and that size classes had grown to be

super-mature. NMFS began to account for this situation in 2012 by closing the Elephant Trunk Access Area (partially contained within survey strata 8) to protect a new population of small scallops. Nevertheless, it was found that the open access grounds contain an economically exploitable sea scallop population that with continued monitoring can remain sustainable.

Chapter 3

QUANTIFYING SEA SCALLOP FISHING EFFORT AND A LOOK AT OTHER MID-ATLANTIC BIGHT EPIFAUNAL ORGANISMS

3.1 Introduction

This chapter is a continuation of the work done in Chapter 2 to further explore the behavior of the sea scallop, but also to briefly investigate the practices of the sea scallop fishermen through analysis of fishing and dredging effort. Additionally, it will be shown that the scallop survey seafloor images could be used to quantify and analyze other species of epifaunal organisms by looking at a subset of images from within the Elephant Trunk Access Area.

3.1.1 Closed Area

The purpose of this study is to take a cursory look at the effects that varied dredging effort has on the sea scallop and other epibenthic fauna within the Mid-Atlantic Bight. During the 1990s, it was discovered through stock assessments that the sea scallop (*Placopecten magellanicus*) population within the Mid-Atlantic Bight was being overfished. To counteract this problem, the major sea scallop fishing grounds were put on rotational closings. Once closed, a scallop fishing ground was off limits to commercial fishing. The combination of fishing ground closures and imposed yearly catch limits led to the rebound of the sea scallop populations (Murawski *et al.*, 2000).

During the 2011 AUV sea scallop survey, the Elephant Trunk access ground was closed. As a result, the area was off limits to all dredging activity with the exception of dredging performed for stock assessment purposes. Analysis of the side-scan backscatter data for all of the Mid-Atlantic Bight AUV scallop surveys from Chapter 2 revealed that the escarpment that is produced by the dragging of the dredge along the seafloor, known as a dredge scar, was identifiable and measureable (Appendix E and H). The epibenthic organisms residing on the seafloor, including sea scallops, sea stars, sponges, crabs, and skates, are captured by a trawling dredge. The organisms that are unintentionally caught are known as bycatch. Three of the sea scallop survey missions from Chapter 2 were within the Elephant Trunk Access Area, and therefore were found to have minimal area dredged. Three similar missions (depth, water temperature) were chosen from the remaining missions that had correspondingly high dredging effort (>18% area dredged in the side-scan mosaic), and that were outside of the closed access ground.

This study used an image survey method to compare non-dredged seafloor from within a protected closed area to missions that were found to be heavily dredged. The images were analyzed for a suite of marine species, but the focus was on the sea scallop and its predators: the rock crab (*Cancer irroratus)*, the common sea star (*Asterias spp.*), and the sand star (*Astropecten americnaus*). This study utilizes densities of organisms along with diversity analysis to explore non-dredged and dredged seafloor. In addition, dredged area and fishing effort data was used to explore the behavior of commercial fishing vessels and the implications to the Mid-Atlantic Bight sea scallop population.

3.1.2 Study Area

The research location for this study was chosen based upon previously collected data during July of 2011 within the Mid-Atlantic Bight. The Mid-Atlantic Bight is the geographic bend of shallow coastline along the eastern United States. It is officially defined as the area of the continental shelf from Cape Hatteras, North Carolina to Cape Cod, Massachusetts. The New York Bight is located within the greater Mid-Atlantic Bight, and encompasses the shores of New York and New Jersey.

Figure 3.1 shows a map of the Mid-Atlantic Bight. The yellow pins represent the locations that images were analyzed for this study. The northern three pins (Unprotected 1, 2, and 3) represent the unprotected (dredged) scallop fishing grounds within the New York Bight. The depth within the study area of the New York Bight ranged from 42 – 46 m. The southern three pins (Protected 1, 2, and 3) outside the mouth of Delaware Bay, reside within the then closed access scallop fishing grounds of the Elephant Trunk. The depth of the Elephant Trunk was similar to the protected area ranging from 47 m to 53 m. The environmental conditions (shown in Table 3.1) of the two sites were comparable, notably near bed water temperature, which only varied by 1°C between the sets of missions.

Mission Subset	Temperature (°C)	Salinity (ppt)	Depth (m)
U1	**8.9**	**33**	**42.1**
U2	**8.6**	**33**	**45.6**
U3	**8.5**	**33**	**45.4**
P1	**7.6**	**33**	**46.9**
P2	**7.3**	**33**	**53.8**
P3	**7.4**	**33**	**48.8**

Table 3.1 Environmental and bathymetric data for the dredged (U1, U2, and U3) and non-dredged missions (P1, P2, and P3).

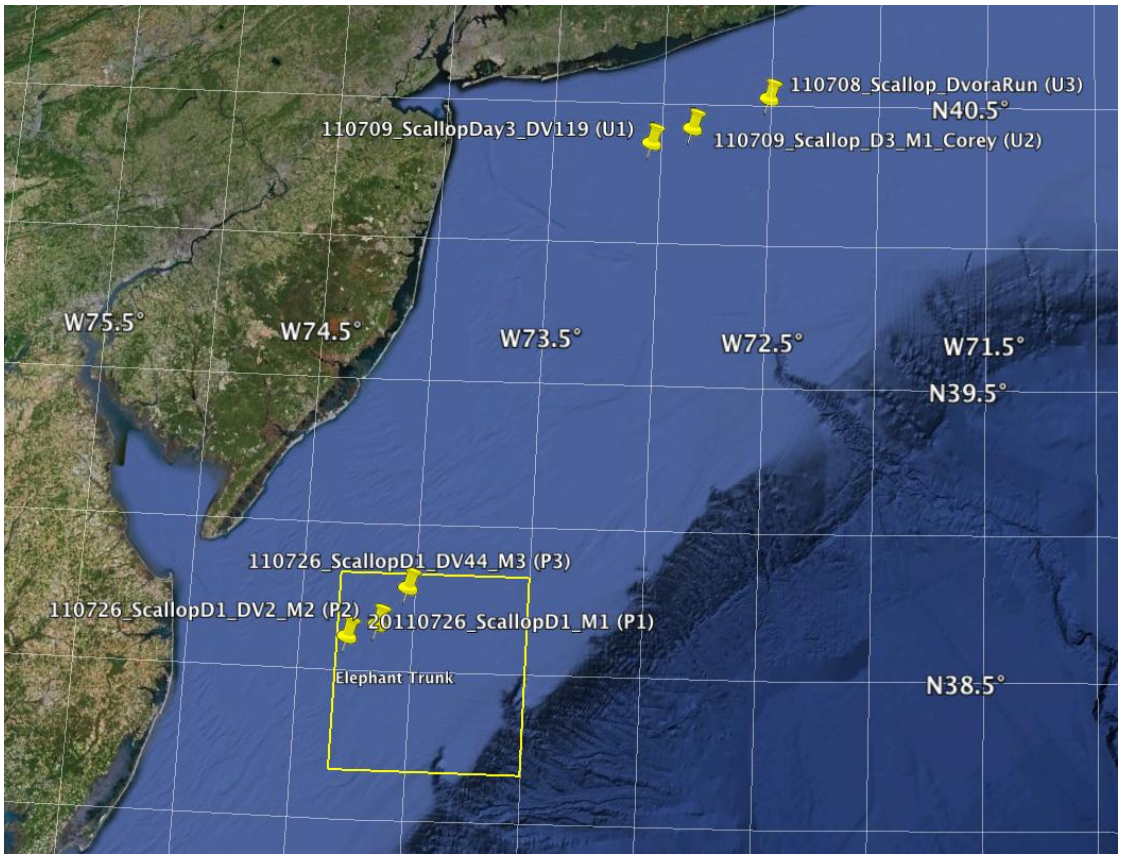

Figure 3.1: Study area of non-dredged (missions P1, P2, P3) versus heavily dredged (U1, U2, U3) sea scallop survey missions. Note that each mission is a subset of a sea scallop survey mission.

3.2 Methods

3.2.1 Image Analysis

Conventional marine stock assessment surveys are done utilizing a dredge or seining net. Recently, different image capture techniques are being employed to survey marine populations (Stokesbury, 2002). The image capture techniques offer a means of making stock assessments without having to cause potential harm to the organisms by capturing them, or altering the morphology of the seafloor (NMFS, 2010). Another advantage offered by utilizing image surveying is that it has been shown to have a theoretical efficiency of 1 (true value) compared to the 0.3 to 0.6 documented efficiency for dredging (NMFS, 2010).

The data collected for this study was done in July of 2011 in the Mid-Atlantic Bight. The F/V CHRISTIAN AND ALEXA served as the research platform and transportation between the sites. The data was collected over the course of two trips that spanned five days each at sea. The northern dredged sites were surveyed at the beginning of July, while the non-dredged Elephant Trunk sites were surveyed during late-July.

The benthic images gathered at the locations were done so utilizing an autonomous underwater vehicle (AUV). The AUV was programmed to run transects at an altitude of 2 m above the seafloor. The AUV performed up to eight transects at each location. Each transect was up to 1.5 km long.

The images gathered by the AUV were done so using an underwater camera that is attached to the nose of the vehicle. The lens of the camera has a horizontal viewing angle of 49.92°. The resolution of the camera is 800 x 600. Since the viewing angle of the camera lens was known, and the AUV ran the transects at a

constant height, it is possible to calculate the true dimensions of each pixel of an image. See Sections 2.3.1 – 2.3.4 for a more in depth discussion of the AUV camera system and image sizing methodology.

Each AUV mission ran within the locations yielded up to eight transects. Three missions were chosen from the protected and unprotected locations, and from them the images of two contiguous transect were analyzed. The transects analyzed were chosen by a random number generator, and the contiguous line (either the previous or next line) was chosen by coin flip. In total, 6,000 images were analyzed at each location (12,000 in total).

Two analyzers looked at the images from each site separately. For quality assurance purposes, a separate batch of 3,000 images was analyzed by the two analyzers and it was found that their results were in 93% agreement. Each image was viewed for the purpose of counting the number of specimens from 15 species (Table 3.2). Seven of the species (*Dipturus laevis, Raja eglantera, Leucoraja erinacea, Leucoraja garmani, Malacoraja senta, Amblyraja radiate,* and *Leucoraja ocellata*) were all skates, and were thus counted as one category. The other species counted separately were the common sea star (*Asterias forbesi*), the sand star (*Astropecten americanus*), the rock crab (*Cancer irroratus*), the summer flounder (*Paralichthys dentatus*), the sea scallop (*Placopecten magellanicus*), and the sulfur sponge (*Clionata celata*). The occurrence of a sea scallop in the same image as a sea star or rock crab was also recorded. Additionally, the sea scallops were sized within the images.

The densities for each species category were calculated separately for the protected and unprotected areas. The densities were found by dividing the total count

of an organism by the surveyed area. The surveyed area was calculated by multiplying the length of the transect by the mean image width for that transect

.

Common Name	Species Name
Common Sea Star	*Asterias forbesi*
Sand Star	*Astropecten americanus*
Monkfish	*Lophius sp.*
Rock Crab	*Cancer irroratus*
Skate	Family: Rajidae
Barndoor Skate	*Dipturus laevis*
Clearnose Skate	*Raja eglantera*
Little Skate	*Leucoraja erinacea*
Rosette Skate	*Leucoraja garmani*
Smooth Skate	*Malacoraja senta*
Thorny Skate	*Amblyraja radiate*
Winter Skate	*Leucoraja ocellata*
Summer Flounder	*Paralichthys dentatus*
Yellowtail Flounder	*Limanda ferruginea*
Sea Scallop	*Placopecten magellanicus*
Sulfur Sponge	*Cliona celata*

Table 3.2: Benthic organisms identified and enumerated from the 12,000 image subset.

3.2.2 Statistical Analysis

The data was then analyzed for both the heavily dredged and non-dredged groups utilizing three different statistical methods. The first method used was the Simpson Diversity Index:

$$D = \sum_{i=1}^{S} \frac{n_i(n_i - 1)}{N(N-1)} \qquad \text{Eq. 3.1}$$

Simpson's index is a measure of concentration of species (Pielou, 1966). N is the total number of organisms counted. The variable n_i represents the number of individuals per species. The summation is done for the total number of species (S) counted. The index measures the probability that two specimens chosen at random from the entire sample of all organisms will be of the same species (DeJong, 1975). *D* ranges from 0 to 1. As *D* approaches 1, the diversity of the sample decreases.

The second method used was the Shannon-Wiener index:

$$H = -\sum_{i=1}^{S} p_i \ln p_i \qquad \text{Eq. 3.2}$$

The Shannon-Wiener index is a measure of uncertainty (DeJong, 1975). *H* is a dimensionless number. An *H* of 0 represents a sample of no diversity, while a higher *H* represents increasing diversity. The variable p_i is estimated by calculating n_i/N. Again, the summation is done for the total number of species.

The third method used was a t-test:

$$t = \frac{\overline{x_1} - \overline{x_2}}{\sqrt{\left(\frac{\sum(x_1 - \overline{x_1})^2 + \sum(x_2 - \overline{x_2})^2}{N_1 + N_2 - 2}\right)\left(\frac{1}{N_1} + \frac{1}{N_2}\right)}} \qquad \text{Eq. 3.3}$$

The t-test is used to compare the same species among the protected area and the unprotected area. The variable $\overline{x_1}$ is the mean of the population of a species in the

protected area, and $\overline{x_2}$ represents the mean of the same species in the unprotected area. The N variables represent the number of missions in each sample. The pooled variance formula was chosen over the separate variance formula because the variances were different between the samples and the number of missions within each sample was equal.

3.2.3 Dredge Scar Area

Fishing effort was measured by two different proxies. The first proxy was the percent area dredged for a survey mission. In order to quantify the dredge scar area within each survey mission, the side-scan sonar backscatter data had to be processed within SonarWiz (see Section 2.3.6). Once a side-scan mosaic was produced, the path of the dredge scars was digitized using the digitizer tool in SonarWiz (Figure 3.2). The data file containing the path data of the digitized dredge scars was then exported as a .csv file. The data file was then imported into Matlab for parsing in order to calculate dredge path length. Total dredge path length (l_D) for the mission was then multiplied by 4.572 m (the width of a New Bedford commercial scallop dredge) to calculate dredge area. Percent area dredged (A_D) was then found by dividing the total dredged area by the product of 40 m (the across-track swath length of the side-scan sonar) and the total survey line length (l_T) for a mission.

$$A_D = \frac{4.572 l_D}{40 l_T} 100 \qquad \text{Eq. 3.4}$$

The second fishing effort proxy was NOAA vessel monitoring system (VMS) data. Each VMS data point consists of a latitude, longitude, and fishing time measured in hours. The data was binned into 3 minute squares. Fishing time is approximated by logging the length of time for a location that fishing vessels are traveling at trawl

speeds (1.5 and 5 knots). Each scallop mission was assigned the nearest neighbor effort value.

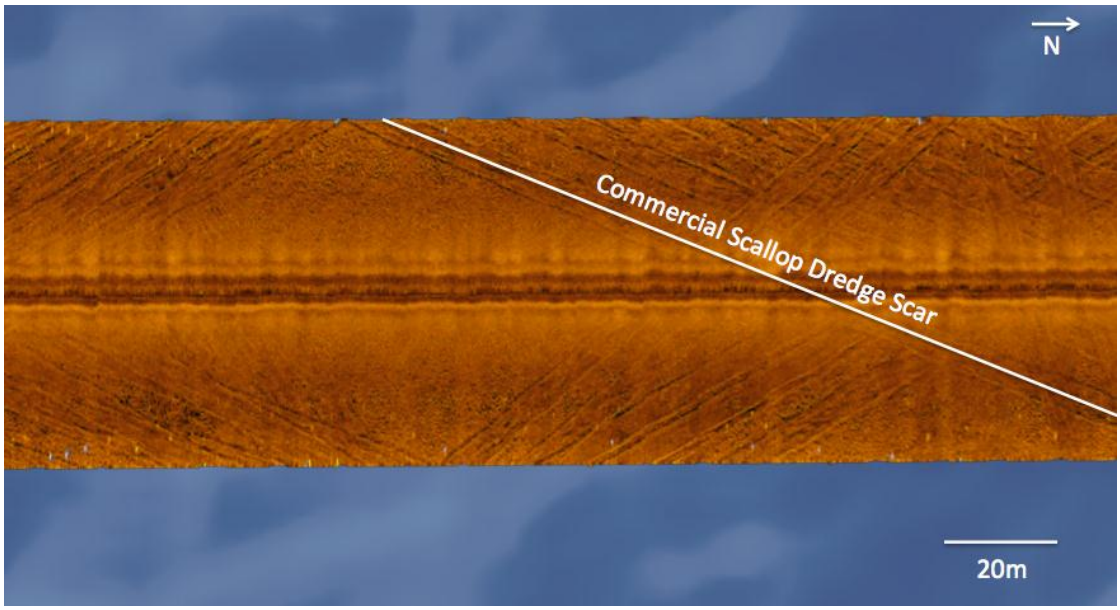

Figure 3.2: Section of a side-scan sonar mosaic of the seafloor from mission U2 (110709_Scallop_D3_M1_Corey) showing multiple intersecting commercial scallop dredge scars.

3.3 Results

3.3.1 Species Diversity Analysis

The calculated densities for each species from both the protected and unprotected areas are plotted in Figure 3.3. Note that the missions in this study, U1-3 and P1-3, are just subsets of larger sea scallop survey missions from Chapter 2; therefore the scallop densities will vary from the parent mission data presented in Chapter 2. The closed area missions had the highest abundance of surveyed organisms with a total of 37,770 organisms compared to the unprotected area with 6,280 organisms. The majority of the population in the closed area was composed of sand stars (95% of all organisms), which also had the highest density amongst all of the data. The rock crab and common sea star densities were also higher in the protected area versus the unprotected area. The sea scallops had a higher density of 0.1934 scallops/m^2 in the unprotected area compared to the Elephant Trunk sea scallop population. The common sea star remained almost constant at densities of 0.0021 and 0.0026 sea stars/m^2.

Table 3.3 shows the calculated Simpson's diversity indices and Shannon-Wiener indices calculated for both study groups. The Simpson's diversity index was greater than 0.77 in both instances, showing that there was little diversity between the samples. The Shannon-Wiener index was 0.56 for the unprotected area and 0.25 for the protected area. The low Shannon-Wiener values are in agreement with the Simpson's diversity indices. The low diversities are likely due to the overwhelming sea star population in the protected area and the high sea scallop population in the unprotected area, suggesting that a species will take a dominant position whether the area is heavily dredged or protected.

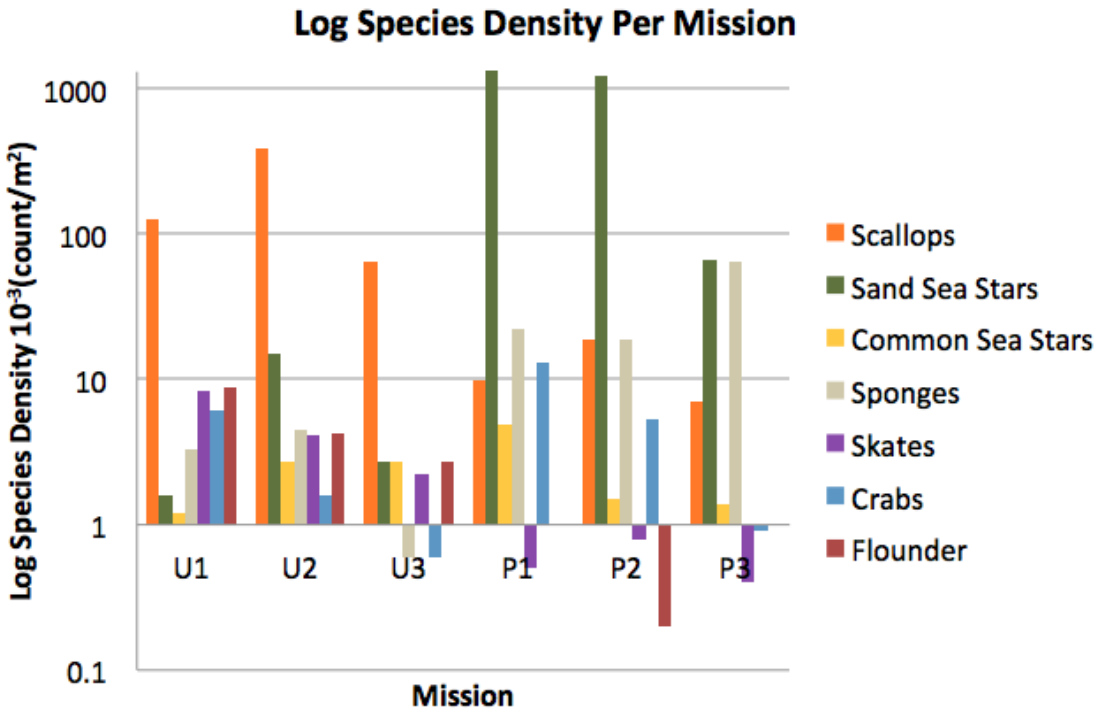

Figure 3.3: Log plot of the benthic organism species densities for each protected (P1, P2, P3) and unprotected (U1, U2, U3) missions. The relationship of scallop densities and sand sea star densities are inversed from protected to unprotected missions. Note the density units are 10^{-3} of the y-axis value.

Sample	Simpson's Diversity	Shannon-Weiner
U1	0.48	1.13
U2	0.86	0.38
U3	0.73	0.67
U (all)	0.78	0.56
P1	0.95	0.15
P2	0.93	0.19
P3	0.44	0.96
P (all)	0.90	0.25

Table 3.3 Simpson's Diversity and Shannon-Wiener Indices for the dredged (U1-3) and non-dredged missions (P1-3). Simpon's Diversity values approaching 1 represent a lower diversity. Shannon-Weiner values approaching 0 represent a lower diversity.

Organism	t-test	p
Sand Star	1.93	>0.1
Common Sea Star	0.43	>0.1
Crabs	0.90	>0.1
Flounder	5.76	<0.01
Skates	2.42	<0.1
Sponges	2.14	<0.1
Scallops	2.79	<0.05
Total Organisms Counted	1.68	>0.1
Scallop Size	3.88	<0.05
Simpson's Diversity	1.30	>0.1
Shannon-Weiner	0.86	>0.1

Table 3.4: T-test analysis of each identified species between the dredged (U1-3) and non-dredged (P1-3) missions. Degrees of freedom is 4 (6 missions – 2). p is probability that the difference observed in species densities between the dredged and non-dredged areas is by random chance. The threshold for $p<0.1$ is $t \geq 2.13$ and for $p<0.05$, $t \geq 2.78$.

Student's t-tests were done on the separate species, the Simpson's diversity index, and the Shannon-Wiener index (Table 3.4). The t-tests show that there is $p < 0.1$ for the skate and sponge populations, showing that there is statistical evidence that the differences observed between the protected and unprotected populations for those species were not by chance. The flounder population was found to have the highest confidence level with $p < 0.01$. The statistical analysis of the Simpson's and Shannon-Wiener diversity indices have $p > 0.1$, meaning that the results of those studies are not statistically significant. T-test analysis of the mission scallop densities was 2.79 ($p < 0.05$). The mean scallop size was larger in the protected area and the t-test shows that there is >95% confidence that the difference in shell heights between the two mission is not by chance. The potential causes for the shell height difference are: biasing of the population due to harvesting by size-selective dredges, two different scallop size classes inhabiting the unprotected and protected sites, differing availability or competition for food (phytoplankton), or predation by other benthic organisms.

3.3.2 Sea Scallop Fishing Effort

The results of the side-scan sonar dredge area analysis are included in Table 3.5. Dredge area percentages varied from 0% to 38%. The more densely dredged missions were concentrated in survey strata 1 – 3. Survey stratum 2 was heavily dredged, while strata 1 and 3 both had missions with near 0 dredged area percentages. The southern strata did not show evidence of consistent dredging efforts by scallop vessels. The missions in the Elephant Trunk were found to have near 0 (<2%) dredge scar area, which was expected as it was a more limited area. The dredge scar from the NMFS survey dredge was viewable in the side-scan sonar mosaic for mission P2

(110726_ScallopD1_DV2_M2). The NMFS survey took place in May 2011, which shows that a dredge scar can remain for at least 3 months.

Figure 3.4 plots the relationship between the image survey calculated scallop densities and the dredge scar analysis. The plot gives insight into the resource allocation methodology of the fishermen. Considerable dredging effort (>15% area dredged) occurs for areas with a scallop density greater than 0.06 scallops/m^2.

The size selectivity of commercial scallop dredges was found to have an effect on shell height distributions for the scallop missions. Figure 3.5 shows that for missions that had non-trivial seafloor dredging (>5% area dredged), there exists an inverse relationship between dredging and mean shell height. Comparing the image survey shell height distribution statistics to the dredge data reveals that increased dredging positively skews the distributions (Figure 3.6).

The VMS data is plotted in Figure 3.7. Vessel fishing efforts were found to be parallel to the depth contours. North of the Hudson Shelf Valley, fishing effort is concentrated between the 32 m and 47 m depth contours off of Long Island. South of the Hudson Shelf Valley, concentrated fishing effort trends southward to the east of the 47 m depth contour. The map reveals that sea scallop survey strata 4-7 are areas of low fishing effort. Fishing effort was found to correlate to scallop density (Figure 3.8), which aligns with the expected conclusion that fishing vessels will allocate increased time and effort to higher density scallop strata.

A comparison of the two fishing effort proxies was done in Figure 3.9. It was found that there exists an exponential relationship between VMS fishing effort and the side-scan sonar dredge area method. The reason for the exponential relationship rather than a linear relationship may be due to the VMS data integrating over the entire year,

including time after this study was conducted. The dredge scars would not have existed at the time of the side-scan surveys. This could have been the cause of the high fishing effort at low percent area dredged outliers on the plot.

Mission Name	Survey Strata	Scallop Density (Scallop/m^2)	Dredge Area %	Fishing Effort (hours)
110708SM2	1	0.12	17.5	33.3
110708ScallopD2M4	1	0.15	22.2	37.5
110708ScallopD2	1	0.07	0.4	33.3
110708ScallopDvoraRun (U3)	2	0.18	18.3	83.6
110709ScallopD3M1 (U2)	2	0.06	38	195
110709ScallopDay3DV119 (U1)	3	0.09	26.4	314
110710DV117	3	0.02	1.3	0.5
110710DV118	3	0.01	1.6	1
110710M1ArtiesRun	3	0.06	27.7	265
110711DV115	4	0.004	1.5	7.4
110729D4DV0113M4	4	0.001	2.7	0.01
110728D3R8M5	5	0.02	2.6	3.6
110729D4DV0105M2	5	0.01	4.7	2.3
110729D4DV0106M1	5	0.03	7	4.3
110729D4DV0112M3	5	0.01	1.4	2.6
110728D3DV062M3	6	0.02	0.2	8.9
110728D3DV063M4	6	0.01	12	32
110728D3R6M1	6	0.02	2.9	1.8
110727D2R2M2	7	0	0.5	0.5
110727D2R3M3	7	0	0	0.9
110727D2R4M4	7	0	0.3	0.5
110727D2R5M5	7	0	0.2	0.1
110728D3R7M2	7	0.004	0.1	2.6
110726ScallopD1DV2M2 (P2)	8	0.01	2.1	85
110726ScallopD1DV44M3 (P3)	8	0.006	1.7	37
110726ScallopD1M1 (P1)	8	0.01	0.7	30
110727ScallopD2R1M1	8	0.001	0.9	1.5

Table 3.5: Results of the dredge scar area analysis and vessesl monitoring system nearest neighbor values.

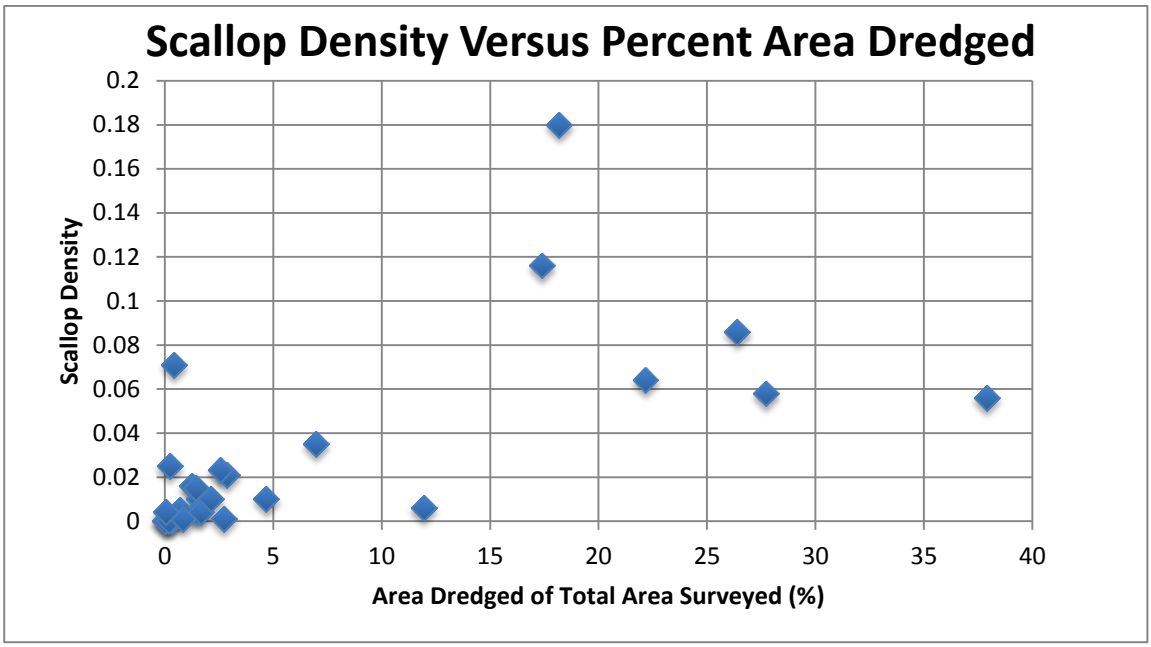

Figure 3.4: Plot of dredged seafloor area versus scallop density. The plot shows that fishing vessels will allocate considerable dredging effort (>15% area dredged) when the scallop density is greater than 0.06 scallops/m^2

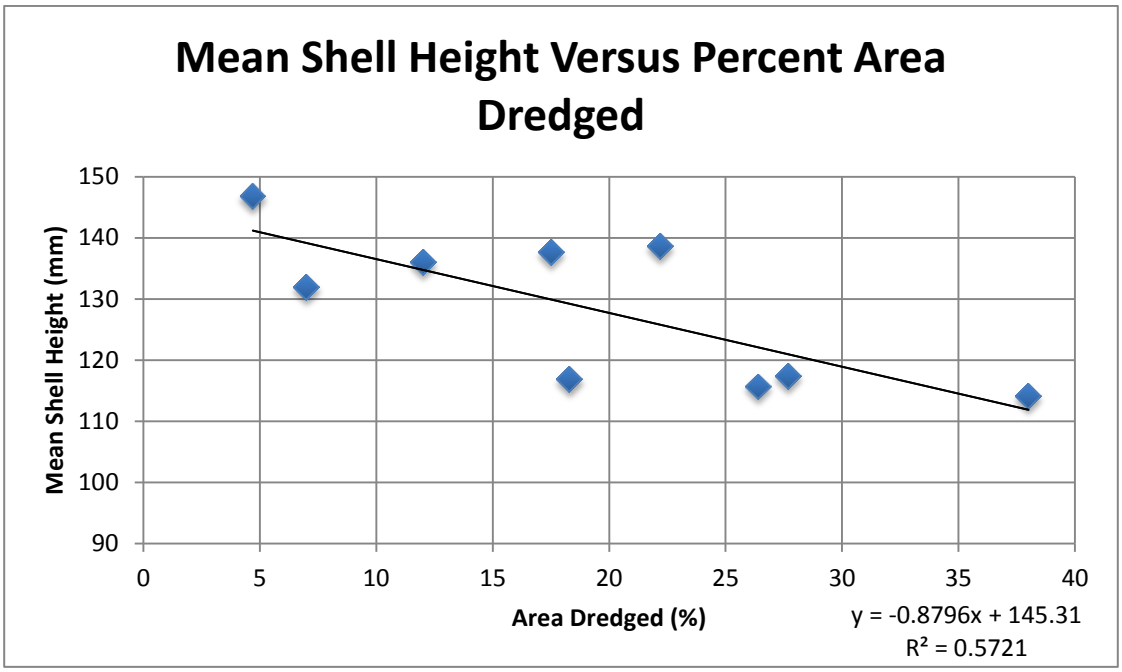

Figure 3.5: A plot showing the inverse relationship that exists between mean sea scallop shell height and dredging for scallop missions that showed minimal dredging effort (>5% area dredged).

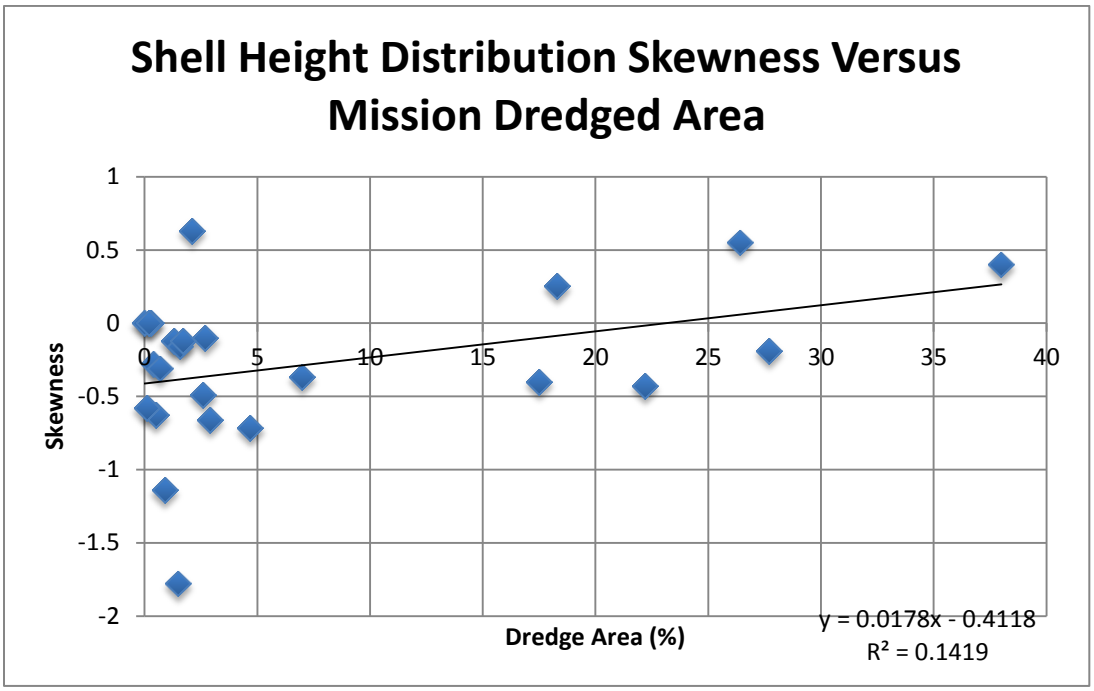

Figure 3.6: Plot of shell height distribution skewness compared to seafloor dredge area. Increased dredging shifts the shell height distribution more positive due to size selectivity of the commercial scallop dredge.

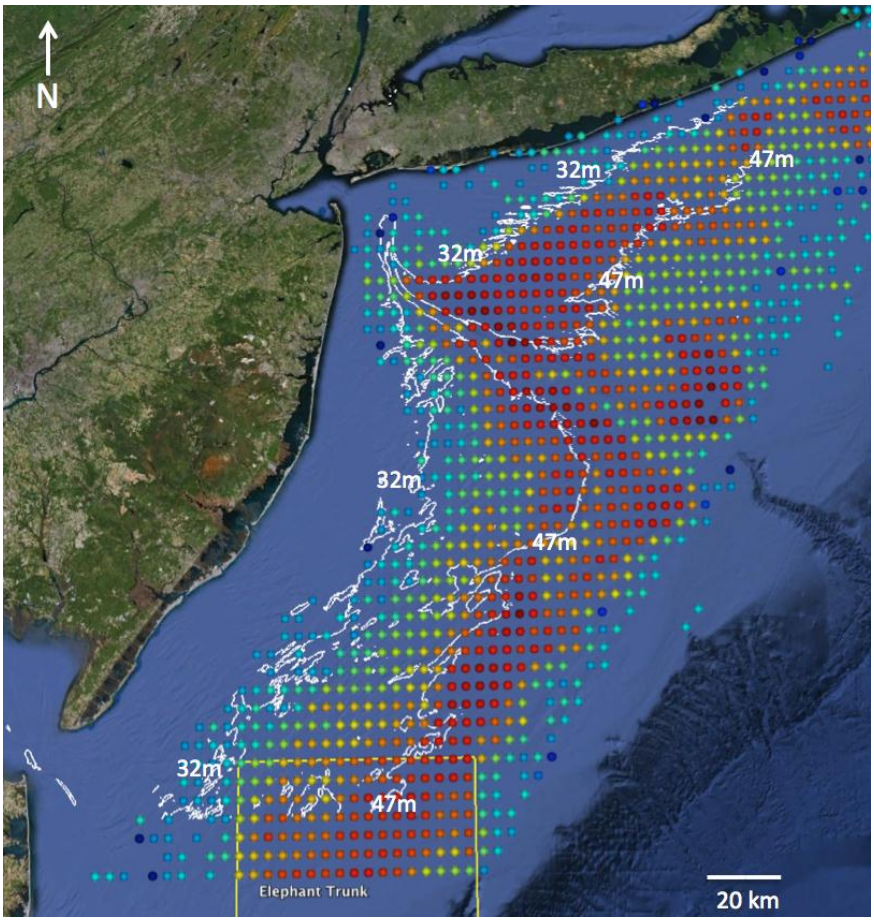

Figure 3.7: Map showing VMS fishing effort data (log transform). Fishing effort trends parallel with depth contour. South of Hudson Shelf Valley, fishing effort is concentrated seaward of the 47 m depth contour. North of Hudson Canyon, fishing effort is concentrated between the 32 and 47 m contour.

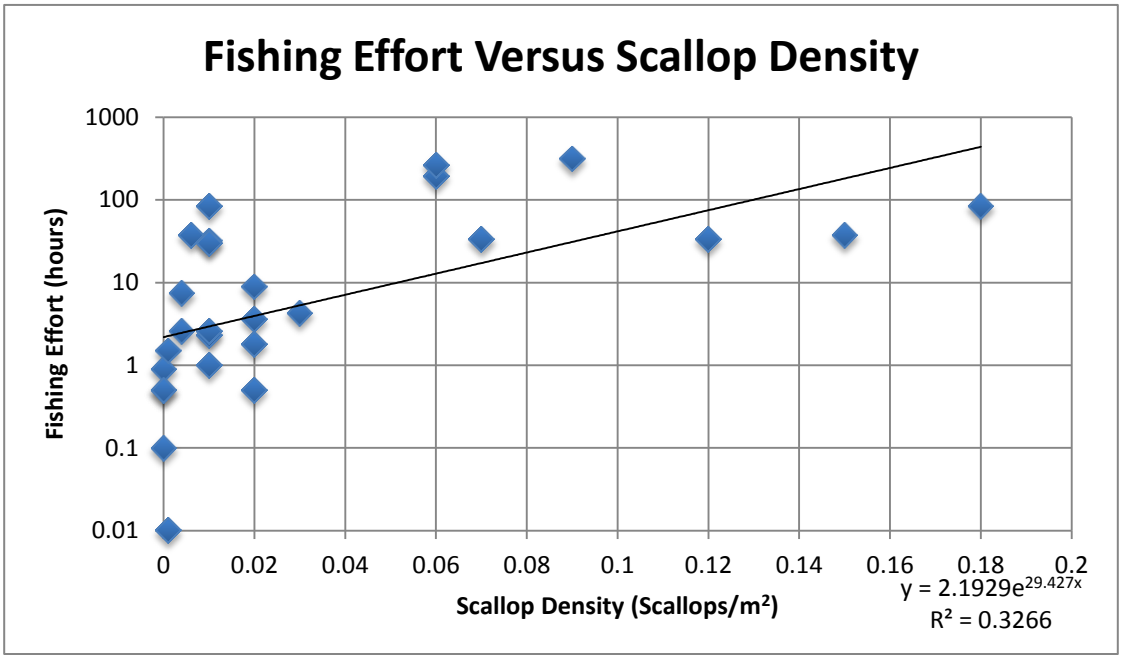

Figure 3.8: Plot of VMS fishing effort versus sea scallop density.

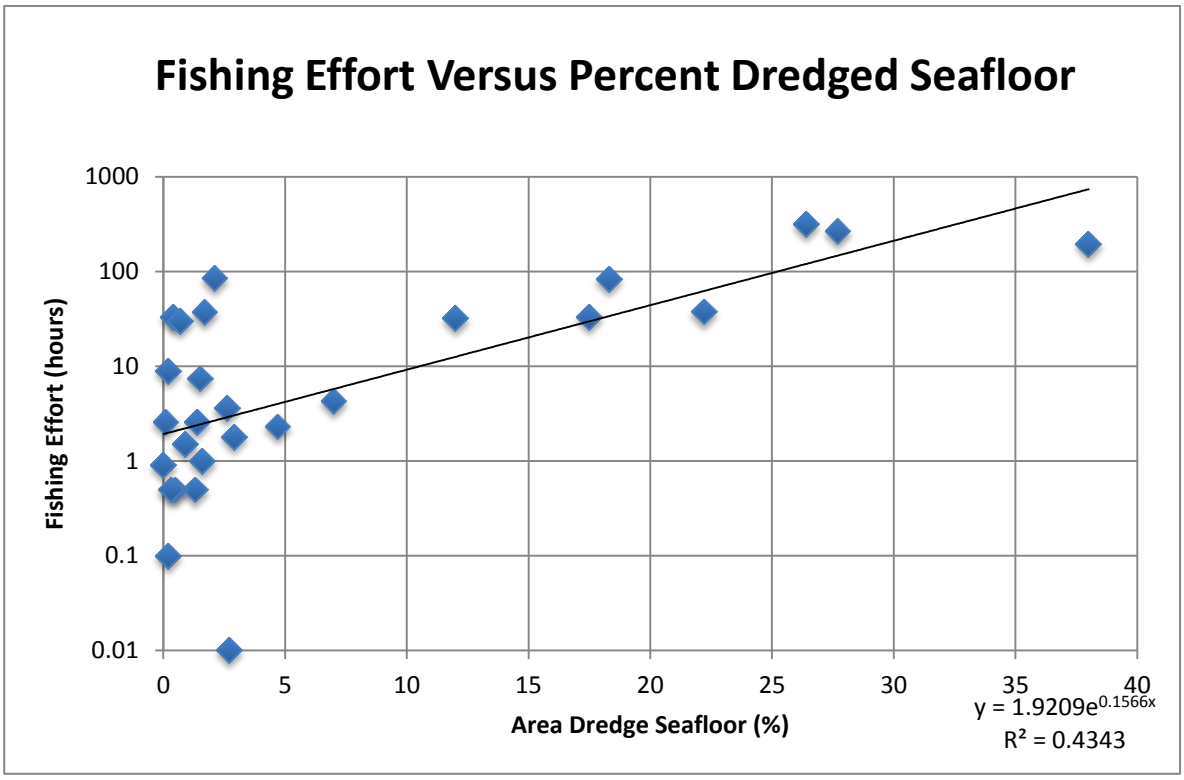

Figure 3.9: A semi-log plot of the two fishing effort proxies used in this study: VMS data and side-scan sonar derived percent area dredged. There exists an exponential relationship between the two methods.

3.4 Discussion and Conclusion

3.4.1 Species Diversity Analysis

Scallop fishing in the Mid-Atlantic Bight is done by dragging commercial dredges across the seafloor. The dredges are known to flatten the morphology of the seafloor and catch a variety of seafloor dwelling creatures: including sea scallops, sea stars, sponges, skates, etc. (NMFS, 2010). While the heavily dredged seafloor missions were found to have a higher sea scallop density, the closed area was found to have a higher density of benthic organisms, while simultaneously having the lower density of scallops. All of the species catalogued in this study are typically caught as bycatch during scallop trawls (catalogued during survey dredges in July, 2011). The closed access ground showed little evidence of dredging, therefore, it follows that the populations of those creatures would have benefited without artificial removal by dredging. The low scallop densities found within the Elephant Trunk match closely to other survey missions near the access ground. There could be other causes for the low scallop density in the closed access ground, such as high mortality from parasites or from a major storm (Stokesbury *et al.*, 2007).

The statistical analysis of the results of this study show that variation amongst half of the species could not be attributed to dredging with a high confidence. The Simpson's and Shannon-Wiener diversity indices have been known to be largely skewed when there is the presence of a single dominant species population, which was true in both survey areas (DeJong, 1975). This diversity study was meant to be a cursory look at the implications of dredging on benthic organism populations, and how the scallop image data set could be used to explore other organism populations. Future work could include a temporal component of a single access ground as it

rotated from closed to open, in order to establish baseline conditions, and how the introduction of dredging affects benthic habitat. Monitoring of the abundances of other major fauna could be explored for interspecies population dynamics.

The image based scallop counting and sizing efforts in Chapter 2 were able to be completed in 120 hours. During those 120 hours, 249,564 images were analyzed (2,080 images/hour) and 16,451 scallops were identified and sized. This study greatly increased the number of enumerated species, resulting in 44,000 organisms being analyzed from only 12,000 images. The increased organism density slowed analysis to 600 images/hour for the 12,000 images, resulting in a completion time of 20 hours. Therefore, image analysis rate roughly decreased by a third (0.3) when the abundance of the organism of interest was roughly tripled (2.67). This shows that organism density of interest can have a major impact on the necessary analysis time, and that this tradeoff must be considered during the planning stages of an image based stock assessment.

3.4.2 Fishing Effort

Two methods of approximating fishing effort were incorporated into this study. Using a method pioneered by Newton (1975), side-scan sonar imagery was used to identify and quantify dredge scar area on the seafloor. The percentage of dredged seafloor for a mission was used as a measure of fishing effort. The size selectivity of the scallop dredge has been shown to positively skew shell height distributions with increased dredging effort, which explains the positive distribution skewness in some of the northern survey missions. Chapter 2 found that the overall scallop density in the surveyed strata was 0.027 scallops/m^2. This study found that twice that value was

the approximate threshold for when scallop vessels would exert considerable dredging effort.

Limited days at sea necessitate the efficient use of resources; therefore, through experience and knowledge, the scallop fishermen aim to concentrate fishing effort on more populated scallop strata. The VMS data revealed that scallop vessel fishing effort correlated with the scallop density of the strata, showing the relative success of the fishermen at efficiently balancing time at sea with fishing effort.

Chapter 4

CONCLUSIONS

4.1 Stock Assessment

The use of an AUV allowed for the photographic and acoustic mapping of 313 km of seafloor within the Mid-Atlantic Bight over the span of 10 days. This is the first sea scallop stock assessment performed by an AUV, and it was found that the implemented digital counting and sizing methods were in accordance with traditional dredge based stock assessments. The major findings of this study are:

1. In 2011, the overall sea scallop density within the open access grounds of the Mid-Atlantic Bight was 0.027 scallops/m^2 and was most concentrated in the waters south of Long Island in survey strata 1, 2, and 3.
2. The sea scallop population was found to be extremely mature with only 0.2% of the population being recruit sized.
3. Sea scallop density was found to peak at a near bed water temperature of 9°C.
4. Scallop populations were found to organize at length scales larger than 300 m, but a structuring was not always evident.
5. Sea scallop shell height distributions are normally negatively skewed, except in the case of highly dredged strata.
6. For this survey, analysis of a randomly selected subset of 50,000 images out of the total 250,000 images would have resulted in an uncertainty of +/- 9% of the organism density.

7. Organism of interest density within an image set can significantly increase analysis time.
8. There was an exponential correlation between VMS fishing effort data and scallop dredging fishing effort resolved from the side-scan sonar mosaics, indicating that VMS data is a reliable proxy for scallop fishing effort.

The AUV makes an ideal platform for the completion of a sea scallop stock assessment. The ability to quickly deploy and retrieve the AUV from a support vessel allows for the rapid acquisition of photographic and acoustic data that can be analyzed during down time or after the completion of the cruise. Imaging the seafloor is a noninvasive way to survey the scallop population, while also gathering data about the small scale spatial structuring of the population, seafloor texture and morphology, and water quality data.

4.2 Future Work

Future sea scallop surveys could be complemented by the use of an AUV. This study was able to quantify scallop density and spatial behavior on sandy seabed; therefore, a scallop survey on a coarser texture seabed could offer a contrasting dataset. Because the AUV has been shown to have an extremely accurate navigation system, able to precisely survey a designated area of seafloor, a sea scallop habitat study would be a logical next step. The methodologies developed for the completion of the scallop stock assessment could also be applied to the assessment of other benthic organisms.

One of the major challenges of this study was the analysis of all of the seafloor images. Development of an automated scallop detection algorithm for seafloor images

would drastically lower the analysis time of a stock assessment. Crowd sourcing of the images has been shown to be an effective way to filter through large datasets. Given that scallop identification can be easily taught, sea scallop images are an ideal candidate for crowd sourcing. The website www.subseaobservers.com was developed as a crowd sourcing website featuring the sea scallop image dataset analyzed for this study. Users on the site are trained to identify and size scallops using the same identifications and methods used in this thesis. Data from the users of the website can be compared to the findings of this thesis as a way to explore and scientifically validate the use of crowd sourcing in scientific research.

REFERENCES

Adams, C. F., Harris, B. P., Marino II, M. C., & Stokesbury, K. D. (2010). Quantifying sea scallop bed diameter on Georges Bank with geostatistics. Fisheries Research, 106(3), 460-467.

Barbeau, M. A., & Scheibling, R. E. (1994). Behavioral mechanisms of prey size selection by sea stars (*Asterias vulgaris* Verrill) and crabs (*Cancer irroratus*) preying on juvenile sea scallops (*Placopecten magellanicus* (Gmelin)). Journal of experimental marine biology and ecology, 180(1), 103-136.

Brand. (2006). Scallop ecology: Distributions and behavior. In Developments in Aquaculture and Fisheries Science: Vol. 35. *Scallops: Biology, ecology and aquaculture* (pp. 651-744). Elsevier.

Bulit, C., Díaz-Avalos, C., Signoret, M., & Montagnes, D. J. (2003). Spatial structure of planktonic ciliate patches in a tropical coastal lagoon: an application of geostatistical methods. Aquatic microbial ecology, 30(2), 185-196.

Caddy, J. F. (1989). A perspective on the population dynamics and assessment of scallop fisheries, with special reference to the sea scallop, *Placopecten magellanicus* Gmelin. *Marine invertebrate fisheries: Their assessment and management*. John Wiley and Sons, New York, New York, 559-589.

Cranford, P. J., & Gordon, D. C. (1992). The influence of dilute clay suspensions on sea scallop (Placopecten magellanicus) feeding activity and tissue growth. Netherlands Journal of Sea Research, 30, 107-120.

Cranford, P. J., & Grant, J. (1990). Particle clearance and absorption of phytoplankton and detritus by the sea scallop Placopecten magellanicus(Gmelin). Journal of Experimental marine biology and Ecology, 137(2), 105-121.

Currie, D. R., & Parry, G. D. (1996). Effects of scallop dredging on a soft sediment community: a large-scale experimental study. *Marine ecology progress series. Oldendorf*, *134*(1), 131-150.

DeJong, T. M. (1975). A comparison of three diversity indices based on their components of richness and evenness. Oikos, 222-227.

DuPaul, W. D., & Rudders, D. B. (2008). An Assessment of Sea Scallop Abundance and Distribution in Selected Closed Areas: Georges Bank Area I and II, Nantucket Lightship and Elephant Trunk.

Field, M. E., & Duane, D. B. (1976). Post-Pleistocene history of the United States inner continental shelf: Significance to origin of barrier islands. *Geological Society of America Bulletin*, *87*(5), 691-702.

Fisheries of the United States. (2012). Fisheries of the united states. Silver Spring, MD: National Marine Fisheries Service Office of Science and Technology

Gibbs, R. J. (1981). Sites of river-derived sedimentation in the ocean. *Geology*, *9*(2), 77-80.

Goff, J. A., Mayer, L. A., Traykovski, P., Buynevich, I., Wilkens, R., Raymond, R., ... & Jenkins, C. (2005). Detailed investigation of sorted bedforms, or "rippled scour depressions," within the Martha's Vineyard Coastal Observatory, Massachusetts. *Continental Shelf Research*, *25*(4), 461-484.

H. Rep. No. 5946, 109th Cong., 178 (2006).

Harry, D. L., & Sawyer, D. S. (1992). A dynamic model of extension in the Baltimore Canyon Trough region. *Tectonics*, *11*(2), 420-436.

Hautmann, M. (2010). The first scallop. *Paläontologische Zeitschrift*, *84*(2), 317-322. doi:10.1007/s12542-009-0041-5

Hennen, D. R., & Hart, D. R. (2012). Shell height-to-weight relationships for Atlantic sea scallops (Placopecten magellanicus) in offshore US waters. *Journal of Shellfish Research*, *31*(4), 1133-1144.

Hutchinson, D. R., & Grow, J. A. (1985). New York Bight fault. *Geological Society of America Bulletin*, *96*(8), 975-989.

Johnson, H. P., & Helferty, M. (1990). The geological interpretation of side-scan sonar. *Reviews of Geophysics*, *28*(4), 357-380.

Kostylev, V. E., Todd, B. J., Fader, G. B., Courtney, R. C., Cameron, G. D., & Pickrill, R. A. (2001). Benthic habitat mapping on the Scotian Shelf based on multibeam bathymetry, surficial geology and sea floor photographs. Marine Ecology Progress Series, 219, 121-137.

Kraft, J. C. (1971). Sedimentary facies patterns and geologic history of a Holocene marine transgression. *Geological Society of America Bulletin*, *82*(8), 2131-2158.

Larsen, P. F., and R. M. Lee (1978). Observations on the abundance, distribution and growth of post-larval sea scallops, Placopecten magellanicus, on Georges Bank. *Nautilus* 92.3, 112-116.

Law, C. G. (2007). The impact of spatial and temporal variability of larval transport on the distribution and population dynamics of the sea scallop (*placopecten magellancius*). PhD Dissertation, Rutgers, 296 pages.

Lurton, X. (2000). Swath bathymetry using phase difference: theoretical analysis of acoustical measurement precision. *Oceanic Engineering, IEEE Journal of*, *25*(3), 351-363.

Mackinson, S., Freeman, S., Flatt, R., & Meadows, B. (2004). Improved acoustic surveys that save time and money: integrating fisheries and ground-discrimination acoustic technologies. *Journal of Experimental marine biology and ecology*, *305*(2), 129-140.

Marawski, S., Wigley, S., Fogarty, M., Rago, P., & Mountain, D. (2005). Effort distribution and catch patterns adjacent to temperate MPAs. *Journal of Marine Science* , 1150-1167.

Matheron, G. (1963). Principles of geostatistics. *Economic geology*, *58*(8), 1246-1266.

McBride, R. A., & Moslow, T. F. (1991). Origin, evolution, and distribution of shoreface sand ridges, Atlantic inner shelf, USA. *Marine Geology*, *97*(1), 57-85.

McNinch, J. E. (2004). Geologic control in the nearshore: shore-oblique sandbars and shoreline erosional hotspots, Mid-Atlantic Bight, USA. *Marine Geology*, *211*(1), 121-141.

Merrill, A. S. (1959). A comparison of Cyclopecten nanus (Verrill and Bush) and Placopecten magellanicus (Gmelin). Harvard University Museum of Comparative Zoology. *Occas. pap. on Molluscs*, *2*, 209-228.

Naidu, K. S., and Robert, G. (2006). Fisheries sea scallop, Placopecten magellanicus. *Developments in Aquaculture and Fisheries Science*, *35*, 869-905.

Nebel, S. H., Trembanis, A. C., & Barber, D. C. (2011). Shoreline analysis and barrier island dynamics: decadal scale patterns from Cedar Island, Virginia. *Journal of Coastal Research*, *28*(2), 332-341.

Newton, R. S., & Stefanon, A. (1975). Application of side-scan sonar in marine biology. *Marine Biology*, *31*(3), 287-291.

NMFS (National Marine Fisheries Service Northeast Fisheries Science Center). (2010). *50th northeast regional stock assessment workshop (50th SAW) assessment report.* Ref Doc 10-17, US Dept Commerce, Northeast Fisheries Science Center, Woods Hole, MA, p 844.

Pielou, E. C. (1967). The use of information theory in the study of the diversity of biological populations. In *Proc. Fifth Berkeley Symposium on Math. Stat. and Prob* (pp. 163-77).

Raineault, A. C. Trembanis, and D. Miller. 2011. Mapping benthic habitats in Delaware Bay and the coastal Atlantic: acoustic techniques provide greater coverage and high resolution in complex shallow water environments. Estuaries and Coasts.

Raineault, N. A., Trembanis, A. C., Miller, D. C., & Capone, V. (2013). Interannual changes in seafloor surficial geology at an artificial reef site on the inner continental shelf. Continental Shelf Research.

Rosenkranz, G. E., Gallager, S. M., Shepard, R. W., & Blakeslee, M. (2008). Development of a high-speed, megapixel benthic imaging system for coastal fisheries research in Alaska. *Fisheries Research*, *92*(2), 340-344.

Rothschild, B. J., Adams, C. F., Sarro, C. L., & Stokesbury, K. D. (2009). Variability in the relationship between sea scallop shell height and meat weight. *ICES Journal of Marine Science: Journal du Conseil*, *66*(9), 1972-1977.

Roughgarden, J., & Smith, F. (1996). Why fisheries collapse and what to do about it. *Proceedings of the National Academy of Sciences*, *93*(10), 5078-5083.

Sawyer, D. S., Swift, B. A., Sclater, J. G., & Toksöz, M. N. (1982). Extensional model for the subsidence of the northern United States Atlantic continental margin. Geology, 10(3), 134-140.

Schettino, A., & Turco, E. (2009). Breakup of Pangaea and plate kinematics of the central Atlantic and Atlas regions. *Geophysical Journal International*, *178*(2), 1078-1097.

Schick, D. F., & Feindel, S. C. (2005). Maine scallop fishery: monitoring and enhancement. *Final report to the Northeast Consortium*.

Schlee, J. S. (1973). Atlantic continental shelf and slope of the United States: sediment texture of the northeastern part (p. 64). US Government Printing Office.

Seiler, J., Friedman, A., Steinberg, D., Barrett, N., Williams, A., & Holbrook, N. J. (2012). Image-based continental shelf habitat mapping using novel automated data extraction techniques. Continental Shelf Research.

Stevenson, J. A., & Dickie, L. M. (1954). Annual growth rings and rate of growth of the giant scallop, Placopecten magellanicus (Gmelin) in the Digby area of the Bay of Fundy. *Journal of the Fisheries Board of Canada*, *11*(5), 660-671.

Stokesbury, K. (2002). Estimation of sea scallop abundance in closed areas of georges bank, USA. *Transactions of the American Fisheries Society , 131*, 1081-1092.

Stokesberry, K., & Harris, B. (2006). Impact of limited short-term sea scallop fishery on epibenthic community of Georges Bank closed areas. *Marine Ecology Progress Series* , 85-100.

Swift, D. J. P. (1976). Coastal Sedimentation. *Marine Sediment Transport and Environmental Management*. John Wiley and Sons, New York, NY, 255-310.

Trehu, A. M., Klitgord, K. D., Sawyer, D. S., & Buffler, R. T. (1989). Atlantic and Gulf of Mexico continental margins. *Geophysical framework of the continental United States: Geological Society of America Memoir*, *172*, 349-382.

Trembanis, A. C., & Hume, T. M. (2011). Sorted bedforms on the inner shelf off northeastern New Zealand: spatiotemporal relationships and potential paleo-environmental implications. *Geo-Marine Letters*, *31*(3), 203-214.

USACE, C. (2002). Coastal Engineering Manual.

Appendix A

AUV MISSION BUBBLE PLOTS

A.1 Introduction

A bubble plot is a data visualization method that spatially plots the scallop abundance data according to the geographic coordinates recorded with each image. The bubble plots are plotted in planform view and are oriented so that north is up. The larger the bubble, the more scallops that were present in that particular image (refer to the provided scale on each plot). The survey design of each mission is clearly evident when all of the images are plotted.

A.2 AUV Mission Bubble Plots

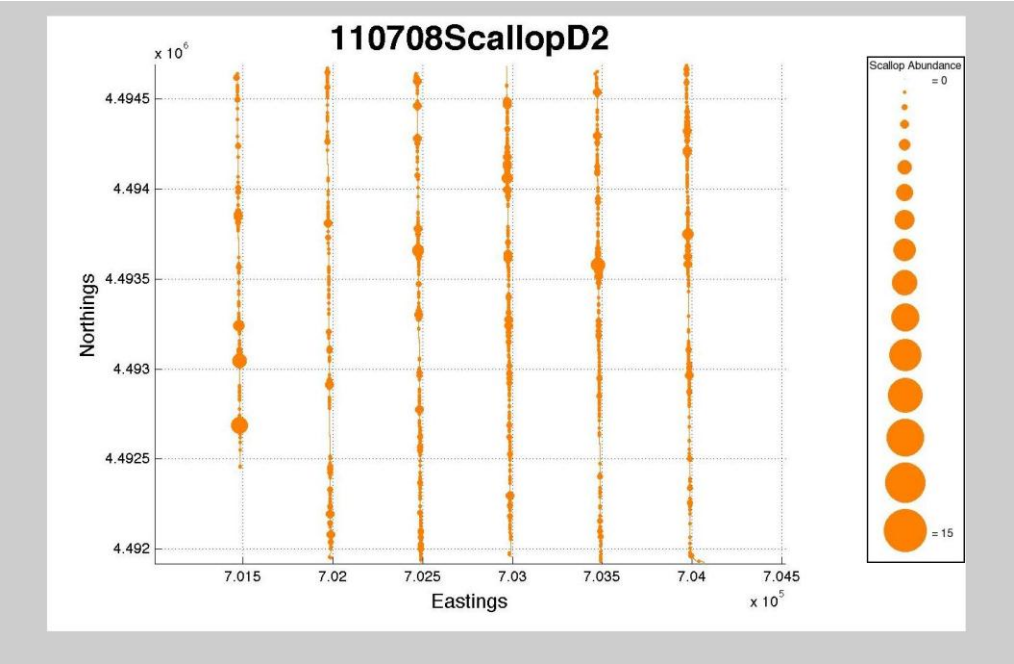

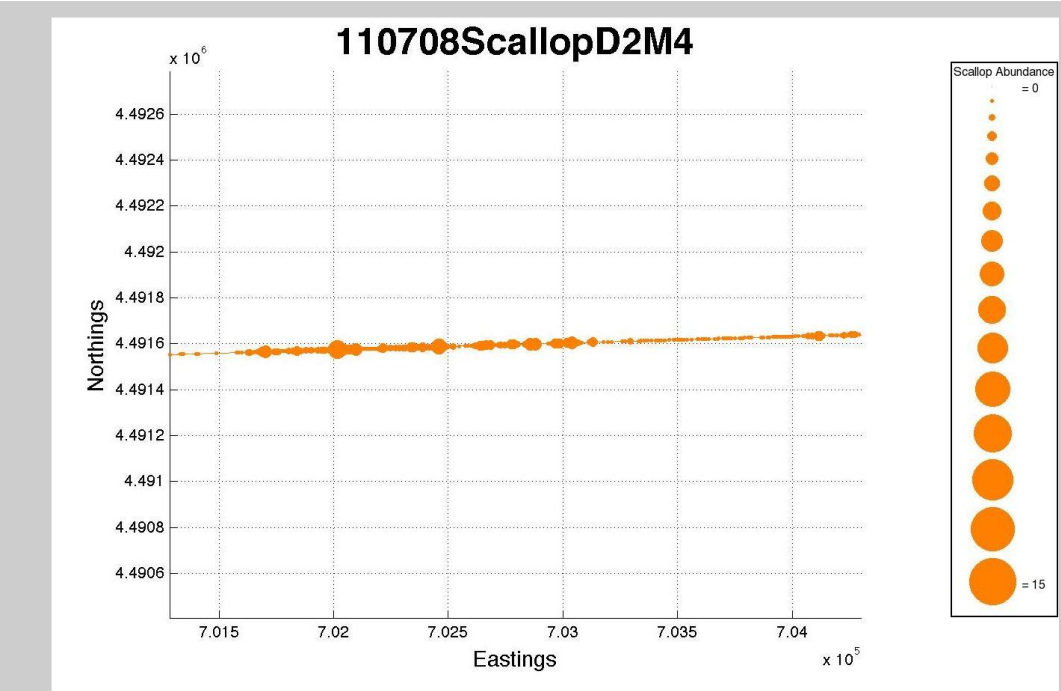
110708ScallopD2M4
x 10^6
4.4926
4.4924
4.4922
4.492
4.4918
4.4916
4.4914
4.4912
4.491
4.4908
4.4906
Northings
7.015
7.02
7.025
7.03
7.035
7.04
Eastings
x 10^5
Scallop Abundance
= 0
= 15

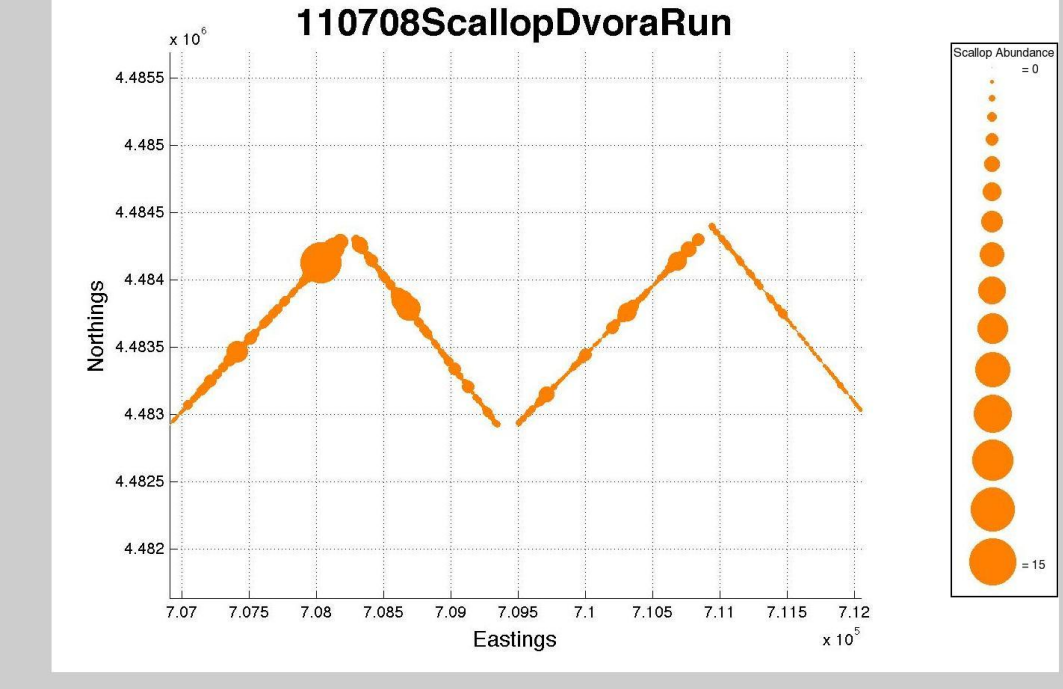
110708ScallopDvoraRun
x 10^6
4.4855
4.485
4.4845
4.484
4.4835
4.483
4.4825
4.482
Northings
7.07
7.075
7.08
7.085
7.09
7.095
7.1
7.105
7.11
7.115
7.12
Eastings
x 10^5
Scallop Abundance
= 0
= 15

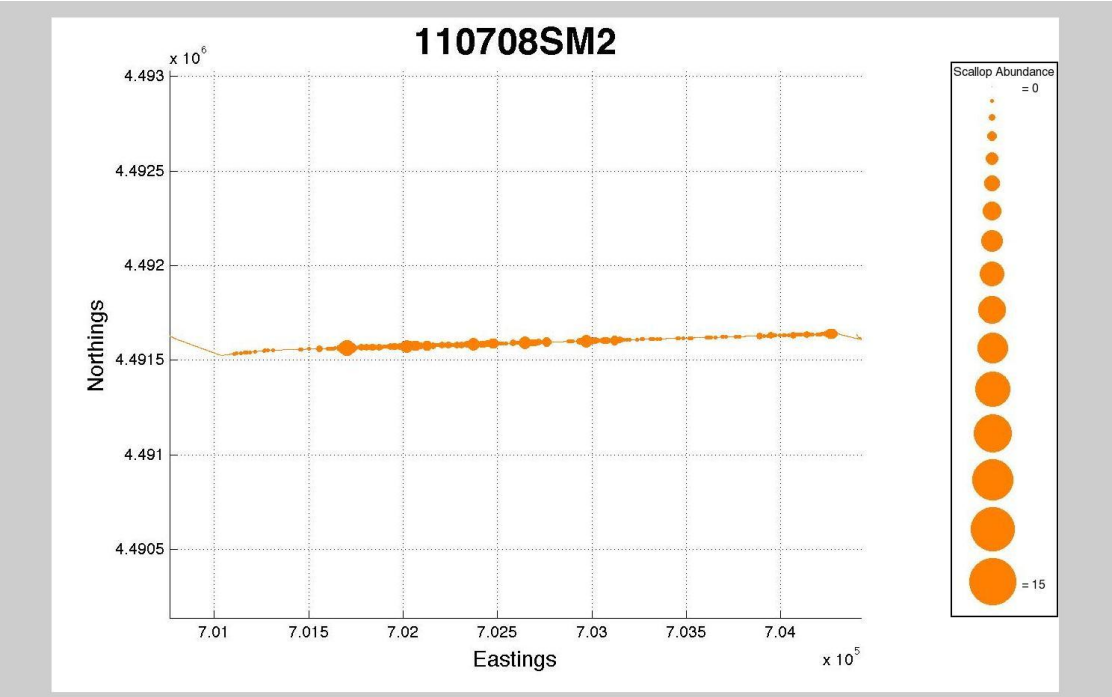
110708SM2
x 10^6
4.493
4.4925
4.492
4.4915
4.491
4.4905
Northings
7.01
7.015
7.02
7.025
7.03
7.035
7.04
Eastings
x 10^5
Scallop Abundance
= 0
= 15

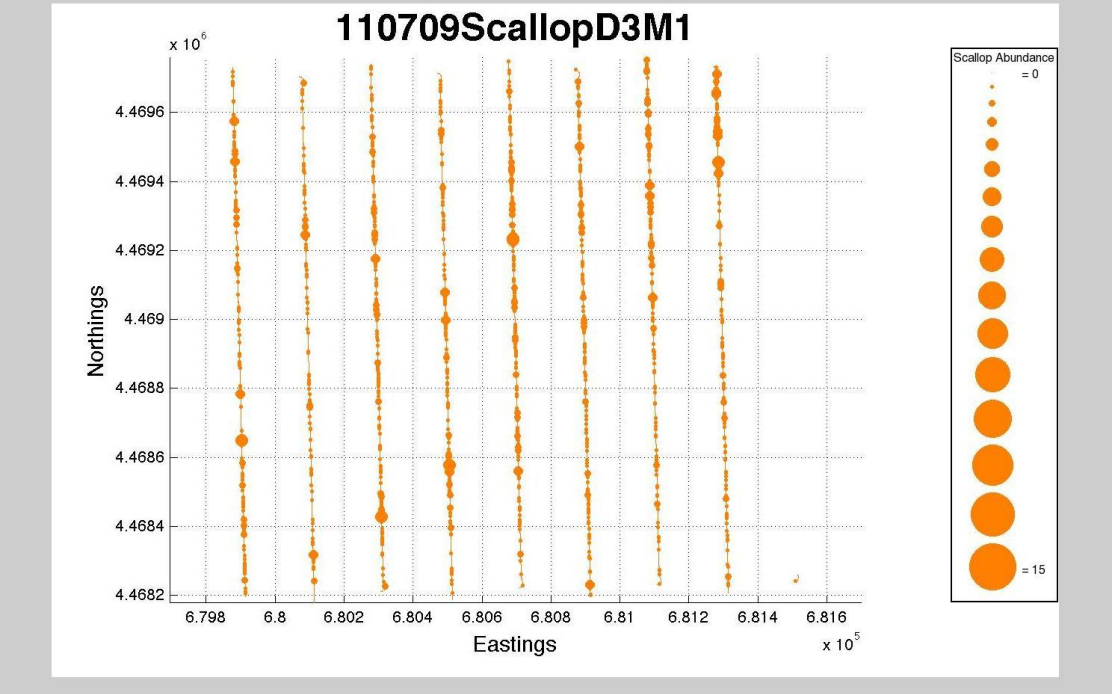
110709ScallopD3M1
x 10^6
4.4696
4.4694
4.4692
4.469
4.4688
4.4686
4.4684
4.4682
Northings
6.798
6.8
6.802
6.804
6.806
6.808
6.81
6.812
6.814
6.816
Eastings
x 10^5
Scallop Abundance
= 0
= 15

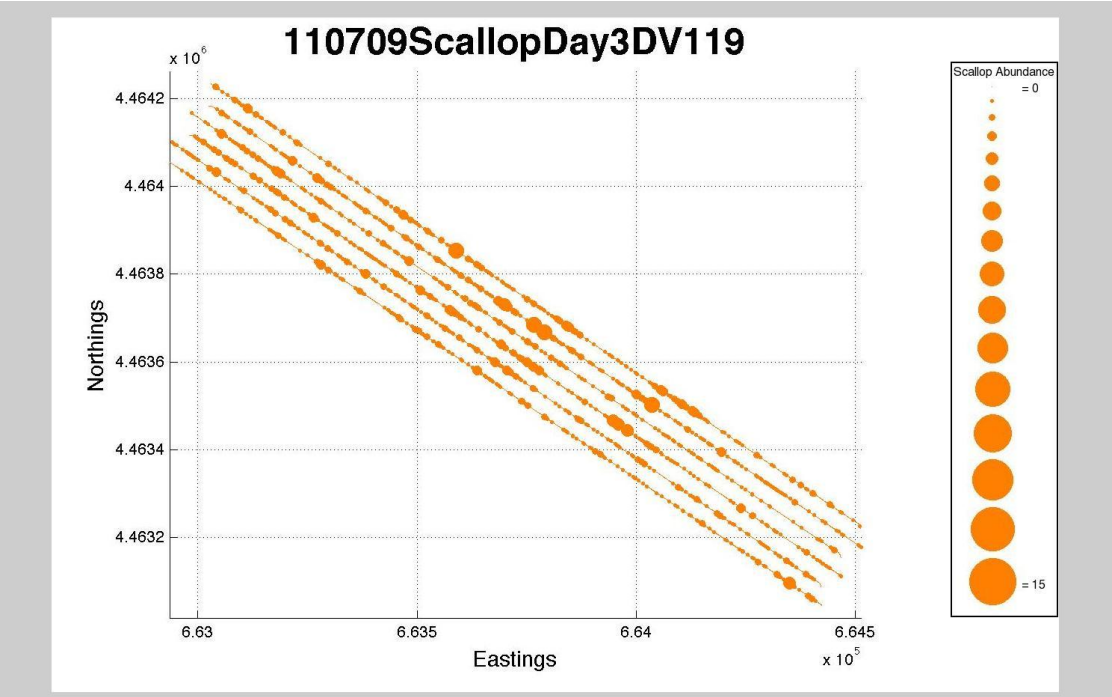
110709ScallopDay3DV119
x 10^6
4.4642
4.464
4.4638
4.4636
4.4634
4.4632
Northings
6.63
6.635
6.64
6.645
x 10^5
Eastings
Scallop Abundance
= 0
= 15

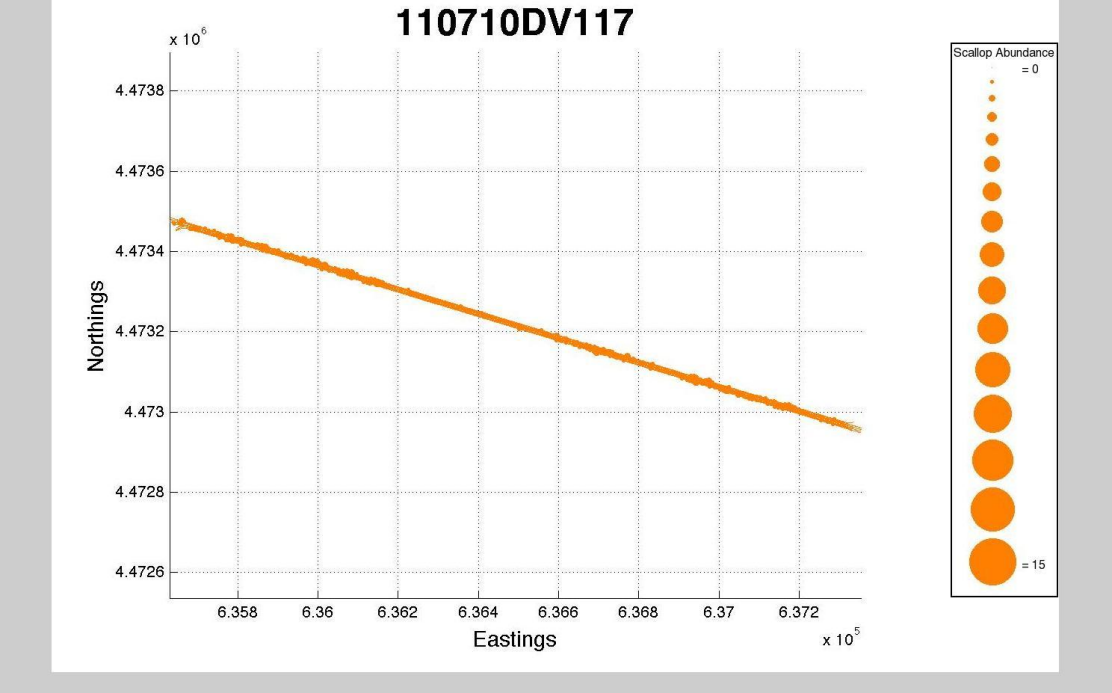
110710DV117
x 10^6
4.4738
4.4736
4.4734
4.4732
4.473
4.4728
4.4726
Northings
6.358
6.36
6.362
6.364
6.366
6.368
6.37
6.372
x 10^5
Eastings
Scallop Abundance
= 0
= 15

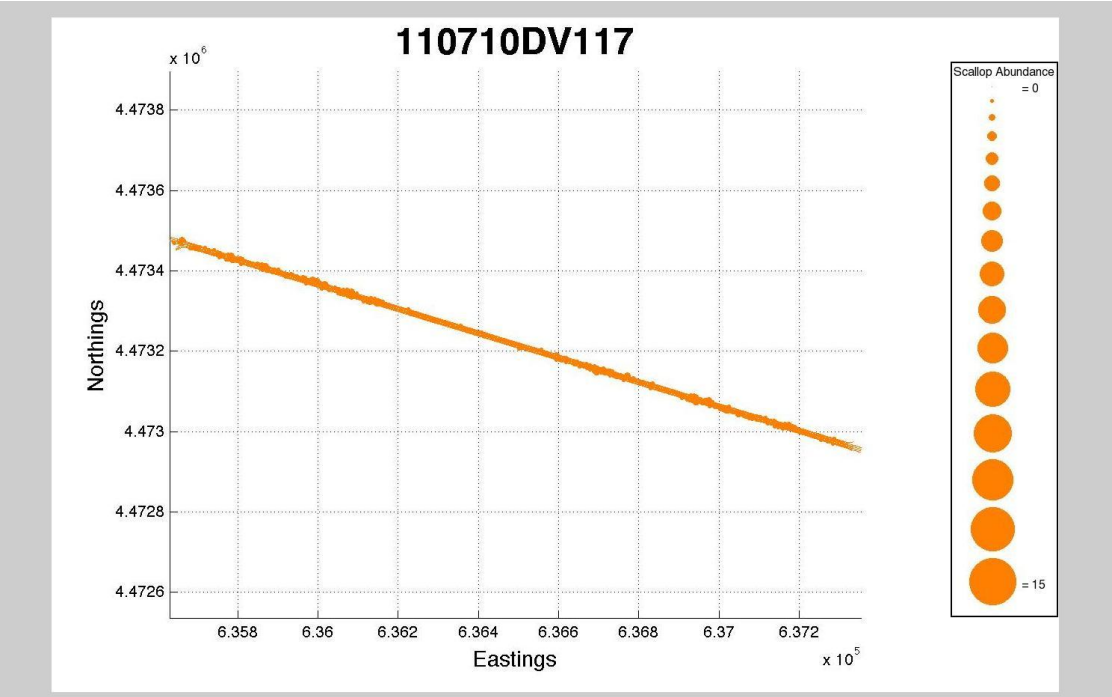
110710DV117
x 10^6
4.4738
4.4736
4.4734
4.4732
4.473
4.4728
4.4726
Northings
6.358
6.36
6.362
6.364
6.366
6.368
6.37
6.372
Eastings
x 10^5
Scallop Abundance
= 0
= 15

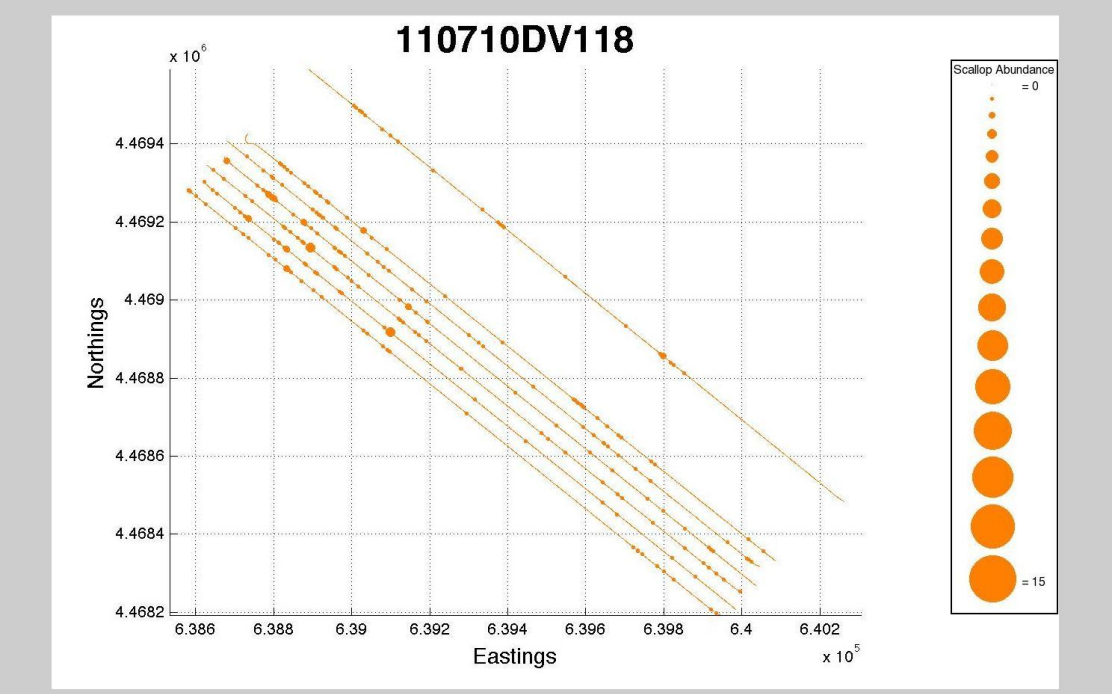
110710DV118
x 10^6
4.4694
4.4692
4.469
4.4688
4.4686
4.4684
4.4682
Northings
6.386
6.388
6.39
6.392
6.394
6.396
6.398
6.4
6.402
Eastings
x 10^5
Scallop Abundance
= 0
= 15

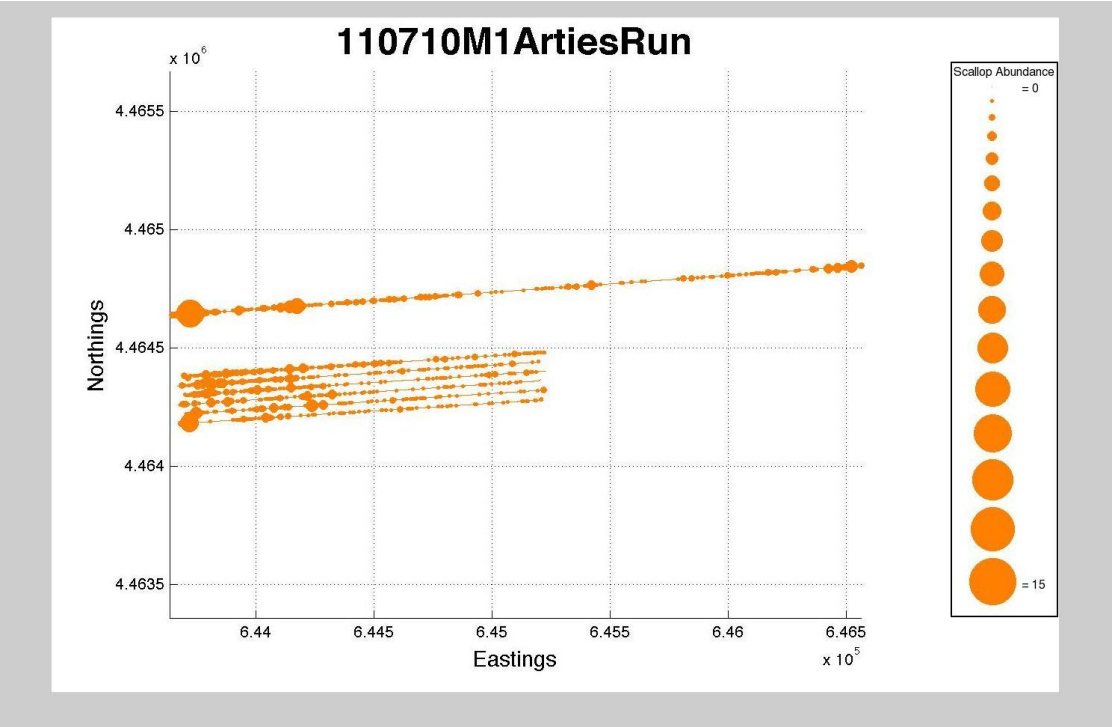
110710M1ArtiesRun
x 10^6
4.4655
4.465
4.4645
4.464
4.4635
Northings
6.44
6.445
6.45
6.455
6.46
6.465
Eastings
x 10^5
Scallop Abundance
= 0
= 15

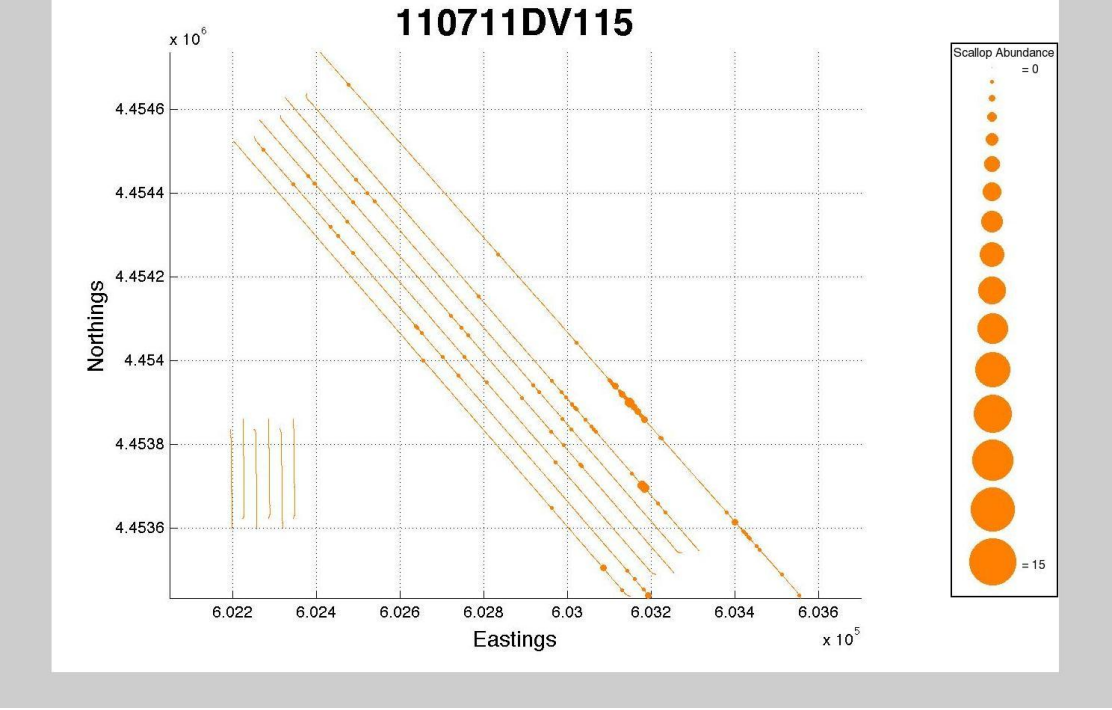
110711DV115
x 10^6
4.4546
4.4544
4.4542
4.454
4.4538
4.4536
Northings
6.022
6.024
6.026
6.028
6.03
6.032
6.034
6.036
Eastings
x 10^5
Scallop Abundance
= 0
= 15

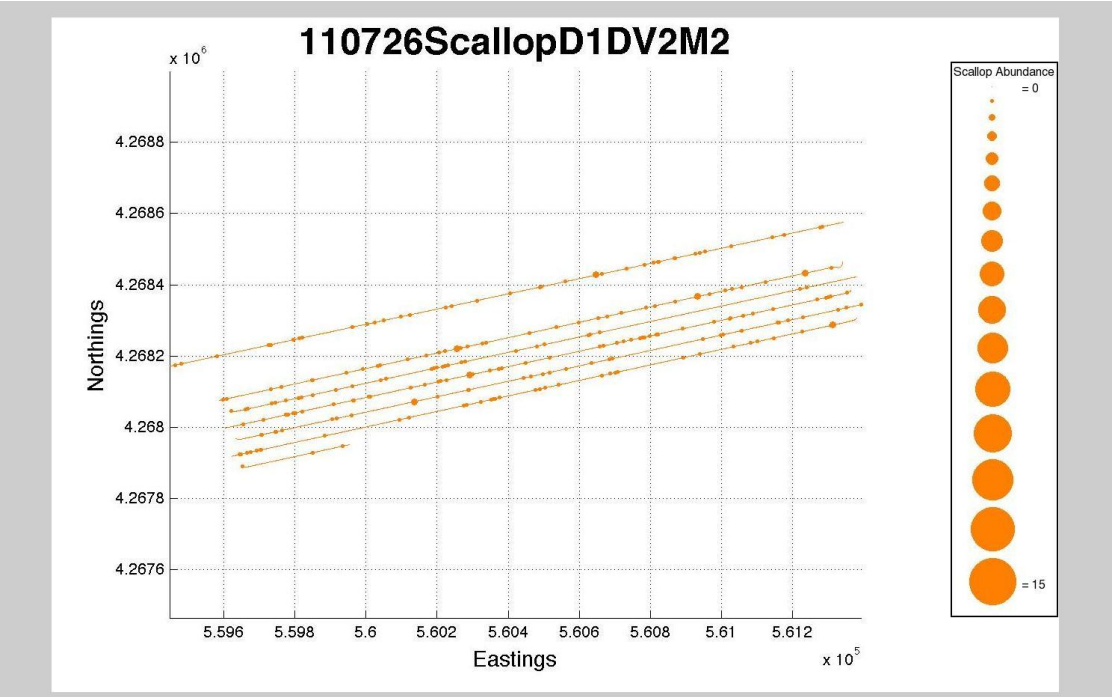
110726ScallopD1DV2M2
x 10^6
4.2688
4.2686
4.2684
4.2682
4.268
4.2678
4.2676
Northings
5.596
5.598
5.6
5.602
5.604
5.606
5.608
5.61
5.612
Eastings
x 10^5
Scallop Abundance
= 0
= 15

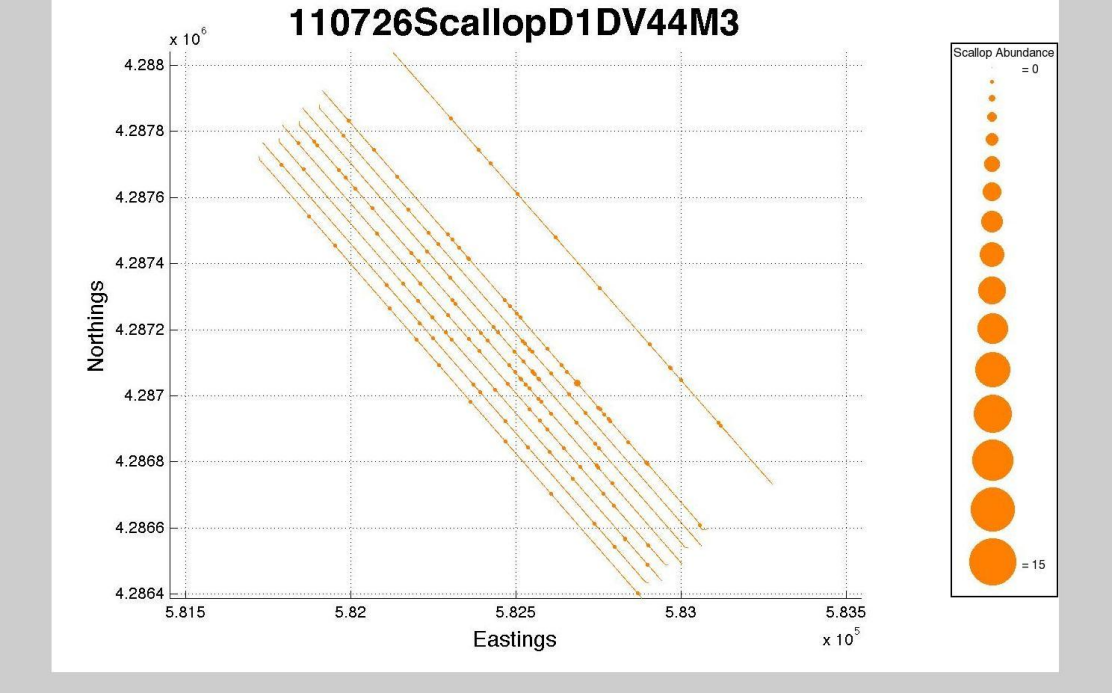
110726ScallopD1DV44M3
x 10^6
4.288
4.2878
4.2876
4.2874
4.2872
4.287
4.2868
4.2866
4.2864
Northings
5.815
5.82
5.825
5.83
5.835
Eastings
x 10^5
Scallop Abundance
= 0
= 15

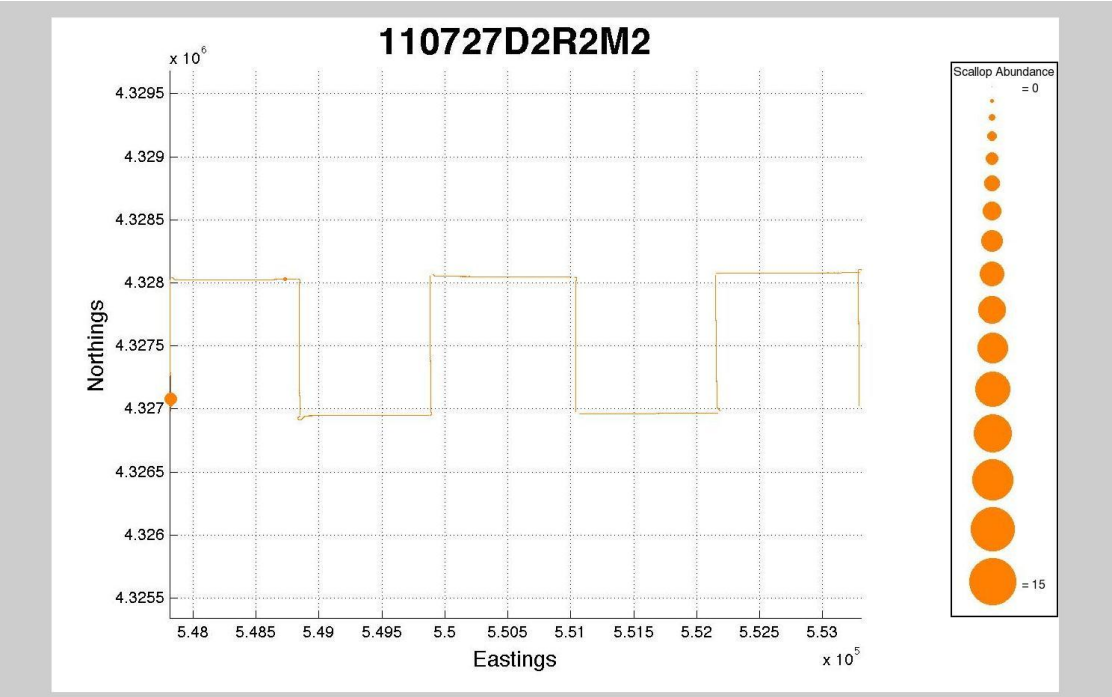
110727D2R2M2
x 10^6
4.3295
4.329
4.3285
4.328
4.3275
4.327
4.3265
4.326
4.3255
Northings
5.48
5.485
5.49
5.495
5.5
5.505
5.51
5.515
5.52
5.525
5.53
Eastings
x 10^5
Scallop Abundance
= 0
= 15

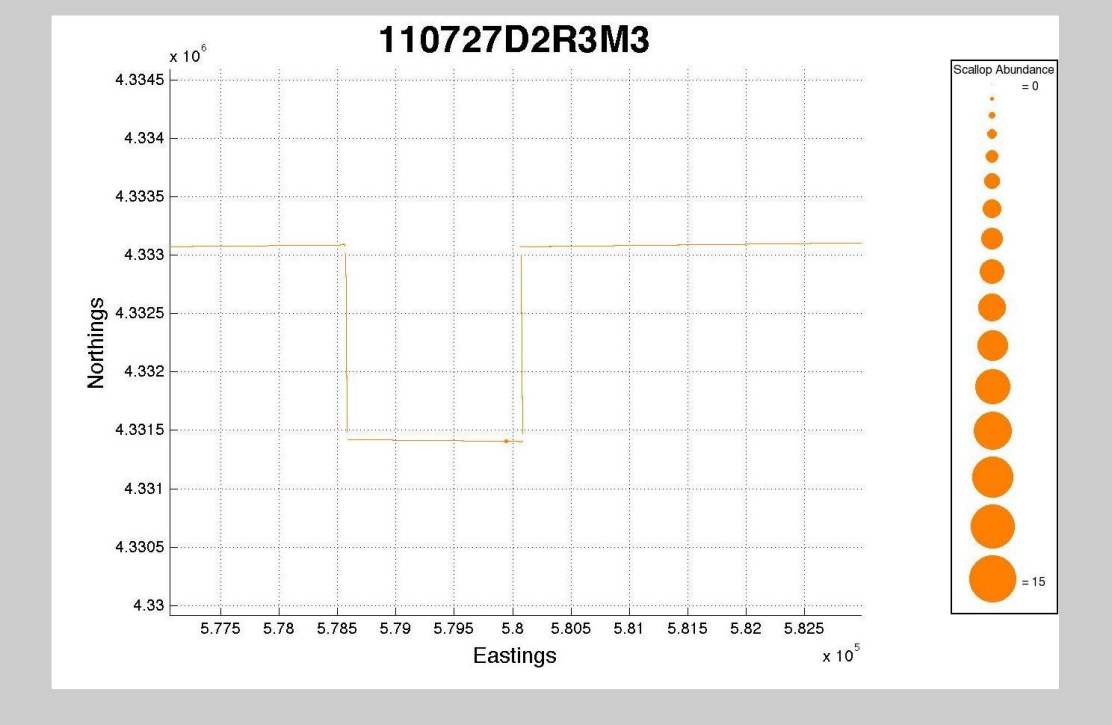
110727D2R3M3
x 10^6
4.3345
4.334
4.3335
4.333
4.3325
4.332
4.3315
4.331
4.3305
4.33
Northings
5.775
5.78
5.785
5.79
5.795
5.8
5.805
5.81
5.815
5.82
5.825
Eastings
x 10^5
Scallop Abundance
= 0
= 15

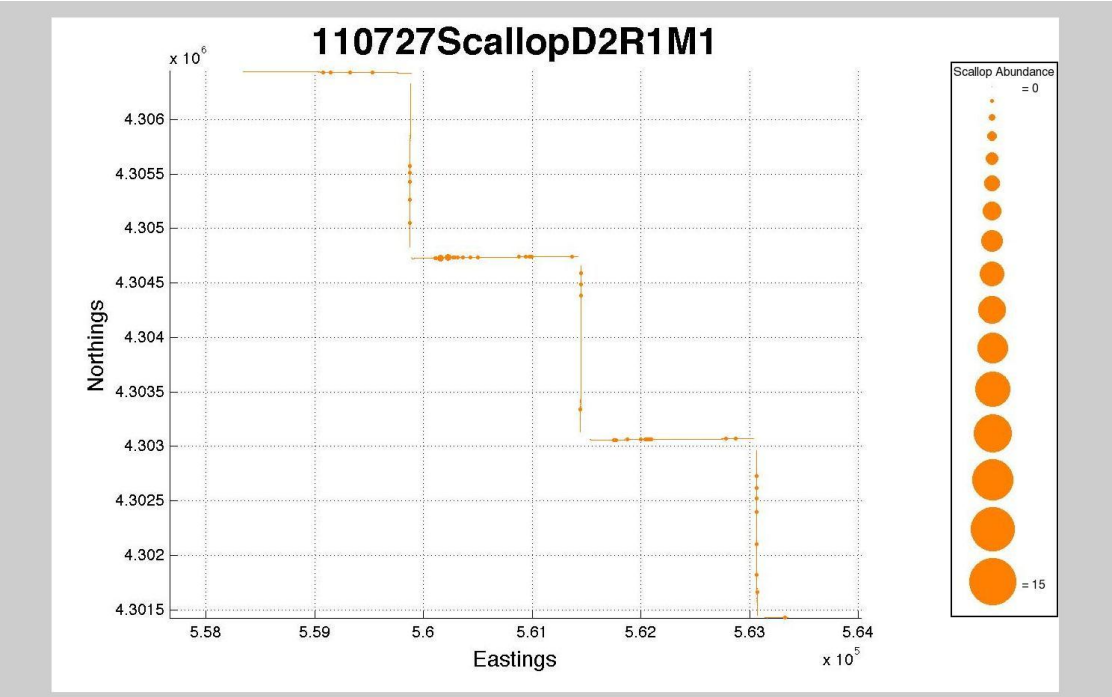
110727ScallopD2R1M1
x 10^6
4.306
4.3055
4.305
4.3045
4.304
4.3035
4.303
4.3025
4.302
4.3015
Northings
5.58
5.59
5.6
5.61
5.62
5.63
5.64
Eastings
x 10^5
Scallop Abundance
= 0
= 15

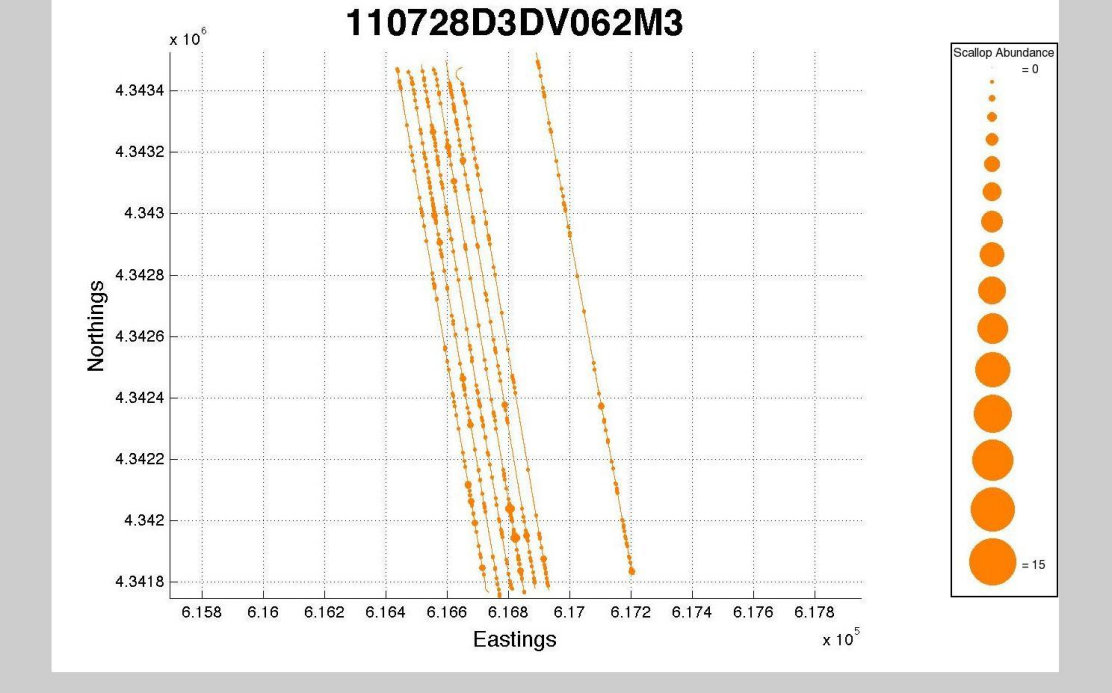
110728D3DV062M3
x 10^6
4.3434
4.3432
4.343
4.3428
4.3426
4.3424
4.3422
4.342
4.3418
Northings
6.158
6.16
6.162
6.164
6.166
6.168
6.17
6.172
6.174
6.176
6.178
Eastings
x 10^5
Scallop Abundance
= 0
= 15

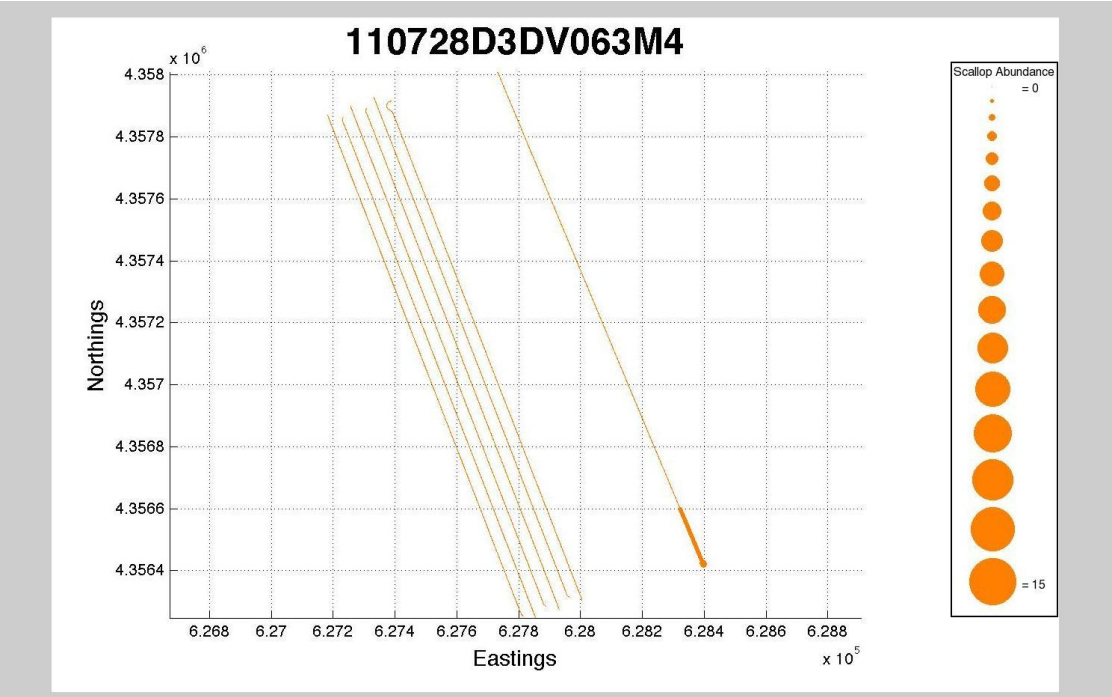
110728D3DV063M4
x 10^6
4.358
4.3578
4.3576
4.3574
4.3572
4.357
4.3568
4.3566
4.3564
Northings
6.268
6.27
6.272
6.274
6.276
6.278
6.28
6.282
6.284
6.286
6.288
Eastings
x 10^5
Scallop Abundance
= 0
= 15

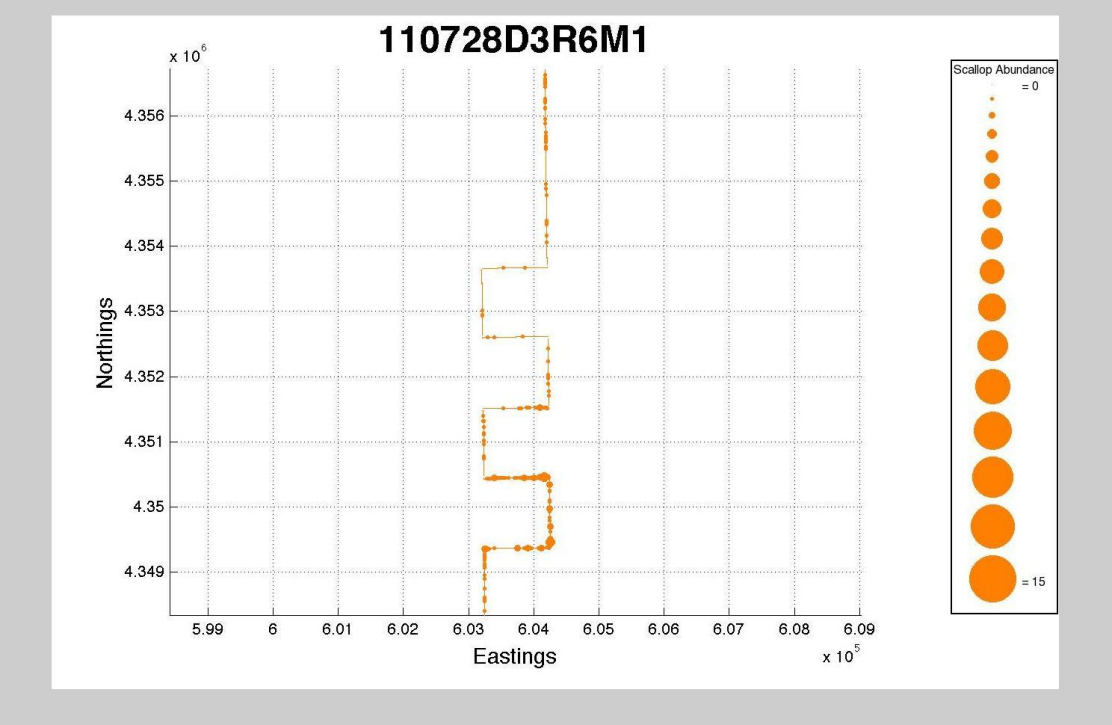
110728D3R6M1
x 10^6
4.356
4.355
4.354
4.353
4.352
4.351
4.35
4.349
Northings
5.99
6
6.01
6.02
6.03
6.04
6.05
6.06
6.07
6.08
6.09
Eastings
x 10^5
Scallop Abundance
= 0
= 15

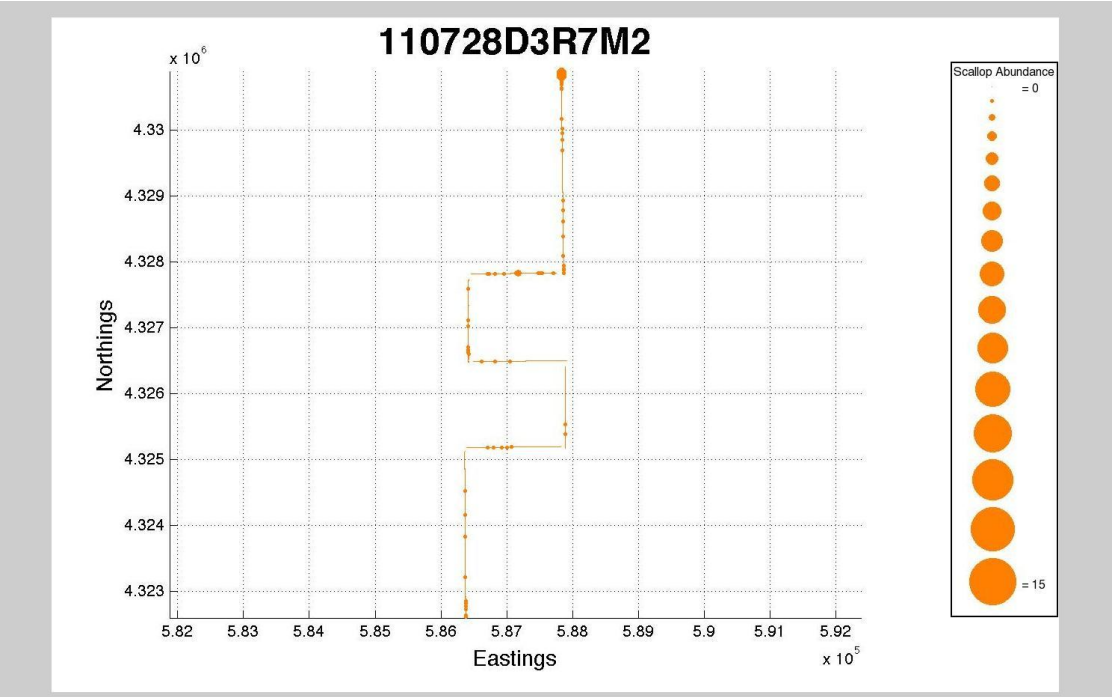
110728D3R7M2
x 10^6
4.33
4.329
4.328
4.327
4.326
4.325
4.324
4.323
Northings
5.82
5.83
5.84
5.85
5.86
5.87
5.88
5.89
5.9
5.91
5.92
Eastings
x 10^5
Scallop Abundance
= 0
= 15

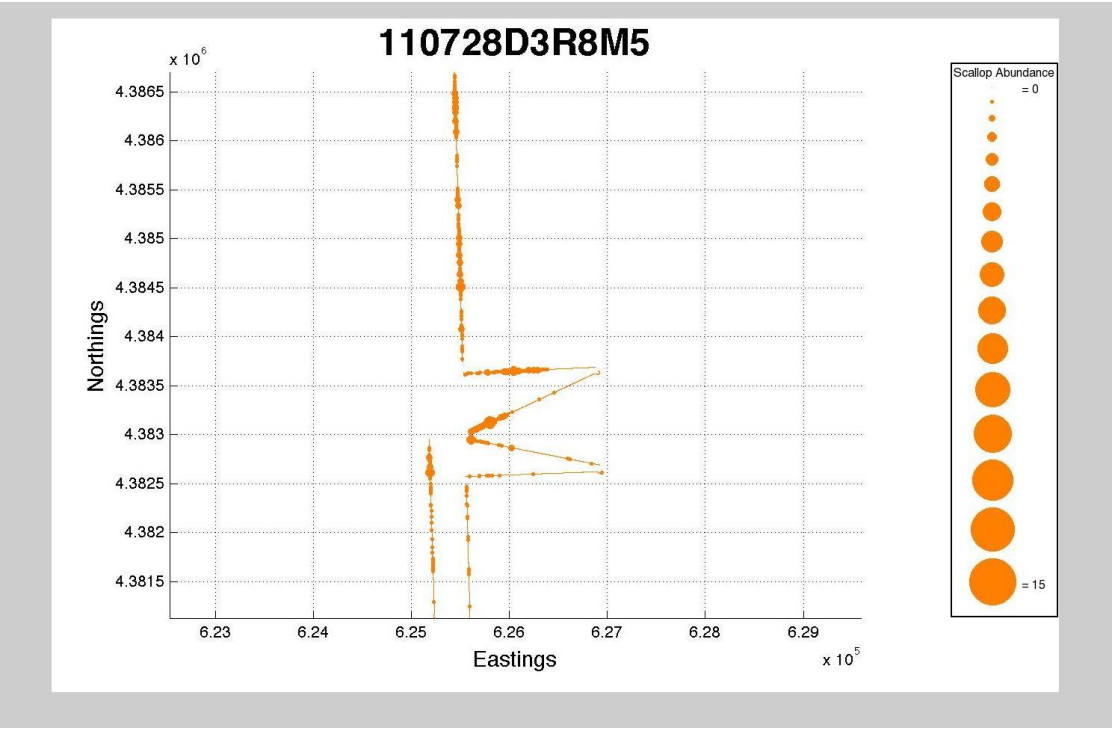
110728D3R8M5
x 10^6
4.3865
4.386
4.3855
4.385
4.3845
4.384
4.3835
4.383
4.3825
4.382
4.3815
Northings
6.23
6.24
6.25
6.26
6.27
6.28
6.29
Eastings
x 10^5
Scallop Abundance
= 0
= 15

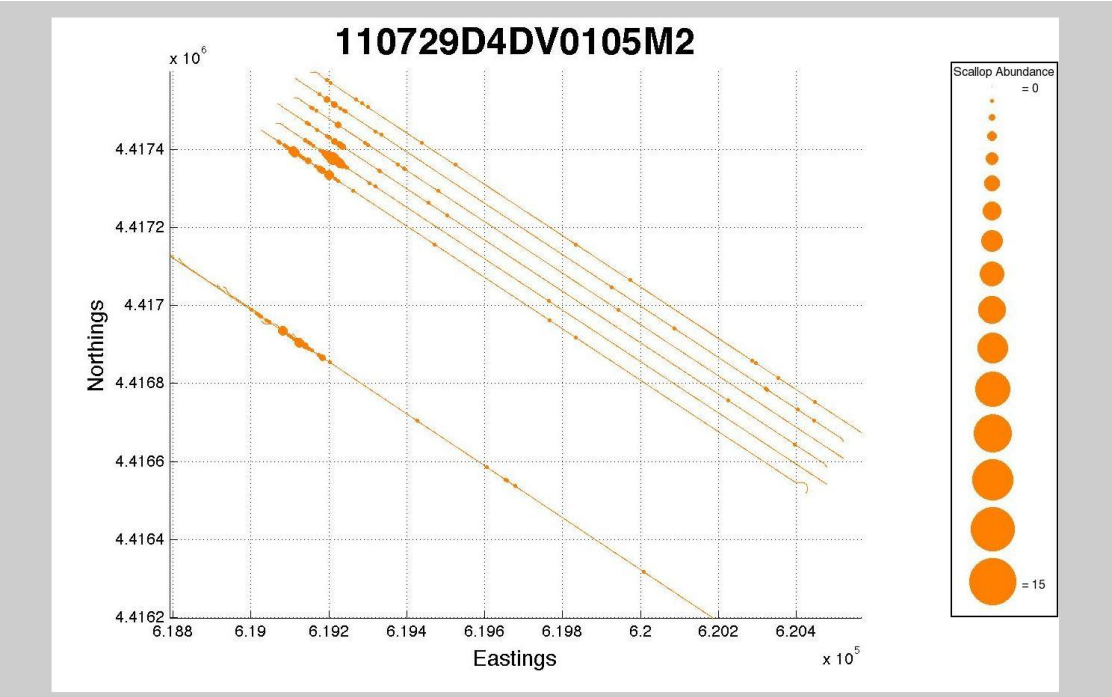
110729D4DV0105M2
x 10^6
4.4174
4.4172
4.417
4.4168
4.4166
4.4164
4.4162
Northings
6.188
6.19
6.192
6.194
6.196
6.198
6.2
6.202
6.204
Eastings
x 10^5
Scallop Abundance
= 0
= 15

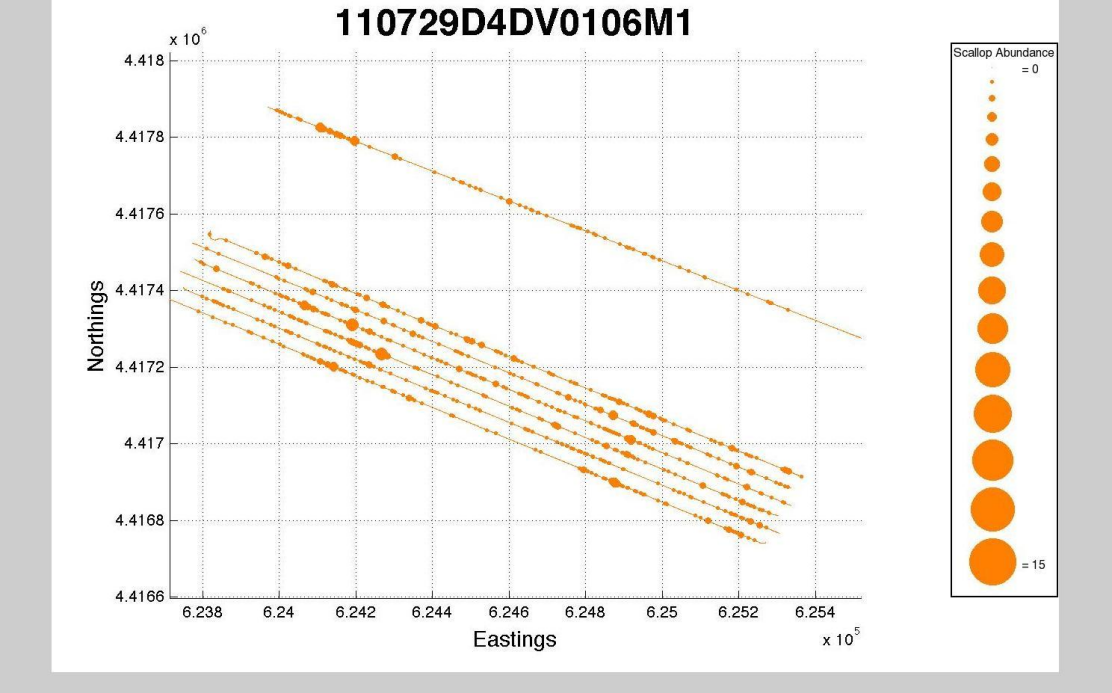
110729D4DV0106M1
x 10^6
4.418
4.4178
4.4176
4.4174
4.4172
4.417
4.4168
4.4166
Northings
6.238
6.24
6.242
6.244
6.246
6.248
6.25
6.252
6.254
Eastings
x 10^5
Scallop Abundance
= 0
= 15

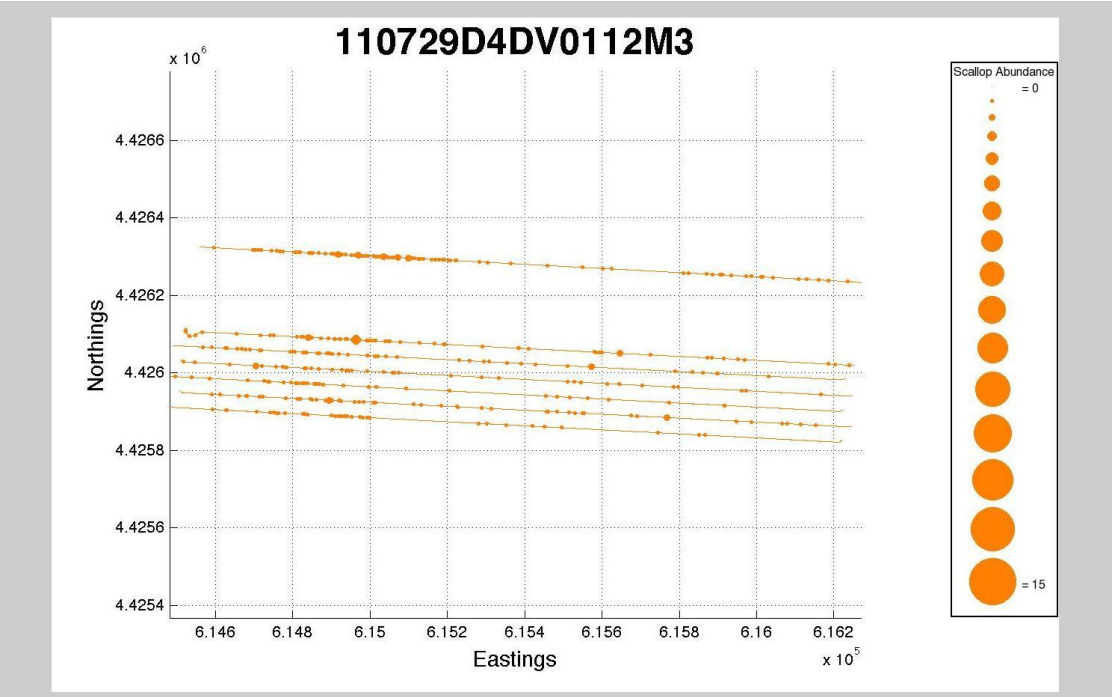
110729D4DV0112M3
x 10^6
4.4266
4.4264
4.4262
4.426
4.4258
4.4256
4.4254
Northings
6.146
6.148
6.15
6.152
6.154
6.156
6.158
6.16
6.162
Eastings
x 10^5
Scallop Abundance
= 0
= 15

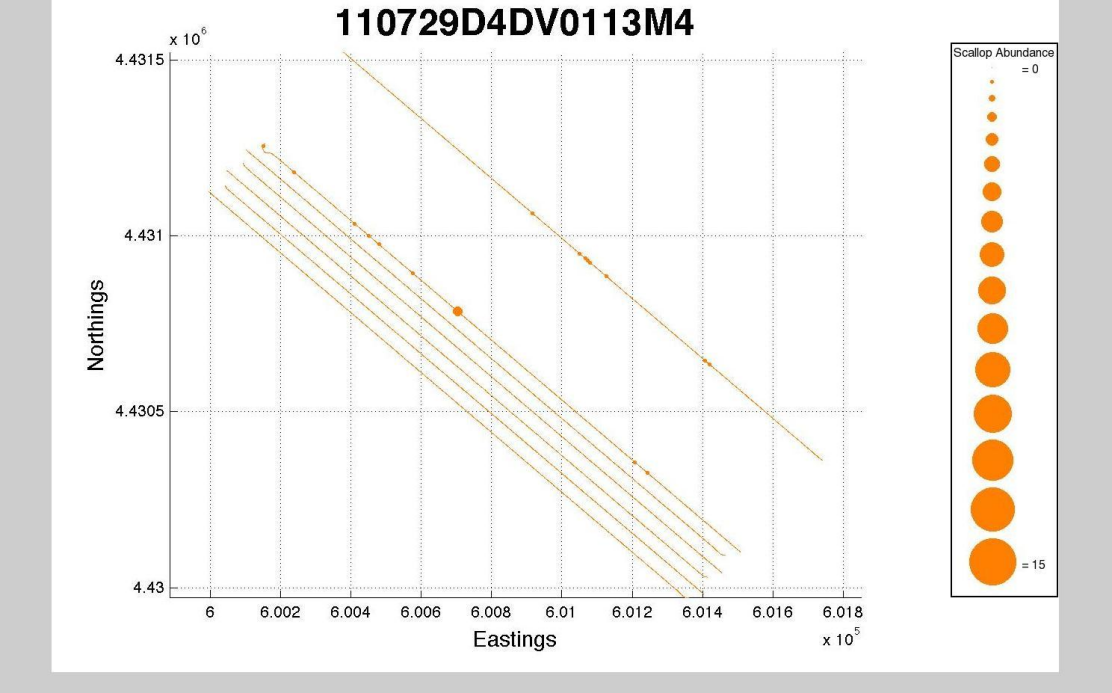
110729D4DV0113M4
x 10^6
4.4315
4.431
4.4305
4.43
Northings
6
6.002
6.004
6.006
6.008
6.01
6.012
6.014
6.016
6.018
Eastings
x 10^5
Scallop Abundance
= 0
= 15

Appendix B

SHELL HEIGHT BOX PLOTS

B.1 Introduction

This appendix includes all box plots for each sea scallop survey stratum. A single box plot corresponds to the sea scallop shell height distribution of one AUV survey mission.

B.2 Shell Height Box Plots

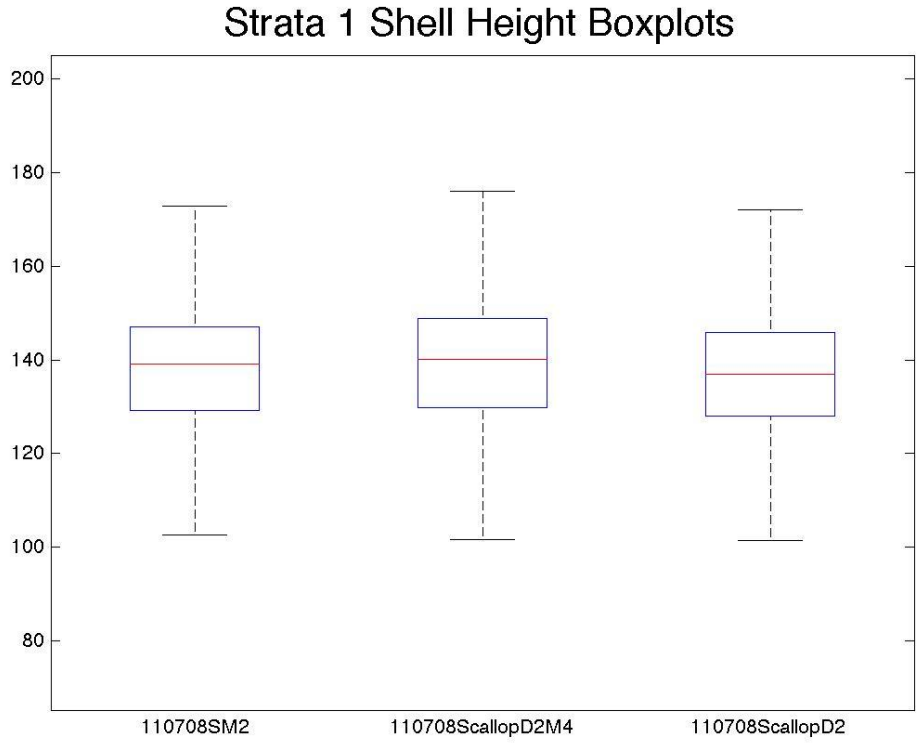

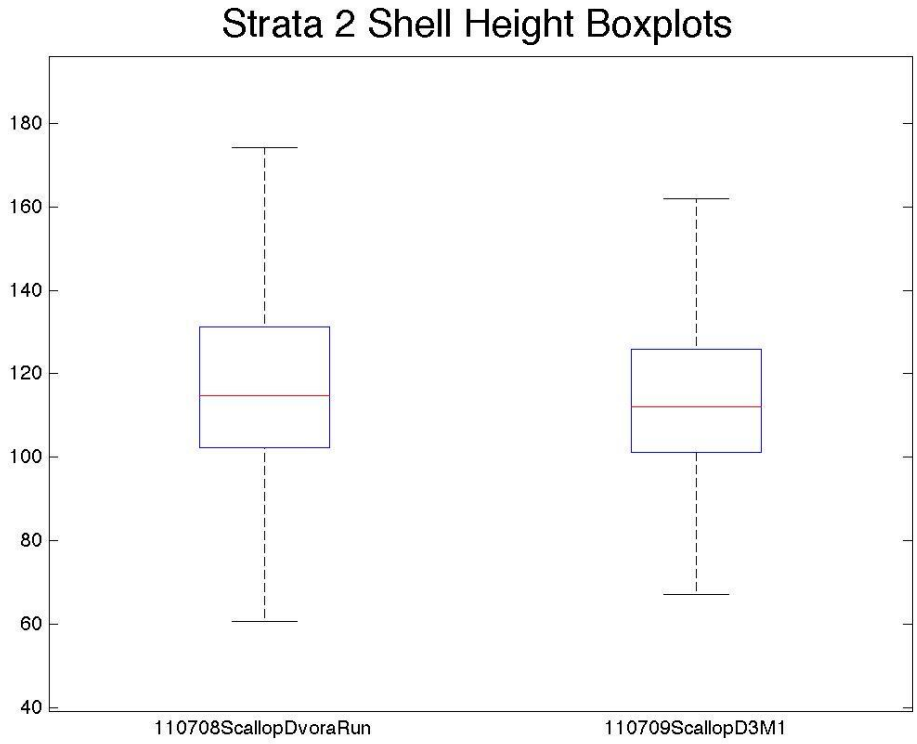
Strata 2 Shell Height Boxplots
180
160
140
120
100
80
60
40
110708ScallopDvoraRun
110709ScallopD3M1

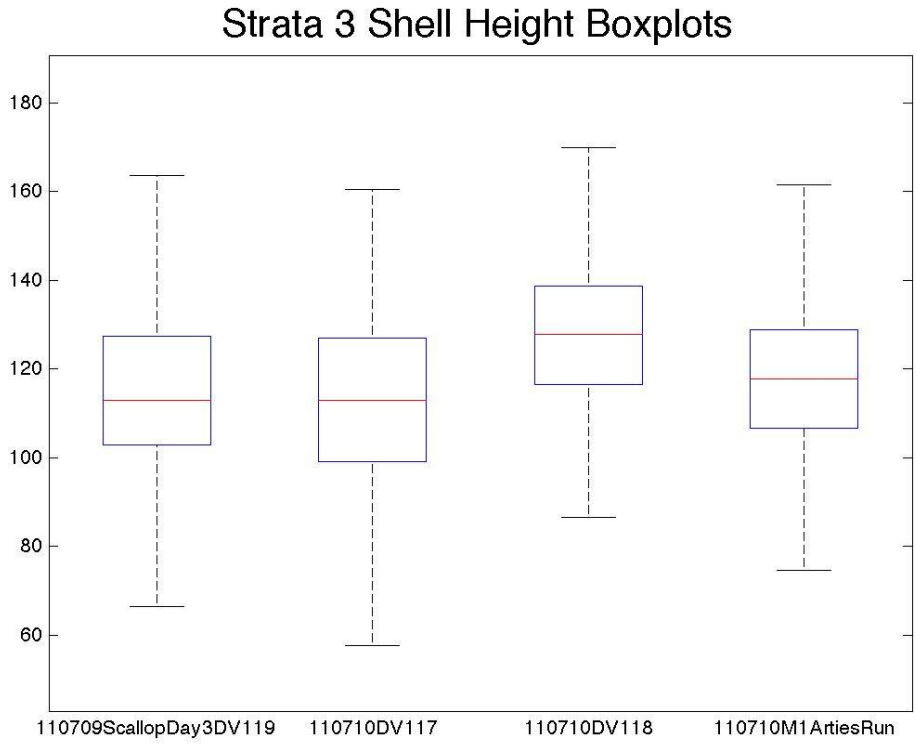
Strata 3 Shell Height Boxplots
180
160
140
120
100
80
60
110709ScallopDay3DV119
110710DV117
110710DV118
110710M1ArtiesRun

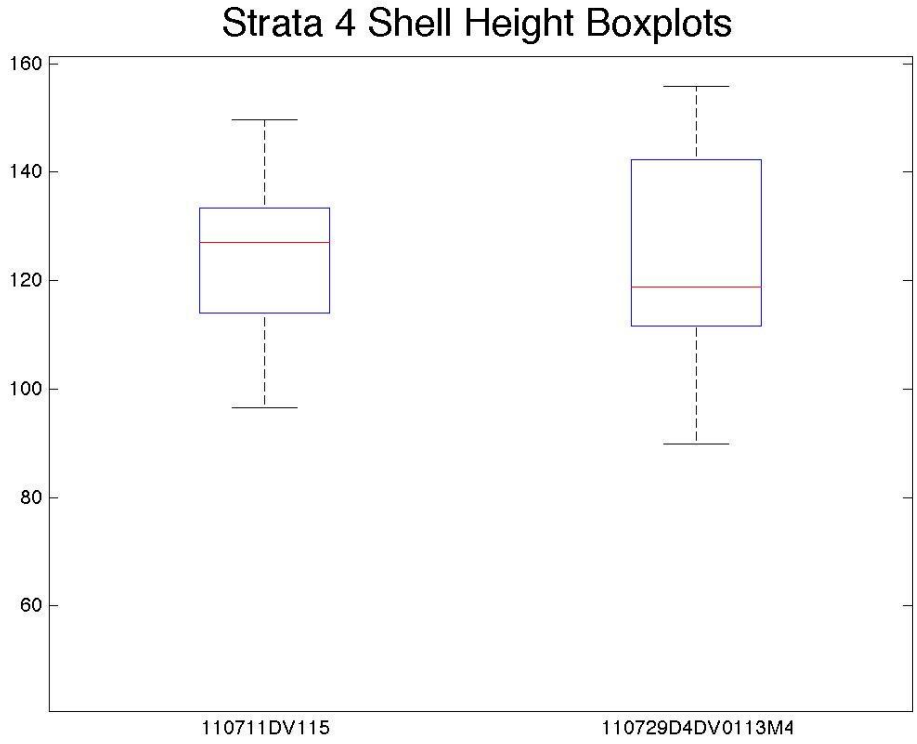
Strata 4 Shell Height Boxplots
160
140
120
100
80
60
110711DV115
110729D4DV0113M4

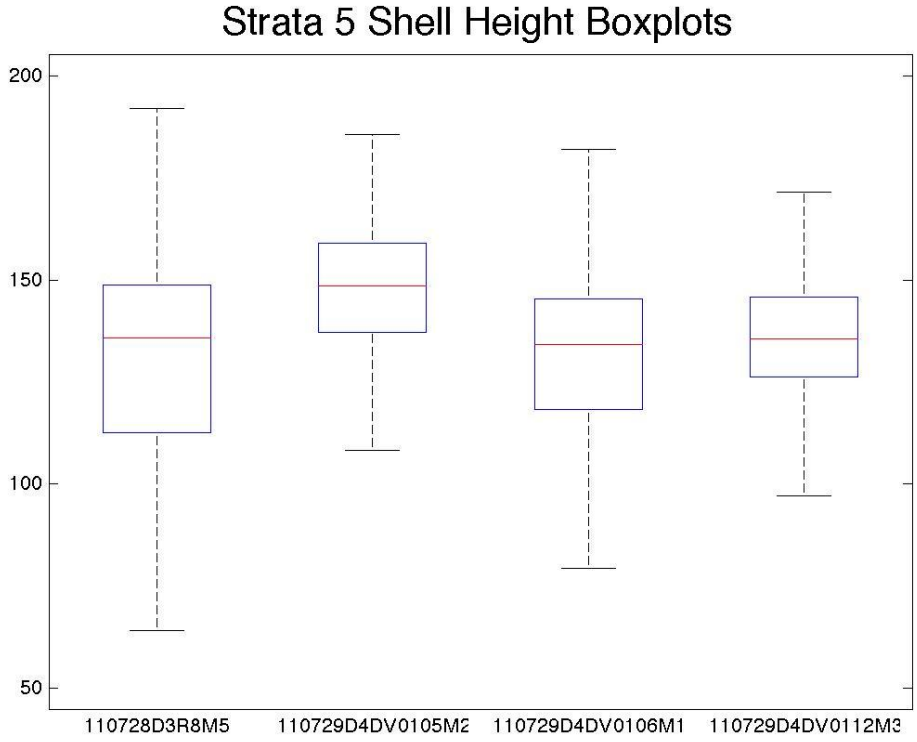
Strata 5 Shell Height Boxplots
200
150
100
50
110728D3R8M5
110729D4DV0105M2
110729D4DV0106M1
110729D4DV0112M3

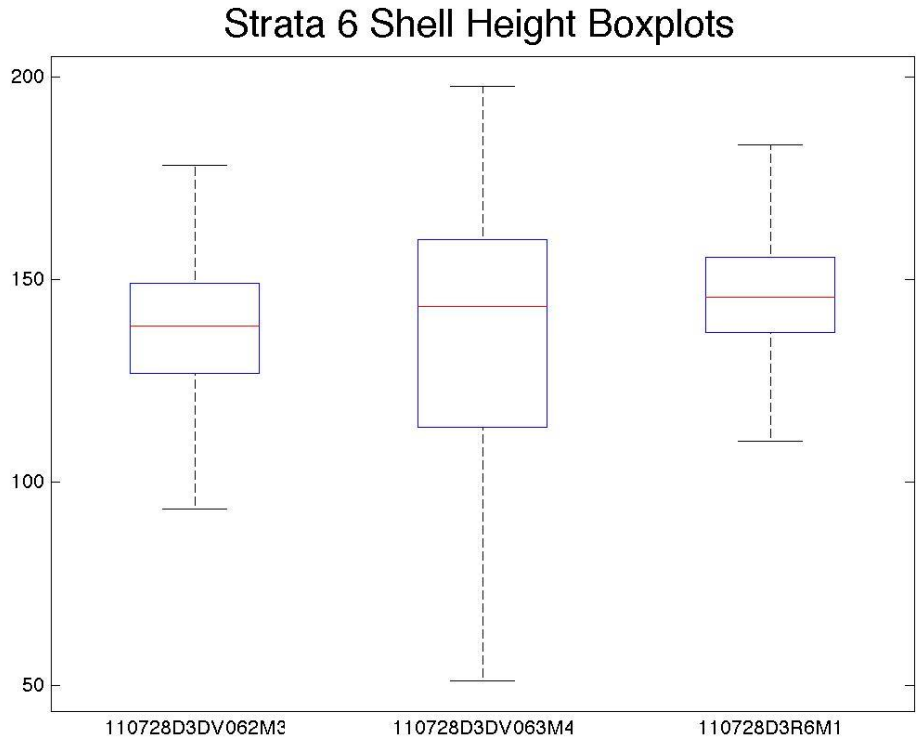
Strata 6 Shell Height Boxplots
200
150
100
50
110728D3DV062M3
110728D3DV063M4
110728D3R6M1

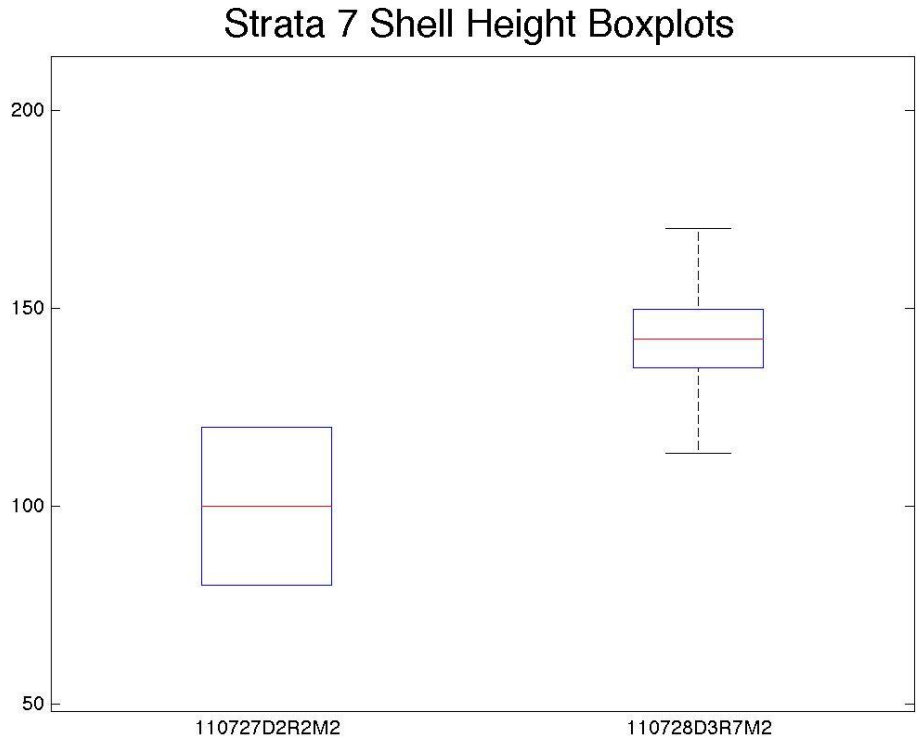
Strata 7 Shell Height Boxplots
200
150
100
50
110727D2R2M2
110728D3R7M2

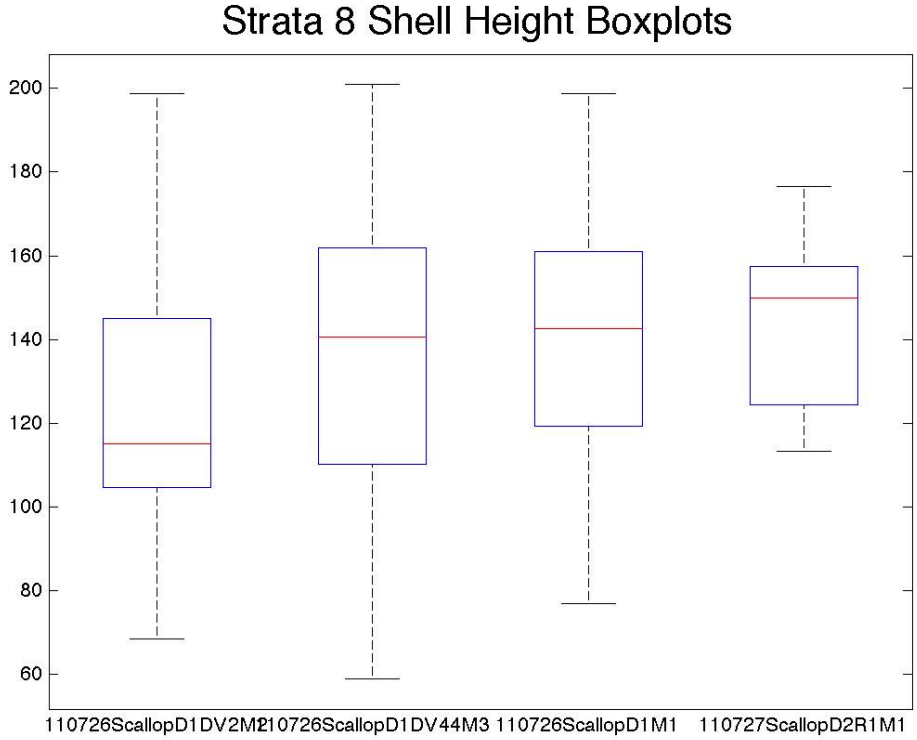
Strata 8 Shell Height Boxplots
200
180
160
140
120
100
80
60
110726ScallopD1DV2M2
110726ScallopD1DV44M3
110726ScallopD1M1
110727ScallopD2R1M1

Appendix C

OMNIDIRECTIONAL VARIOGRAMS

C.1 Introduction

This appendix contains the omnidirectional variograms for each AUV sea scallop survey mission. Each variograms was plotted at half of the maximum lag distance found for the mission. For an in depth review of variograms see Section 2.3.10.

C.2 Sea Scallop Survey Variograms

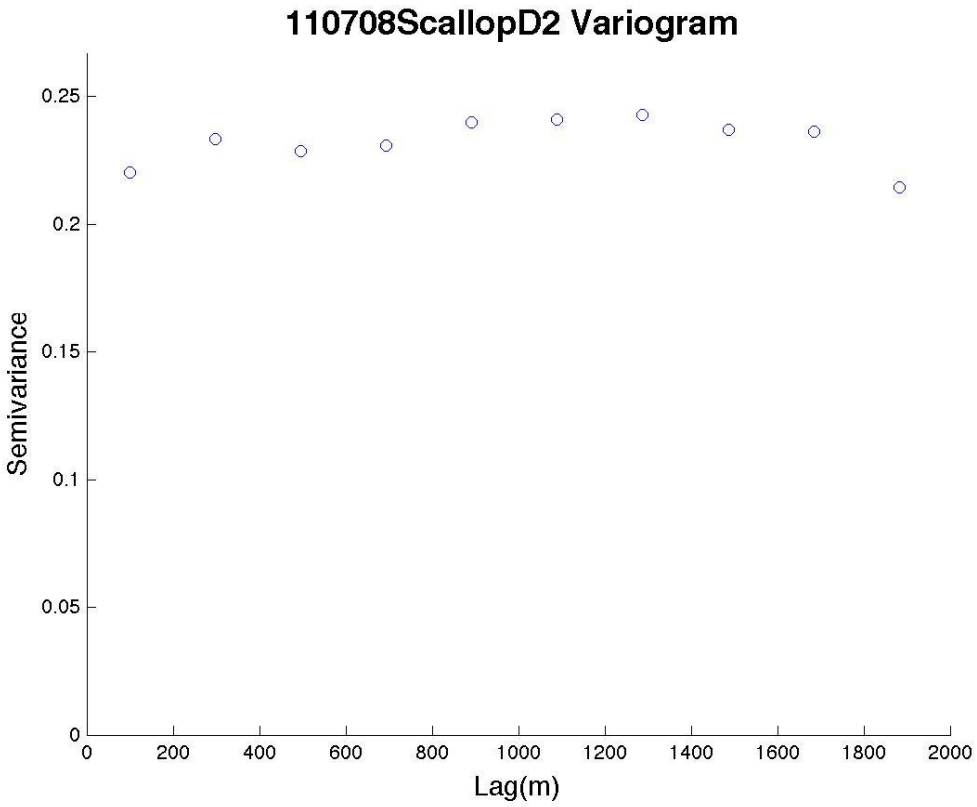

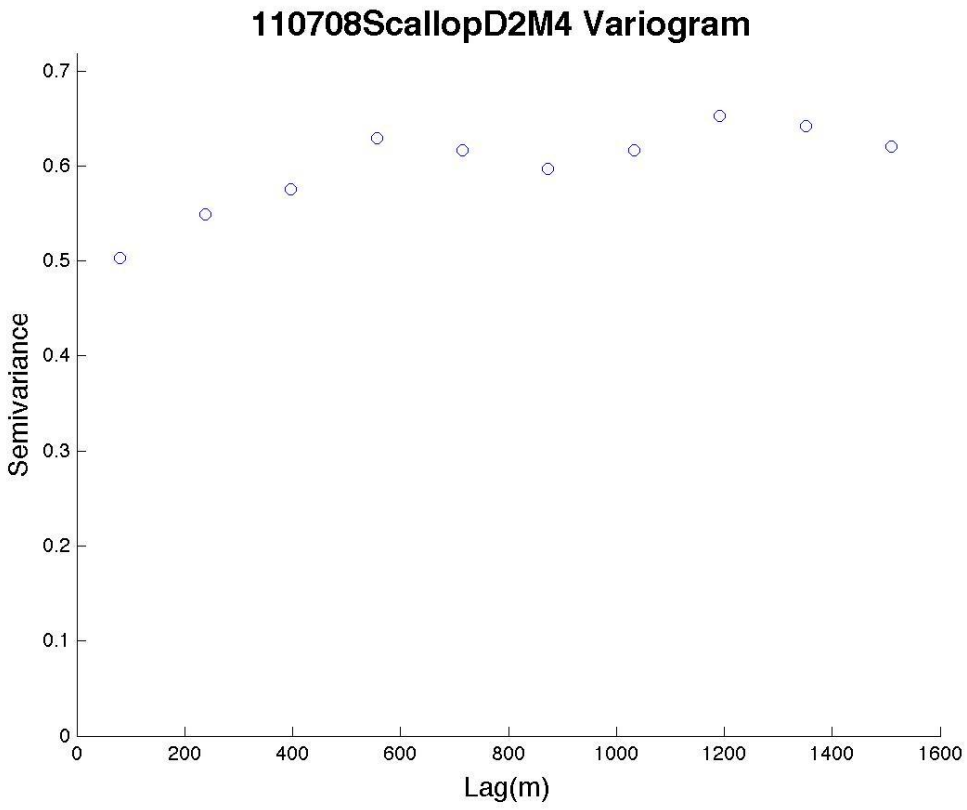
110708ScallopD2M4 Variogram
Semivariance
Lag(m)
0
0.1
0.2
0.3
0.4
0.5
0.6
0.7
0
200
400
600
800
1000
1200
1400
1600

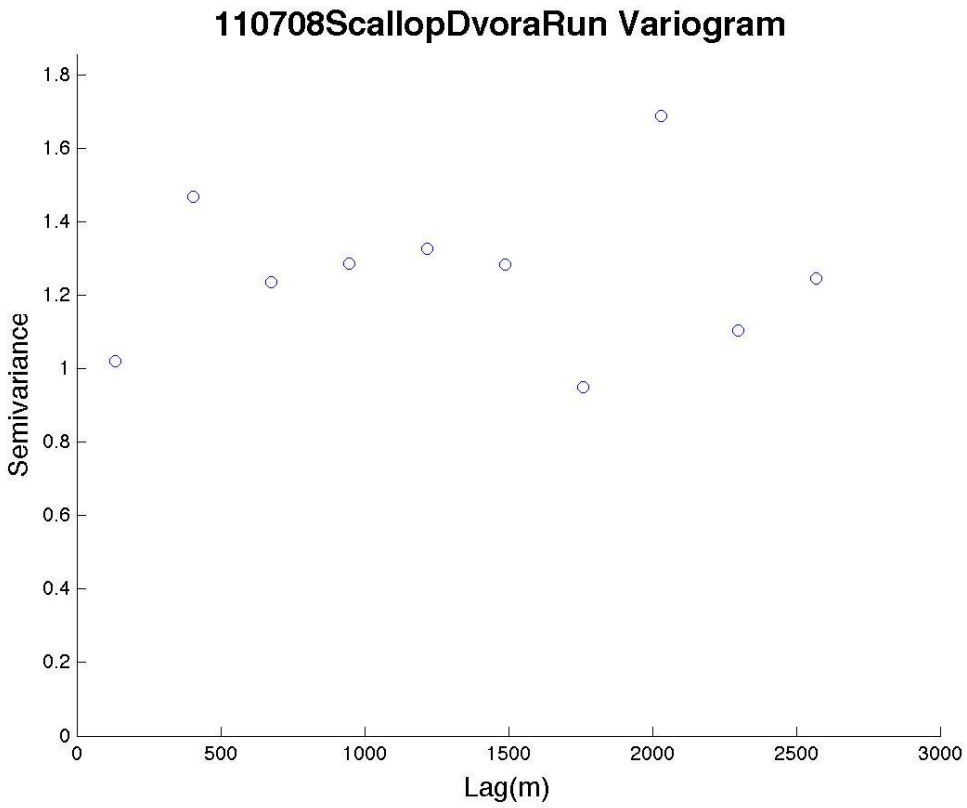
110708ScallopDvoraRun Variogram
Semivariance
Lag(m)
0
0.2
0.4
0.6
0.8
1
1.2
1.4
1.6
1.8
0
500
1000
1500
2000
2500
3000

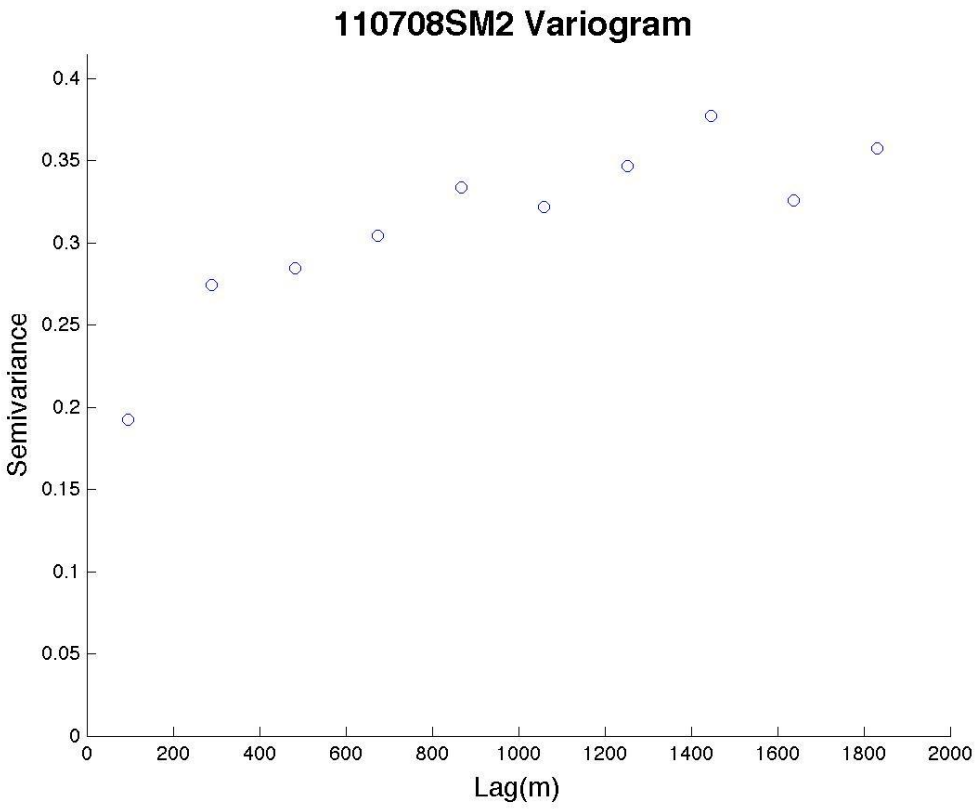
110708SM2 Variogram
Semivariance
Lag(m)
0
0.05
0.1
0.15
0.2
0.25
0.3
0.35
0.4
0
200
400
600
800
1000
1200
1400
1600
1800
2000

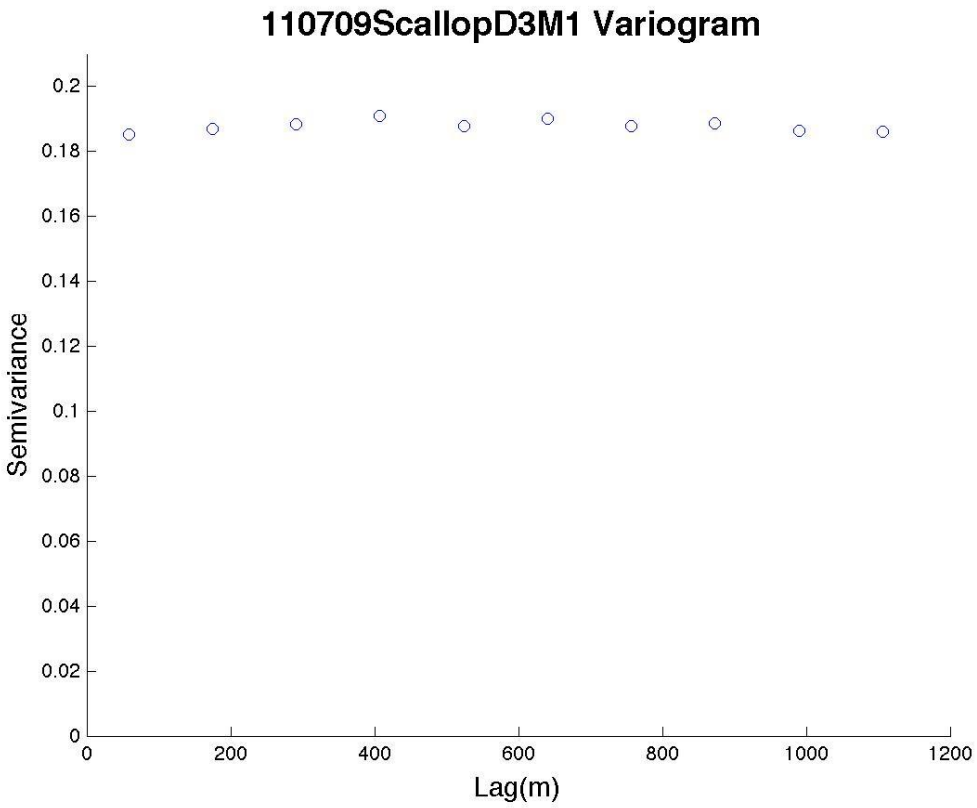
110709ScallopD3M1 Variogram
Semivariance
Lag(m)
0
0.02
0.04
0.06
0.08
0.1
0.12
0.14
0.16
0.18
0.2
0
200
400
600
800
1000
1200

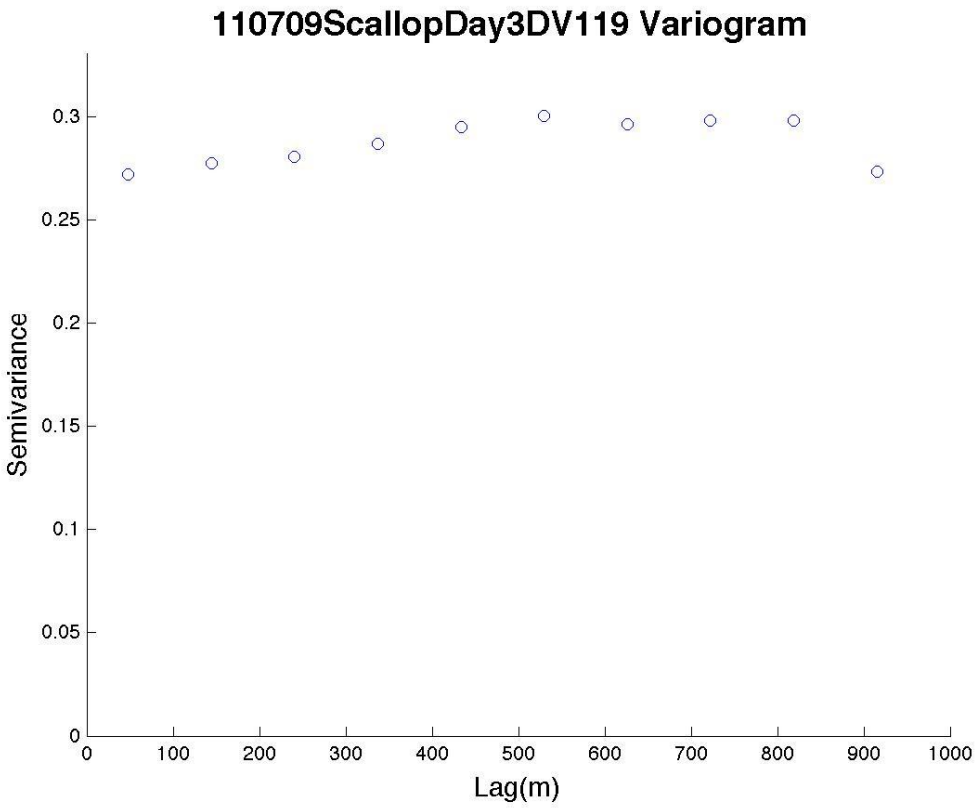
110709ScallopDay3DV119 Variogram
Semivariance
Lag(m)
0
0.05
0.1
0.15
0.2
0.25
0.3
0
100
200
300
400
500
600
700
800
900
1000

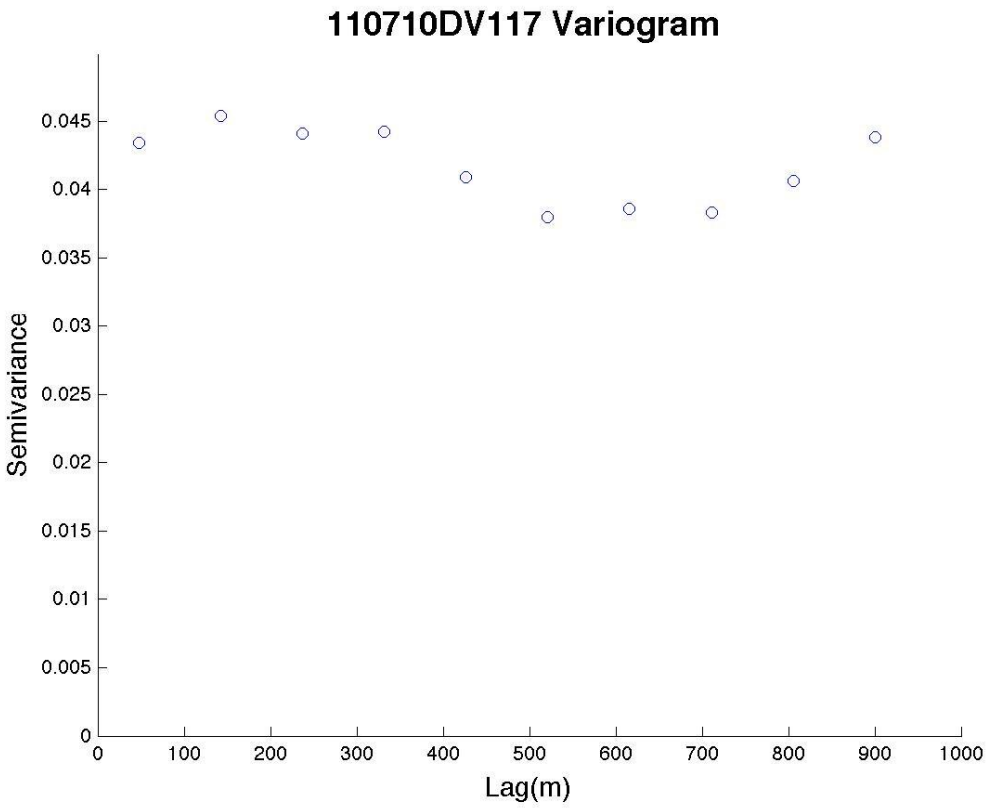
110710DV117 Variogram
Semivariance
Lag(m)
0
0.005
0.01
0.015
0.02
0.025
0.03
0.035
0.04
0.045
0
100
200
300
400
500
600
700
800
900
1000

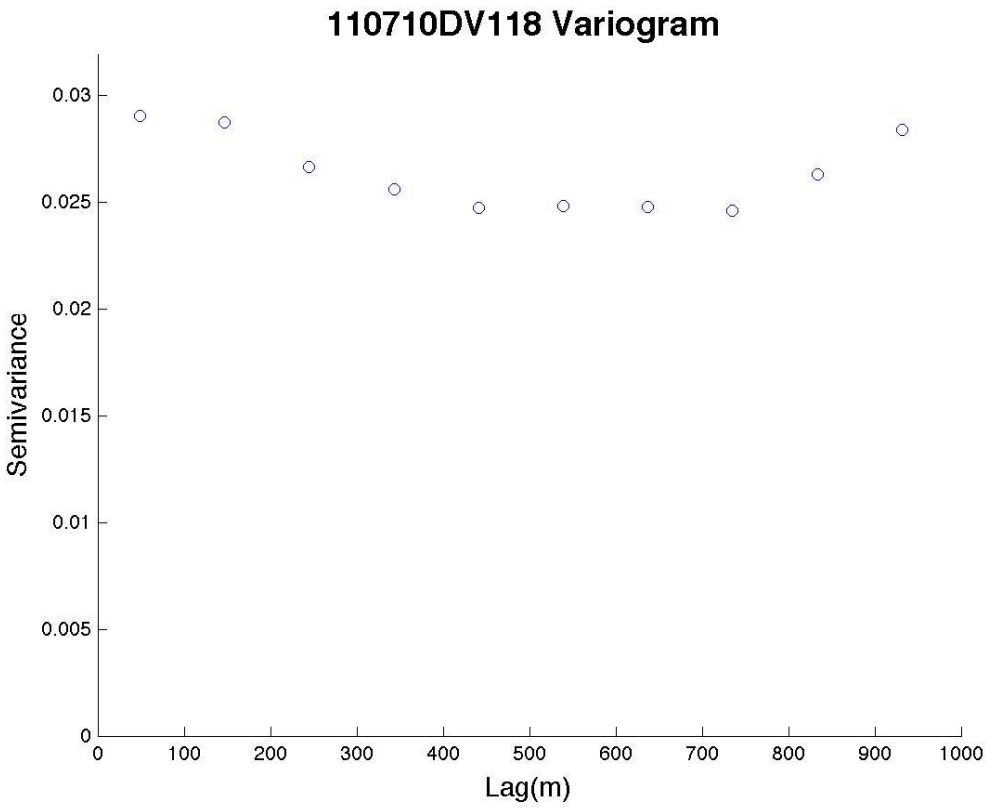
110710DV118 Variogram
Semivariance
Lag(m)
0.03
0.025
0.02
0.015
0.01
0.005
0
0
100
200
300
400
500
600
700
800
900
1000

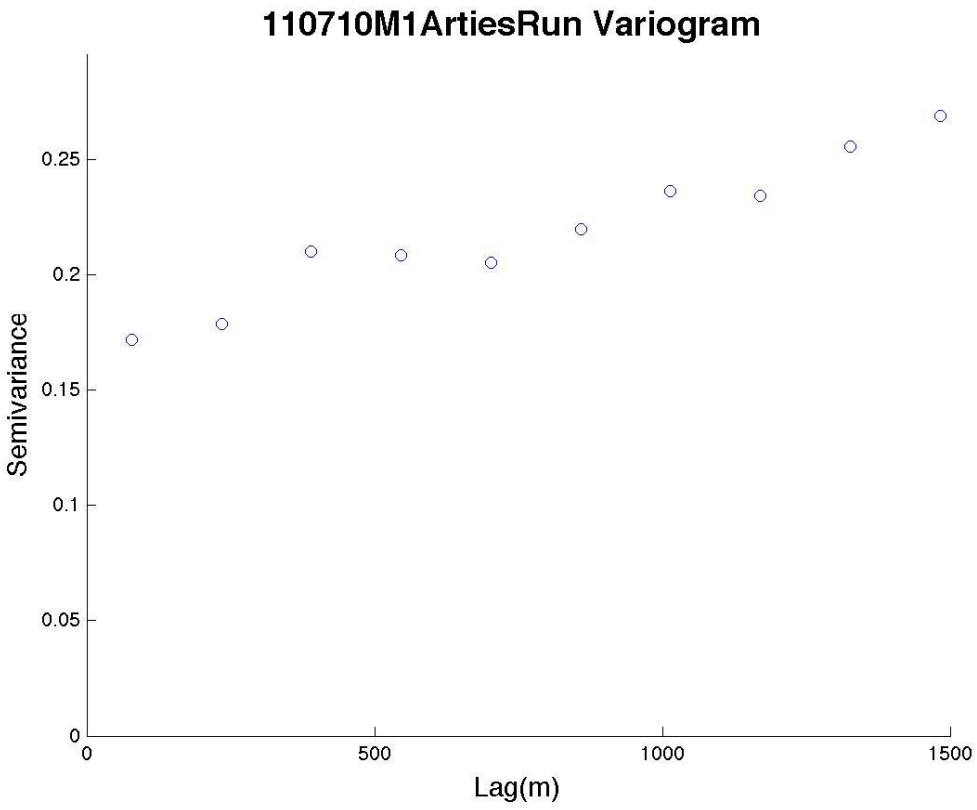
110710M1ArtiesRun Variogram
Semivariance
0
0.05
0.1
0.15
0.2
0.25
0
500
1000
1500
Lag(m)

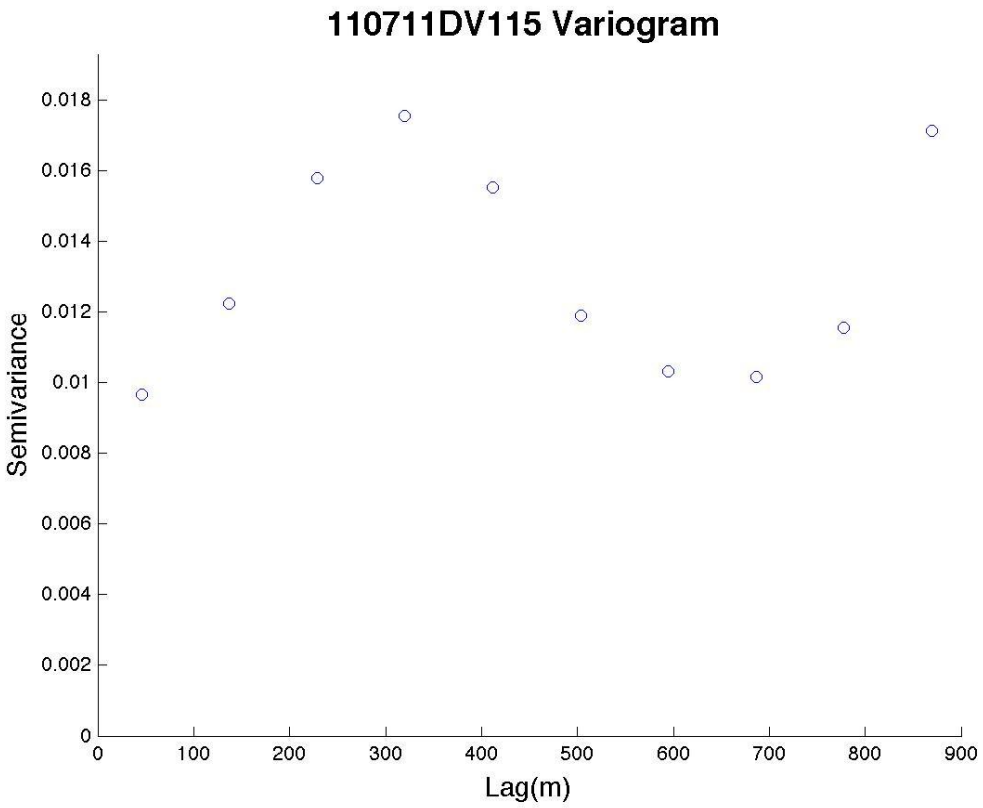
110711DV115 Variogram
Semivariance
Lag(m)
0
0.002
0.004
0.006
0.008
0.01
0.012
0.014
0.016
0.018
0
100
200
300
400
500
600
700
800
900

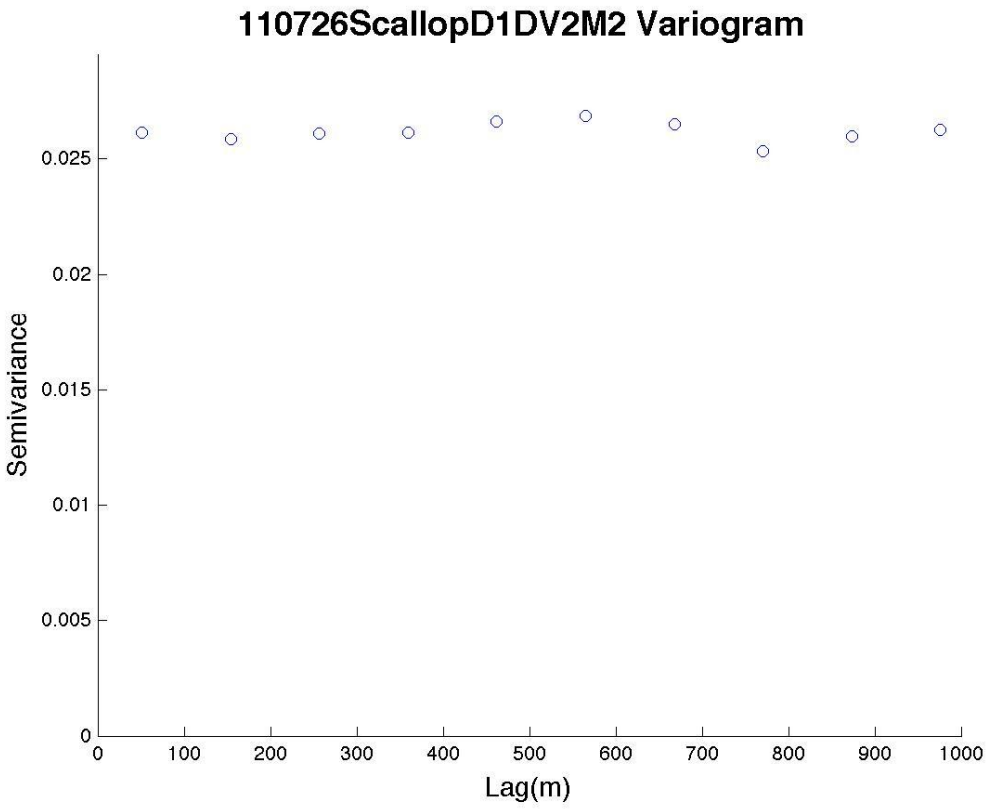
110726ScallopD1DV2M2 Variogram
Semivariance
0
0.005
0.01
0.015
0.02
0.025
0
100
200
300
400
500
600
700
800
900
1000
Lag(m)

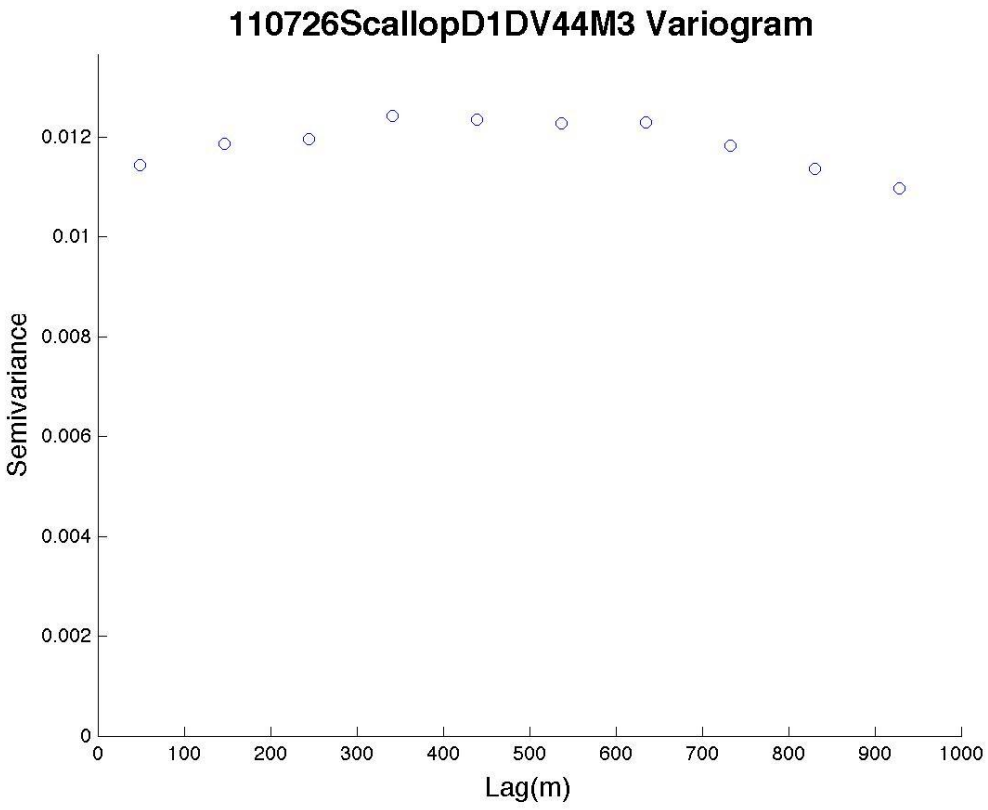
110726ScallopD1DV44M3 Variogram
Semivariance
Lag(m)
0
0.002
0.004
0.006
0.008
0.01
0.012
0
100
200
300
400
500
600
700
800
900
1000

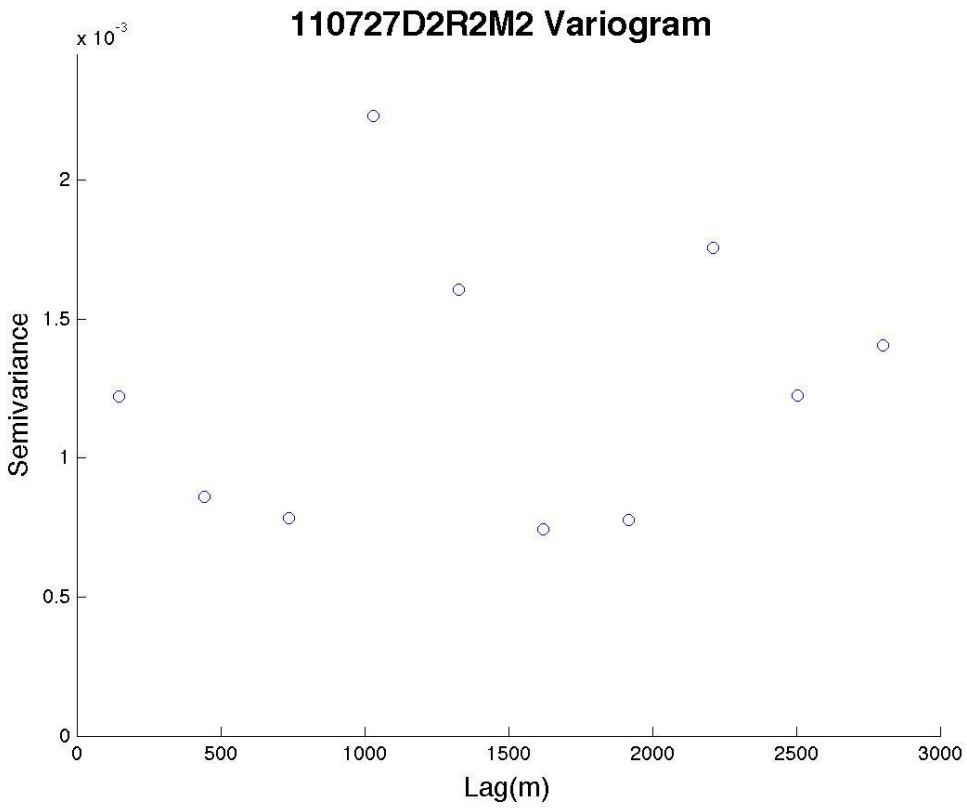
110727D2R2M2 Variogram
x 10^-3
Semivariance
Lag(m)
0
0.5
1
1.5
2
0
500
1000
1500
2000
2500
3000

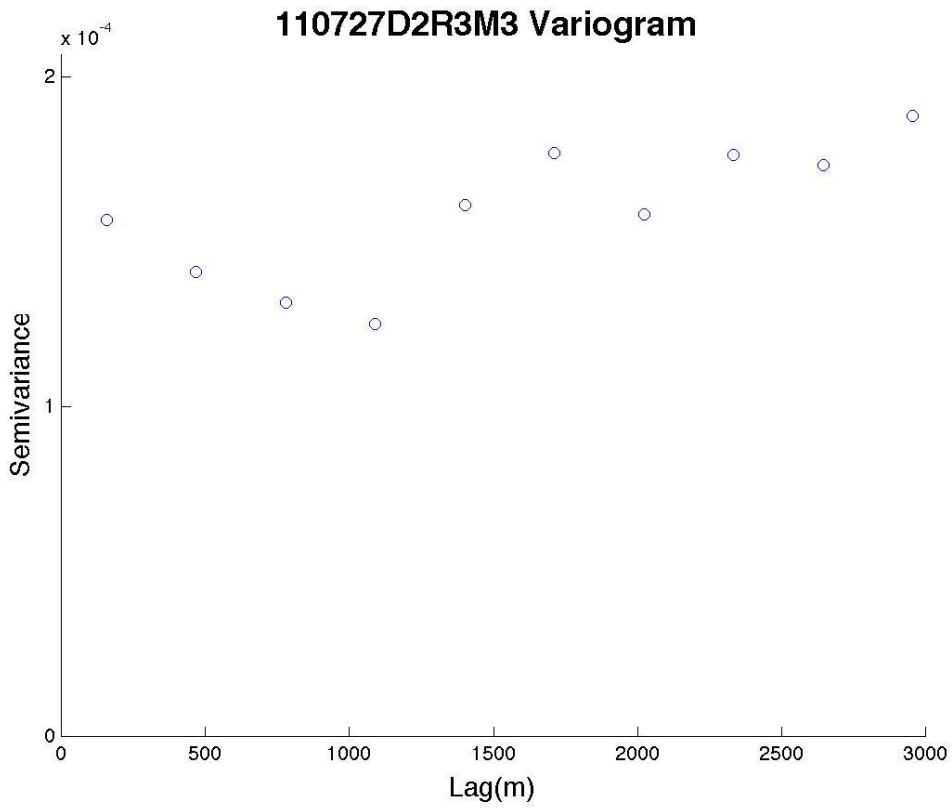
110727D2R3M3 Variogram
x 10^-4
2
1
0
Semivariance
0
500
1000
1500
2000
2500
3000
Lag(m)

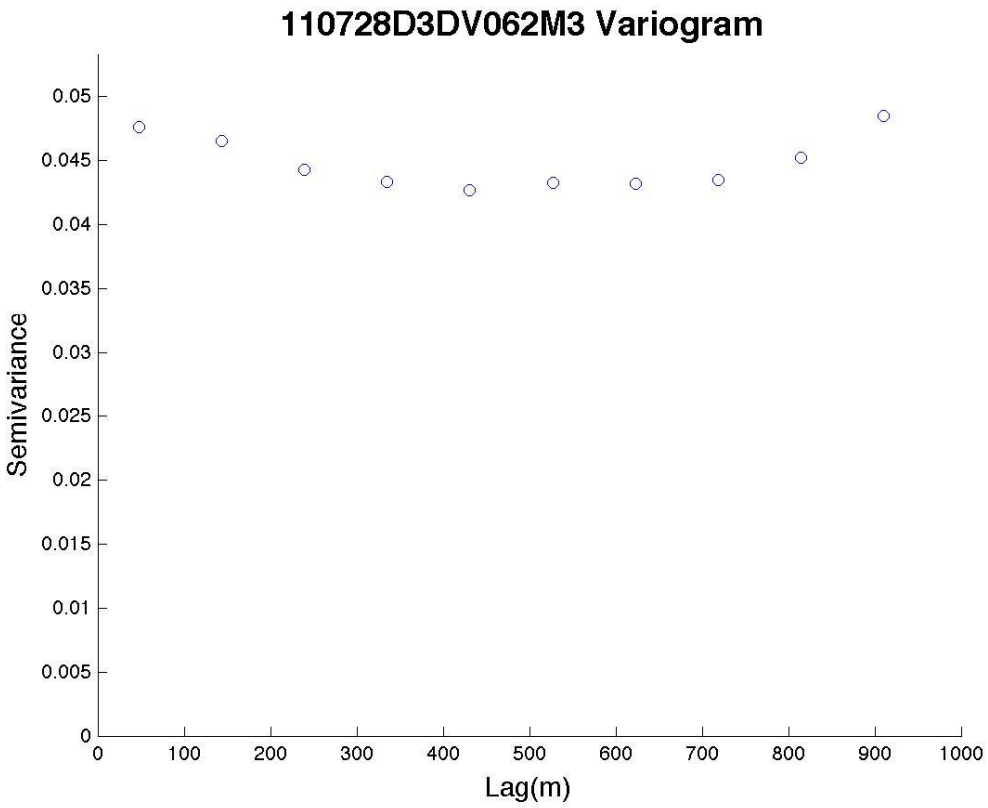
110728D3DV062M3 Variogram
Semivariance
Lag(m)
0
0.005
0.01
0.015
0.02
0.025
0.03
0.035
0.04
0.045
0.05
0
100
200
300
400
500
600
700
800
900
1000

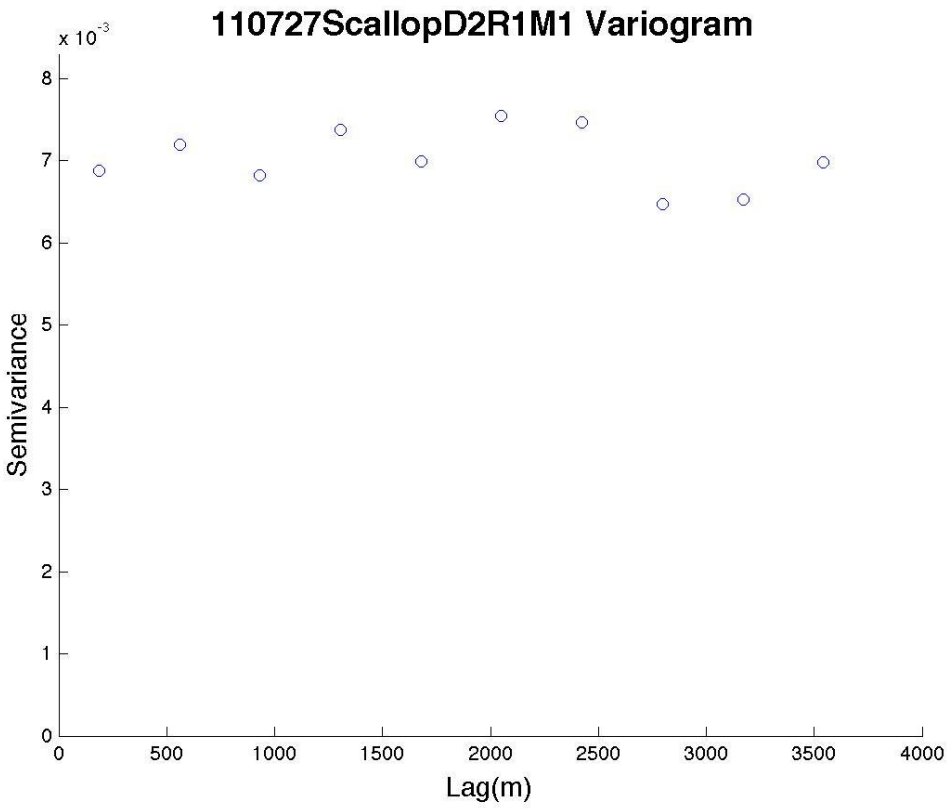
110727ScallopD2R1M1 Variogram
x 10^-3
Semivariance
Lag(m)
0
1
2
3
4
5
6
7
8
0
500
1000
1500
2000
2500
3000
3500
4000

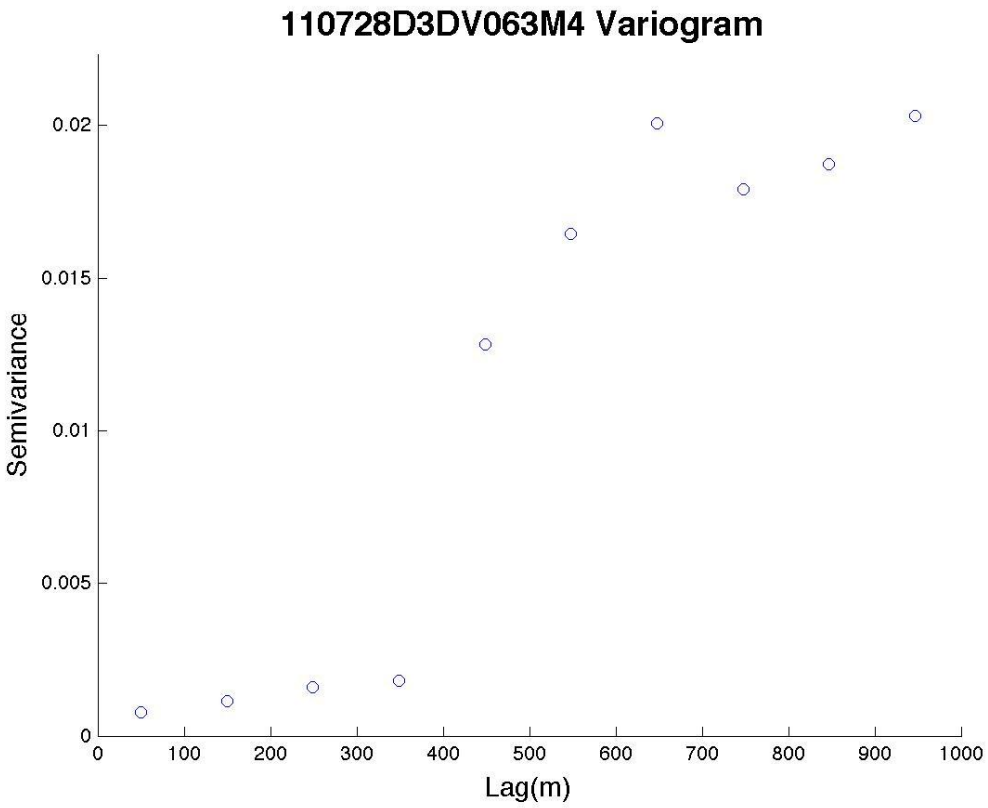
110728D3DV063M4 Variogram
Semivariance
Lag(m)
0
0.005
0.01
0.015
0.02
0
100
200
300
400
500
600
700
800
900
1000

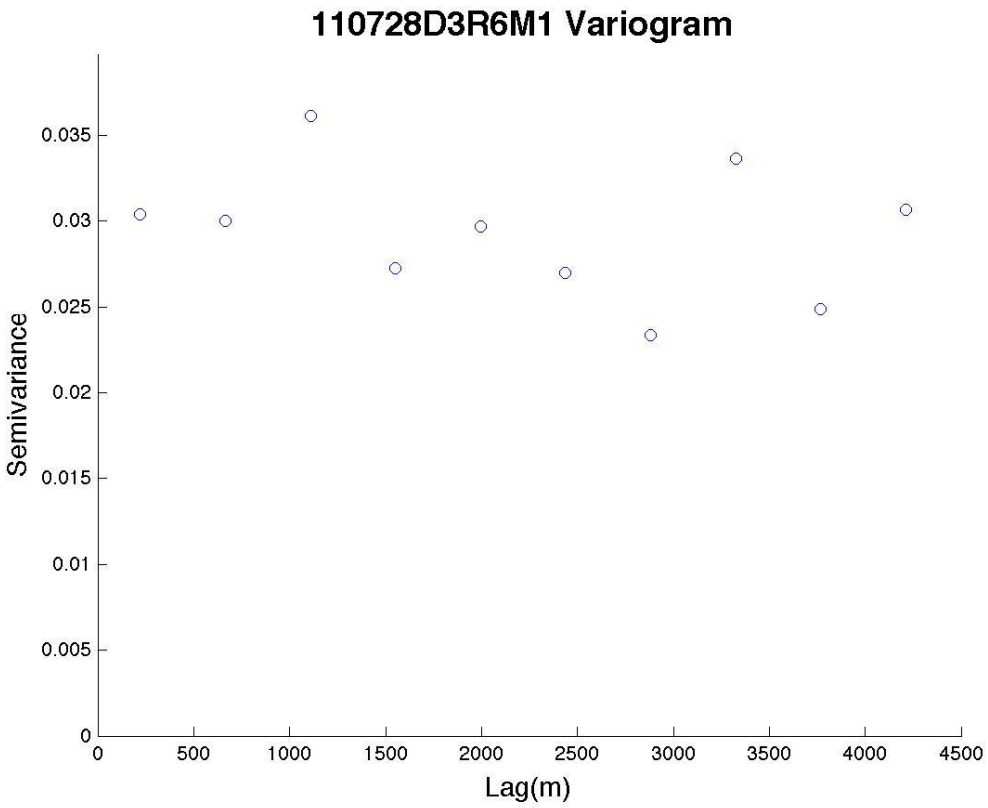
110728D3R6M1 Variogram
Semivariance
Lag(m)
0
0.005
0.01
0.015
0.02
0.025
0.03
0.035
0
500
1000
1500
2000
2500
3000
3500
4000
4500

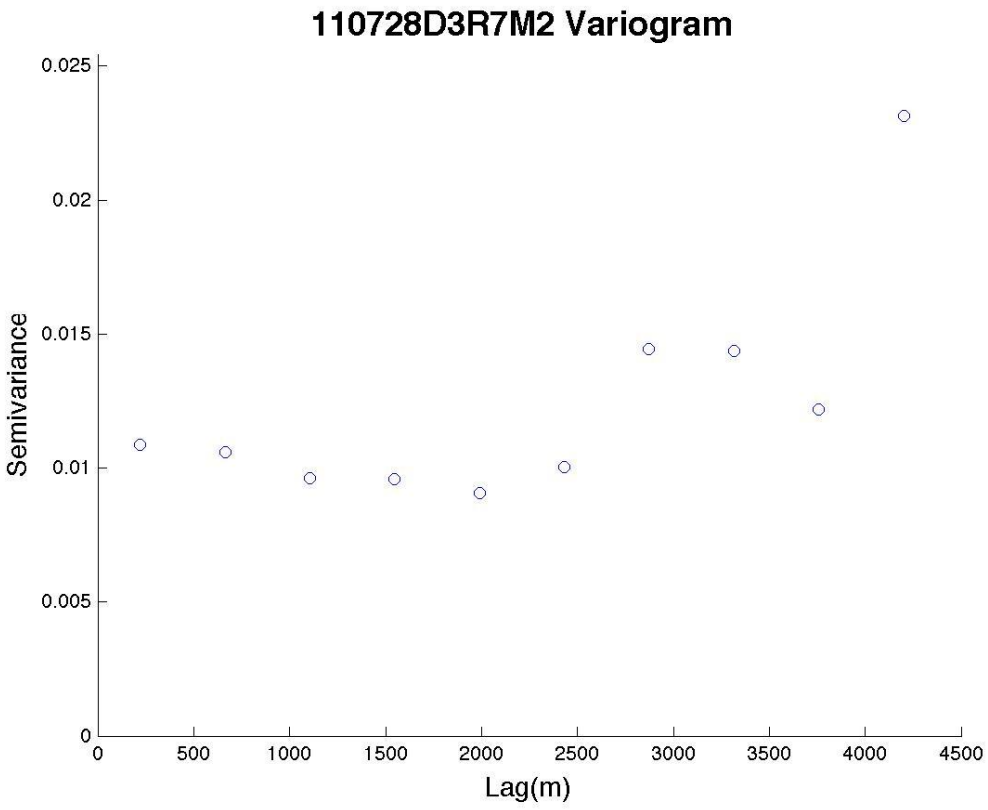
110728D3R7M2 Variogram
Semivariance
Lag(m)
0.025
0.02
0.015
0.01
0.005
0
0
500
1000
1500
2000
2500
3000
3500
4000
4500

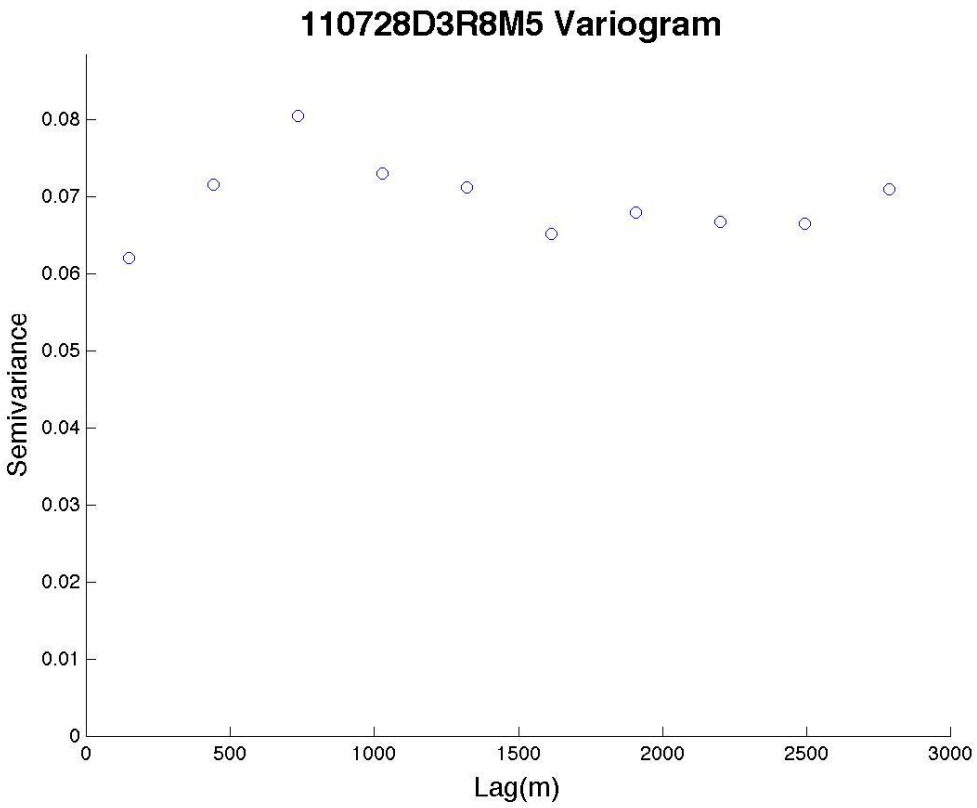
110728D3R8M5 Variogram
Semivariance
Lag(m)
0
0.01
0.02
0.03
0.04
0.05
0.06
0.07
0.08
0
500
1000
1500
2000
2500
3000

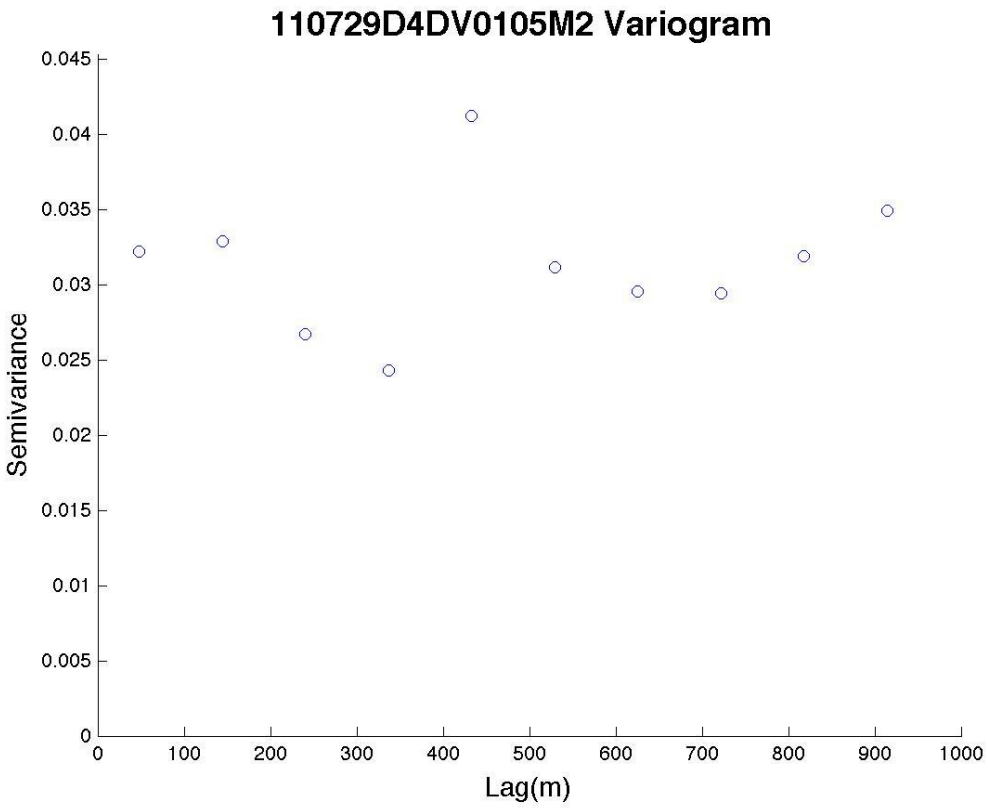
110729D4DV0105M2 Variogram
Semivariance
Lag(m)
0.045
0.04
0.035
0.03
0.025
0.02
0.015
0.01
0.005
0
0
100
200
300
400
500
600
700
800
900
1000

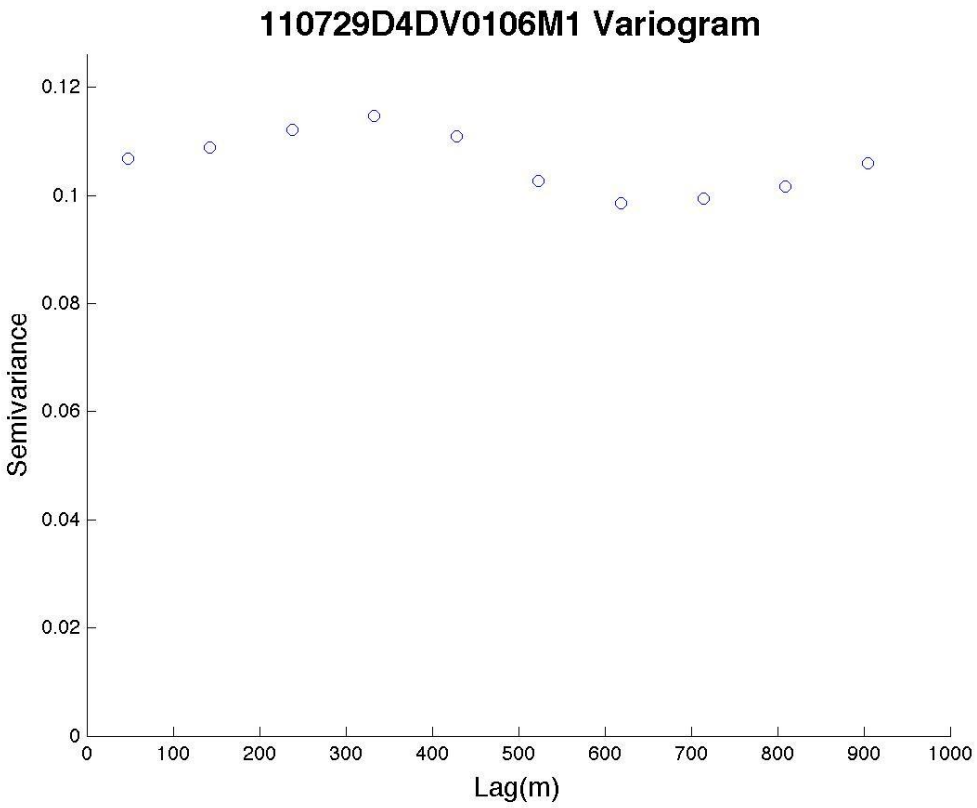
110729D4DV0106M1 Variogram
Semivariance
Lag(m)
0
0.02
0.04
0.06
0.08
0.1
0.12
0
100
200
300
400
500
600
700
800
900
1000

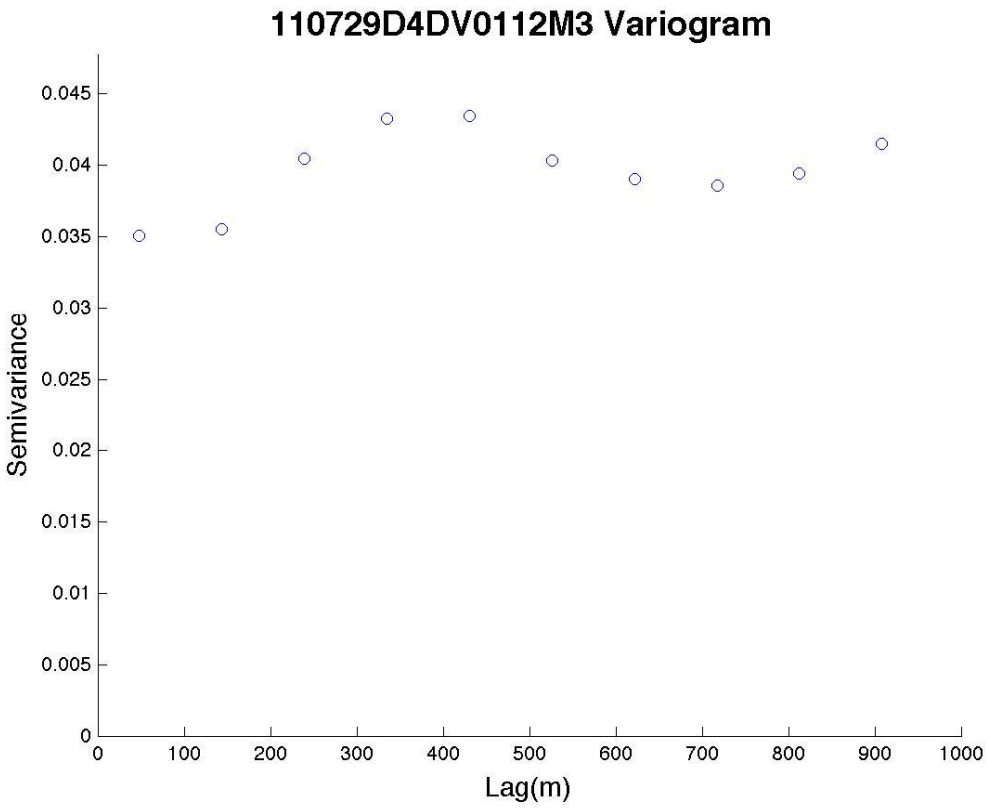
110729D4DV0112M3 Variogram
Semivariance
Lag(m)
0
0.005
0.01
0.015
0.02
0.025
0.03
0.035
0.04
0.045
0
100
200
300
400
500
600
700
800
900
1000

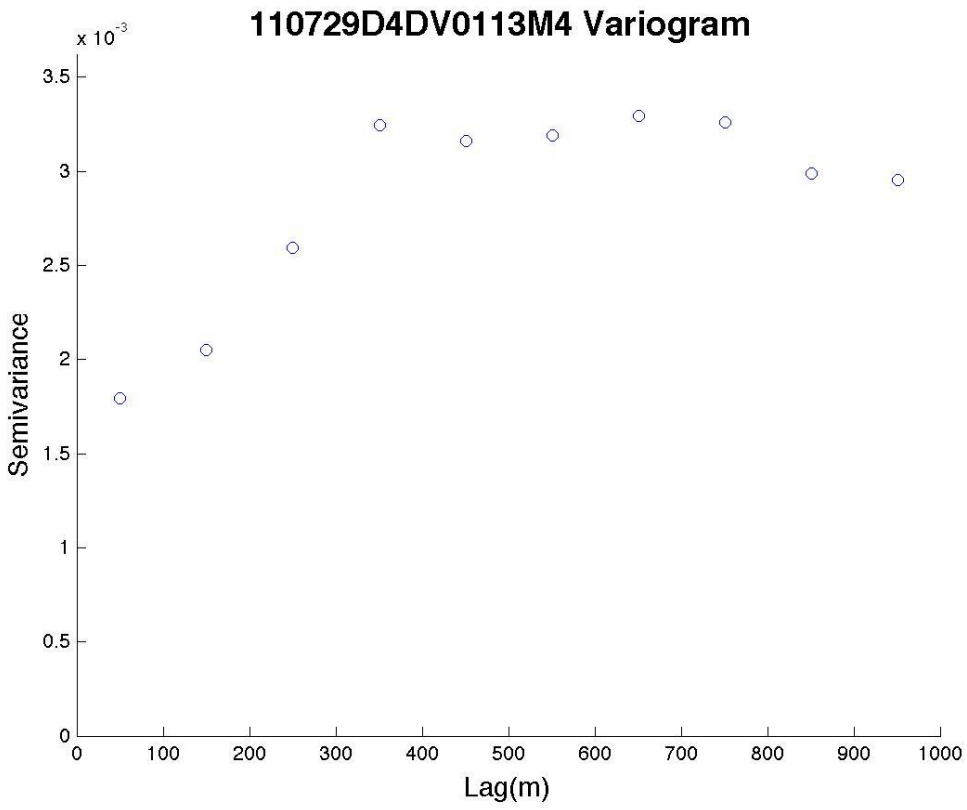
110729D4DV0113M4 Variogram
x 10^-3
3.5
3
2.5
2
1.5
1
0.5
0
Semivariance
0
100
200
300
400
500
600
700
800
900
1000
Lag(m)

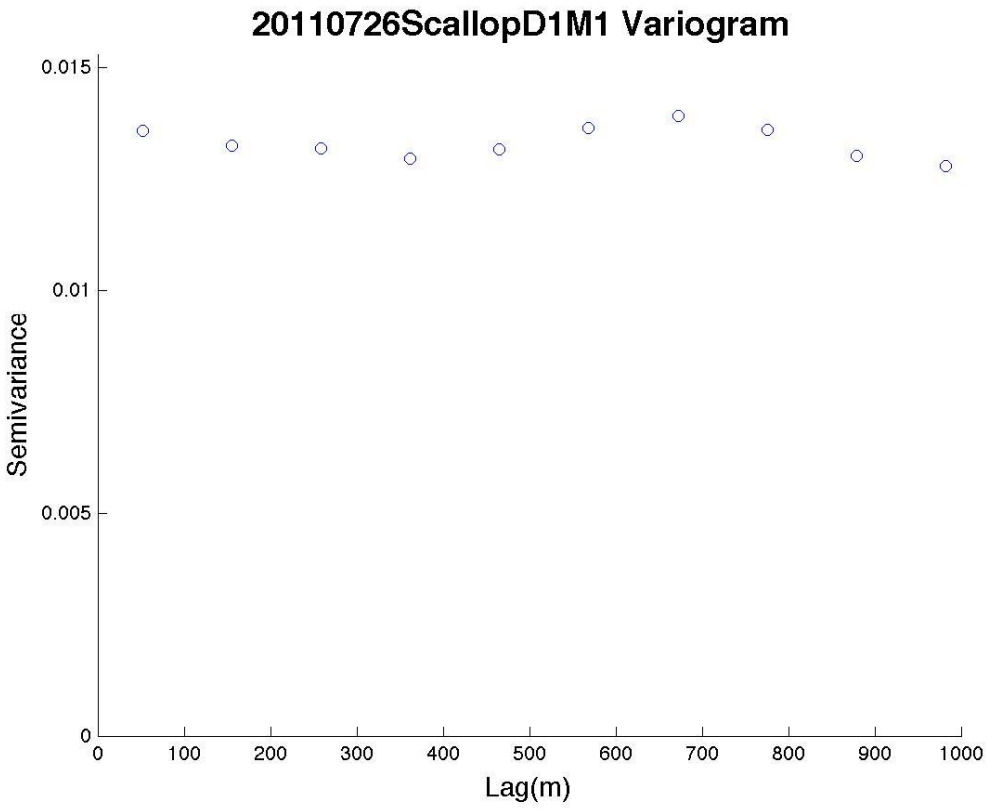
20110726ScallopD1M1 Variogram
Semivariance
Lag(m)
0.015
0.01
0.005
0
0
100
200
300
400
500
600
700
800
900
1000

Appendix D

SHELL HEIGHT HISTOGRAMS

D.1 Introduction

This appendix contains the photogrammetric sea scallop shell height histograms for each AUV survey mission. The bars are colored to coordinate to the sea scallop size classes: recruit (shell height less than 70 mm), sublegal (shell height between 70 mm and 101.6 mm), and mature (shell height greater than or equal to 101.6 mm).

D.2 Shell Height Histograms

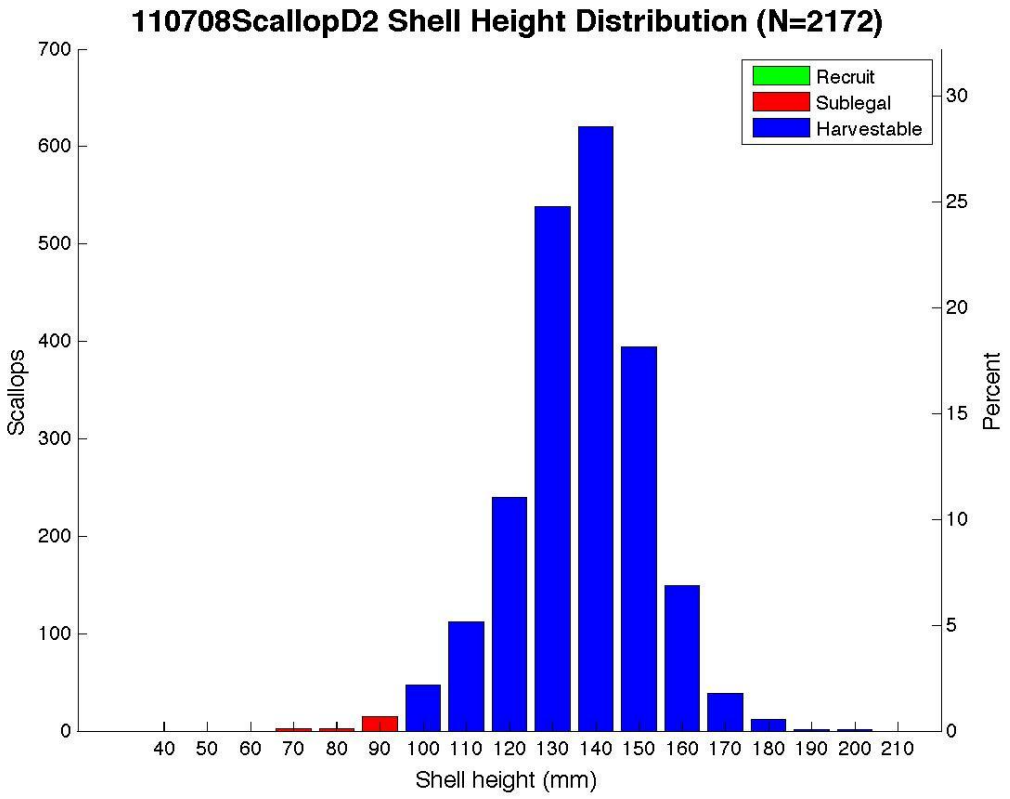

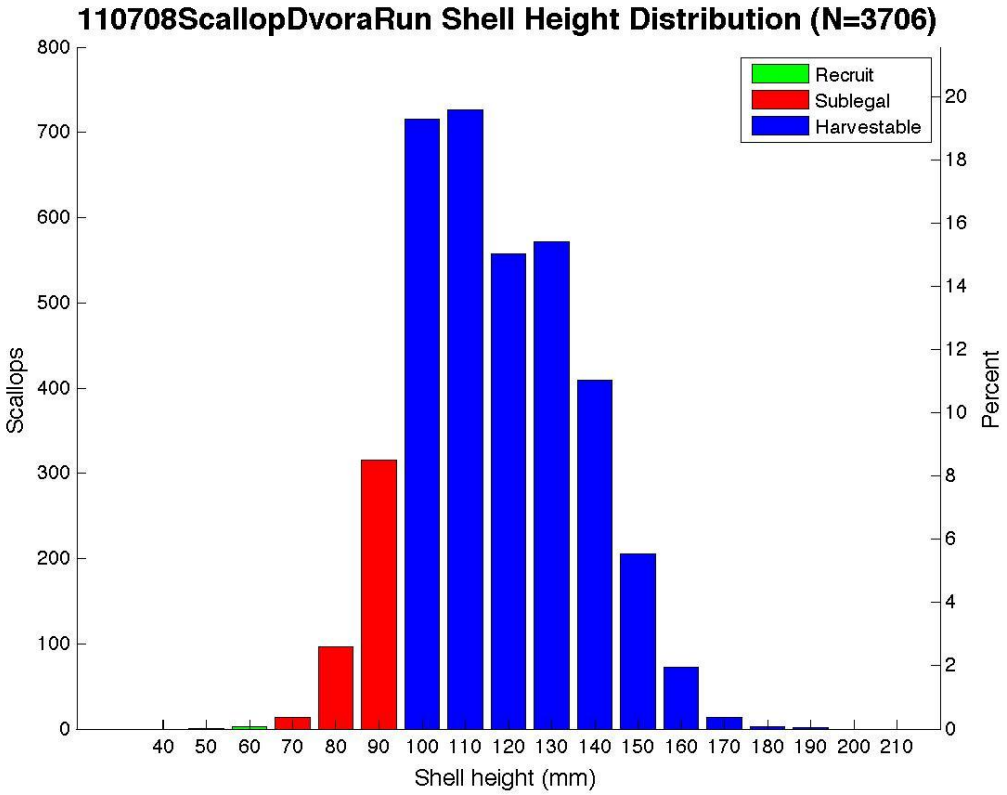
110708ScallopDvoraRun Shell Height Distribution (N=3706)
Recruit
Sublegal
Harvestable
Scallops
Percent
Shell height (mm)
0
100
200
300
400
500
600
700
800
0
2
4
6
8
10
12
14
16
18
20
40
50
60
70
80
90
100
110
120
130
140
150
160
170
180
190
200
210

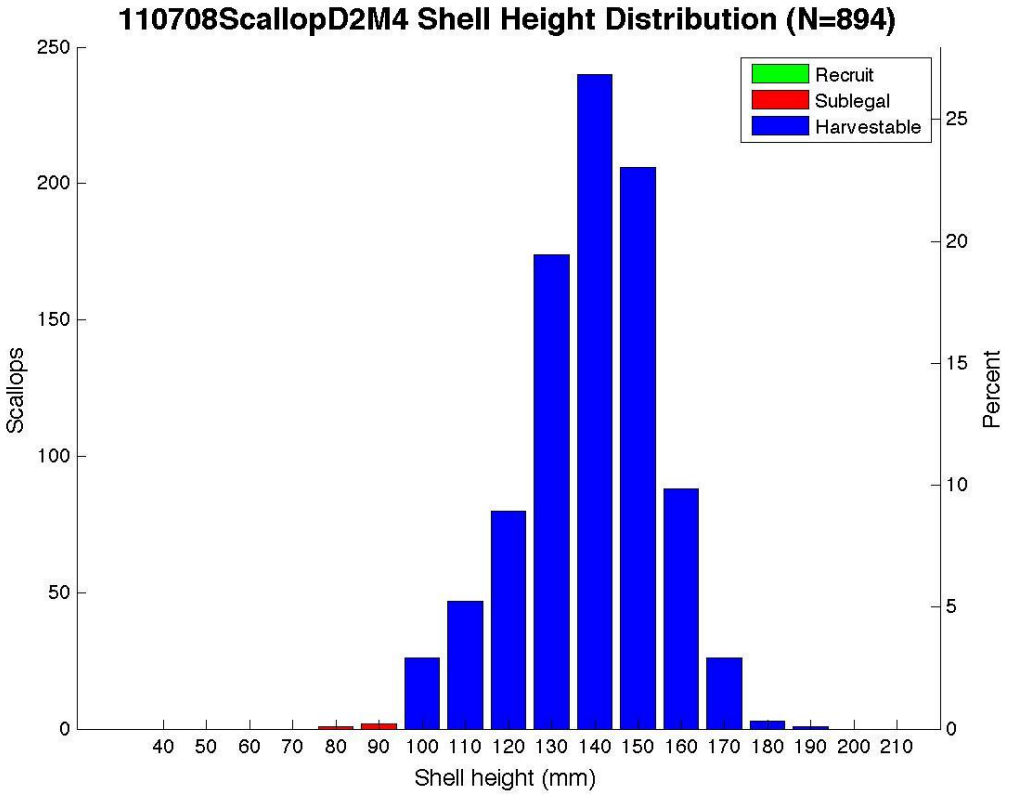
110708ScallopD2M4 Shell Height Distribution (N=894)
Recruit
Sublegal
Harvestable
Scallops
Percent
Shell height (mm)
0
50
100
150
200
250
0
5
10
15
20
25
40 50 60 70 80 90 100 110 120 130 140 150 160 170 180 190 200 210

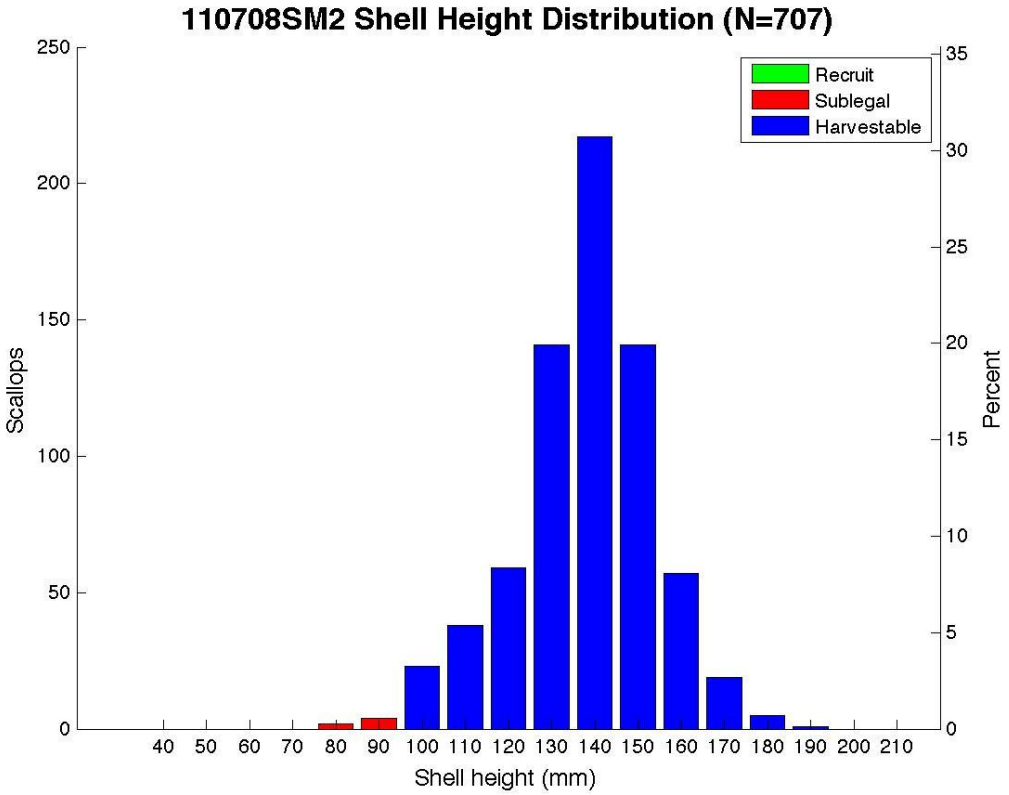
110708SM2 Shell Height Distribution (N=707)
Recruit
Sublegal
Harvestable
Scallops
Percent
Shell height (mm)
0
50
100
150
200
250
0
5
10
15
20
25
30
35
40 50 60 70 80 90 100 110 120 130 140 150 160 170 180 190 200 210

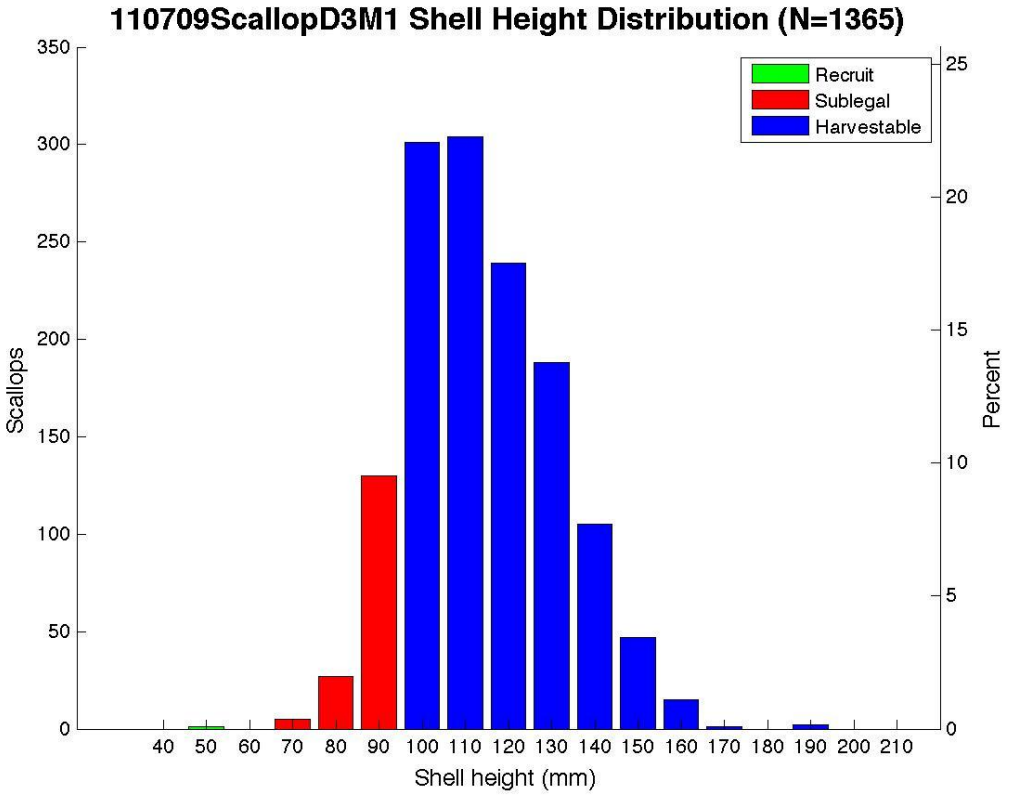
110709ScallopD3M1 Shell Height Distribution (N=1365)
Recruit
Sublegal
Harvestable
Scallops
Percent
Shell height (mm)
0
50
100
150
200
250
300
350
0
5
10
15
20
25
40
50
60
70
80
90
100
110
120
130
140
150
160
170
180
190
200
210

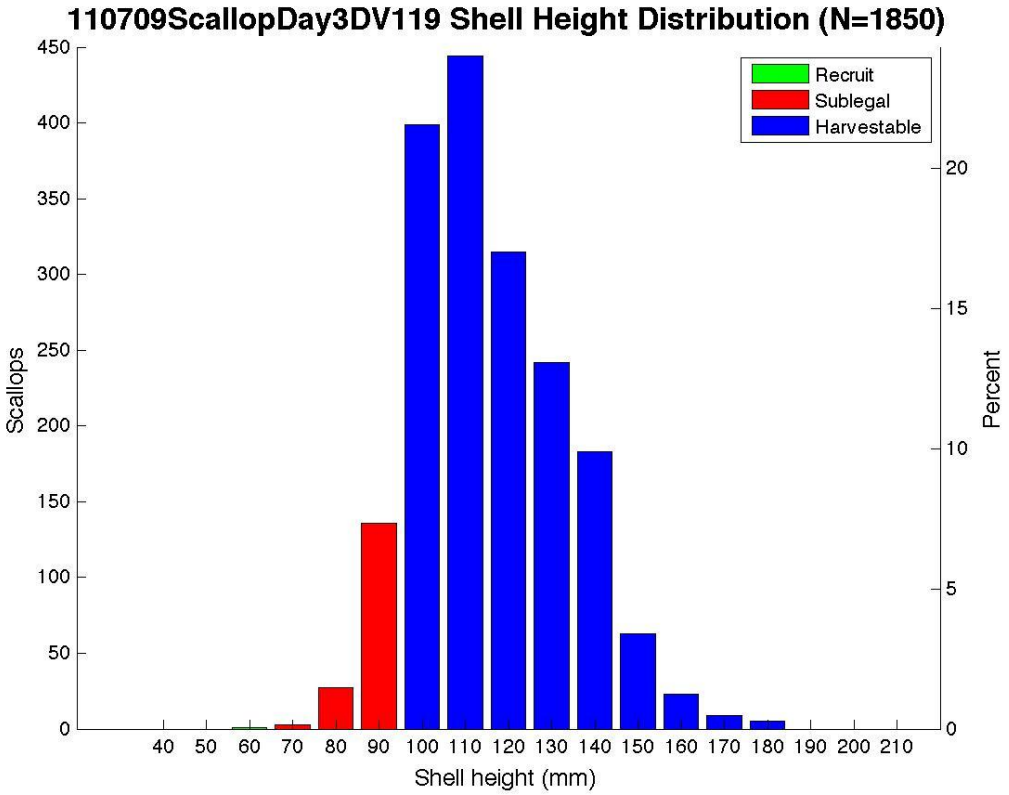
110709ScallopDay3DV119 Shell Height Distribution (N=1850)
Recruit
Sublegal
Harvestable
Scallops
Percent
Shell height (mm)
0
50
100
150
200
250
300
350
400
450
0
5
10
15
20
40
50
60
70
80
90
100
110
120
130
140
150
160
170
180
190
200
210

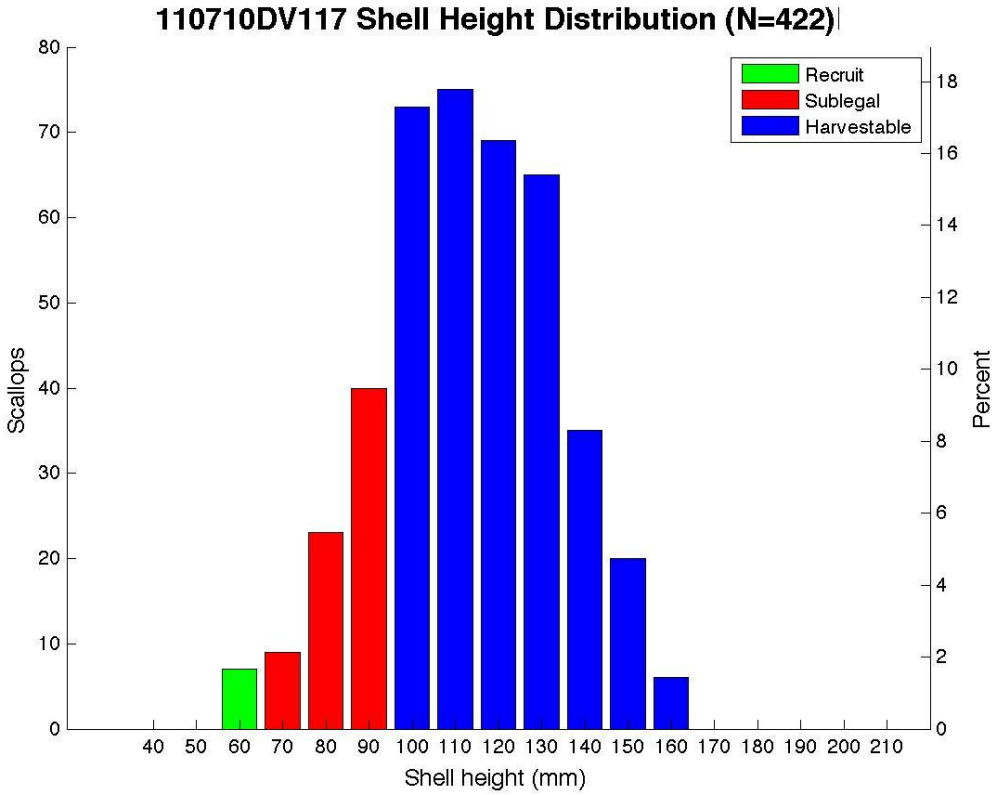
110710DV117 Shell Height Distribution (N=422)
Recruit
Sublegal
Harvestable
Scallops
Percent
Shell height (mm)
0
10
20
30
40
50
60
70
80
0
2
4
6
8
10
12
14
16
18
40 50 60 70 80 90 100 110 120 130 140 150 160 170 180 190 200 210

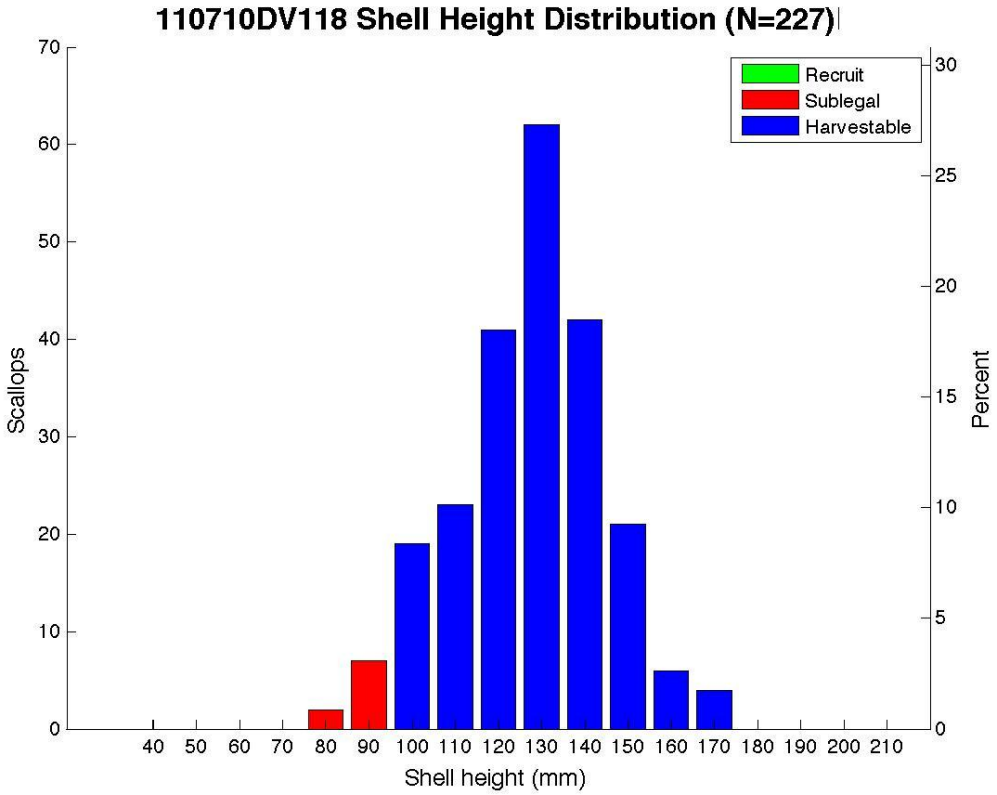
110710DV118 Shell Height Distribution (N=227)
Recruit
Sublegal
Harvestable
Scallops
Percent
Shell height (mm)
0
10
20
30
40
50
60
70
0
5
10
15
20
25
30
40 50 60 70 80 90 100 110 120 130 140 150 160 170 180 190 200 210

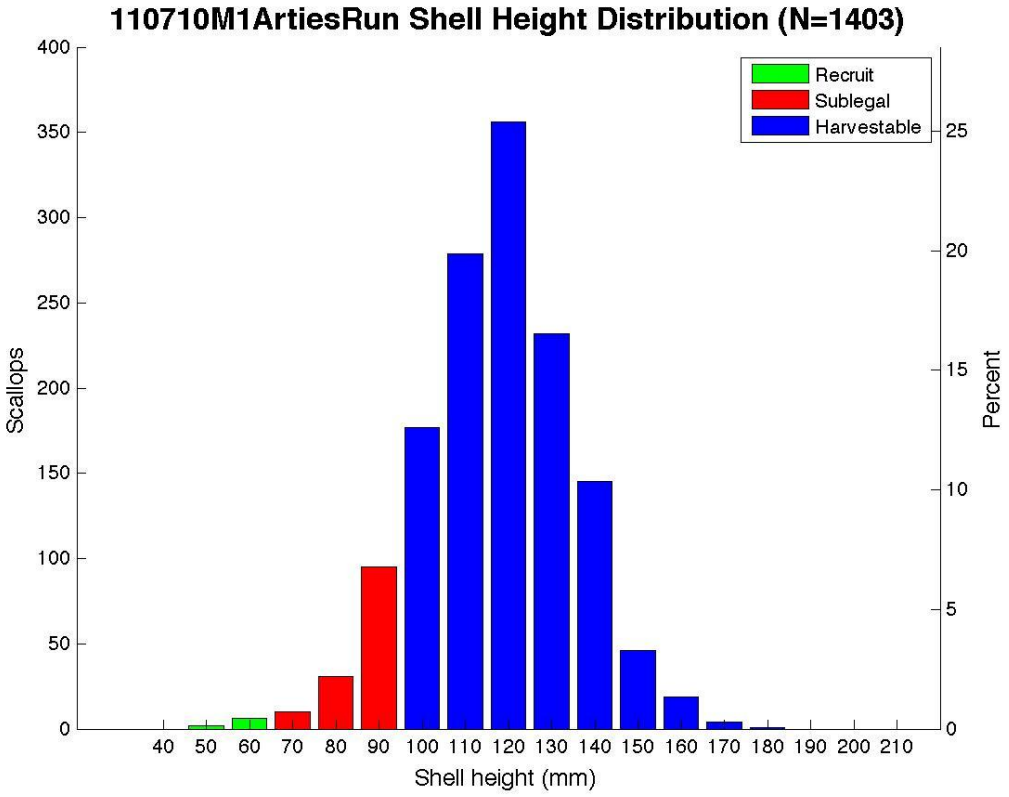
110710M1ArtiesRun Shell Height Distribution (N=1403)
Recruit
Sublegal
Harvestable
Scallops
Percent
Shell height (mm)
0
50
100
150
200
250
300
350
400
0
5
10
15
20
25
40
50
60
70
80
90
100
110
120
130
140
150
160
170
180
190
200
210

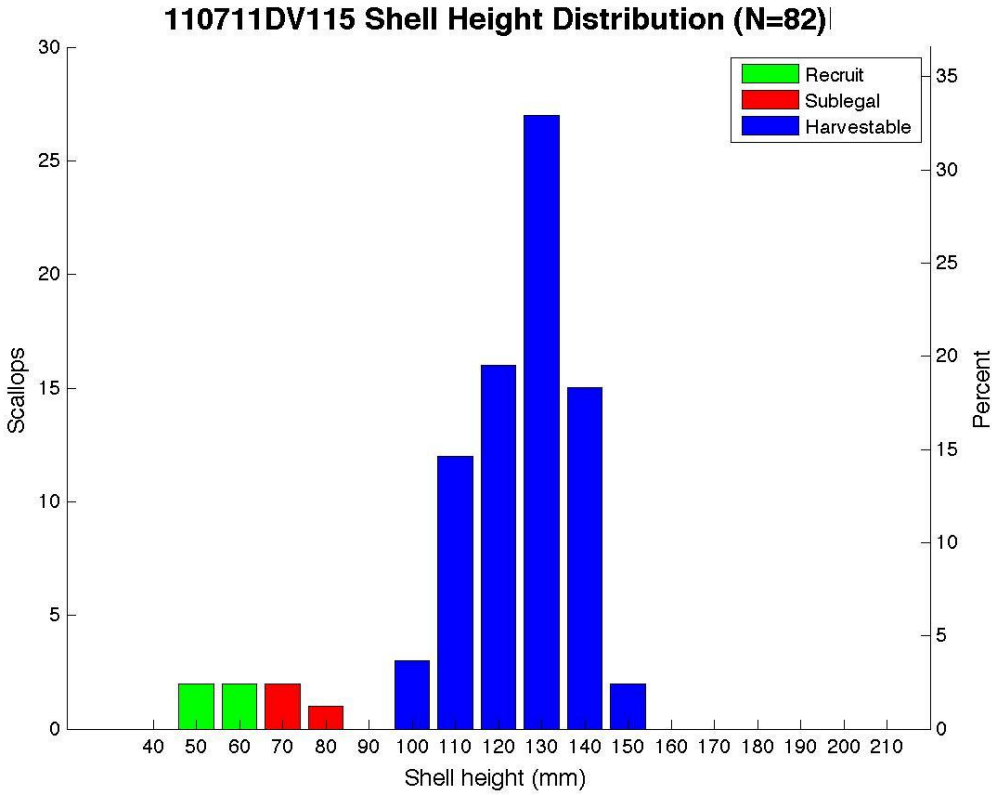
110711DV115 Shell Height Distribution (N=82)
Recruit
Sublegal
Harvestable
Scallops
Percent
Shell height (mm)
0
5
10
15
20
25
30
35
40
50
60
70
80
90
100
110
120
130
140
150
160
170
180
190
200
210

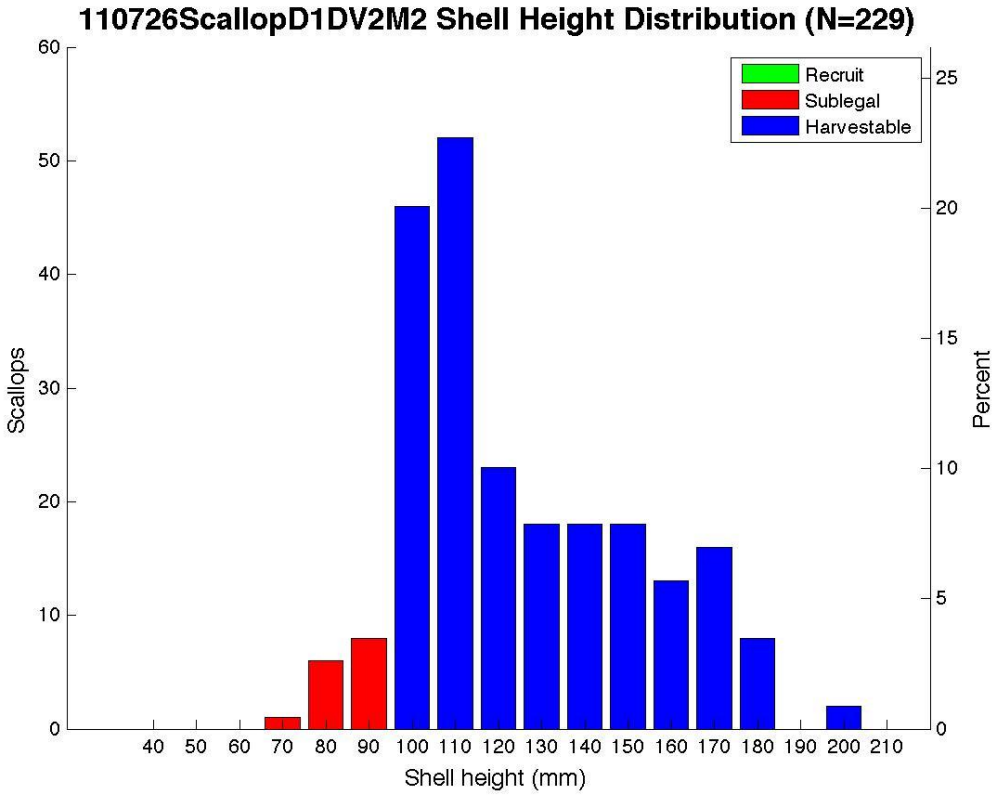
110726ScallopD1DV2M2 Shell Height Distribution (N=229)
Recruit
Sublegal
Harvestable
Scallops
Percent
Shell height (mm)
0
10
20
30
40
50
60
0
5
10
15
20
25
40 50 60 70 80 90 100 110 120 130 140 150 160 170 180 190 200 210

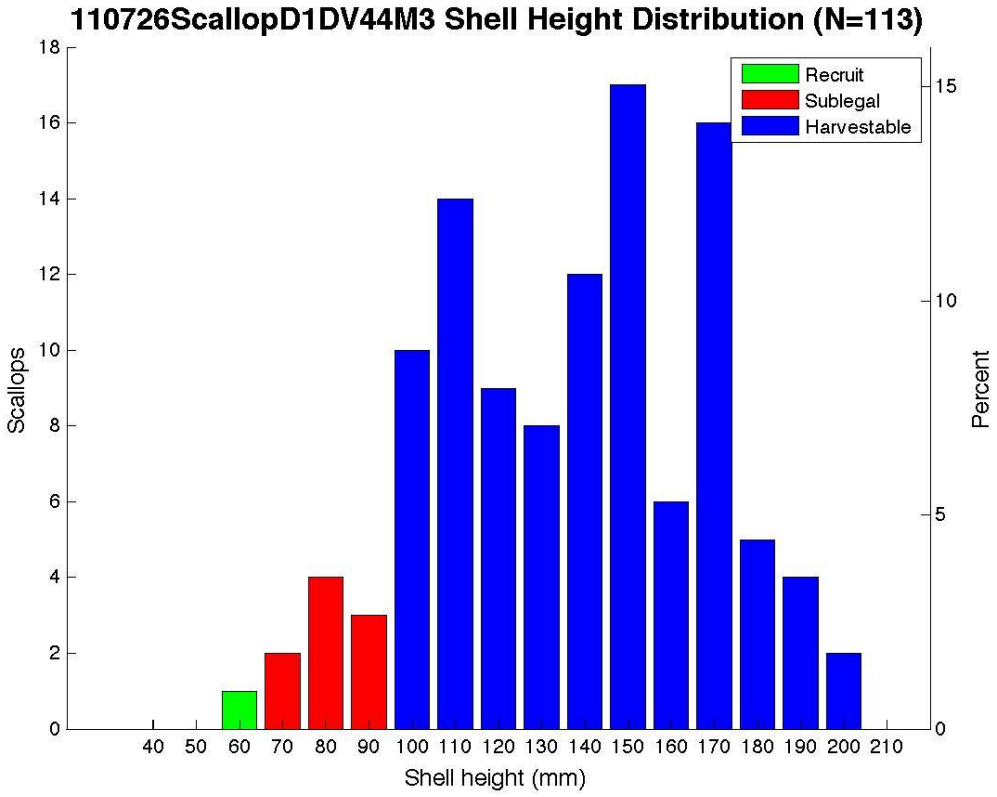
110726ScallopD1DV44M3 Shell Height Distribution (N=113)
Recruit
Sublegal
Harvestable
Scallops
Percent
Shell height (mm)
0
2
4
6
8
10
12
14
16
18
0
5
10
15
40
50
60
70
80
90
100
110
120
130
140
150
160
170
180
190
200
210

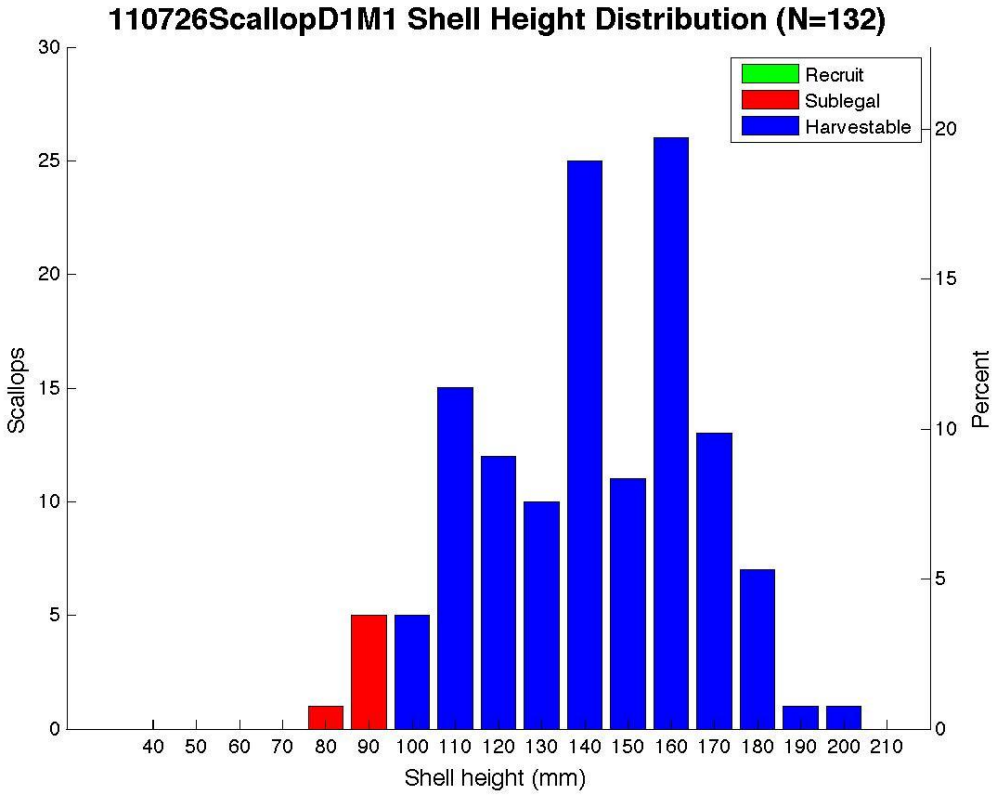
110726ScallopD1M1 Shell Height Distribution (N=132)
Recruit
Sublegal
Harvestable
Scallops
Percent
Shell height (mm)
0
5
10
15
20
25
30
40
50
60
70
80
90
100
110
120
130
140
150
160
170
180
190
200
210

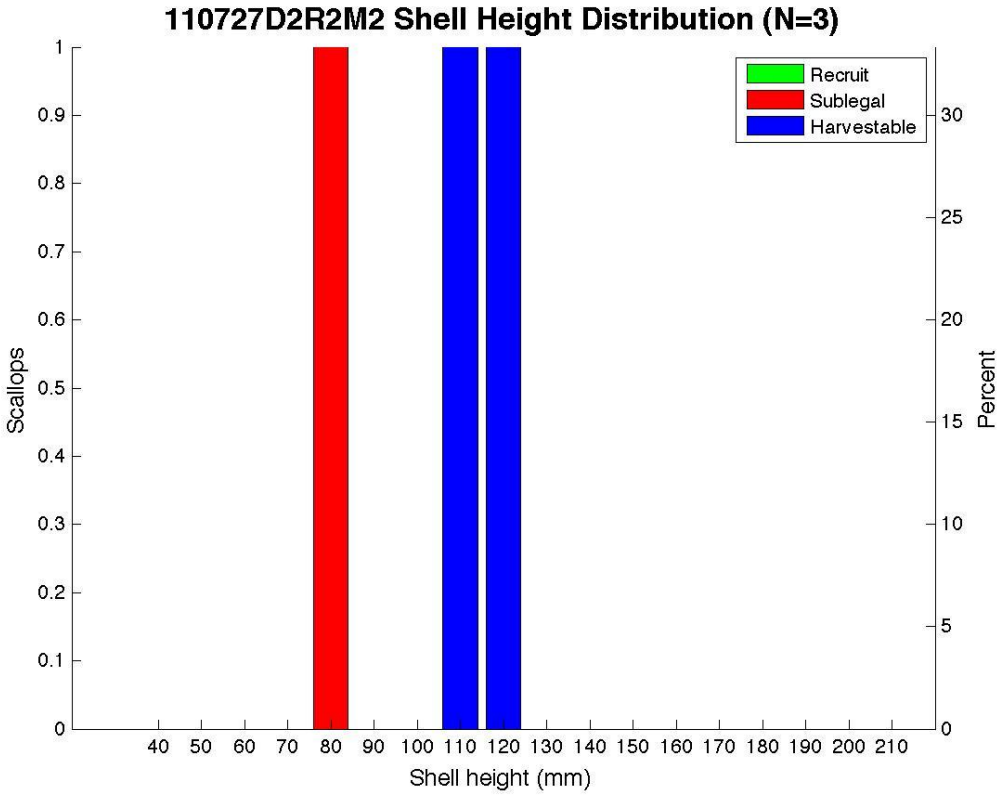
110727D2R2M2 Shell Height Distribution (N=3)
Recruit
Sublegal
Harvestable
Scallops
Percent
Shell height (mm)
0
0.1
0.2
0.3
0.4
0.5
0.6
0.7
0.8
0.9
1
0
5
10
15
20
25
30
40 50 60 70 80 90 100 110 120 130 140 150 160 170 180 190 200 210

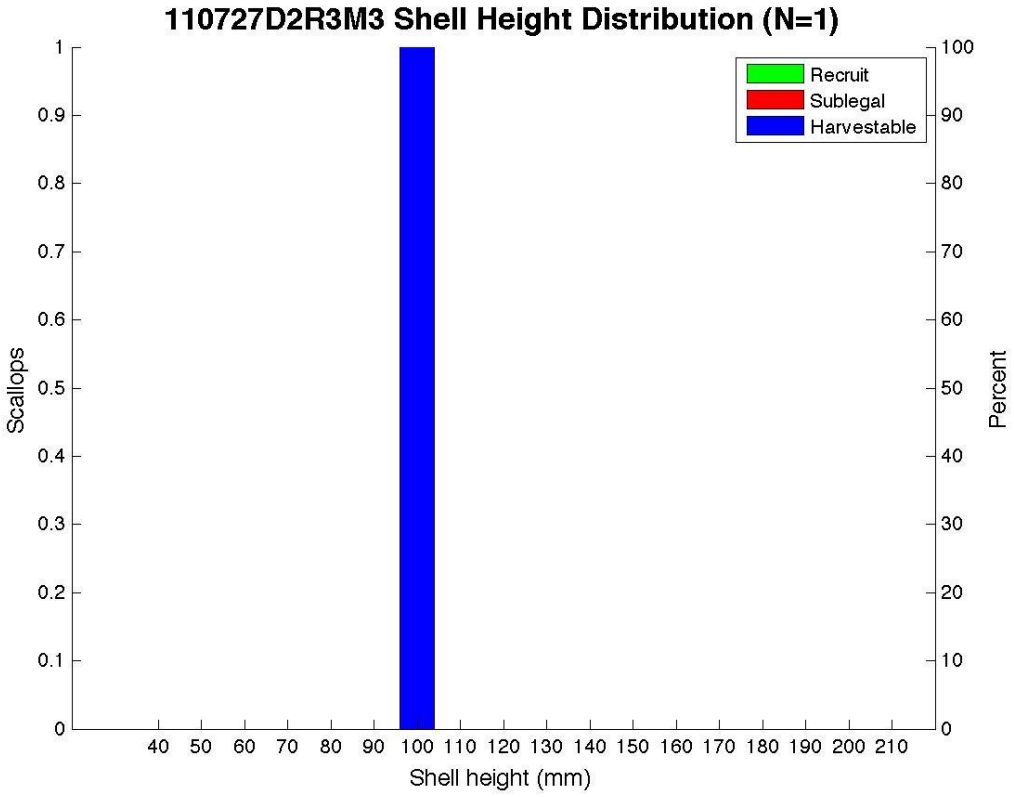
110727D2R3M3 Shell Height Distribution (N=1)
Recruit
Sublegal
Harvestable
Scallops
Percent
Shell height (mm)
0
0.1
0.2
0.3
0.4
0.5
0.6
0.7
0.8
0.9
1
0
10
20
30
40
50
60
70
80
90
100
40 50 60 70 80 90 100 110 120 130 140 150 160 170 180 190 200 210

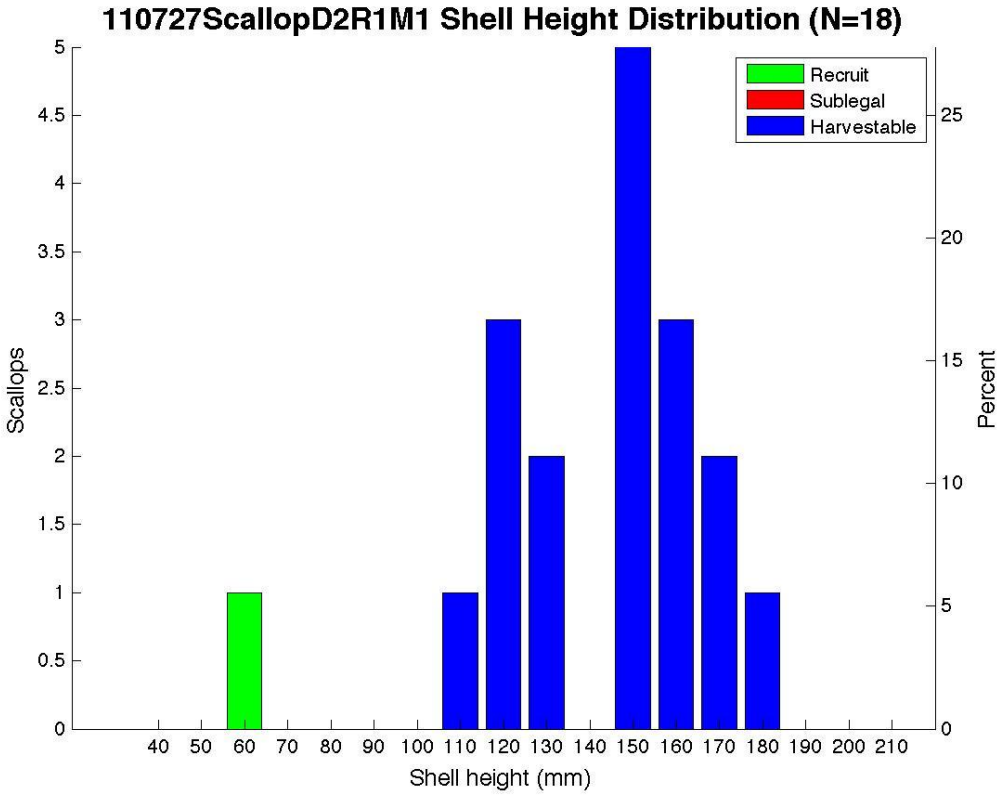
110727ScallopD2R1M1 Shell Height Distribution (N=18)
Recruit
Sublegal
Harvestable
Scallops
Percent
Shell height (mm)
0
0.5
1
1.5
2
2.5
3
3.5
4
4.5
5
0
5
10
15
20
25
40 50 60 70 80 90 100 110 120 130 140 150 160 170 180 190 200 210

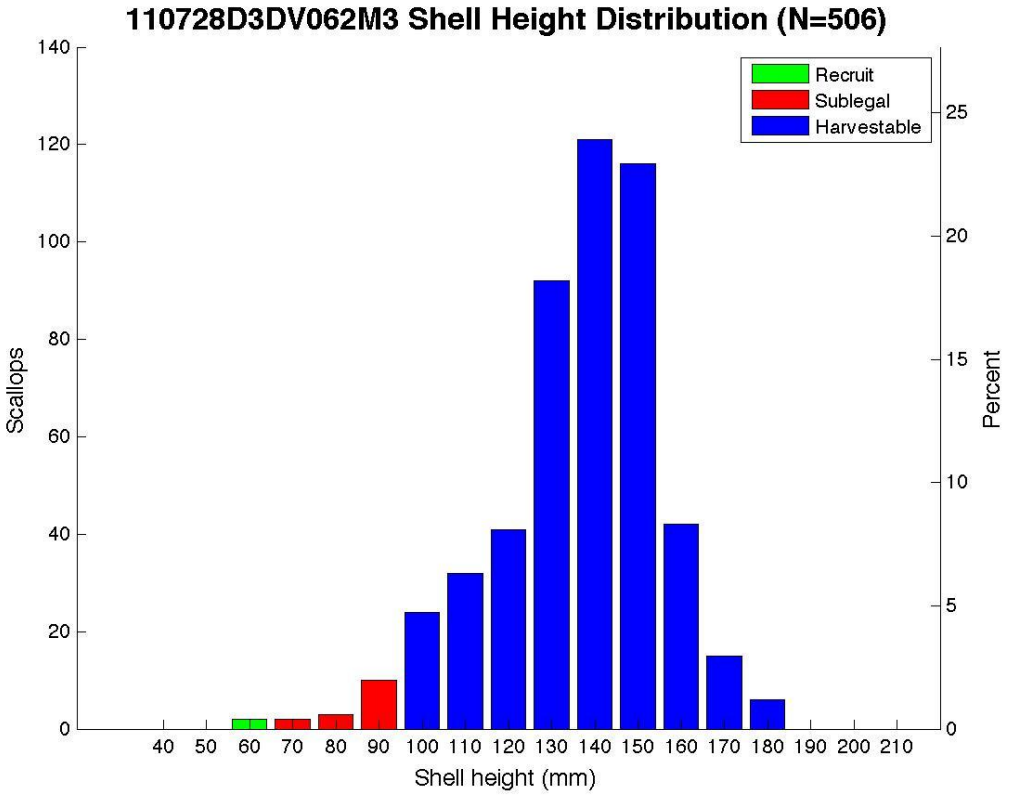
110728D3DV062M3 Shell Height Distribution (N=506)
Recruit
Sublegal
Harvestable
Scallops
Percent
Shell height (mm)
0
20
40
60
80
100
120
140
0
5
10
15
20
25
40 50 60 70 80 90 100 110 120 130 140 150 160 170 180 190 200 210

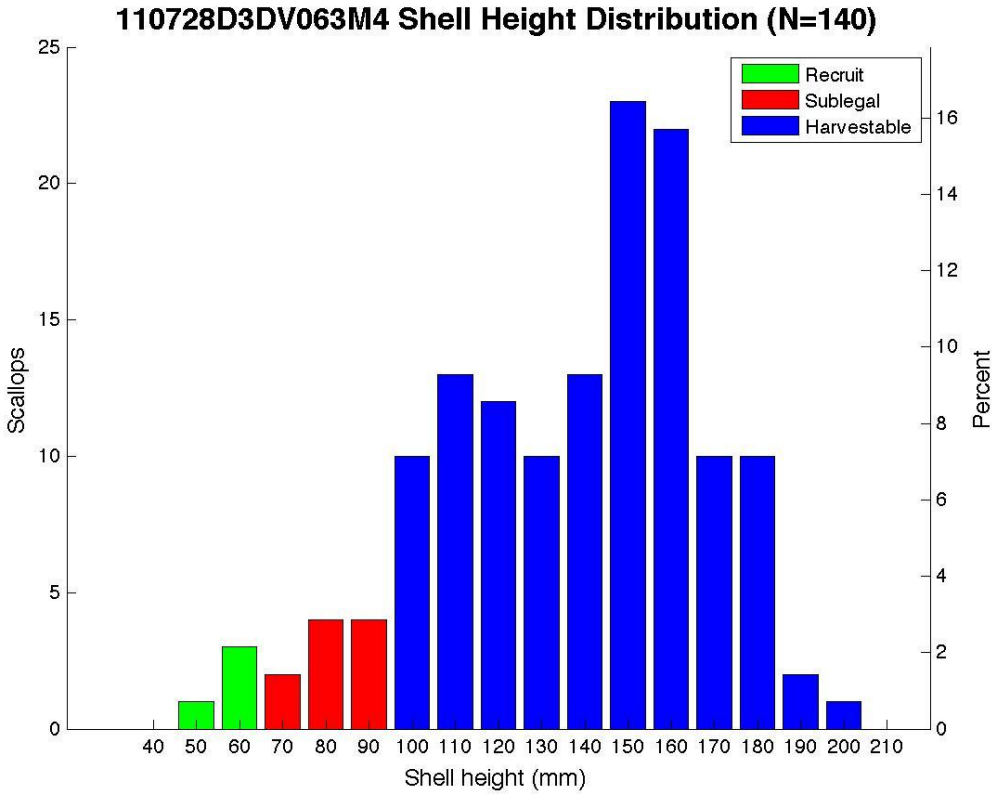
110728D3DV063M4 Shell Height Distribution (N=140)
Recruit
Sublegal
Harvestable
Scallops
Percent
Shell height (mm)
0
5
10
15
20
25
0
2
4
6
8
10
12
14
16
40
50
60
70
80
90
100
110
120
130
140
150
160
170
180
190
200
210

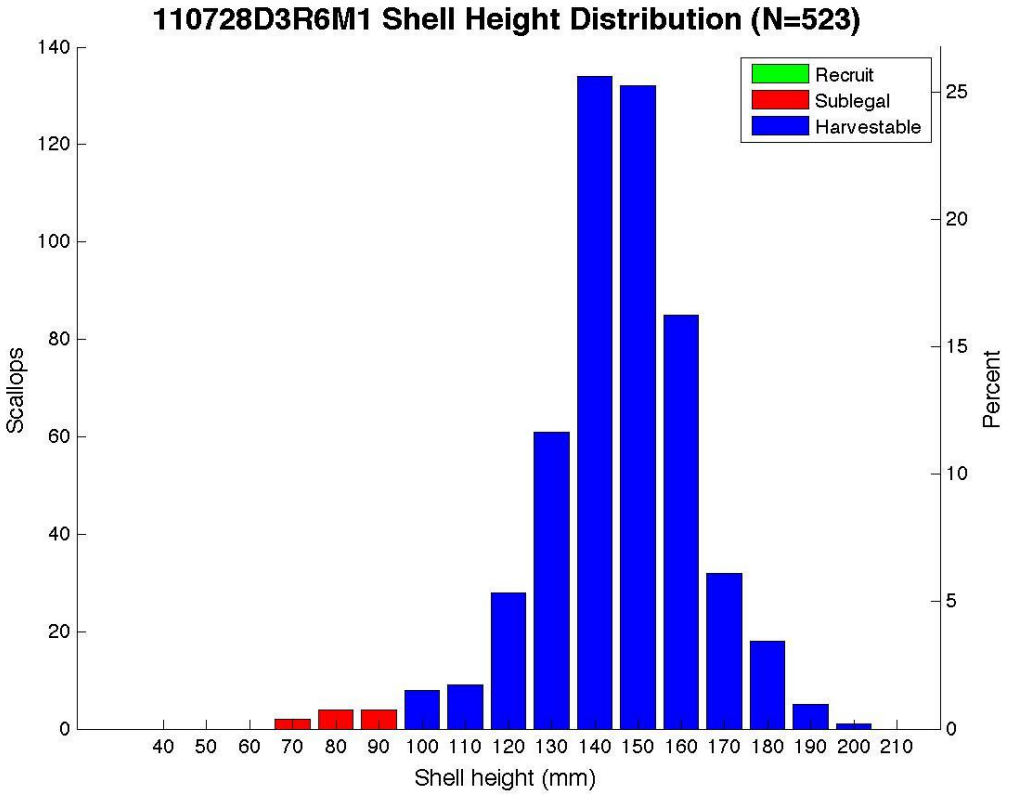
110728D3R6M1 Shell Height Distribution (N=523)
Recruit
Sublegal
Harvestable
Scallops
Percent
Shell height (mm)
0
20
40
60
80
100
120
140
0
5
10
15
20
25
40 50 60 70 80 90 100 110 120 130 140 150 160 170 180 190 200 210

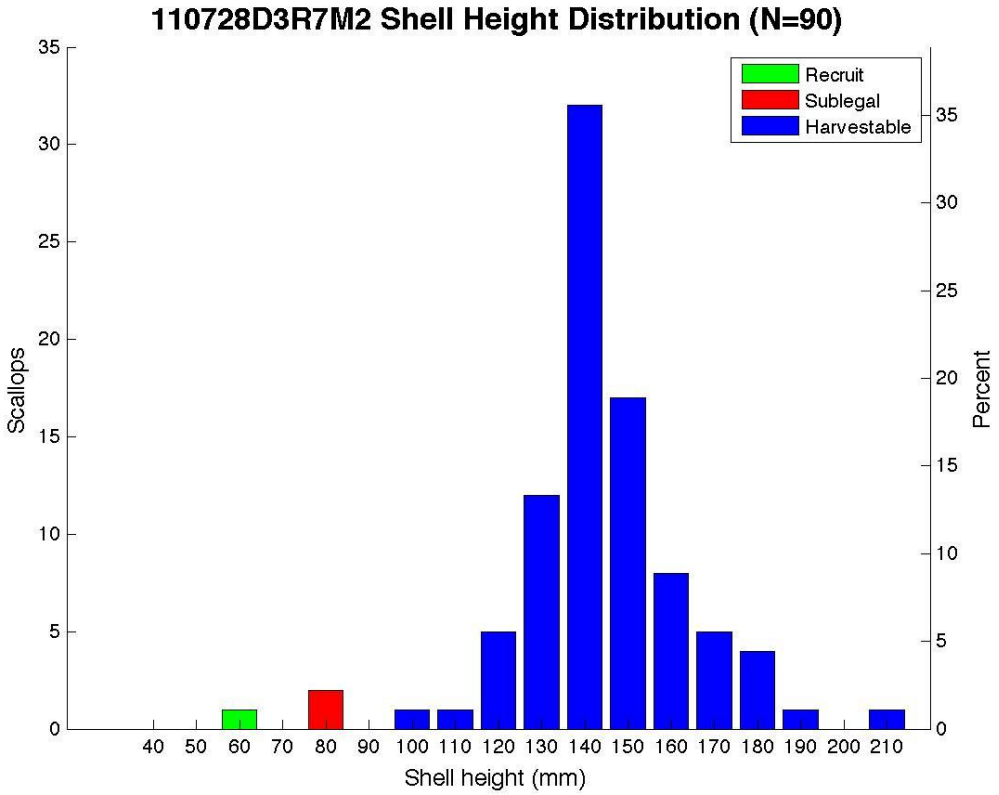
110728D3R7M2 Shell Height Distribution (N=90)
Recruit
Sublegal
Harvestable
Scallops
Percent
Shell height (mm)
0
5
10
15
20
25
30
35
40
50
60
70
80
90
100
110
120
130
140
150
160
170
180
190
200
210

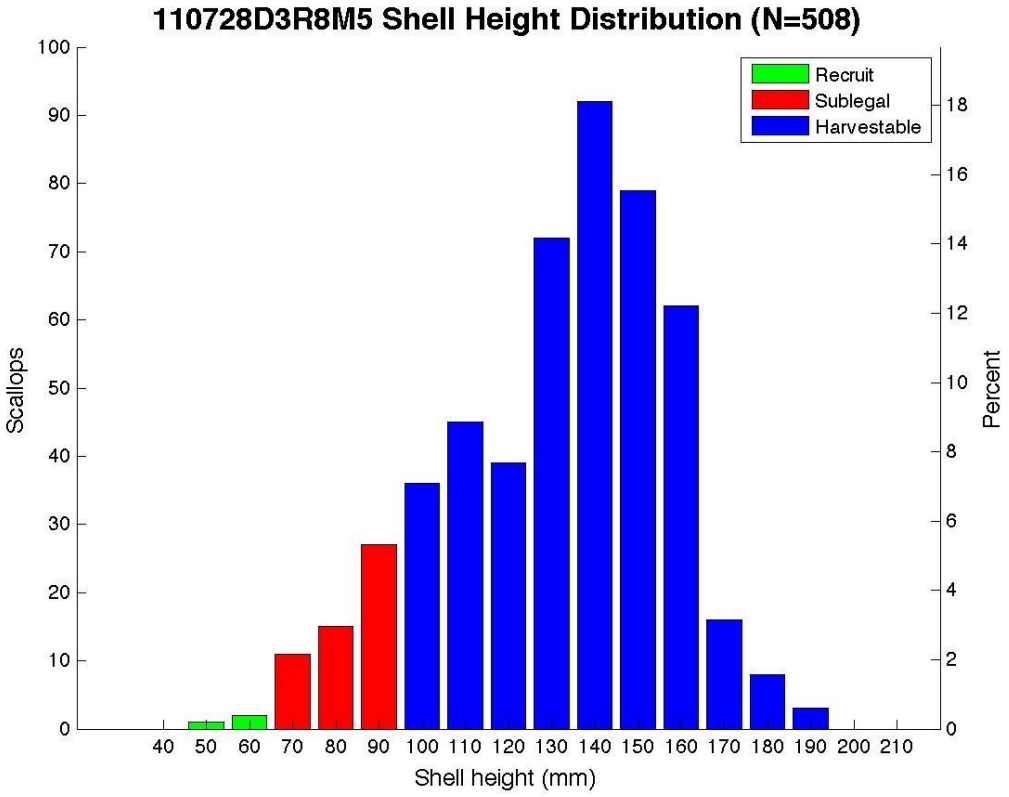
110728D3R8M5 Shell Height Distribution (N=508)
Recruit
Sublegal
Harvestable
Scallops
Percent
Shell height (mm)
0
10
20
30
40
50
60
70
80
90
100
0
2
4
6
8
10
12
14
16
18
40 50 60 70 80 90 100 110 120 130 140 150 160 170 180 190 200 210

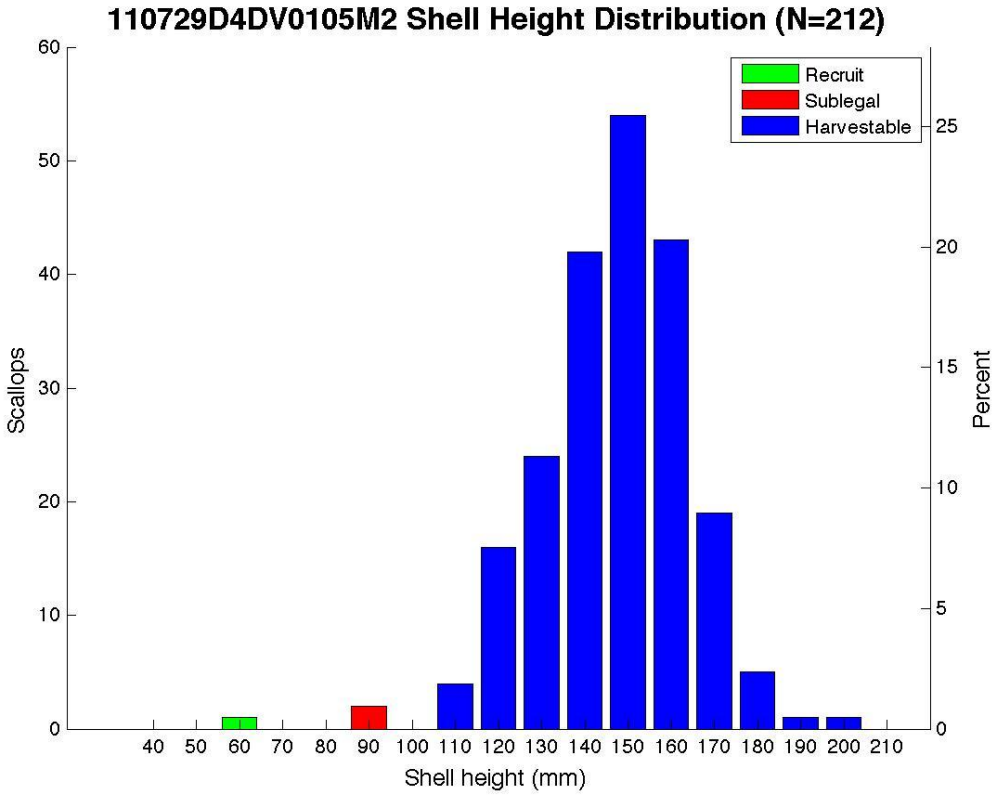
110729D4DV0105M2 Shell Height Distribution (N=212)
Recruit
Sublegal
Harvestable
Scallops
Percent
Shell height (mm)
0
10
20
30
40
50
60
0
5
10
15
20
25
40 50 60 70 80 90 100 110 120 130 140 150 160 170 180 190 200 210

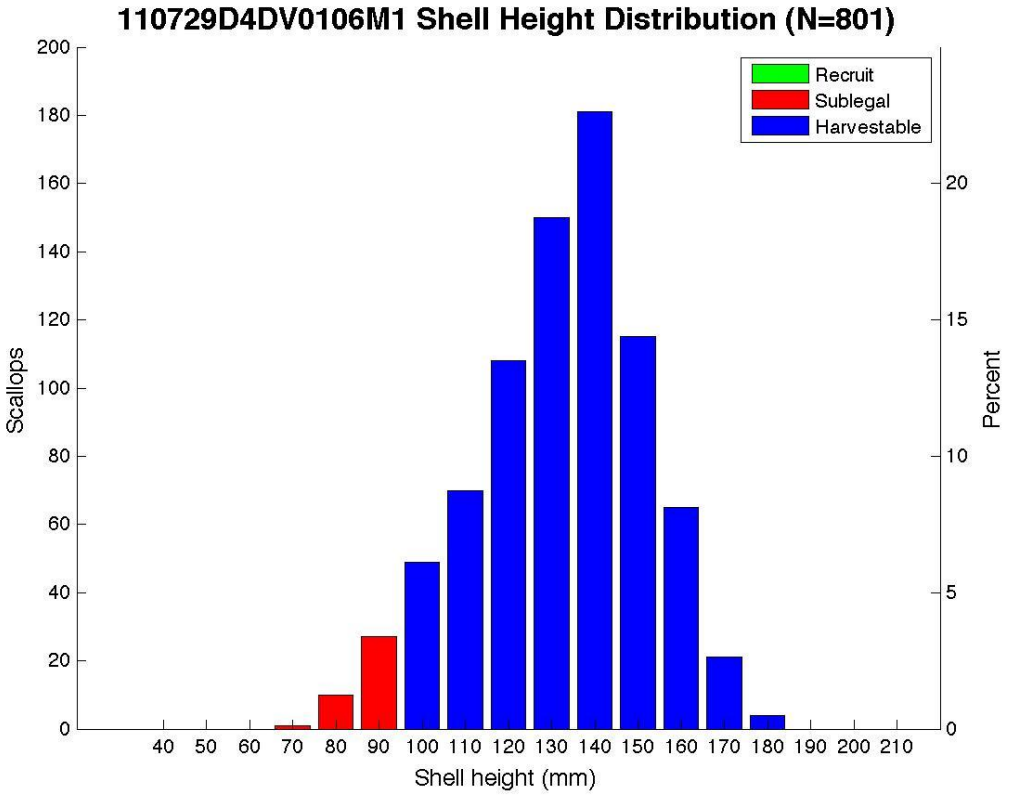
110729D4DV0106M1 Shell Height Distribution (N=801)
Recruit
Sublegal
Harvestable
Scallops
Percent
Shell height (mm)
0
20
40
60
80
100
120
140
160
180
200
0
5
10
15
20
40 50 60 70 80 90 100 110 120 130 140 150 160 170 180 190 200 210

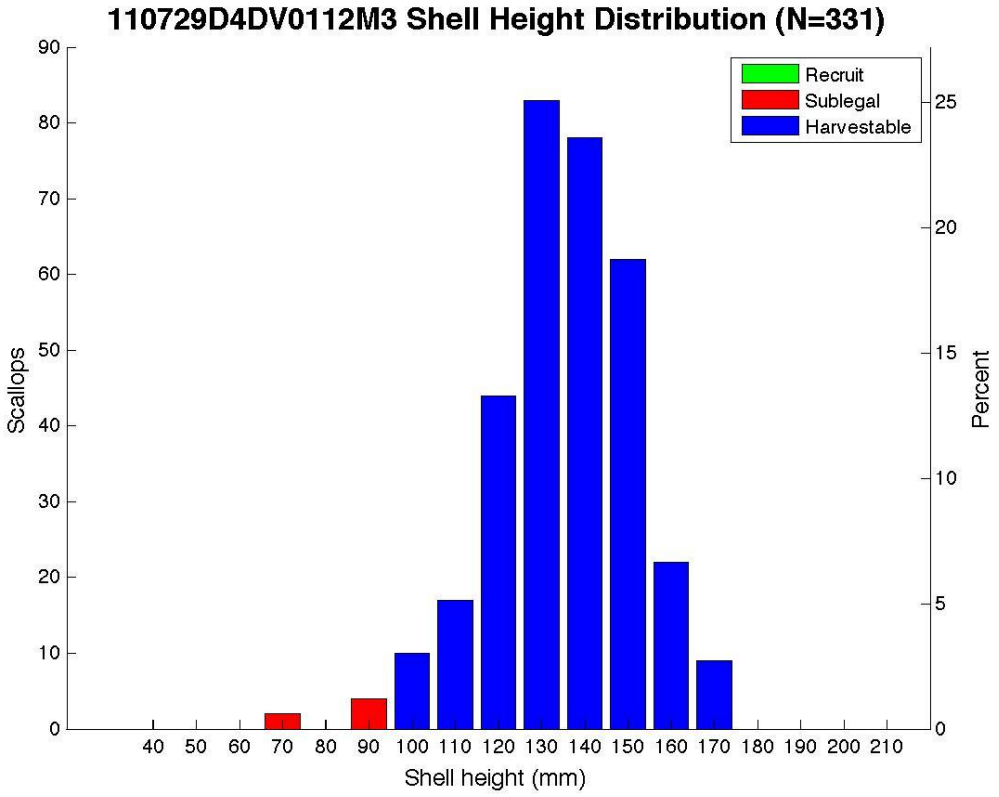
110729D4DV0112M3 Shell Height Distribution (N=331)
Recruit
Sublegal
Harvestable
Scallops
Percent
Shell height (mm)
0
10
20
30
40
50
60
70
80
90
0
5
10
15
20
25
40 50 60 70 80 90 100 110 120 130 140 150 160 170 180 190 200 210

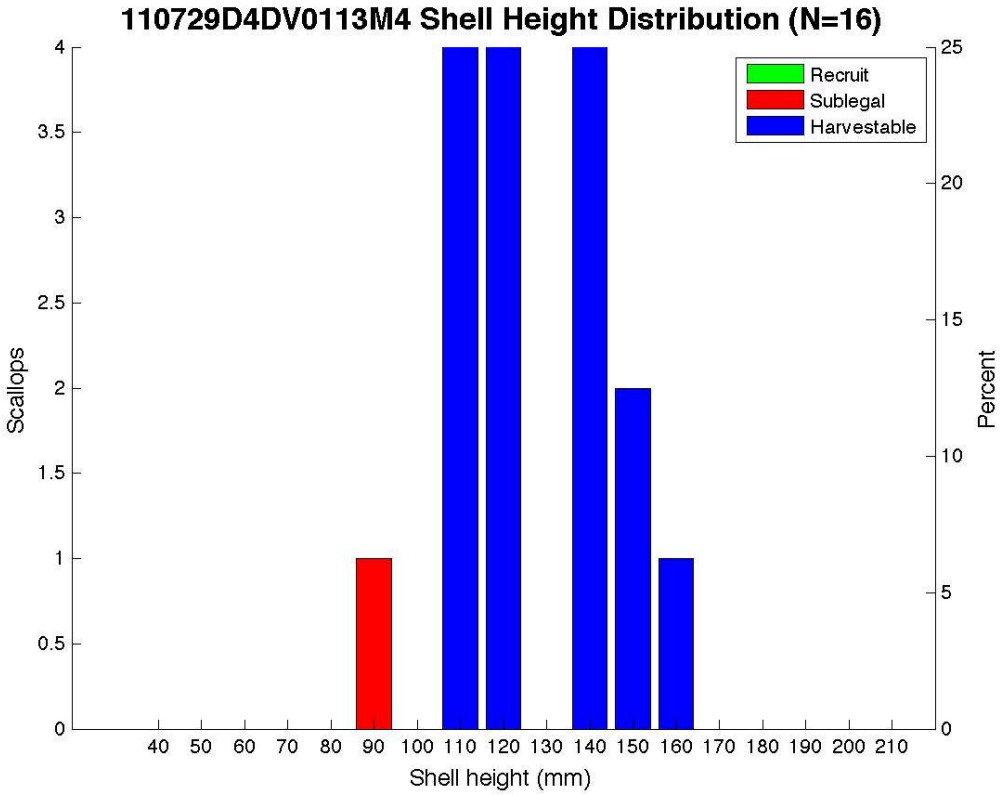
110729D4DV0113M4 Shell Height Distribution (N=16)
Recruit
Sublegal
Harvestable
Scallops
Percent
Shell height (mm)
0
0.5
1
1.5
2
2.5
3
3.5
4
0
5
10
15
20
25
40 50 60 70 80 90 100 110 120 130 140 150 160 170 180 190 200 210

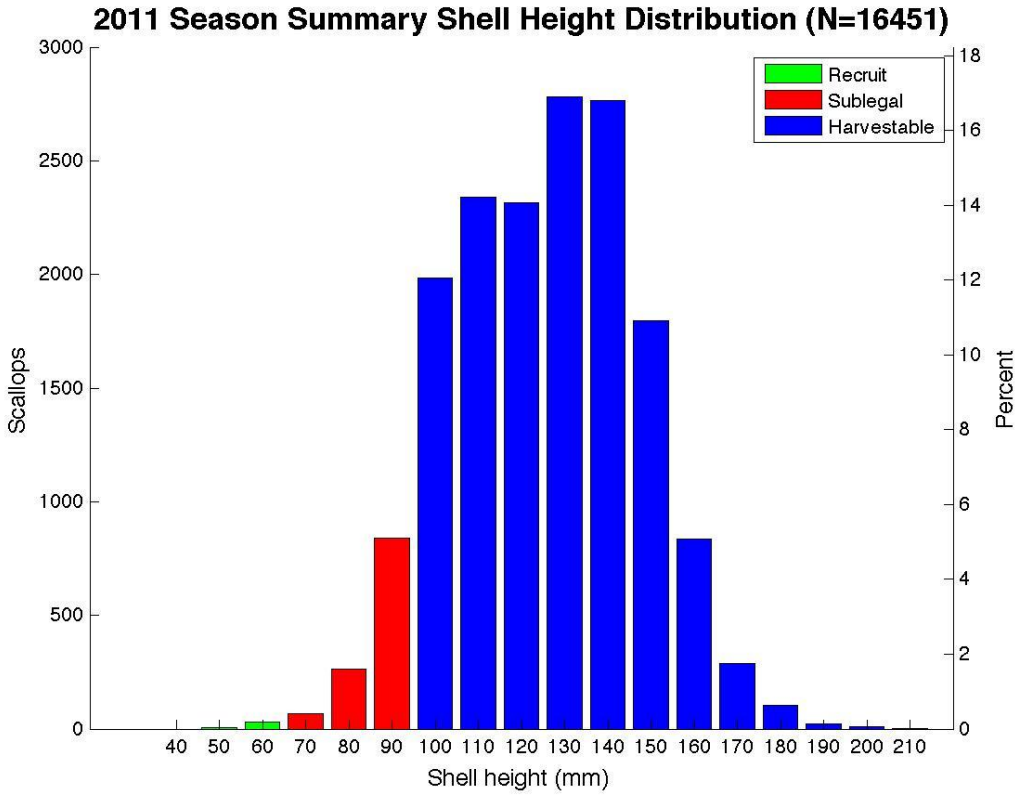
2011 Season Summary Shell Height Distribution (N=16451)
Recruit
Sublegal
Harvestable
Scallops
Percent
Shell height (mm)
0
500
1000
1500
2000
2500
3000
0
2
4
6
8
10
12
14
16
18
40
50
60
70
80
90
100
110
120
130
140
150
160
170
180
190
200
210

Appendix E

SIDE-SCAN MOSAICS WITH DIGITIZED DREDGE SCARS

E.1 Introduction

This appendix contains the side-scan sonar mosaics with digitized dredge scars (white lines) for each AUV survey mission. Areas of bright intensity indicate high backscatter. The mosaics are gridded at 0.25 m resolution. The missions are oriented with north up.

E.2 Side-Scan Sonar Mosaics

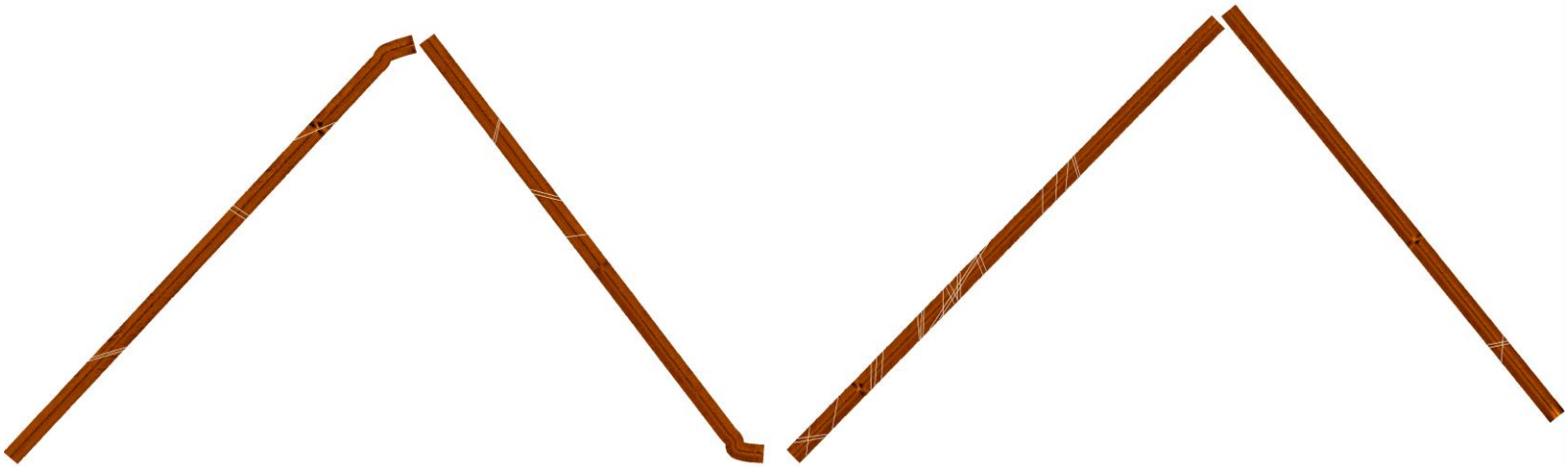

Figure E.1: 110708_Scallop_DvoraRun

Figure E.2: 110708_ScallopD2_M4

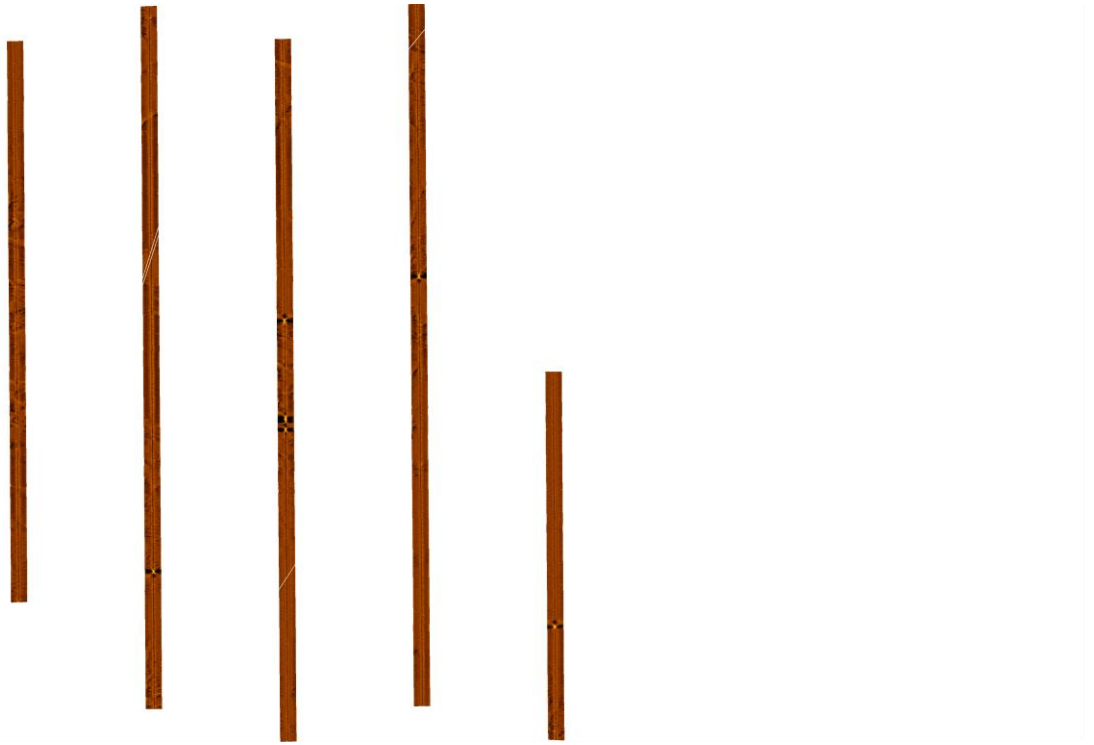

Figure E.3: 110708_ScallopD2

Figure E.4: 110708_SM2

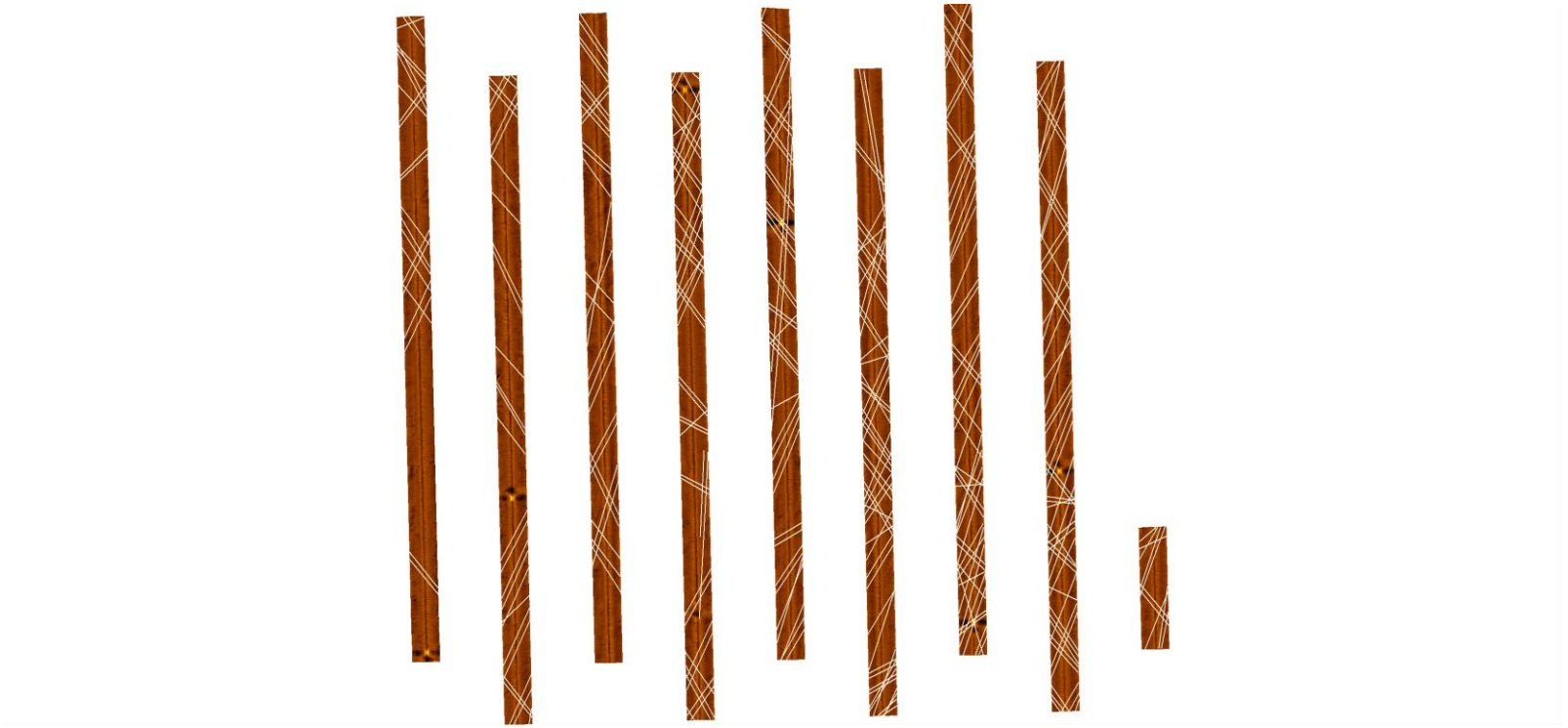

Figure E.5: 110709_Scallop_D3_M1_Corey

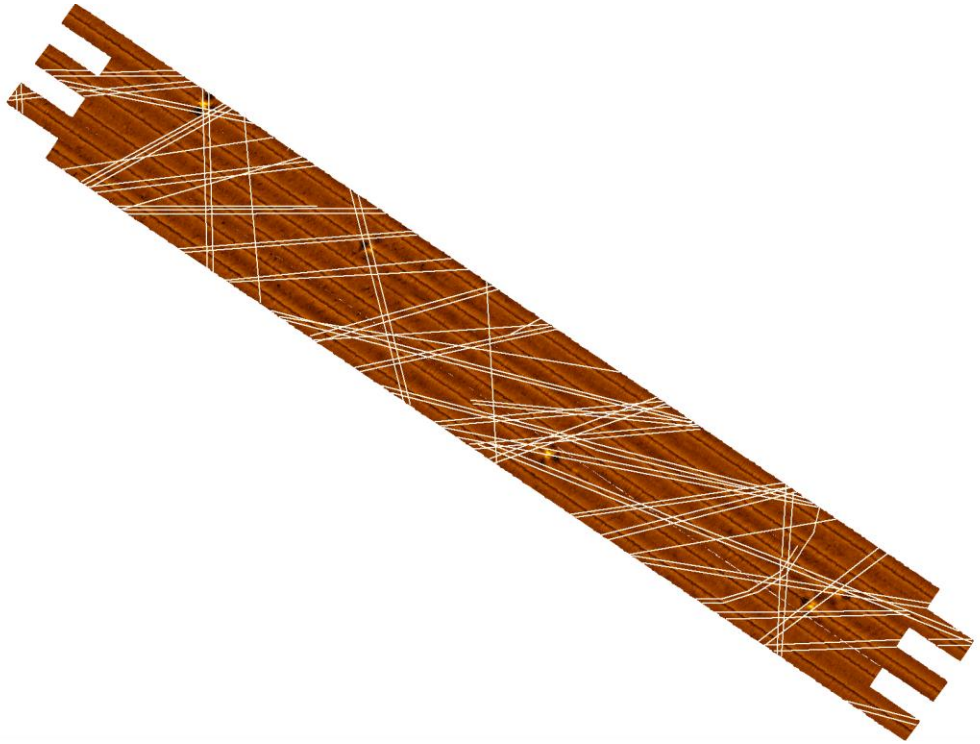

Figure E.6: 110709_ScallopDay3_DV119

Figure E.7: 110710_DV117

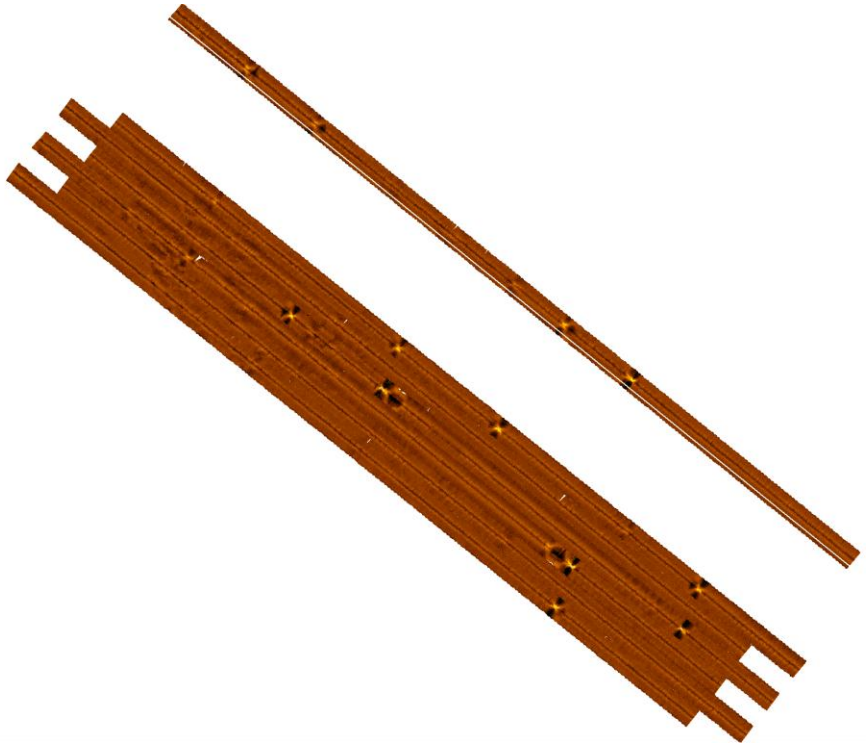

Figure E.8: 110710_DV118

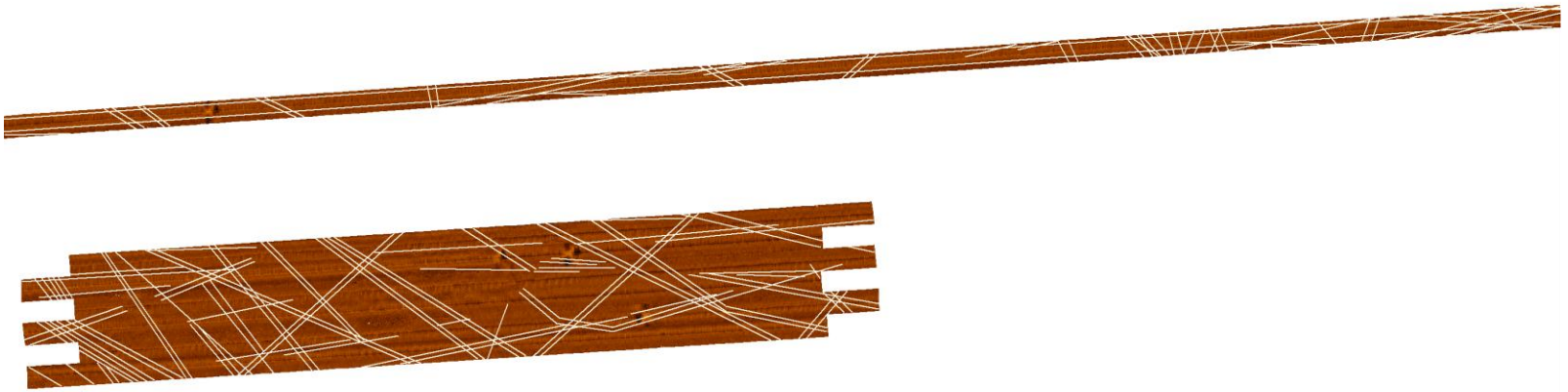

Figure E.9: 110710_M1_ArtiesRun

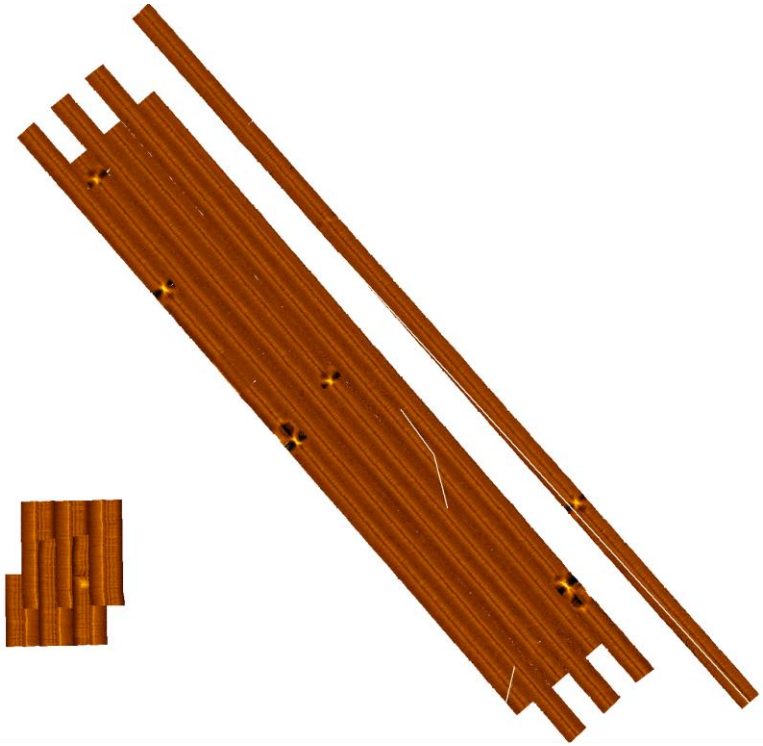

Figure E.10: 110711_DV115

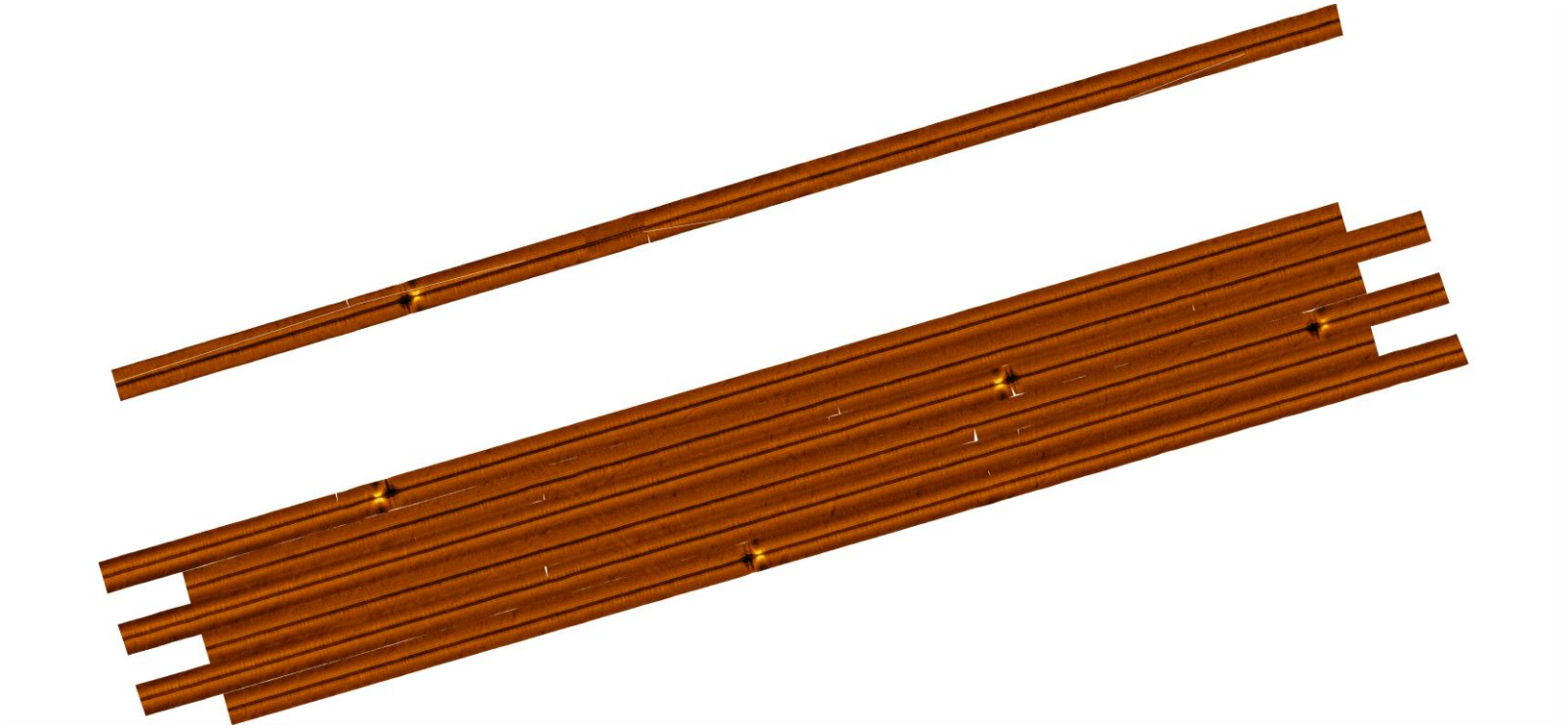

Figure E.11: 110726_ScallopD1_DV2_M2

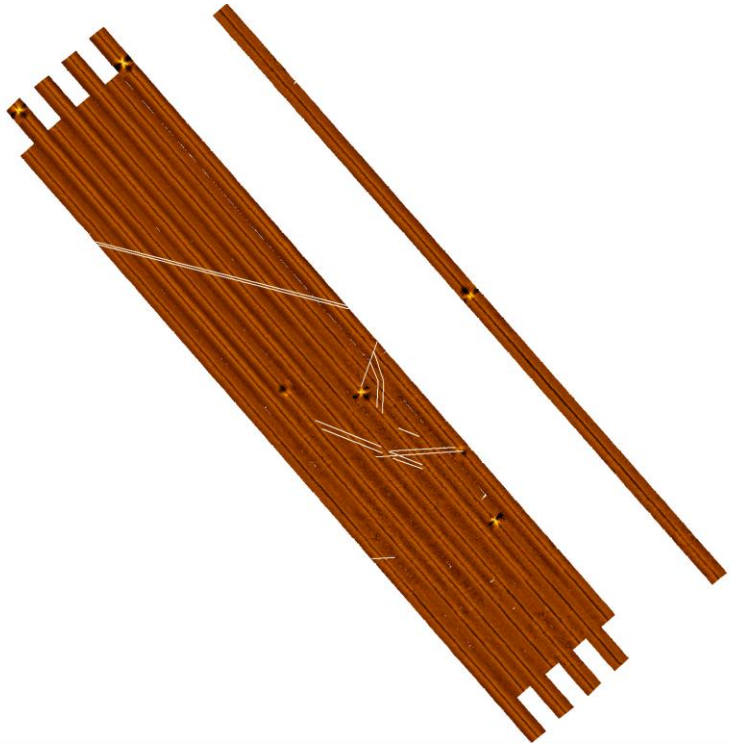

Figure E.12: 110726_ScallopD1_DV44_M3

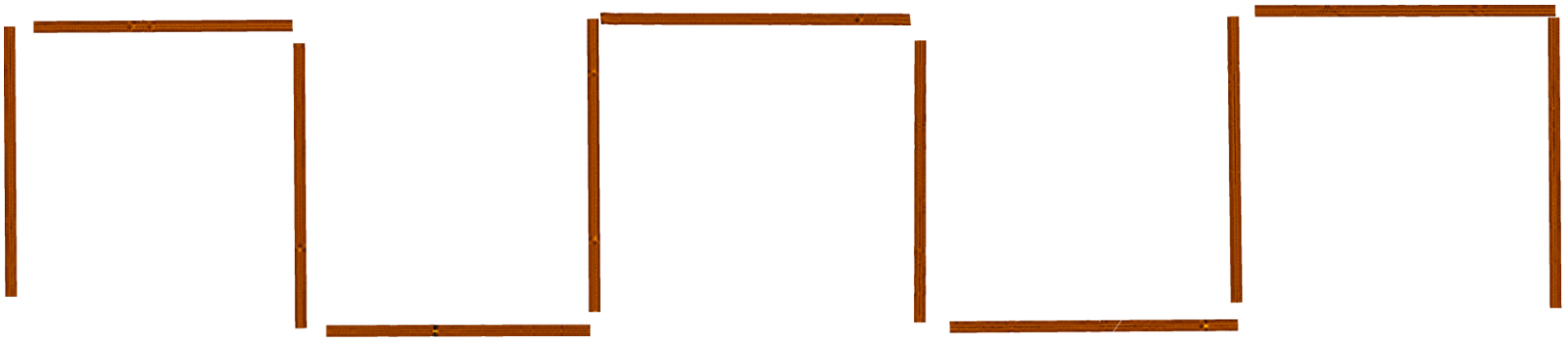

Figure E.13: 110727_D2_R2_M2

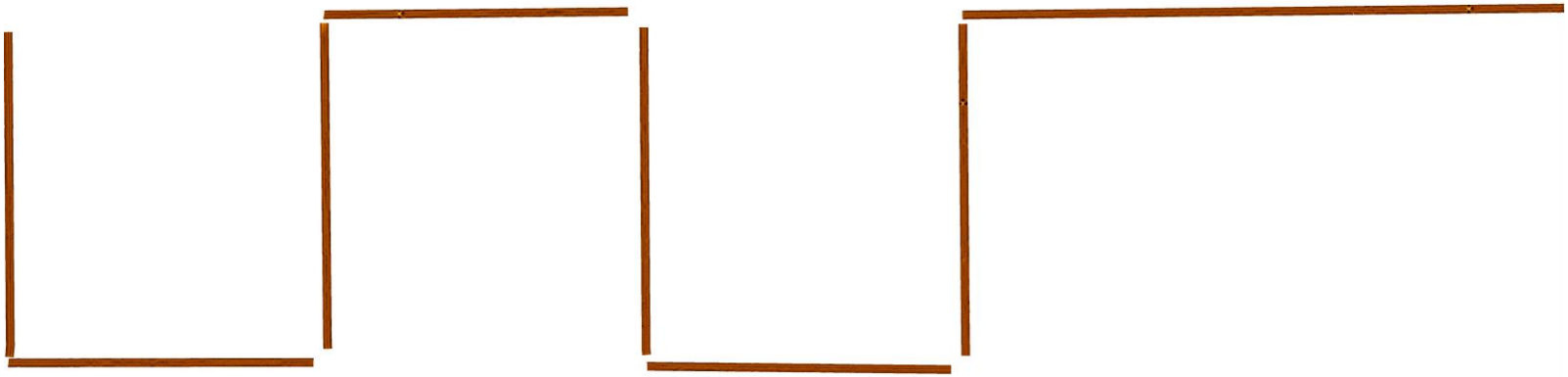

Figure E.14: 110727_D2_R3_M3

Figure E.15: 110726_D2_R4_M4

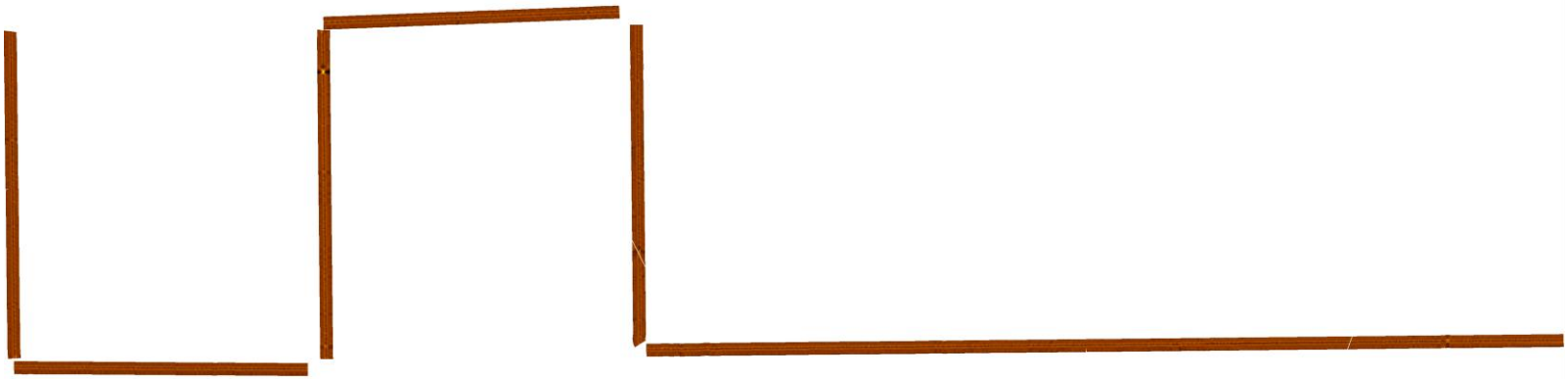

Figure E.16: 110727_D2_R5_M5

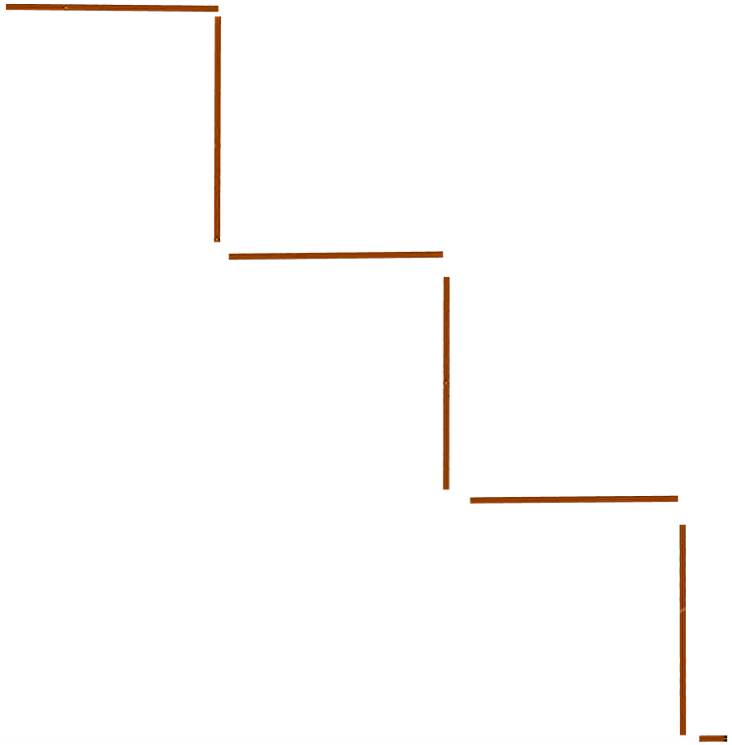

Figure E.17: 110727_ScallopD2_R1_M1

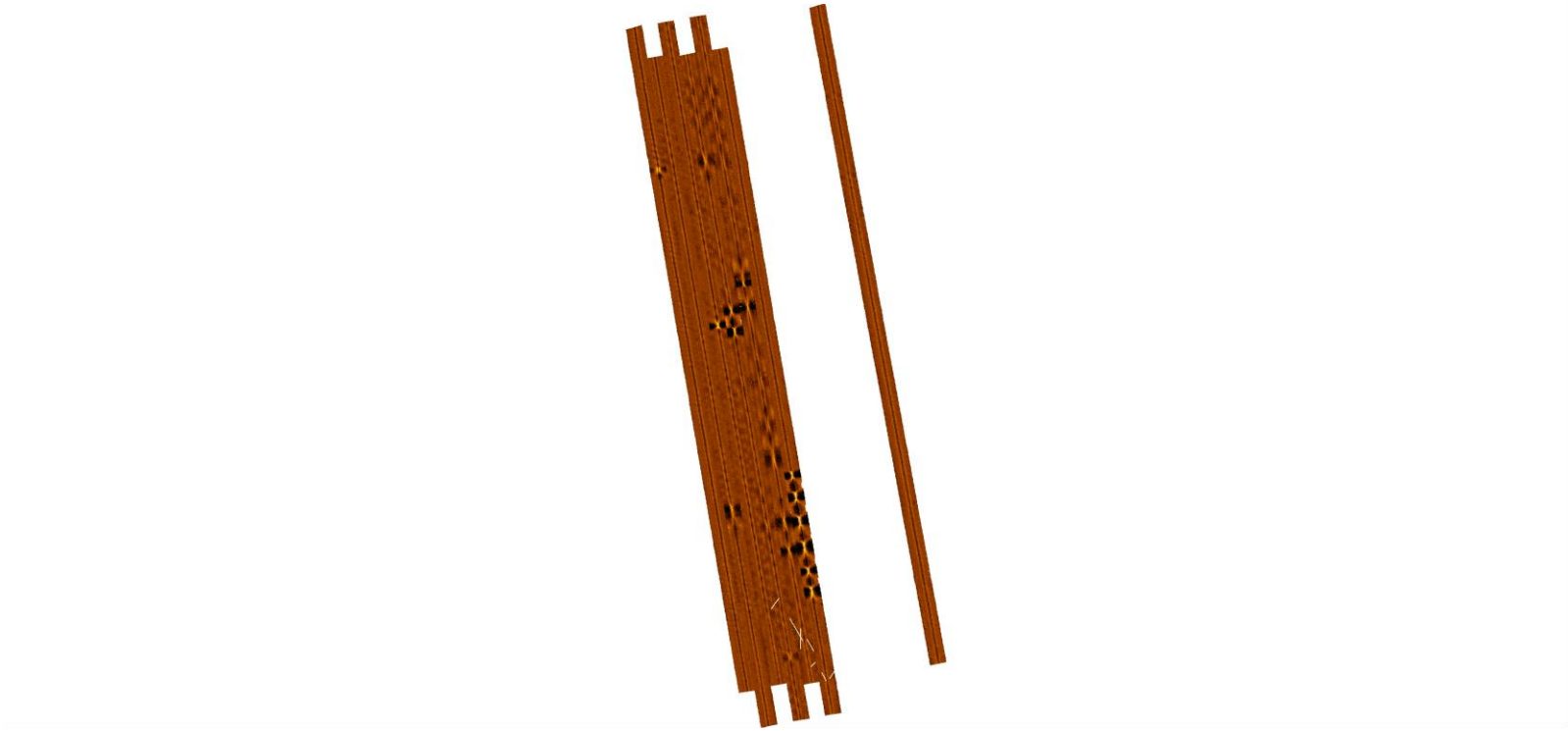

Figure E.18: 110728_D3_DV062_M3

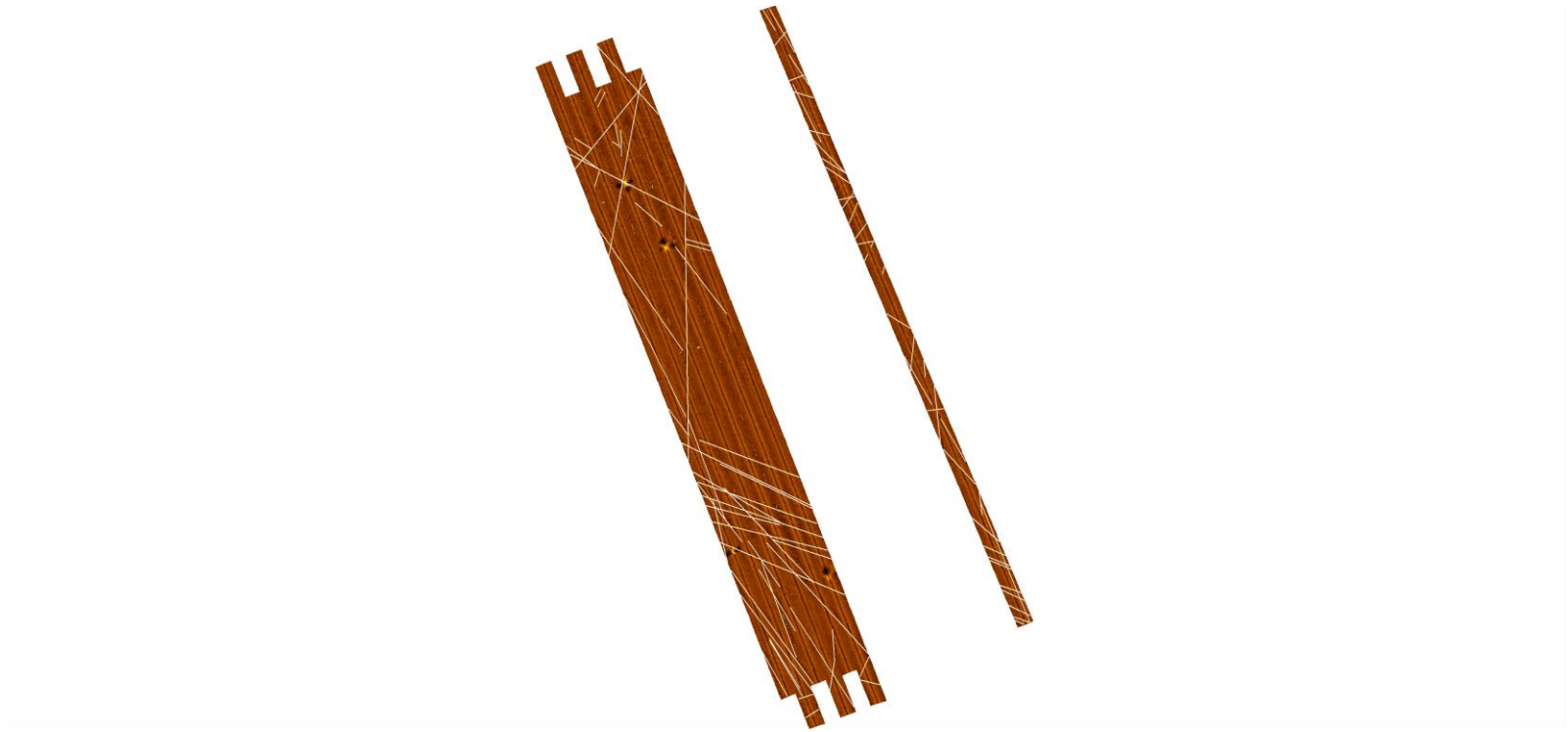

Figure E.19: 110728_D3_DV063_M4

Figure E.20: 110728_D3_R6_M1

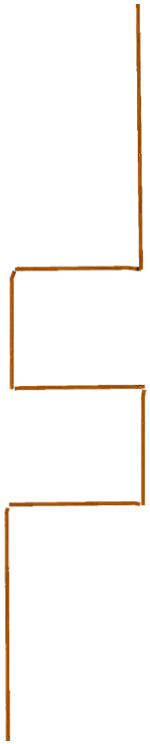

Figure E.21: 110728_D3_R7_M2

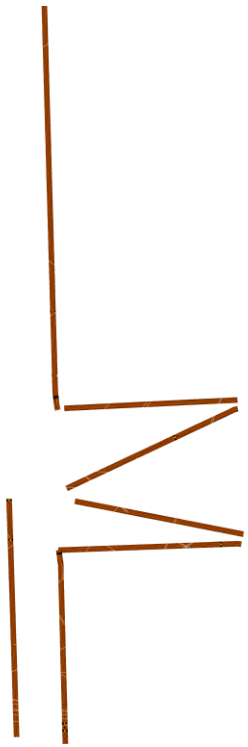

Figure E.22: 110728_D3_R8_M5

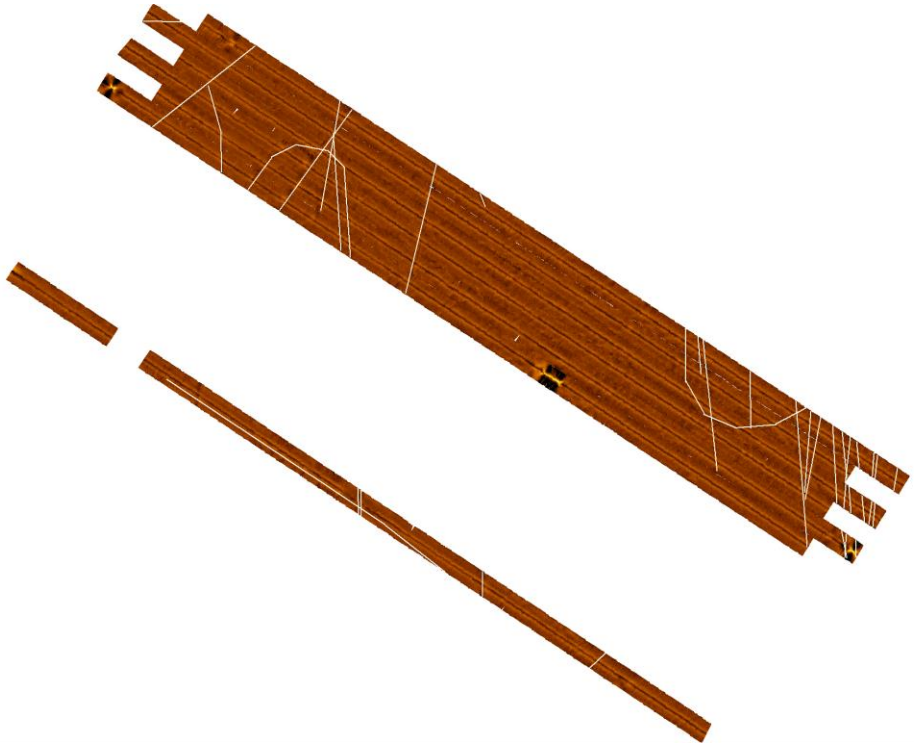

Figure E.23: 110729_D4_DV0105_M2

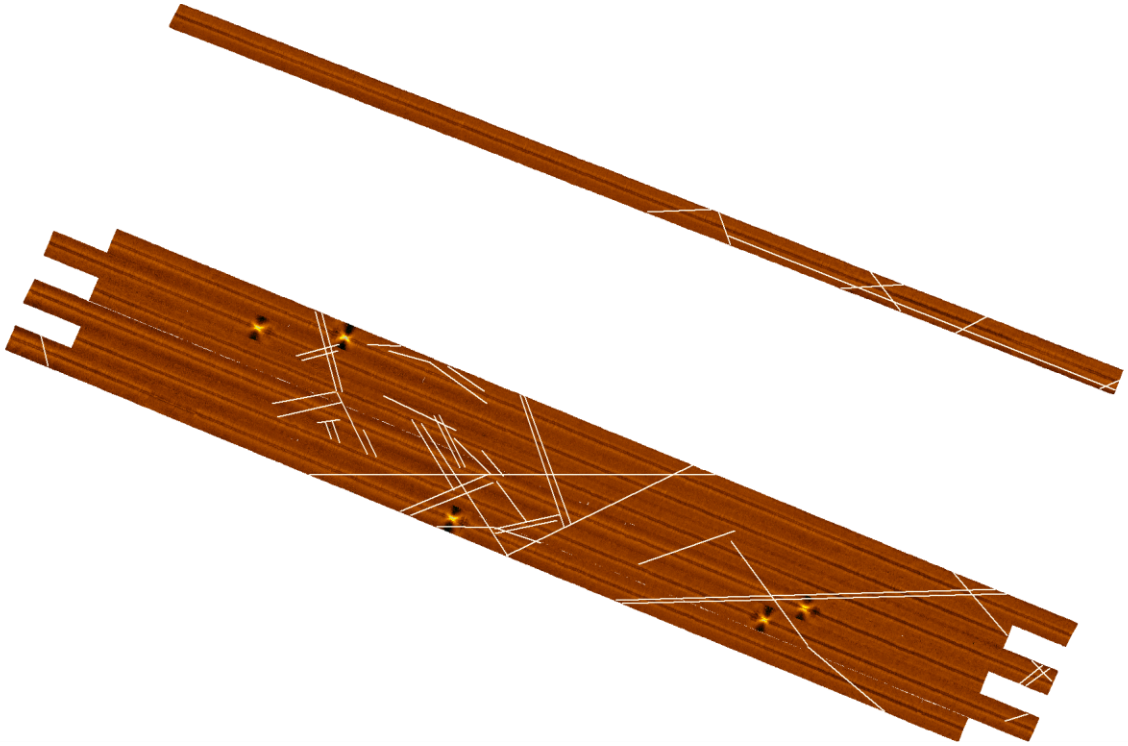

Figure E.24: 110729_D4_DV0106_M1

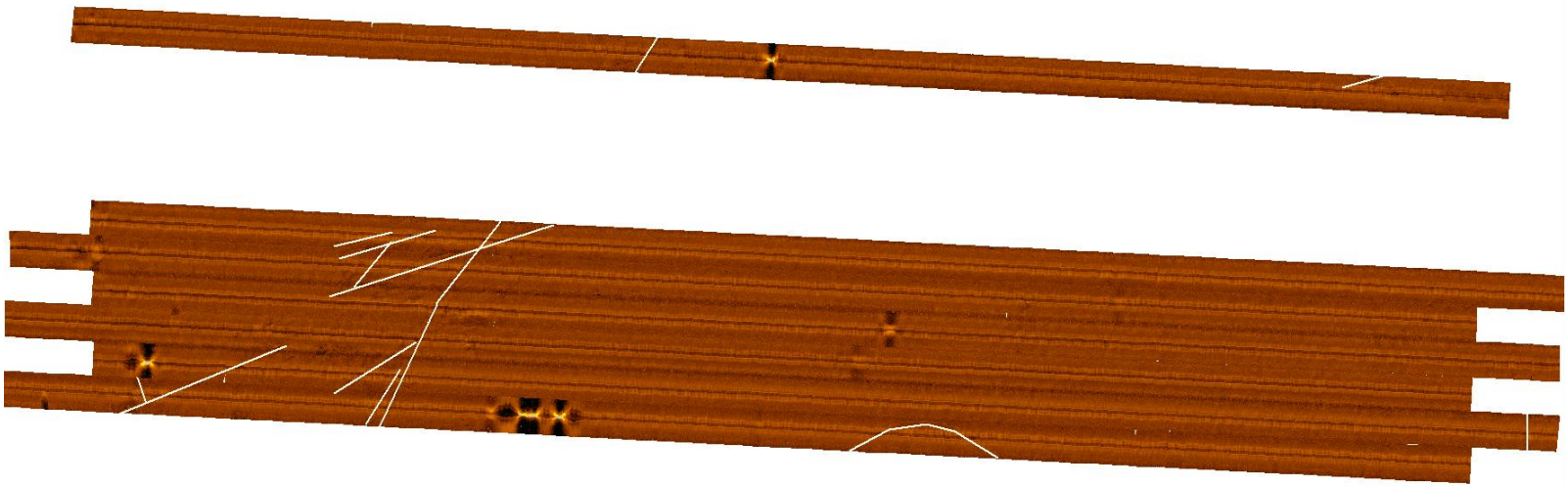

Figure E.25: 110729_D4_DV0112_M3

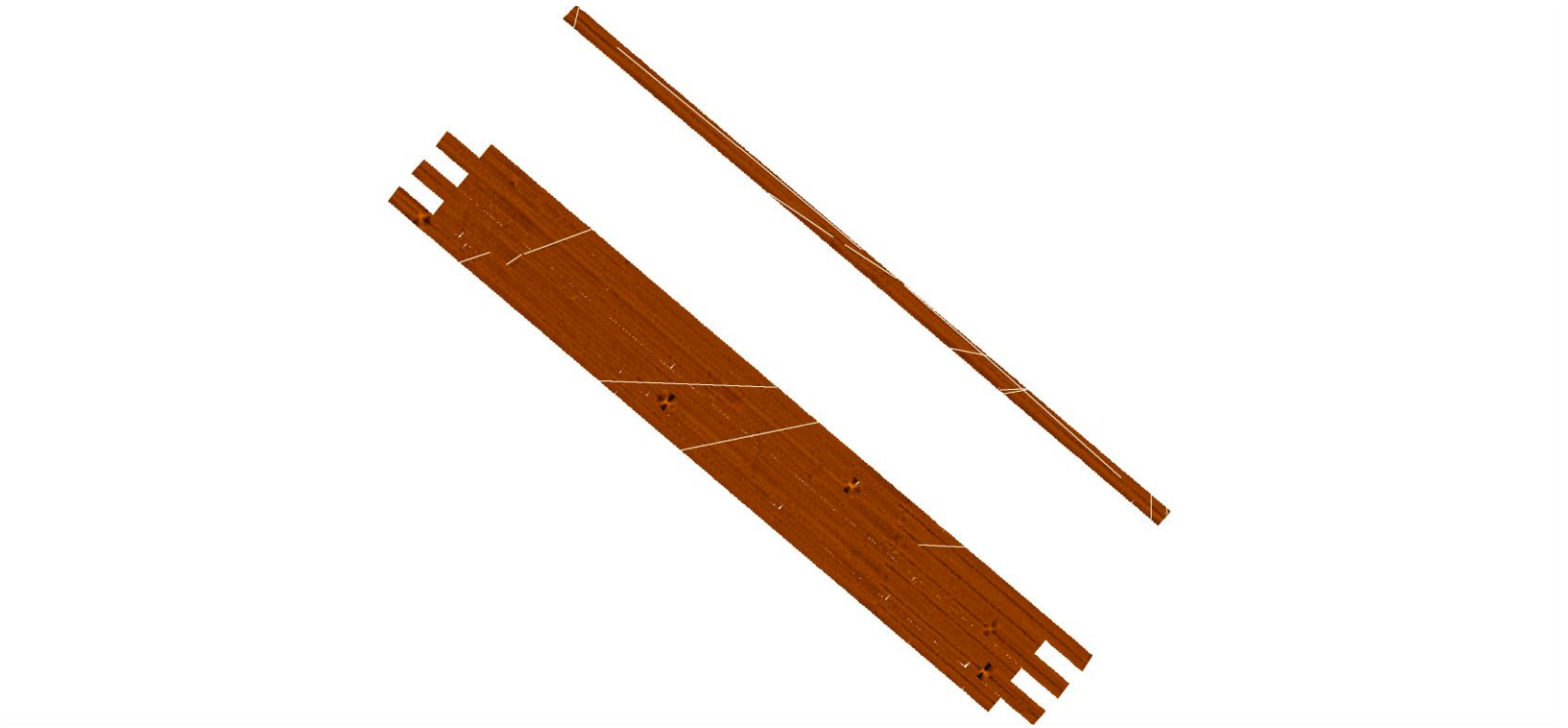

Figure E.26: 110729_D4_DV0113_M4

Figure E.27: 20110726_ScallopD1_M1

Appendix F

MATLAB CODE

F.1 Biomass

```
%Script that steps through the scallop sizing files in the current
%directory and outputs the scallop biomass based on shell height and
depth.
%Justin Walker
%University of Delaware

f = dir;
biomass = {};

for i=4:1:numel(f)
x = f(i).name;
y = importdata(x);



textdata = y.textdata;
data = y.data;
x = regexprep(x,'Sizing.csv','');
x(~isstrprop(x,'alphanum')) = '';

mission = x;


textdata(1,:) = [];
shellheight =  str2num(char(textdata(:,10)))*1000;
depth = data(:,1);

mw=exp(-8.94+2.94*log(shellheight)-.43*log(depth));

biomass(i,:) = {mission, sum(mw)};

end
```

F.2 Semivariogram

```
%Script that takes as input csv files containing image abundace and
location:
% [abundance northing easting]
%Output: Omnidirectional semivariogram
%Justin Walker
%University of Delaware


clear all
numbins =19;
f = dir;

for k=4:1:numel(f)
x = f(k).name;

data = importdata(x);
x = regexprep(x,'.csv','');
x(~isstrprop(x,'alphanum')) = '';

mission = x;
filename =
strcat('/Users/JustinWalker/Desktop/Variograms/',mission,'_Variogram.
jpeg');
filenamedata =
strcat('/Users/JustinWalker/Desktop/Variograms/',mission,'_Variogram.
csv');

x = size(data);
numrows = x(1);

interval = 1;

variance = [];
variogram = [];
variance = zeros(floor(numrows/interval)*numrows-
(floor(numrows/interval)+(floor(numrows/interval)*(floor(numrows/inte
rval)-1)/2)*interval),2);
z = 0;
for i = 1:interval:numrows-1
    for g = i+1:1:numrows
        z = z + 1;
     variance(z,1) = (data(i,1)-data(g,1))^2;
     variance(z,2) = sqrt((data(i,2)-data(g,2))^2+(data(i,3)-
data(g,3))^2);
    end
    i/(numrows-1)
end

y = size(variance);
```

```
numrowsvariance = y(1);
binspaces = linspace(0, max(variance(:,2)),numbins+1);


for j = 1:1:numbins
    totalvariance = 0;
    pairs = 0;
    for k = 1:1:numrowsvariance

        if variance(k,2) >= binspaces(j) && variance(k,2) <=
binspaces(j+1)
            pairs = pairs + 1;
            totalvariance = totalvariance + variance(k,1);
    end
    variogram(j,1) = (binspaces(j)+binspaces(j+1))/2;
    variogram(j,2) = totalvariance/(2*pairs);
    variogram(j,3) = pairs;
    end
end

totalscallops = sum(data(:,1));

if totalscallops > 0


scatter(variogram(1:round(numbins/2),1),variogram(1:round(numbins/2),
2))
    title(strcat(mission,' Variogram (', num2str(totalscallops),'
Scallops)'),'FontSize',18,'fontweight','bold');
    ylabel('\gamma(h) Scallops^2','FontSize',14)
    xlabel('Lag(m)','FontSize',14)
    ylim([0 1.1*max(variogram(1:round(numbins/2),2))])
    saveas(gcf,filename);
    close gcf;
    csvwrite(filenamedata,variogram);
end
end
```

F.3 Dredge Scar Area

```
%A script that steps through a directory containing SonarWiz exported
digitized dredge scar information.  The script parces the SonarWiz
formatted csv file and outputs a rose plot of dredging
directionality, dredge scar length, and dredge scar area.
%Justin Walker
%University of Delaware

f = dir;

for k=4:1:numel(f)
x = f(k).name;
y = importdata(x);

textdata = y.textdata;

textdata = y.textdata;
textdata(1,:) = [];


x = regexprep(x,'.csv','');
x(~isstrprop(x,'alphanum')) = '';

mission = x;
filename =
strcat('/Users/JustinWalker/Desktop/',mission,'_DredgeScarOrientation
.jpeg');

arraysize = size(textdata);
numberrows = arraysize(1);
total = numberrows/4;
coordrow = 0;
coordinates = [];
length = [];
angle = [];
for i=1:1:numberrows
if rem(i,4)==3
coordrow = coordrow + 1;
coordinates(coordrow,:) = str2num(char(textdata(i,7:8)));
end
if rem(i,4)==0
coordrow = coordrow + 1;
coordinates(coordrow,:) = str2num(char(textdata(i,7:8)));
end
end
arraysize = size(coordinates);
numberrows = arraysize(1);
j = 0;
for i=1:2:numberrows
j = j + 1;
```

```
length(j,1) = sqrt((coordinates(i+1,1)-coordinates(i,1))^2 +
(coordinates(i+1,2)-coordinates(i,2))^2);
if (coordinates(i+1,1) - coordinates(i,1))/(coordinates(i+1,2)-
coordinates(i,2)) < 0

    angle(i,1) =  2*pi()+atan((coordinates(i+1,1)-
coordinates(i,1))/(coordinates(i+1,2)-coordinates(i,2)));
    angle(i+1,1) = 2*pi()+atan((coordinates(i+1,1)-
coordinates(i,1))/(coordinates(i+1,2)-coordinates(i,2)))+pi ;
else
    angle(i,1) = atan((coordinates(i+1,1)-
coordinates(i,1))/(coordinates(i+1,2)-coordinates(i,2)));
    angle(i+1,1) = atan((coordinates(i+1,1)-
coordinates(i,1))/(coordinates(i+1,2)-coordinates(i,2)))+pi;
end
end

totalLength = sum(length)
totalArea = sum(length)*4.572
rose(angle);
[t,r] = rose(angle);
p = rose(angle);

set(gca,'View',[-90 90],'YDir','reverse');

[x,y] = pol2cart(t,r);
h = patch(reshape(x,4,[]), reshape(y,4,[]), 'b');
alpha(h, 0.5)

title(strcat(mission,' Dredge Scar Orientation
(N=',num2str(total),')'),'FontSize',18,'fontweight','bold');
h = findall(gcf,'type','line');
% remove the handle for the polar plot line from the array
h(h == p) = [];
% delete all other lines
delete(h);
% find all of the text objects in the polar plot
t = findall(gcf,'type','text');
% delete the text objects
tl = numel(t);
delete(t(16:tl));
delete(t(4));

databox = sprintf(strcat('Dredge Scar
Length:',num2str(round(totalLength)),'m','\nDredge Scar Area:
',num2str(round(totalArea)),'m^2'));

Textbox = annotation('textbox',[0 .15 0 0]);
set(Textbox,'String',databox);
set(Textbox,'FitBoxToText','on');
set(Textbox,'LineWidth',2);
```

```
saveas(gcf,filename);
close gcf;
end
```

F.4 Image Sample Model

```
%mfile to generate random sampling of scallop image counts and
calculate
%abundances
%first load the all count data- one column listing number of scallops
in
%each image
%load allsc
%determine a sampling interval
sublength=1; %define a percentage subset
subset=length(allsc)*(sublength/100);

%next calculate a randomsampling of all the images
%qr=randperm(length(allsc));
%take a subset worth of the images
%qrsubset=allsc(qr(1:floor(subset)));
%calculate sum of counts of subset
%qrsubsum=sum(qrsubset);
%calculate abundance of subset
%qrabund=qrsubsum./floor(subset);
m=20 %number of subsets
n=50 %number of resamplings
%k=100; %set sublength interval
bigM=zeros(m,n); %preallocate matrix
%do sample loop of calculations
for i=1:m;
    for j=1:n;
qr=randperm(length(allsc));
qrsubset=allsc(qr(1:floor(subset)));
%calculate sum of counts of subset
qrsubsum(j,i)=sum(qrsubset);
%calculate abundance of subset
qrabund(j,i)=sum(qrsubset)./floor(subset);
    end
end

stuff=ones(100,20);
stuff2=stuff(:,1).*floor(subset);

%%%this part works don't mess with it%%%
sublength=15; %define a percentage subset
subset=length(allsc)*(sublength/100);

for i=1:100
qr=randperm(length(allsc));
qrsubset=allsc(qr(1:floor(subset)));
%calculate sum of counts of subset
qrsubsum(i)=sum(qrsubset);
%calculate abundance of subset
qrabund(i)=sum(qrsubset)./floor(subset);
```

```
end
%%%

subs2use=0:5:100;
subs2use(1)=1;
bigM=zeros(length(subs2use),100);
for k=1:length(subs2use);
for i=1:100

sublength=subs2use(k); %define a percentage subset
subset=length(allsc)*(sublength/100);

qr=randperm(length(allsc));
qrsubset=allsc(qr(1:floor(subset)));
%calculate sum of counts of subset
qrsubsum(i)=sum(qrsubset);
%calculate abundance of subset
qrabund(i)=sum(qrsubset)./floor(subset);
bigM(k,i)=qrabund(i);

end
end
```

Appendix G

QUALITY CONTROL

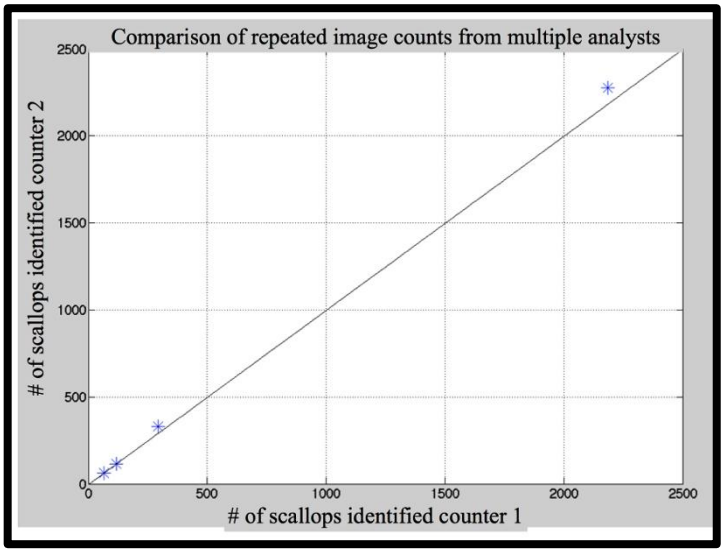

Figure G.1: Plot showing the consistency of repeated image counts by multiple analysts.

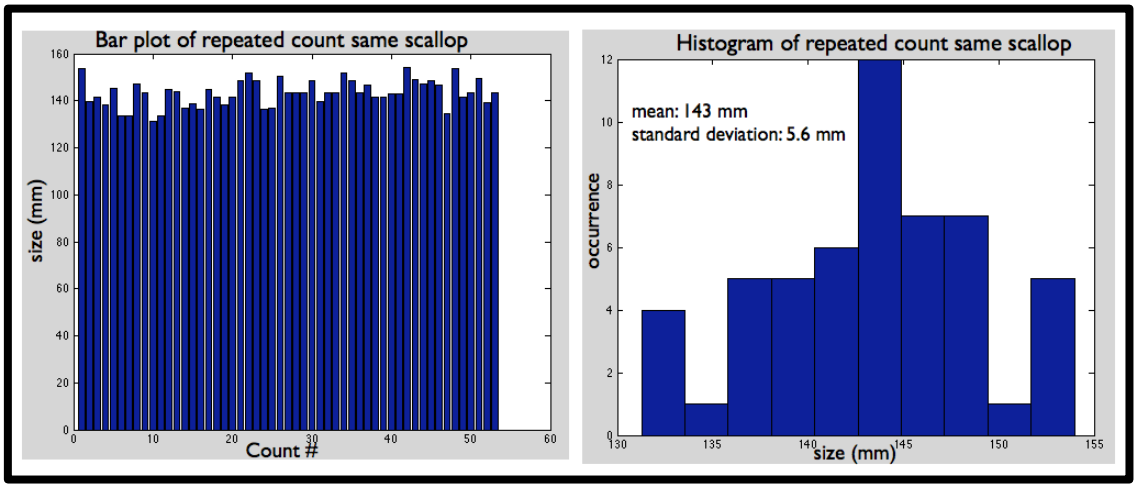

Figure G.2: Results of N=53 repeated digital measurements of the same scallop in a photo by a single analyst.

Appendix H

DREDGE SCAR AREA AND ROSE PLOTS

H.1 Introduction

This appendix contains the dredge scar area calculated for each AUV survey mission from the side-scan sonar mosaics (Appendix E). A rose plot is constructed for each mission showing the dredge strike orientation distribution. See Section 3.2.3 to review how to calculate dredge scar area from the side-scan mosaics.

H.2 Dredge Scar Rose Plots

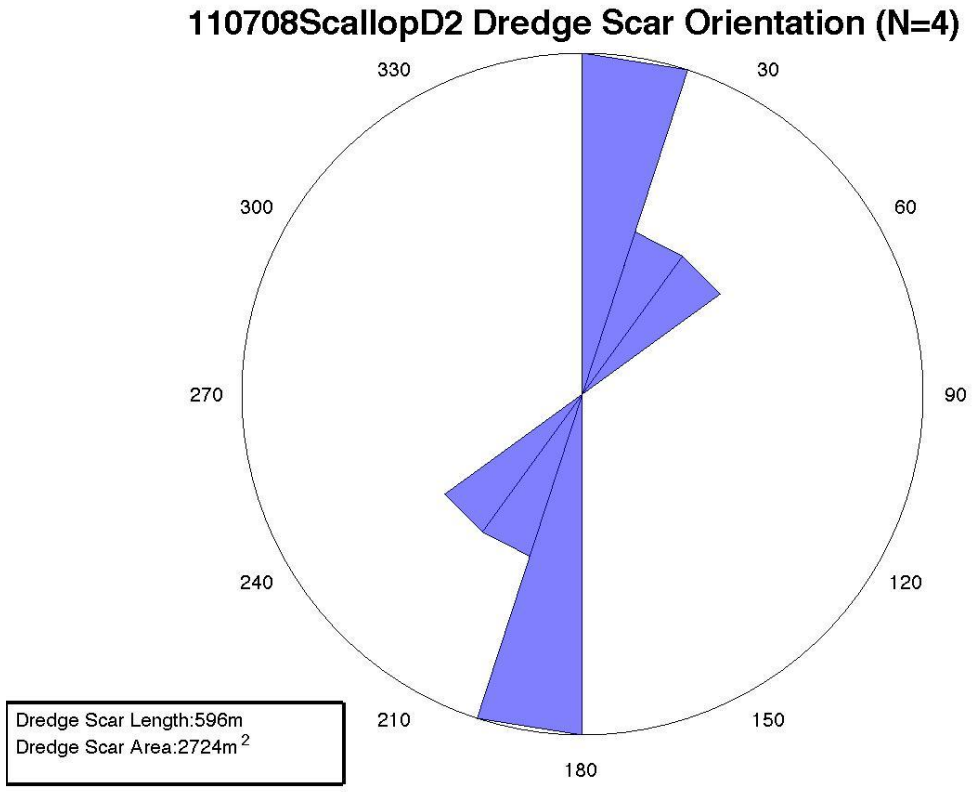

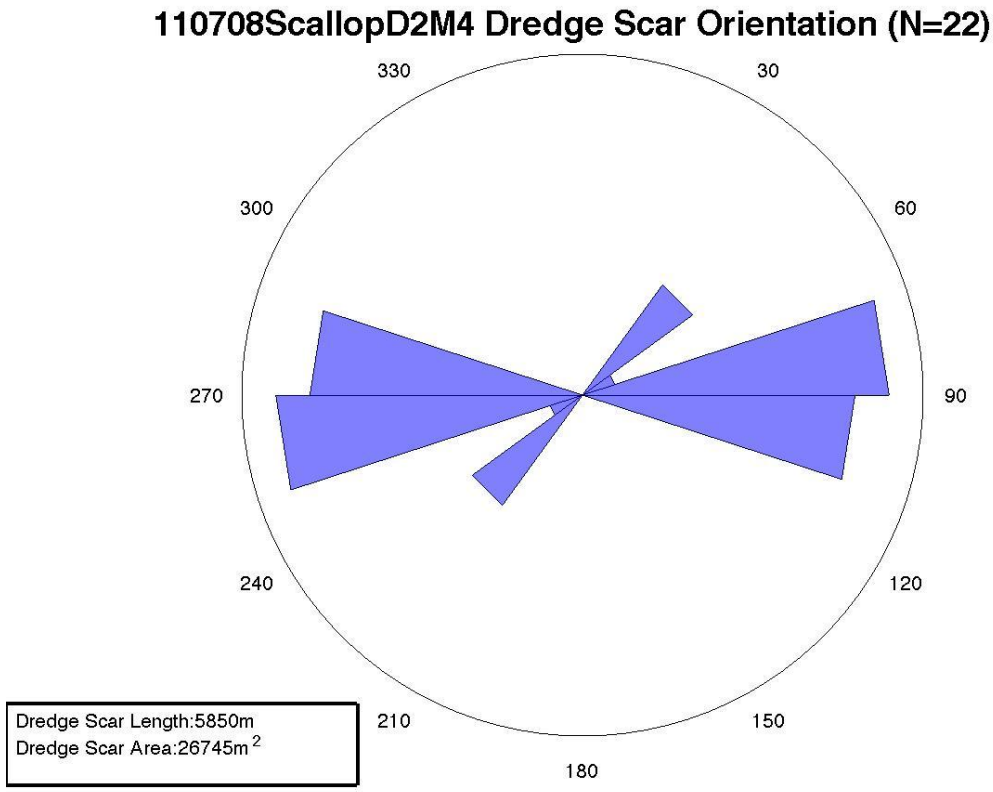
110708ScallopD2M4 Dredge Scar Orientation (N=22)
330
30
300
60
270
90
240
120
210
150
180
Dredge Scar Length:5850m
Dredge Scar Area:26745m 2

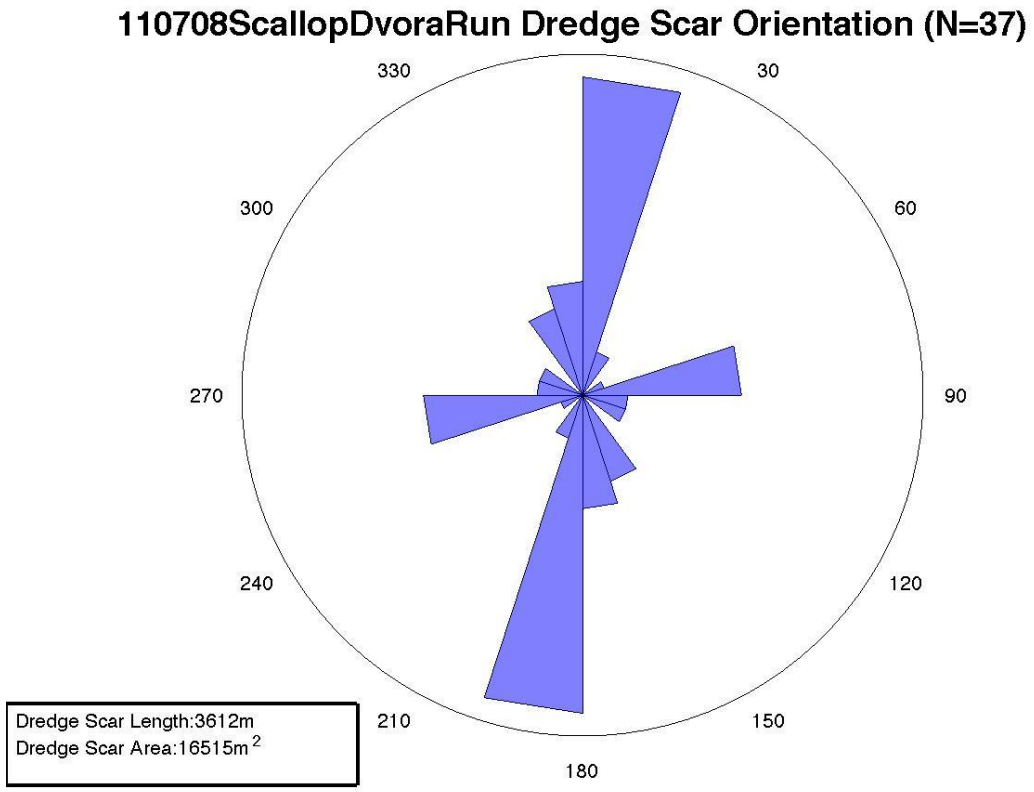
110708ScallopDvoraRun Dredge Scar Orientation (N=37)
330
30
300
60
270
90
240
120
210
150
180
Dredge Scar Length:3612m
Dredge Scar Area:16515m 2

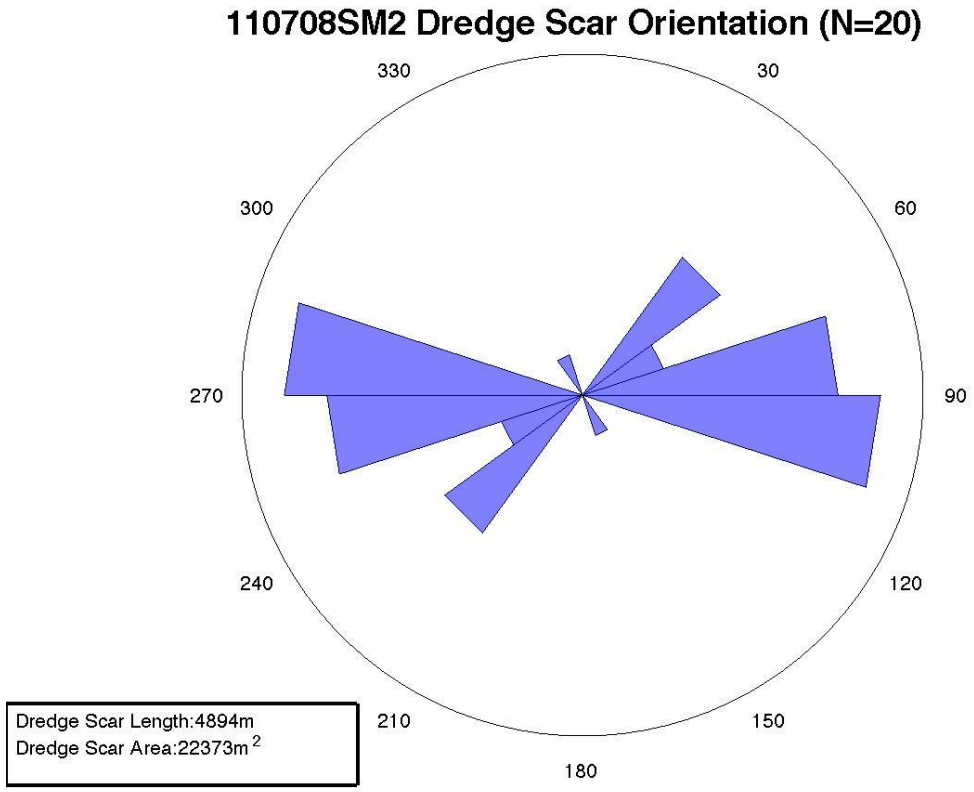
110708SM2 Dredge Scar Orientation (N=20)
330
30
300
60
270
90
240
120
210
150
180
Dredge Scar Length:4894m
Dredge Scar Area:22373m 2

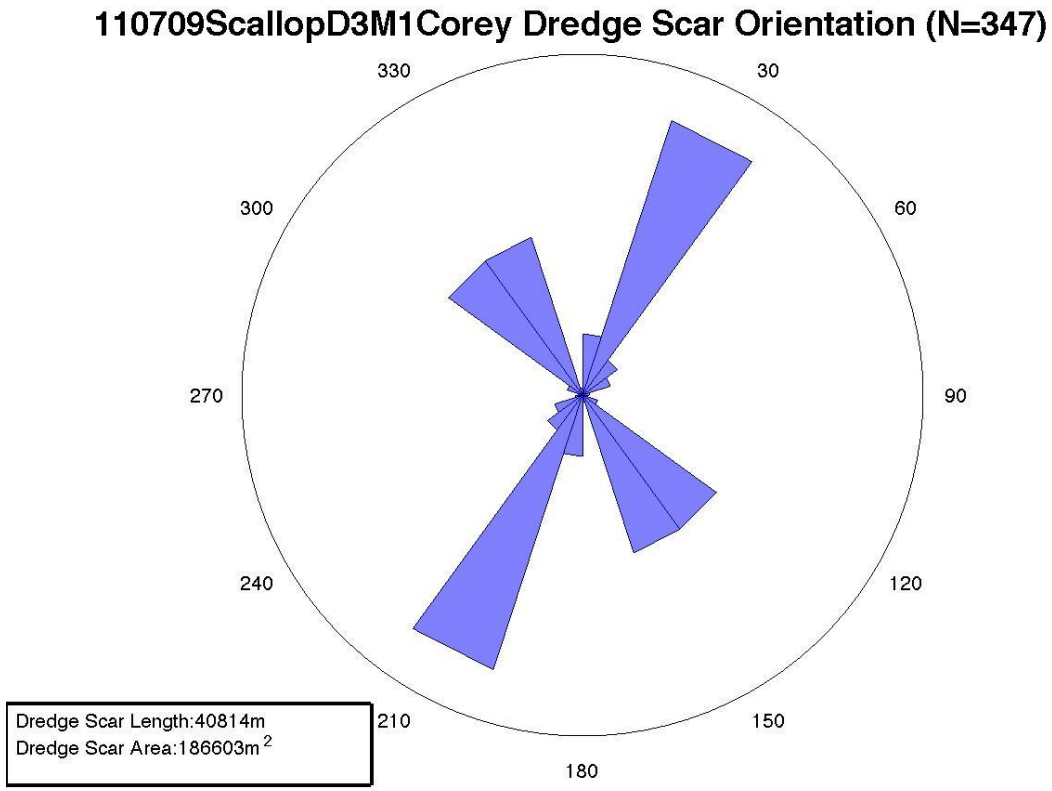
110709ScallopD3M1Corey Dredge Scar Orientation (N=347)
330
30
300
60
270
90
240
120
210
150
180
Dredge Scar Length:40814m
Dredge Scar Area:186603m 2

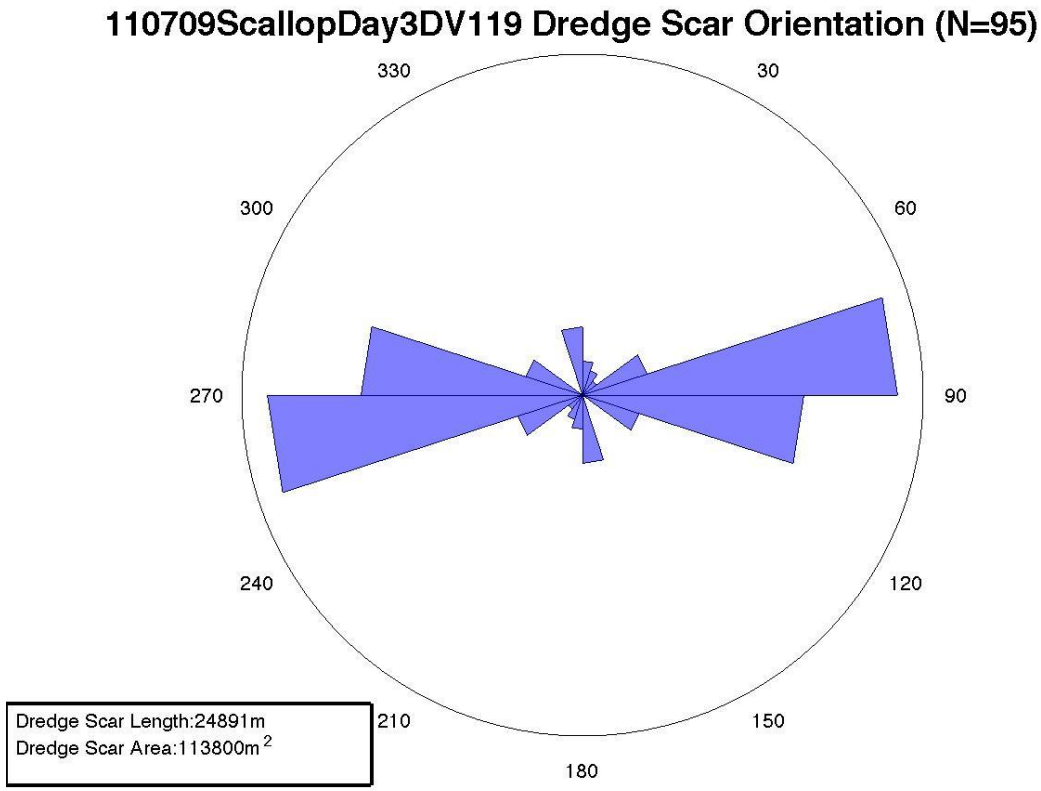
110709ScallopDay3DV119 Dredge Scar Orientation (N=95)
330
30
300
60
270
90
240
120
210
150
180
Dredge Scar Length:24891m
Dredge Scar Area:113800m 2

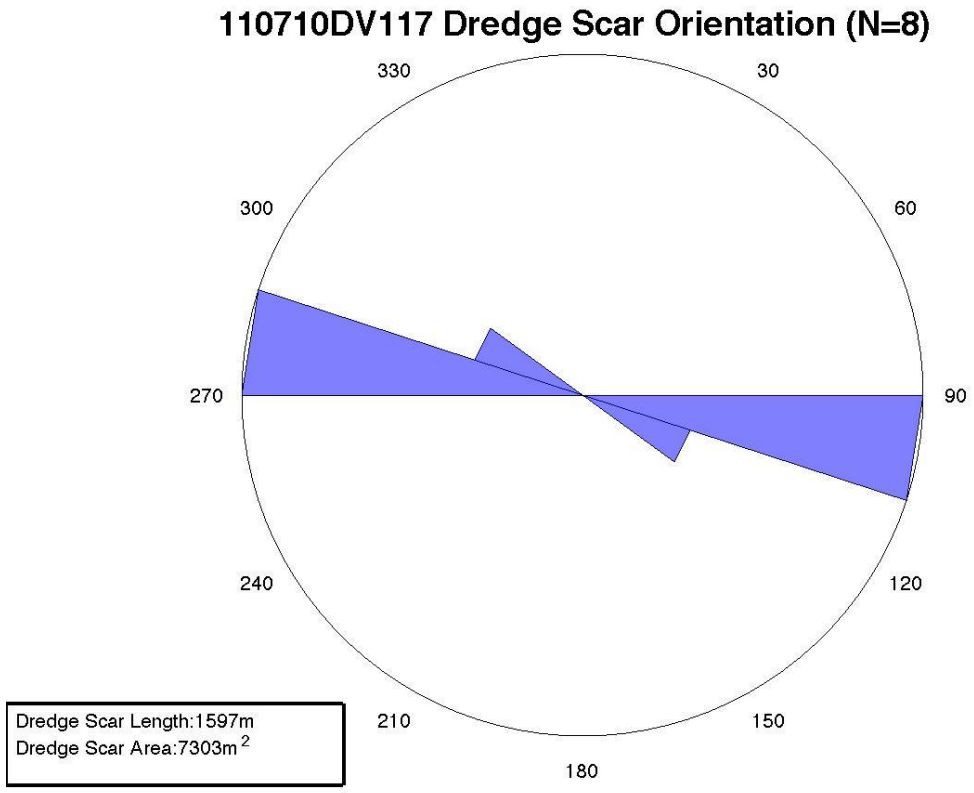
110710DV117 Dredge Scar Orientation (N=8)
330
30
300
60
270
90
240
120
210
150
180
Dredge Scar Length:1597m
Dredge Scar Area:7303m 2

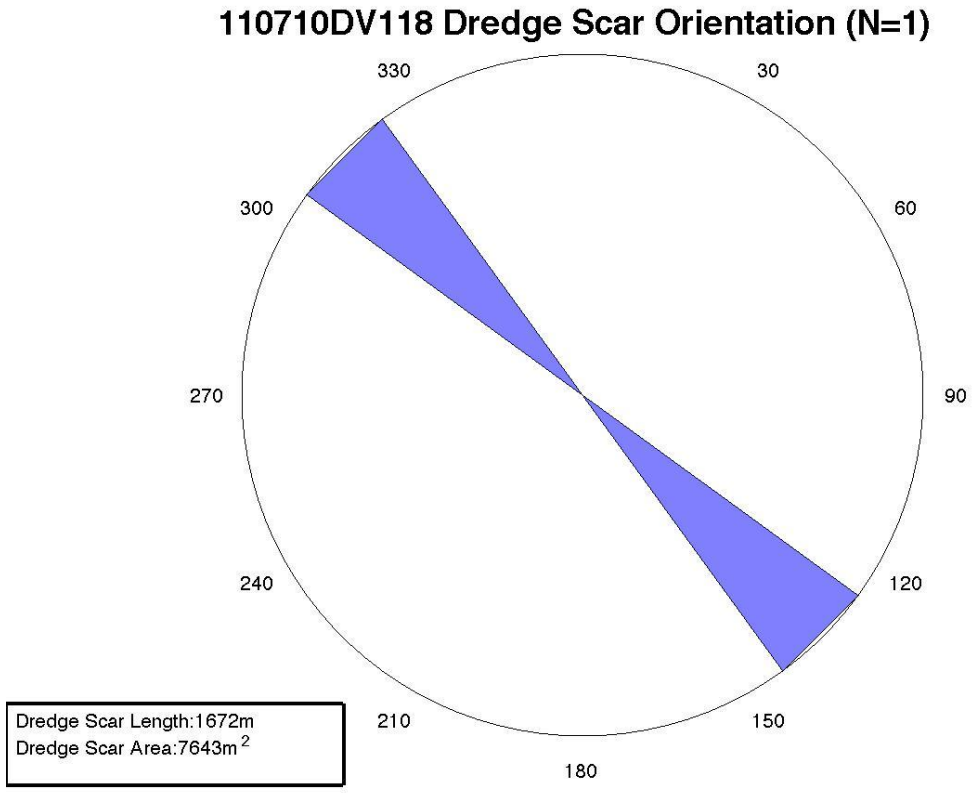
110710DV118 Dredge Scar Orientation (N=1)
330
30
300
60
270
90
240
120
210
150
180
Dredge Scar Length:1672m
Dredge Scar Area:7643m 2

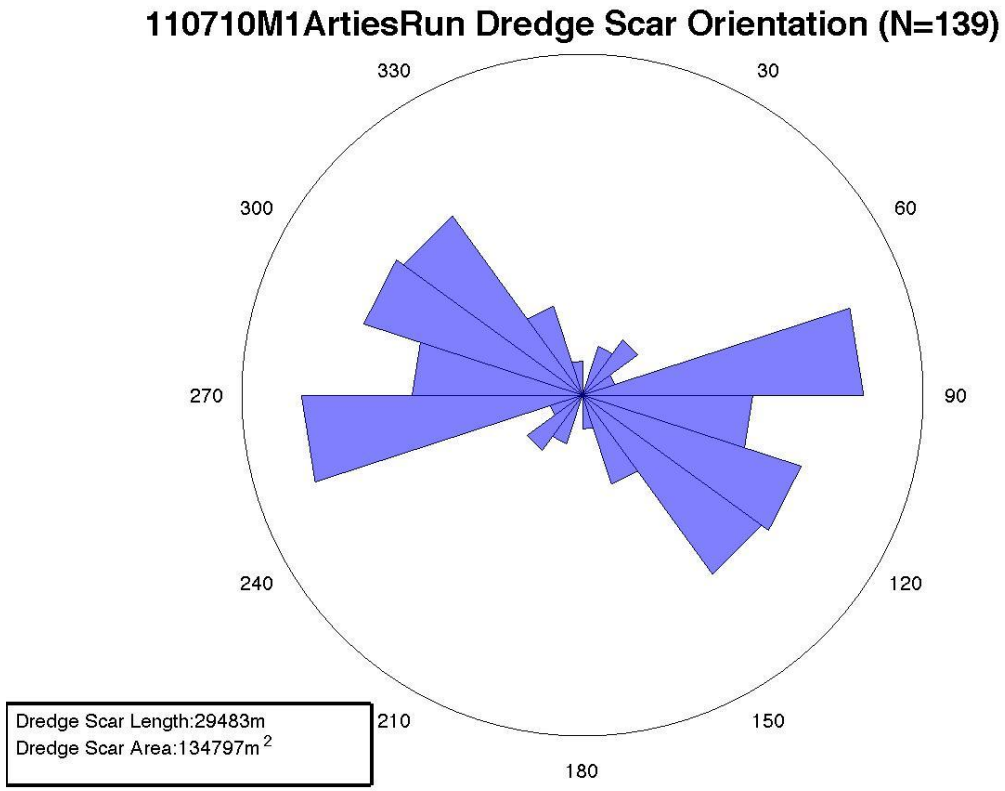
110710M1ArtiesRun Dredge Scar Orientation (N=139)
330
30
300
60
270
90
240
120
210
150
180
Dredge Scar Length:29483m
Dredge Scar Area:134797m 2

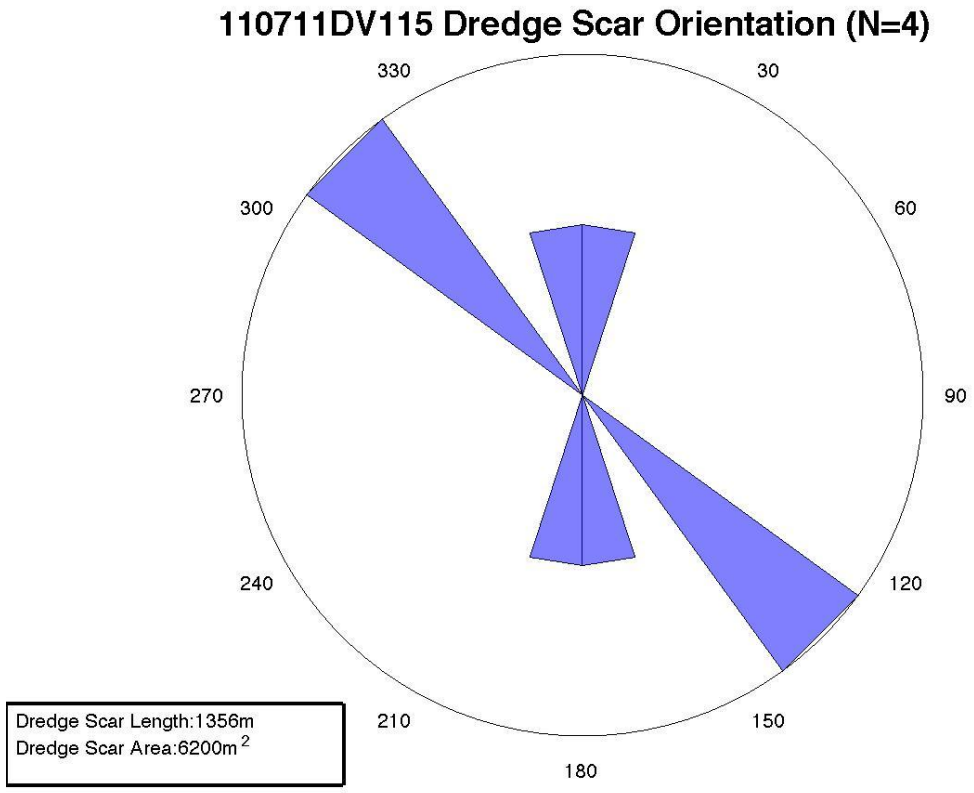
110711DV115 Dredge Scar Orientation (N=4)
330
30
300
60
270
90
240
120
210
150
180
Dredge Scar Length:1356m
Dredge Scar Area:6200m 2

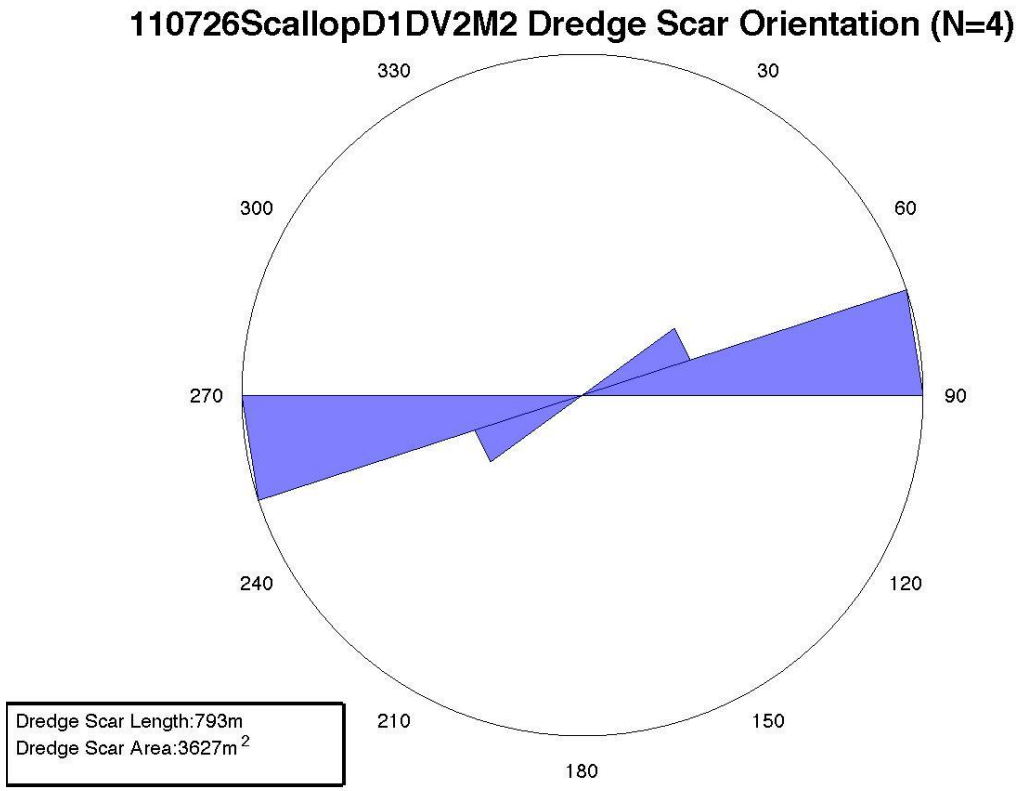
110726ScallopD1DV2M2 Dredge Scar Orientation (N=4)
330
30
300
60
270
90
240
120
210
150
180
Dredge Scar Length:793m
Dredge Scar Area:3627m 2

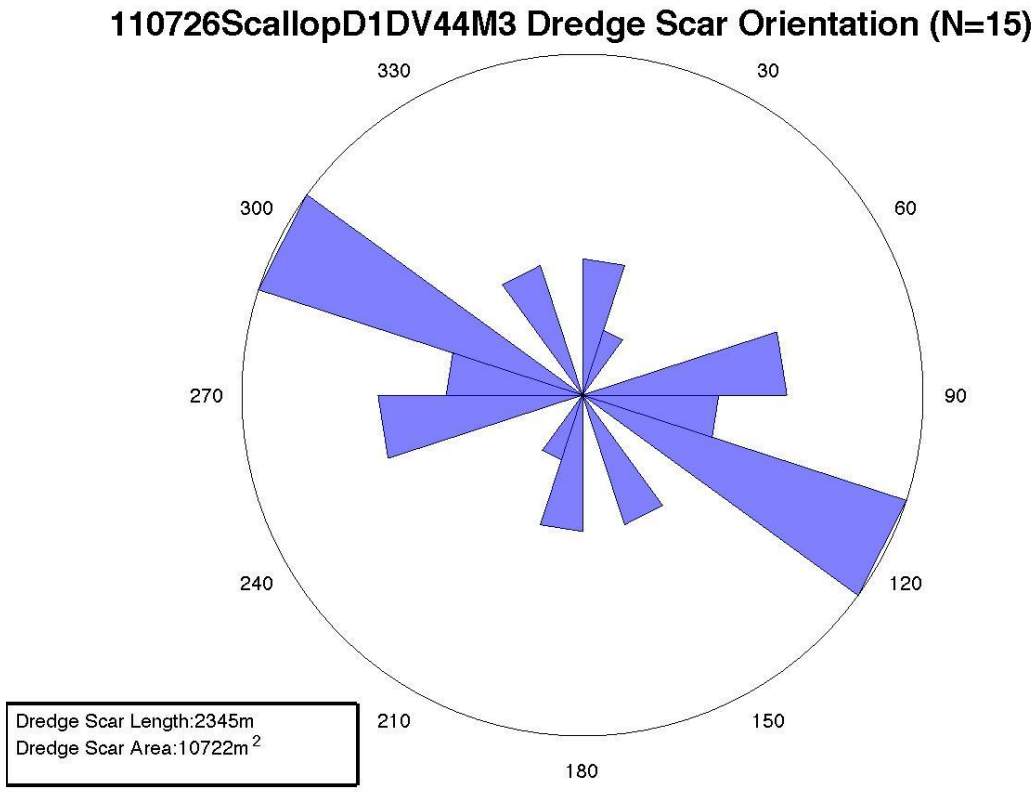
110726ScallopD1DV44M3 Dredge Scar Orientation (N=15)
330
30
300
60
270
90
240
120
210
150
180
Dredge Scar Length:2345m
Dredge Scar Area:10722m 2

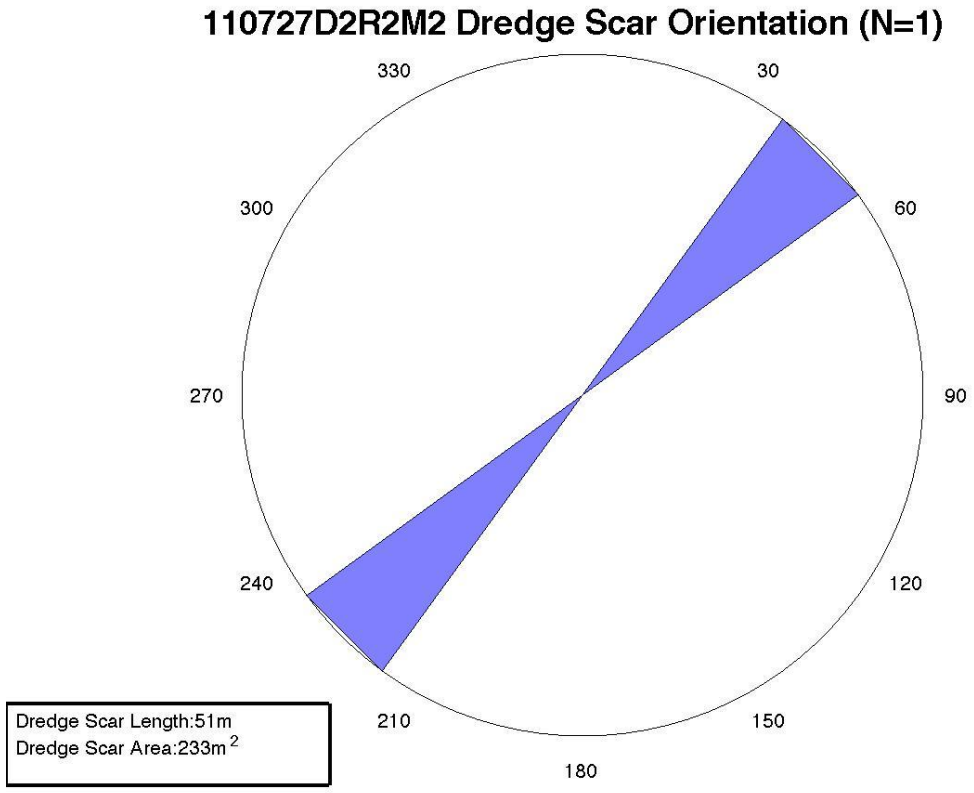
110727D2R2M2 Dredge Scar Orientation (N=1)
330
30
300
60
270
90
240
120
210
150
180
Dredge Scar Length:51m
Dredge Scar Area:233m 2

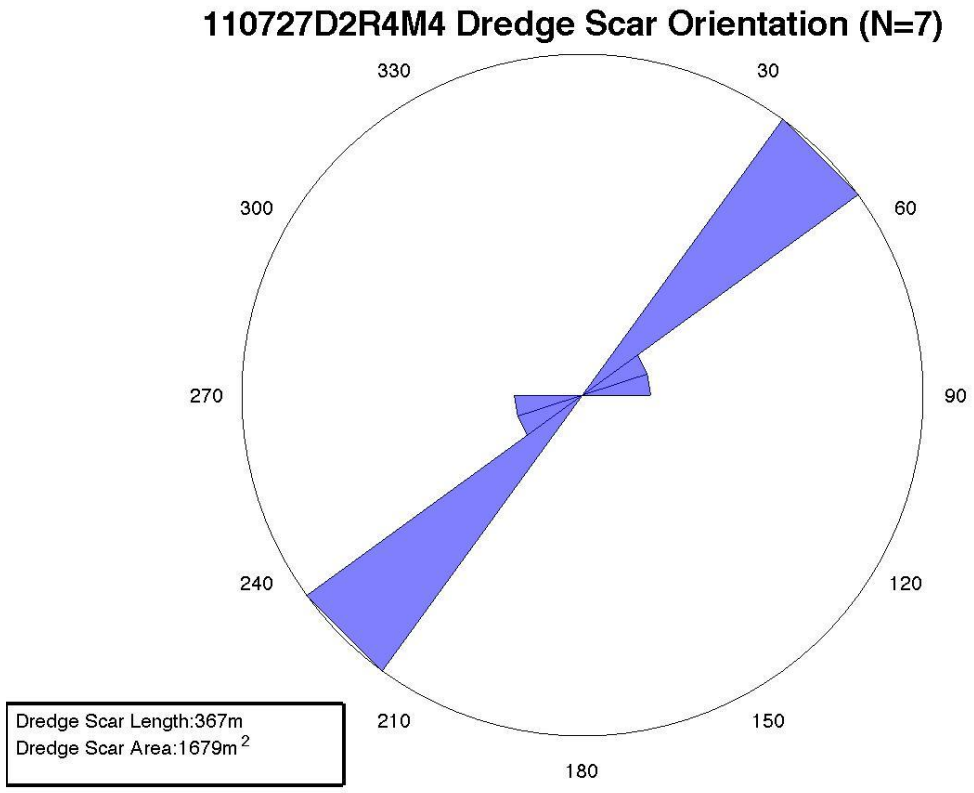
110727D2R4M4 Dredge Scar Orientation (N=7)
330
30
300
60
270
90
240
120
210
150
180
Dredge Scar Length:367m
Dredge Scar Area:1679m 2

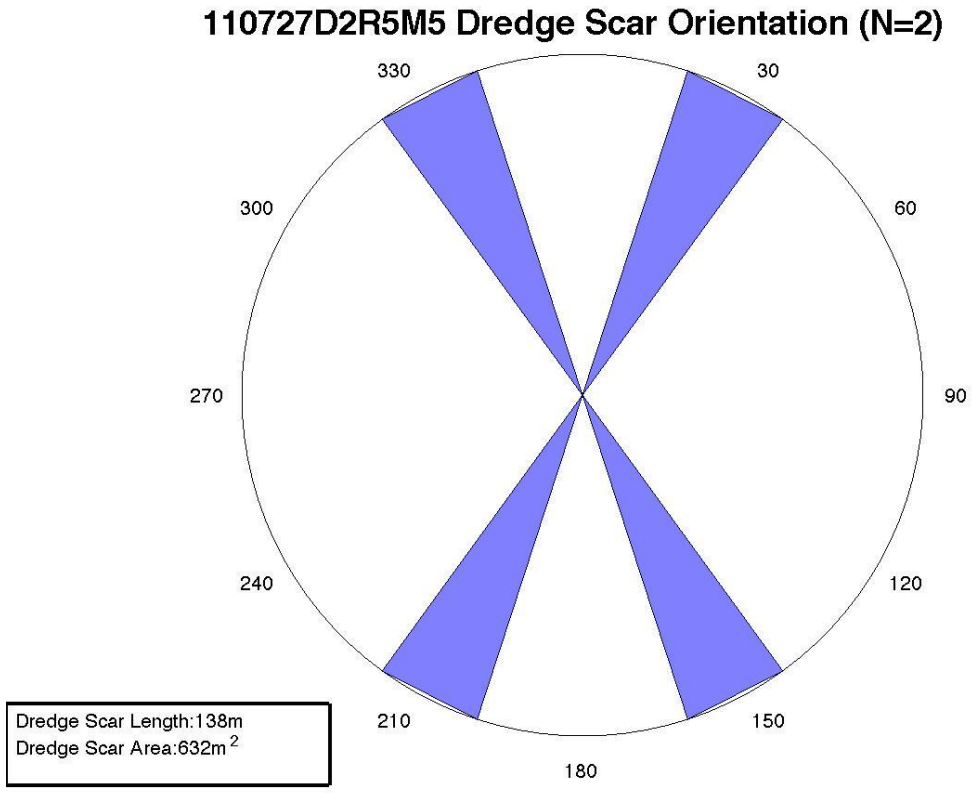
110727D2R5M5 Dredge Scar Orientation (N=2)
330
30
300
60
270
90
240
120
210
150
180
Dredge Scar Length:138m
Dredge Scar Area:632m 2

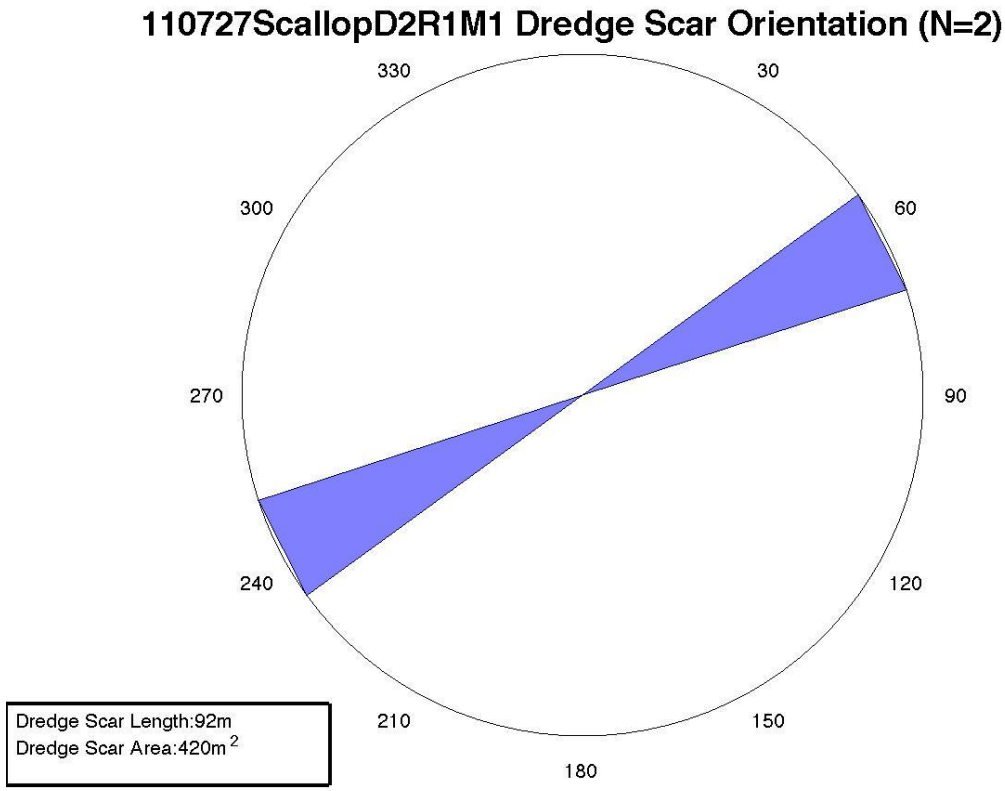
110727ScallopD2R1M1 Dredge Scar Orientation (N=2)
330
30
300
60
270
90
240
120
210
150
180
Dredge Scar Length:92m
Dredge Scar Area:420m 2

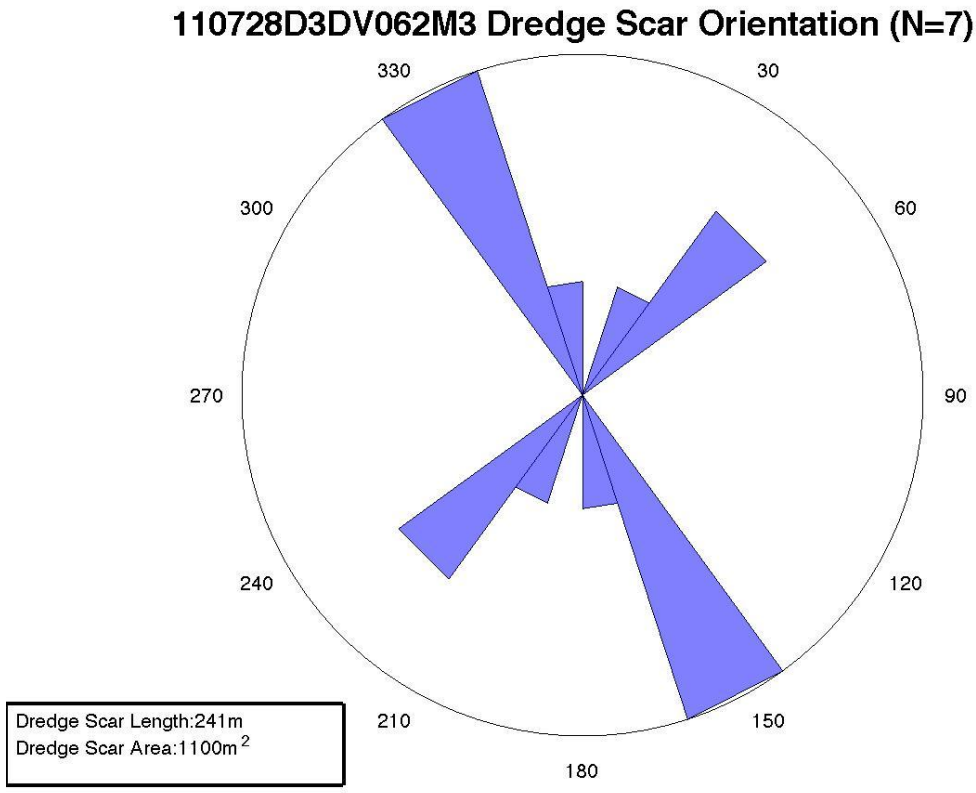
110728D3DV062M3 Dredge Scar Orientation (N=7)
330
30
300
60
270
90
240
120
210
150
180
Dredge Scar Length:241m
Dredge Scar Area:1100m 2

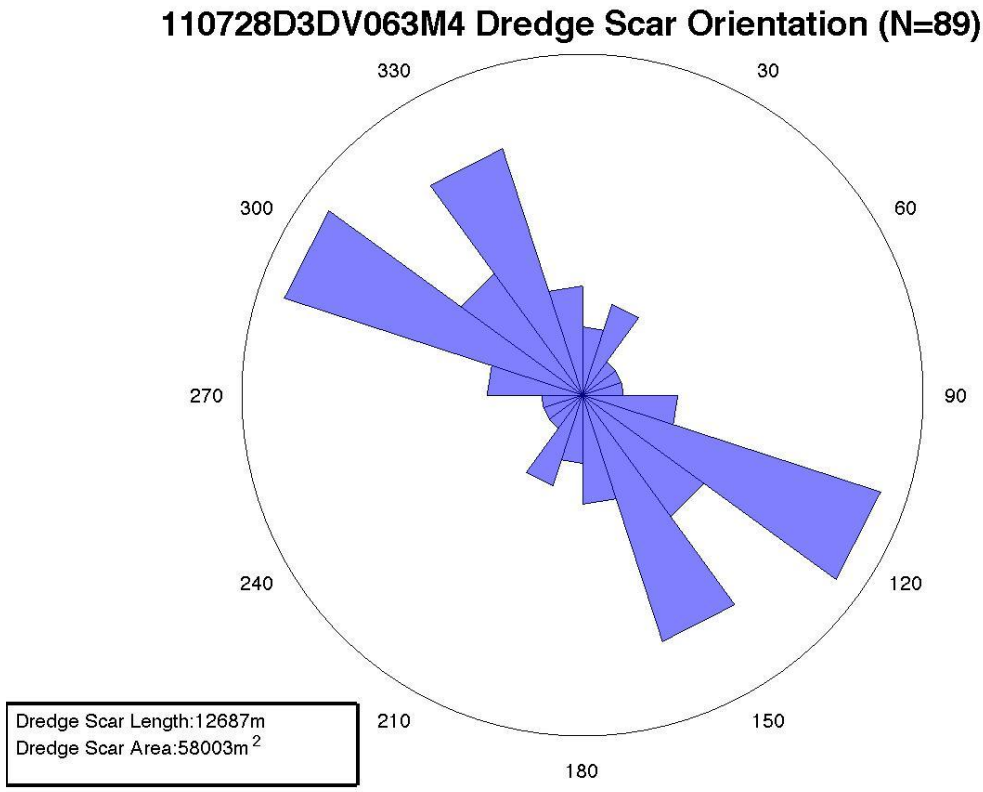
110728D3DV063M4 Dredge Scar Orientation (N=89)
330
30
300
60
270
90
240
120
210
150
180
Dredge Scar Length:12687m
Dredge Scar Area:58003m 2

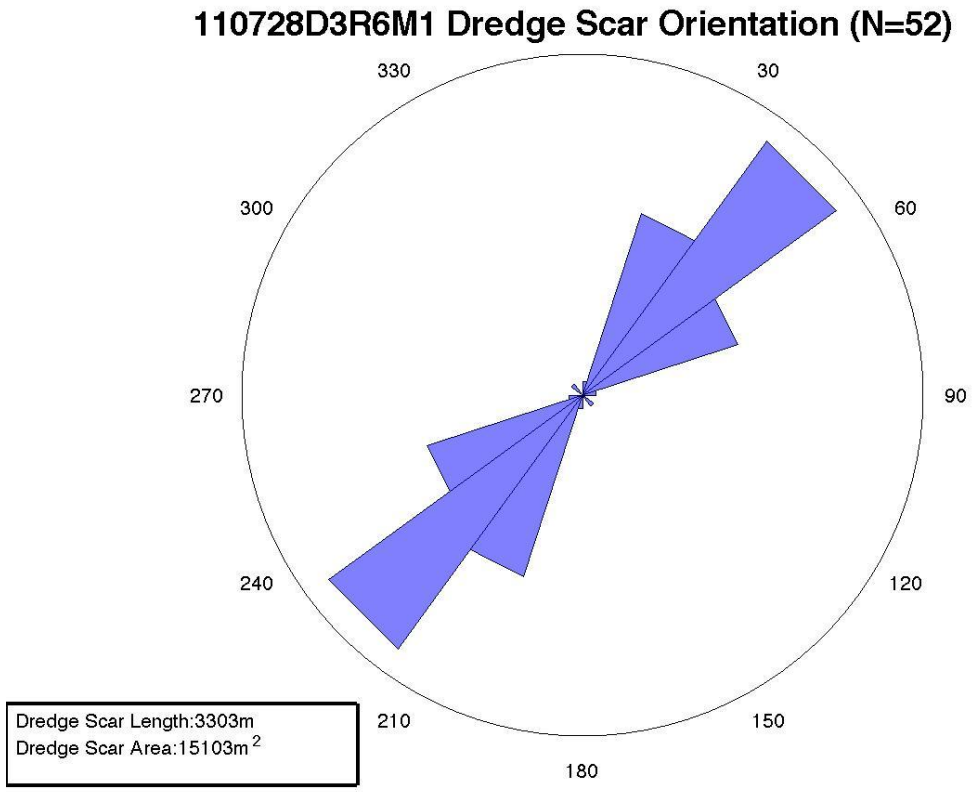
110728D3R6M1 Dredge Scar Orientation (N=52)
330
30
300
60
270
90
240
120
210
150
180
Dredge Scar Length:3303m
Dredge Scar Area:15103m 2

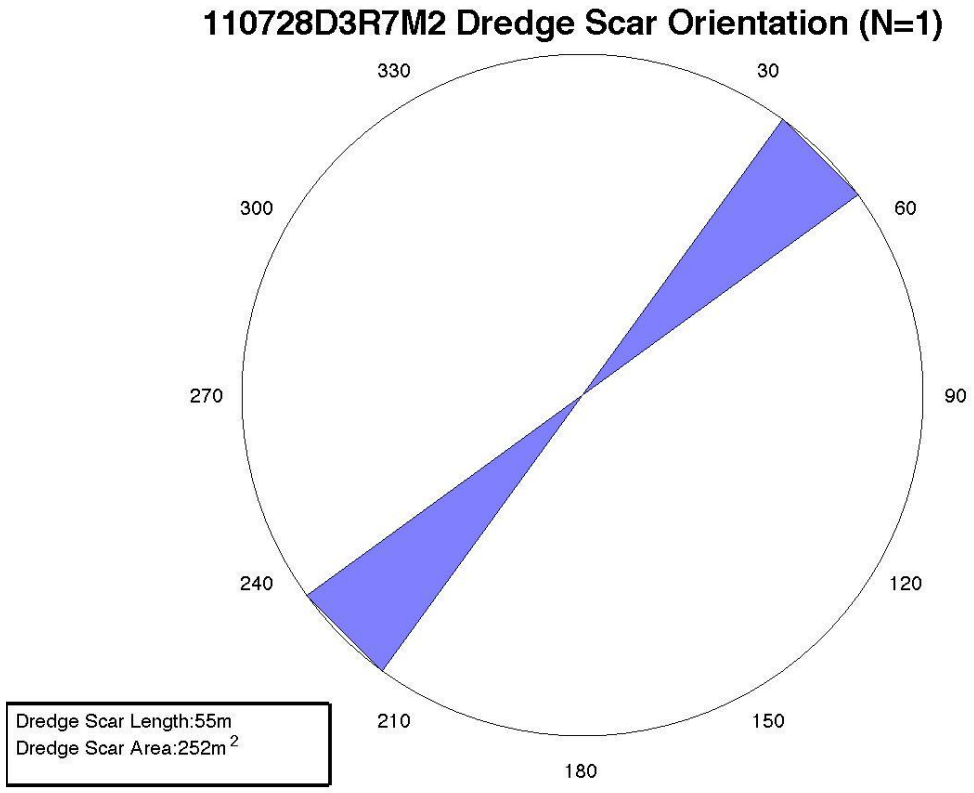
110728D3R7M2 Dredge Scar Orientation (N=1)
330
30
300
60
270
90
240
120
210
150
180
Dredge Scar Length:55m
Dredge Scar Area:252m 2

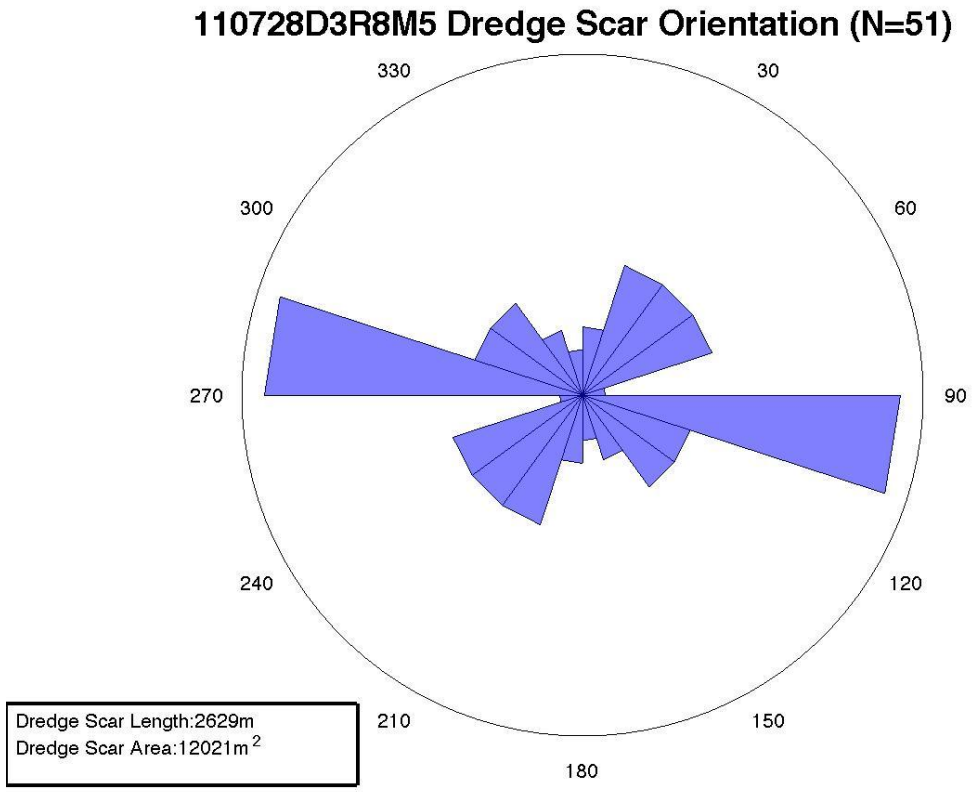
110728D3R8M5 Dredge Scar Orientation (N=51)
330
30
300
60
270
90
240
120
210
150
180
Dredge Scar Length:2629m
Dredge Scar Area:12021m 2

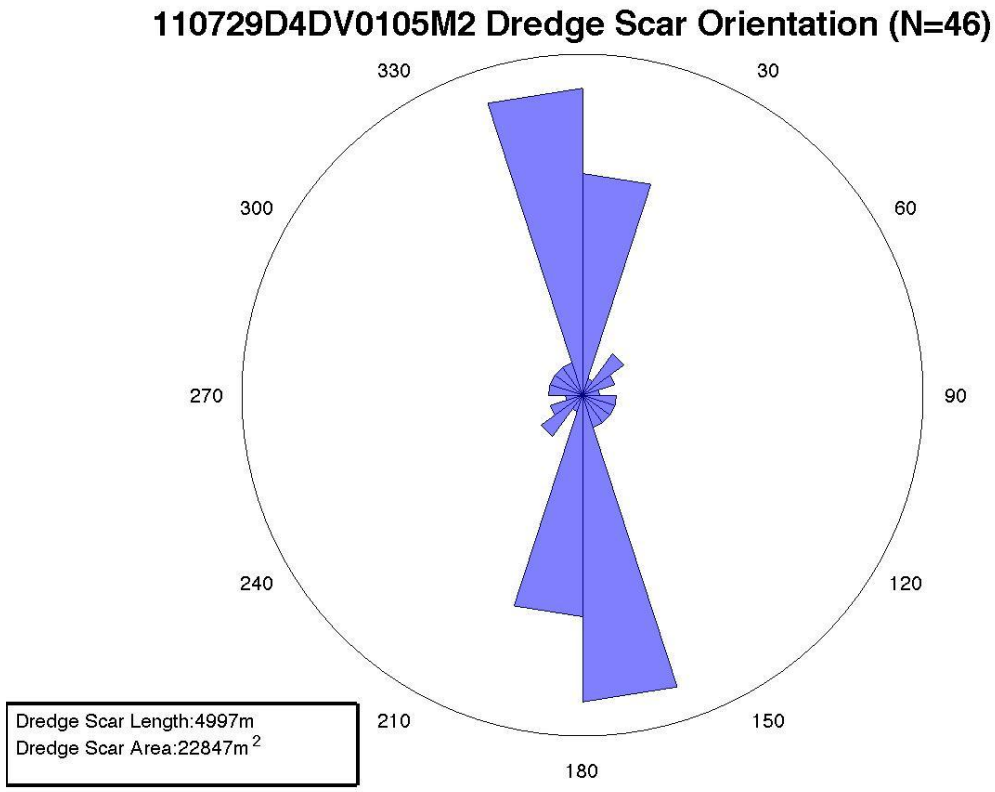
110729D4DV0105M2 Dredge Scar Orientation (N=46)
330
30
300
60
270
90
240
120
210
150
180
Dredge Scar Length:4997m
Dredge Scar Area:22847m 2

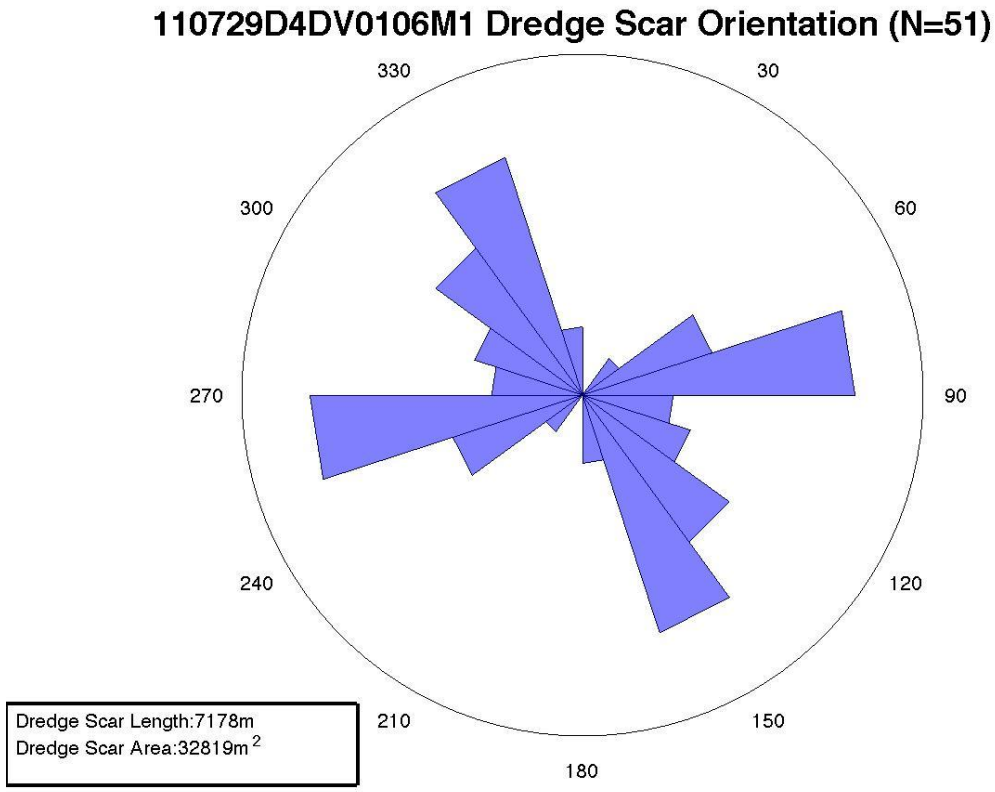
110729D4DV0106M1 Dredge Scar Orientation (N=51)
330
30
300
60
270
90
240
120
210
150
180
Dredge Scar Length:7178m
Dredge Scar Area:32819m 2

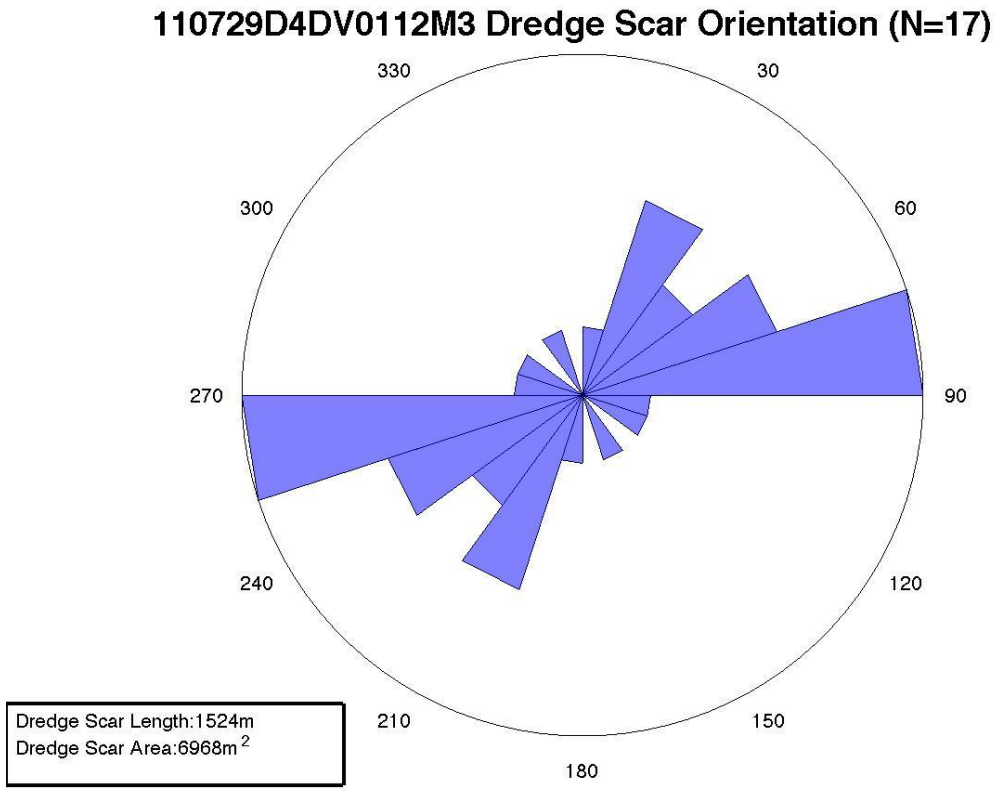
110729D4DV0112M3 Dredge Scar Orientation (N=17)
330
30
300
60
270
90
240
120
210
150
180
Dredge Scar Length:1524m
Dredge Scar Area:6968m 2

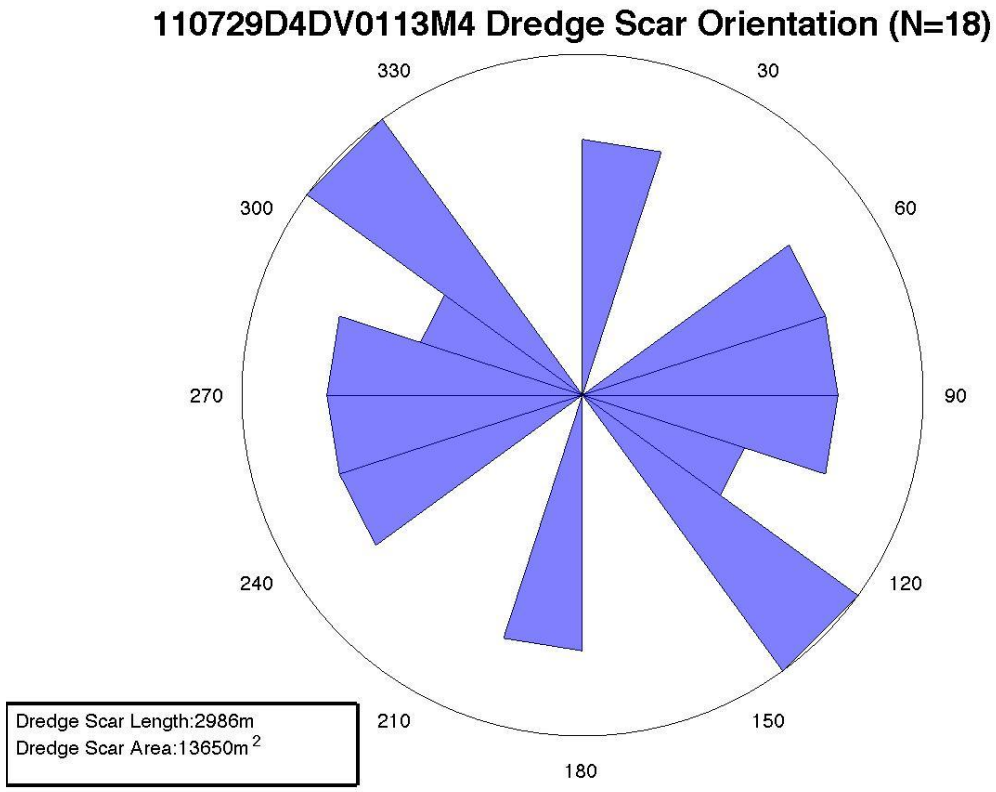
110729D4DV0113M4 Dredge Scar Orientation (N=18)
330
30
300
60
270
90
240
120
210
150
180
Dredge Scar Length:2986m
Dredge Scar Area:13650m 2

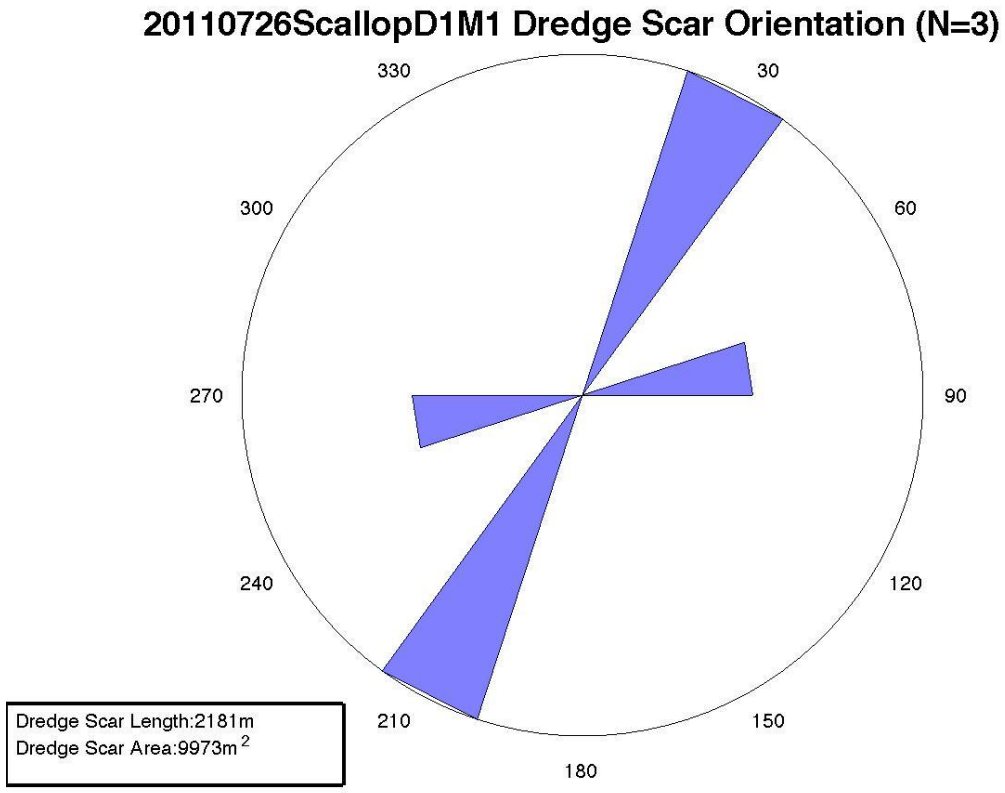
20110726ScallopD1M1 Dredge Scar Orientation (N=3)
330
30
300
60
270
90
240
120
210
150
180
Dredge Scar Length:2181m
Dredge Scar Area:9973m 2